Understanding lipid droplet biogenesis in the central nervous system of Drosophila models of Parkinson's disease

Victor Girard

Numéro National de Thèse : 2020LYSEN083

THESE de DOCTORAT DE L'UNIVERSITE DE LYON
opérée par
l'Ecole Normale Supérieure de Lyon

Ecole Doctorale N° 340
Biologie Moléculaire, Intégrative et Cellulaire (BMIC)

Discipline : Biologie

Soutenue publiquement le 15/12/2020, par :
Victor GIRARD

Understanding lipid droplet biogenesis in the central nervous system of *Drosophila* models of Parkinson's disease

Biogénèse des gouttelettes lipidiques dans le système nerveux central de modèles de la maladie de Parkinson chez la *Drosophile*

Devant le jury composé de :

SIBON, Ody Professeur Université de Groningen (Pays-Bas) Rapporteure
KÜHNLEIN, Ronald Professeur Université de Graz (Autriche) Rapporteur
THIAM, Abdou Rachid Directeur de Recherche ENS Paris Examinateur
Davoust-Nataf, Nathalie Maître de Conférence ENS de Lyon Co-encadrante de thèse
Mollereau, Bertrand Professeur ENS de Lyon Directeur de thèse

ABSTRACT

Neurodegenerative disorders are a worldwide leading cause of disability. Several neurodegenerative disorders including Parkinson's disease (PD) are associated with lipid storage dysregulation in the brain. In particular, the storage of lipids in cytoplasmic organelles, called lipid droplets (LDs), has recently emerged as an important mechanism of the stress response. Several labs including ours, found that LD accumulation in glia may promote neuronal survival in condition of oxidative stress. Interestingly, in the context of neurodegeneration, neurons can also accumulate LDs. The contribution of neuronal and glial cells LDs to neurodegeneration remains a topic of debate. During my PhD, I investigated the mechanisms and consequences of LD accumulation in neurons and glia in two *Drosophila* models of PD.

PD is characterized by the accumulation of misfolded alpha-synuclein (aSyn) in neuronal cytoplasmic inclusions. Interestingly, aSyn contains a lipid-binding domain that shares structural similarities with LD-binding proteins such as perilipins and aSyn can bind synthetic LDs *in vitro,* and induce LD accumulation in yeast by a mechanism that remains unclear. I found that expression of aSyn in association with perilipin impairs LD homeostasis leading to accumulation of LDs in *Drosophila* photoreceptor neurons. Interestingly, I observed that aSyn co-localizes with perilipins on the LD surface in both *Drosophila* photoreceptor neurons and human neuroblastoma cells. I thus propose that aSyn can, by associating with perilipins, stabilize LDs and by this mean promotes LD accumulation. Finally, modulating LD content in photoreceptor impacts aSyn resistance to proteinase K suggesting that LDs are involved in the pathological conversion of aSyn.

Glial cells are early sensors of central nervous system injuries that accumulate LDs in response to neuronal stress to protect neurons from damages associated with lipid peroxidation. We found that Split-ends (Spen), an RNA binding protein previously identified as a glial pro-survival factor during development, maintains LD homeostasis in adult glial cell. In addition, expression of *Spen* was associated with resistance to paraquat-induced neurotoxicity, a pesticide associated with increased risk of PD in human epidemiologic studies. These results suggest that Spen-mediated lipid metabolism functions are important for neuroprotection in PD.

Collectively the results of my thesis provide new evidences for the formation of LDs in both neurons and glial cells and their contribution in the progression of PD pathology.

RESUMÉ DE LA THÈSE

Les maladies neurodégénératives sont l'une des principales causes d'invalidité dans le monde. Certaines de ces maladies, telle que la maladie de Parkinson, sont associées à des dérégulations cérébrales du métabolisme lipidique. En particulier, il a été montré par plusieurs laboratoires dont le nôtre, que l'accumulation d'acide gras sous forme de gouttelettes lipidiques (GLs) dans les cellules gliales est un mécanisme de réponse au stress oxydatif conservé au cours de l'évolution. Des études récentes suggèrent que la formation de GLs dans les neurones pourrait également participer au processus neurodégénératif. Les contributions respectives des cellules gliales et des neurones restent cependant peu étudiées. Au cours de ma thèse, je me suis intéressé aux mécanismes et conséquences pathologiques de l'accumulation de GLs dans les neurones et les cellules gliales.

La maladie de Parkinson est caractérisée par l'accumulation d'alpha-synuclein (aSyn) qui forme des agrégats appelé corps de Lewy dans le cytoplasme des neurones affectés. L'aSyn est une protéine normalement localisée aux synapses, contenant un domaine de liaison aux lipides de type hélice amphipathique, partageant des similarités structurelles avec les protéines se trouvant à la surface des GLs, les périlipines. En effet, l'aSyn peut se lier à la surface de GLs in vitro et l'expression d'aSyn humaine dans la levure induit l'accumulation de GLs. La conservation de ce processus ainsi que sa relevance dans le cadre de la maladie de Parkinson restent cependant à démontrer. Durant ma thèse, j'ai montré que l'expression simultanée de l'aSyn et de périlipines induit l'accumulation de GLs dans les neurones de type photorécepteurs de la rétine de drosophile. J'ai de plus observé qu'une fraction de l'aSyn était localisée à la surface des GLs dans les photorécepteurs de drosophiles ainsi que dans les neuroblastes humains en culture. Mes résultats suggérent que l'association de l'aSyn et des périlipines à la surface de GLs instables, pourrait les stabiliser et ainsi favoriser leur accumulation. Enfin, la présence de GLs dans les photorécepteurs est associée à une plus grande résistance de l'aSyn à la digestion par la protéinase K, suggérant que les GLs seraient impliquées dans le processus de conversion pathologique de l'aSyn vers des formes agrégées.

Les cellules gliales sont les gardiennes de l'intégrité du système nerveux central. En cas de dommages des neurones ou de stress, les cellules gliales accumulent des GLs afin de protéger les neurones de dommages liés à la peroxydation lipidique. Nous avons montré que Split-ends (Spen), une protéine ayant précédemment été identifiée comme facteur de survie des cellules gliales au cours du développement, est impliquée dans le maintien de l'homéostasie des GLs dans les cellules gliales de drosophile adulte. De plus, l'expression de *spen* est associée avec la résistance des mouches au traitement neurotoxique par le Paraquat, un pesticide reconnu comme facteur de risque pour la maladie de Parkinson chez l'homme. Ces résultats suggèrent que les fonctions de Spen dans le maintien de l'homéostasie lipidique dans les cellules gliales sont protectrice contre le stress oxydatif

induit par le paraquat.

Collectivement, les résultats obtenus au cours de ma thèse montrent que le maintien de l'homéostasie des GLs à la fois dans les cellules gliales mais également dans les neurones est important dans les processus pathologiques associés à la maladie de Parkinson.

ACKNOWLEDGMENTS

First of all, I would like to thank the members of the jury for accepting to read and evaluate my PhD thesis.

I am extremely grateful to my two supervisors, Nathalie Davoust and Bertrand Mollereau, for giving me the opportunity to work on this project. During four years, I beneficiated greatly from their knowledge, guidance, excellent advices, and above all else their unwavering support for my ideas and help in executing them. I would also like to thank them for the critical reading of my thesis manuscript.

I also wish to thank Daan van den Brink for many stimulating scientific discussions, fly advices, and support. I would like to extend my gratitude to Florence Jollivet and Gilles Chatelain for their technical expertise with mammalian cell culture, and electronic microscopy respectively. I would also like to thank the other present and past members of the Mollereau team with whom I had the opportunity to interact.

I am grateful to the Fondation pour la Recherche Médicale (FRM) that granted me the financial support indispensable to conduct my fourth year of PhD.

Special thanks to Jean-Noel Arsac who was instrumental in the detection alpha-synuclein by western blot and David Cluet who helped me greatly with the programming of ImageJ quantification macros.

I would also like to acknowledge the assistance of the members of the PLATIM imaging center, and the Arthro-tool facility.

I would like to thank the fly community for valuable advices, and the sharing of transgenic fly lines used in this study.

Finally, I would like to thank my sister, Pauline, for her unconditional support.

TABLE OF CONTENT

FIGURE INDEX

GENE NOMENCLATURE

Fatp: *Drosophila* gene
Fatp: *Drosophila* protein
FATP: Human gene
FATP: Human protein

ABBREVIATIONS

AD	Alzheimer's Disease
ACC	Acetyl-CoA Caxboxylase
AMPA	α-amino-3-hydroxy-5-methyl-4 isoxazolepropionic acid
aSyn	alpha-synuclein
BBB	Blood Brain Barrier
CCT1	CTP: Phosphocholine Cytidylyltransferase 1
CPT2	Carnitine Palmitoyltransferase 2
CS	Citrate Synthase
CSF	Cerebrospinal fluid
DGAT	Diacylglycerol-acyltransferase
EAAT1	excitatory amino acid transporter 1
EPT1	Ethanolaminephosphotransferase 1
FA	Fatty acid
FABP7	Fatty acid Binding Protein 7
FATP	Fatty acid transfer protein
GPAT	Glycerol-3-Phosphate Acyltransferase
HD	Huntington's Disease
HSP	Hereditary Spastic Paraplegia
LD	Lipid droplet
MARCKS	myristoylated alanine-rich protein kinase C substrate
MCT	monocarboxylate transporter
mdy	midway (*Drosophila* DGAT1 homolog)
PAP	Phosphatidic Acid Phosphatase
PD	Parkinson's Disease

PLD	Phospholipase D
ROS	Reactive Oxygene Species
SCD1	stearoyl CoA desaturase 1
Spen	split-ends
Ldsdh1	Lipid droplet subset dehydrogenase 1
PE	Phosphatidylethanolamine
PC	Phosphatidylcholine
SE	Sterol-ester
LPCAT	Lysophosphatidylcholine Acyltransferases
ER	Endoplasmic Reticulum
FIT	Fat Inducing Transmembrane protein
BSCL2	Berardinelli-Seip Congenital Lipodystrophy 2
CIDE	cell death-inducing DFFA-like effector
COPI	Coat Protein complex I
LC3	microtubule-associated protein 1 light chain
PUFA	polyunsaturated fatty acid
CGI-58	Comparative gene identification-58
PKA	Protein Kinase A

INTRODUCTION

Neurodegenerative disorders, such as Alzheimer's (AD) and Parkinson's disease (PD), are the leading cause of disability worldwide (Kyu et al., 2018). It raises an increasing concern as the world population is growing, and life expectancy is extending. Age is the most important risk factor for AD and PD. By 2040, 12 to 17 million people worldwide are expected to live with PD (Dorsey et al., 2018). At this point in time, no curative treatment exists for PD and patients rely only on the treatment of their symptoms. As the number of PD patients increases, PD represents an increasing societal and economic burden for society. Understanding the underlying pathological mechanisms behind these neurodegenerative diseases is an essential step toward the development of new therapies. Accumulating evidences, in animal and cellular models of neurodegenerative disorders, point to a dysregulation of lipid metabolism as an important contributing factor to neuronal survival. In particular, accumulation of lipid storage organelles called lipid droplets (LDs) have been observed in a large variety of neurodegenerative disorders models. Indeed, while neurons are rarely loaded with LDs in healthy animals, mutations in genes involved in LD metabolism have been identified in neurodegenerative disorders. Interestingly, the accumulation of LDs in glia is a conserved mechanism of the stress response both in mammals and insects, that could participate to neuroprotection as well. Previously underestimated in the brain, LD formation represents an exciting new area of investigation in the field of neurodegeneration. During my thesis, I investigated the mechanisms of LD formation in both neurons and glia and their contribution to PD hallmarks using *Drosophila* central nervous system as a model. In my thesis introduction, I will first overview the literature on LD biogenesis and functions, then I will specifically present the current knowledge about LD homeostasis in the brain in health and diseases, and finally I will focus on the contribution of lipid metabolism dysregulation in PD.

1. LD biology

1.1. Generalities about LDs: from inert fat particles to stand alone organelle

1.1.1. An evolutionary conserved organelle of fat storage

The first observation of LDs could be attributed to the Dutch scientist Antonie van Leeuwenhoek that observed “fat particles” with a microscope in sheep adipose tissue in 1723 (Leeuwenhoek and Chamberlayne, 1723). For a long time, LDs were considered inert fat deposits restricted to adipose tissue, but it is now clear that LDs are found in most animal tissues and are dynamic regulators of the stress response.

LDs are constituted of a neutral lipid core, insoluble in water, enclosed in a phospholipid monolayer associated with LD-binding proteins. The neutral lipid core contains esterified fatty acids (FA), mostly triacylglycerols (TAGs) and sterol esters (SE) surrounded by a mix of amphiphilic phospholipids such as phosphatidylcholine (PC) and phosphatidylethanolamine (PE). LDs are found in most living organisms including fungi, plants, animals and some types of bacteria and archaea suggesting that storage of fat in cytoplasmic droplet is an evolutionary ancient mechanism (Chapman et al., 2019; Murphy, 2012).

The observation of LDs can be challenging in tissue-sections, as lipids contained in LDs can be washed away by regular staining protocols and thus sample preparation must be adapted to lipophilic dyes. The most common lipid dyes, which can be used to detect LDs in cell culture, whole-mount, and, frozen tissue-sections include fluorescent dyes such as Nile Red or Bodipy, and non-fluorescent pigment such as Oil Red O (Daemen et al., 2016). LDs can also be identified using electronic microscopy, which allows the identification of homogenous electron-transparent round structure, surrounded by an electron-dense phospholipid monolayer. The absence of a double membrane allows the distinction of LDs from other double membrane vesicles of similar same size (Daemen et al., 2016).

In healthy mammals, LDs accumulate in large quantity in organs dedicated to lipid absorption and storage such as the intestine, white and brown adipose tissue (WAT and BAT respectively) and the liver. LDs are also visible in organs that consume lipids as substrate to produce energy such as skeletal muscles and heart. Finally, LDs accumulate as well in cells that use lipids as precursors for the synthesis of other molecules, such adrenal cortex gland cells producing steroid hormone and immune cells producing eicosanoids (Welte and Gould, 2017). In contrast to the above-mentioned structures, the healthy mammalian brain is not particularly known for LD accumulation. While LDs are rare in some tissues in healthy conditions, stress, and pathologies can induce LDs in virtually all cell types.

In comparison with mammals, healthy *Drosophila,* accumulate LDs at all stages of development from embryos, larvae, and adults, in the fat body, a large structure analogous to mammalian adipose tissue (Figure 1) (Kühnlein, 2012). Indeed, larvae spend their

time eating and accumulating lipids in structure called fat bodies, which are analogous to mammalian adipose tissue. Fat bodies have been extensively used to study LD properties in *Drosophila* (Kühnlein, 2011). Lipids will provide the energy and building blocks necessary for membrane synthesis and the transformation of larval tissues and organs into the future adult fly. Indeed, larvae accumulate LDs in structures called imaginal discs, which contain highly dividing cells that will give rise to the adult legs, wings, eyes and antennae (Fauny et al., 2005; Kühnlein, 2012). In addition, the larvae developing nervous system also accumulate LDs in a subset of glial cells, which are in closed proximity with neuronal progenitors (Bailey et al., 2015; Kis et al., 2015).

As the larvae reach a critical weight, hormonal signaling mediated by ecdysone triggers pupation and metamorphosis, a process during which larval organs are transformed to give rise to the adult organs (Ohhara et al., 2017). In adult flies, LDs are mainly found in adult fat body located in the fly abdomen and head (Arrese and Soulages, 2010; Hwangbo et al., 2004). The fat body acts as a lipid storage organ and releases lipids in the form

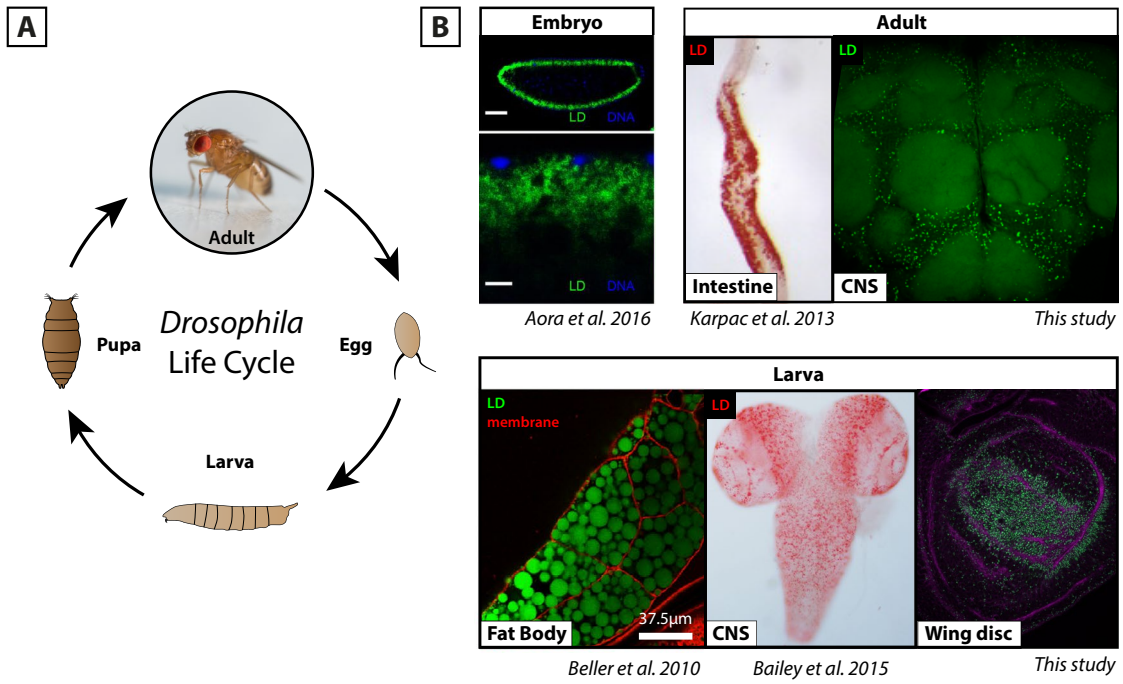

Figure 1. LD accumulate in *Drosophila* tissues at all stages of development

(A) Schematic view of *Drosophila* life cycle. Briefly eggs hatch about one day after egg-laying. The emerging larvae then go through three stages of growth also known as instar. When reaching a critical weight, larvae enter the pupal stage, during which metamorphosis occurs. Finally, the adult emerges from the pupal case. (B) Example of LD accumulation in *Drosophila* tissues during development and adulthood. In embryos, LDs accumulate in the periphery (image from Aora et al. 2016). In larvae, LDs are found mostly in fat body, but also in the central nervous system (CNS, image from Bailey et al. 2015) and in imaginal discs. In adult, LDs accumulate in fat body (not represented here) and other tissues including the intestine (image from Karpac et al. 2013) and the CNS.

of lipoproteins into the circulating hemolymph, the fly equivalent of mammalian blood (Palm et al., 2012). LDs are also found in the gut and in oenocytes, a group of cells with liver-like functions located in the fly abdomen (Gutierrez et al., 2007).

In both healthy mammals and *Drosophila*, LDs accumulate mainly in organs dedicated to lipid storage. Meanwhile, during aging, and pathologies that impair lipid homeostasis such as obesity, lipodystrophies, diabetes, and neurodegeneration, abnormal LDs can accumulate in non-adipose tissue like the brain, and have critical impact on organ functions.

1.1.2. The biogenesis of LDs

In eukaryotes, LD formation takes place at the endoplasmic reticulum (ER) membrane where enzymes of the glycerolipid synthesis pathway first synthesize TAGs by successive addition of three FA to a glycerol backbone (Figure 2).

This process first requires the activation of FA by addition of a Co-Enzyme A (CoA) mediated by FA-CoA synthase such as the FA transport protein (FATP)(Dourlen et al., 2015). The first FA-CoA is then transferred to a glycerol-3-P molecule by Glycerol-3-Phosphate Acyltransferase (GPAT) resulting in the synthesis of lysophosphatidic acid (LPA). Addition of a second FA to LPA, by an Acyl-glycerol-3-phosphate Acyl-transferase (AGPAT), gives rise phosphatidic acid (PA). PA is then converted to DAG by a PA Phosphatase (PAP). The final step is the addition of a third FA onto a DAG molecule by Diacylglycerol-O-acyl transferase (DGAT) to form TAG (Xu et al., 2012).

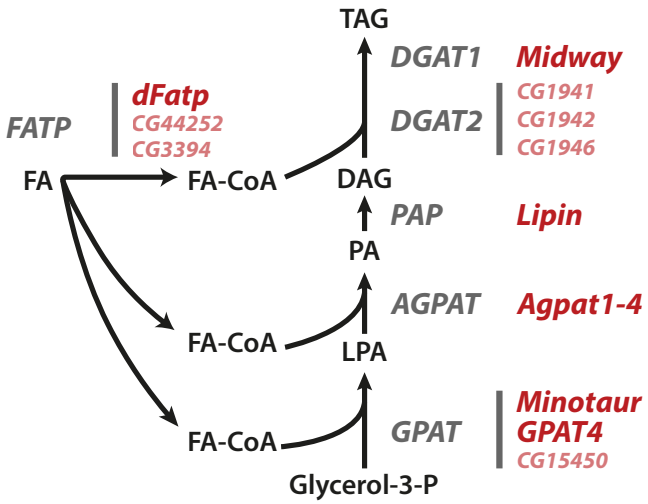

Figure 2. The TAG synthesis pathway and its conservation in Drosophila

Schematic representation of the TAG synthesis pathway. Enzymes are well conserved between human (black) and *Drosophila* (red, or pink if not experimentally confirmed). FA, fatty acid; FATP, fatty acid transport protein; GPAT, glycerol-3-phosphate acyltransferase; LPA, lysophophatidic acid; AGPAT, 1-acylglycerol-3-phosphate O-acyltransferase; PA, phosphatidic acid; PAP, phosphatidic acid phosphatase; DAG, diacylglycerol; DGAT, diacylglycerol O-acyltransferase; TAG, triacylglycerol.

Newly synthesized TAGs are concentrated within the ER phospholipids bilayer to form a lens. This lens then progressively expands with the intervention of ER-resident proteins, such as Seipin (encoded by BSCL2 in humans) and Fat Inducing Transmembrane proteins 2 (FIT2). Finally, the emerging LD buds off from the ER to become an independent organelle (Figure 3).

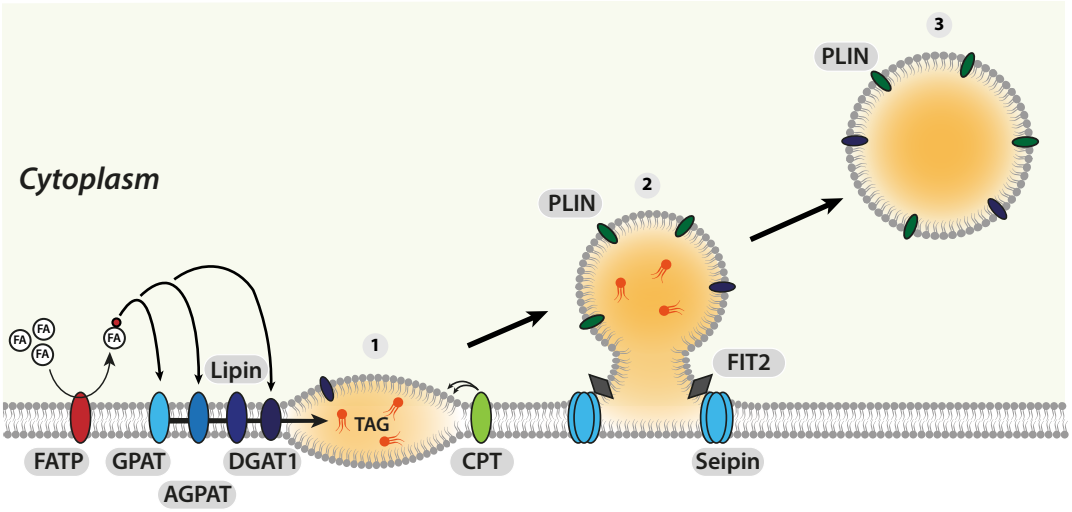

Figure 3. The steps of LD biogenesis

Schematic representation of the three main steps of LD formation at the ER. (1) ER resident enzymes synthetize TAGs that accumulate within the ER bilayer to form a lens. (2) The lens is progressively growing by simultaneous addition of TAGs and phospholipids. This step requires also Seipin and FIT2 proteins that stabilize the forming LD (3) the LD buds off into the cytosol.

Seipin proteins form mobile foci in the ER membrane, that recognize growing lens and facilitate the maturation of future LDs (Wang et al., 2016). The lack of Seipin, destabilizes LD formation and leads to the accumulation of small nascent LDs and abnormally large ones (Fei et al., 2011; Tian et al., 2011; Wang et al., 2016). Deficiency in Seipin is associated with a severe form of congenital generalized lipodystrophy called Berardinelli-Seip syndrome, characterized by a nearly complete loss of adipose tissue (Agarwal et al., 2003). In *Drosophila*, mutation of *Seipin* leads to a severe reduction of fat body as well and to the formation of ectopic LDs in salivary glands (Tian et al., 2011). Seipin interacts with LD assembly protein-1 (LDAF1) to form a complex that associates with forming lenses to stabilize the formation of LDs (Chung et al., 2019). Finally is has been reported that Seipin could facilitate the recruitment of a LD formation complex containing proteins such as TAG synthase, *Lro1* in yeast, or GPAT in mammalian adipocytes, at the site of LD formation

(Choudhary et al., 2020; Pagac et al., 2016).

As mentioned earlier, the final step of LD biogenesis is the budding of the new LDs from the ER into the cytosol. Control of the budding direction is in part regulated by the asymmetry in phospholipid and protein composition of the ER phospholipid monolayer surrounding the lens. A decrease in surface tension of the ER cytosolic face, favors the LD budding into the cytosol (Ben M'barek et al., 2017; Chorlay and Thiam, 2018). The budding of the newly formed LDs into the cytosol is also facilitated by proteins such as Fat storage-inducing transmembrane proteins 1-2 (FIT1 and 2) that normally reside at the ER membrane and accumulate at LD biogenesis sites (Choudhary et al., 2015; Henne et al., 2018). In absence of FIT2, LDs remain trapped inside the ER membrane (Choudhary et al., 2015). While FIT2 could bind TAG, its exact function in LD biogenesis remains unclear.

The molecular actors of LD formation including TAG synthesis enzymes and Seipin are well conserved in insects (Heier and Kühnlein, 2018). Indeed, the *Drosophila* genome contains three genes encoding GPATs, four genes encoding AGPATs, (Agpat1-4) one gene encoding PAP (*Lipin*), one gene encoding DGAT1 (*Midway*), and three uncharacterized genes encoding putative DGAT2 (*CG1941*, *CG1942/Dgat2*, and *CG1946*) (Heier and Kühnlein, 2018). *Drosophila* carries also three homologs of FATP (*dFatp*, *CG44252* and *CG3394*) (see Figure 2) (Dourlen et al., 2015). With its versatile genetics, *Drosophila* provides a very powerful model to study LD biology *in vivo*. For example, LD deposition in the retina is dependent on *dFatp* expression. The knockdown of *dFatp* prevents LD accumulation, while *dFatp* overexpression increases lipid storage in *Drosophila* retina glial cells (Van Den Brink et al., 2018).

As the newly formed LD emerges and becomes an independent organelle, it takes away a fraction of the ER outer phospholipid-layer, as well as several proteins normally residing in the ER membrane. The LD surface is associated with various LD-binding proteins: ER-proteins captured by the LD when budding from the ER outer membrane (Class I) and specific cytosolic proteins targeting the LD phospholipid monolayer directly (Class 2). Collectively, these LD-binding proteins form the LD proteome, which contributes to the maintenance and dynamic turnover of LDs.

1.2. A functional overview of the LD proteome

1.2.1. Establishing the LD proteome

Proteomic analysis of LDs isolated from yeast, plants, insects and mammals revealed that LDs contain a common subset of conserved proteins involved in lipid metabolism that maintains LD structure, expansion, and degradation (Beller et al., 2006; Bersuker et al., 2018; Cermelli et al., 2006; Currie et al., 2014; Hamada et al., 2020; Krahmer et al., 2013; Pyc et al., 2017). LDs can also carry proteins involved in non-metabolic functions such as inter-organelles contacts and protein degradation. For example, proteomic analysis of

LDs isolated from *Drosophila* third-instar larvae fat body, revealed a list of more than 130 proteins including lipid metabolism enzymes such as lipases, but also small GTPase of the Rab protein family and protein chaperones (Figure 4) (Beller et al., 2006). Unexpectedly, LDs isolated from *Drosophila* embryos can even carry histones (Cermelli et al., 2006). These histones carried by LDs are involved in a defense mechanism against intracellular

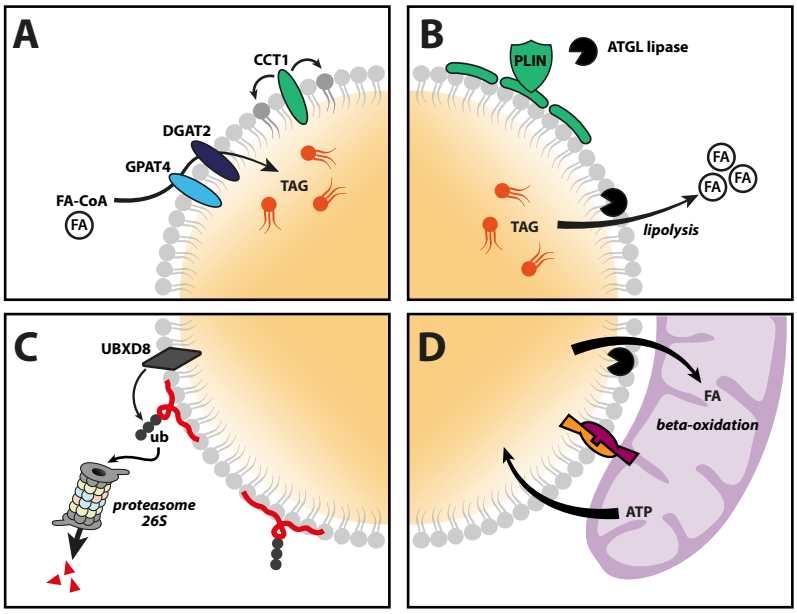

Figure 4. The functions of LD-binding proteins

Schematic representation of four examples of LD-binding protein functions. (A). Enzymes of the TAG and phospholipid synthesis pathways are targeted to the LD surface and promote LD growth (B). Perilipins are the most abundant proteins at the surface of LDs and act as shield against cytosolic lipases such as ATGL. (C). LD-protein abundance is regulated by the Ubiquitin Proteasome System (UPS) including the ubiquitin ligase UBDX8 that signals proteins for degradation. (D). LDs interact with other organelles such as mitochondria through protein tethering complex. The proximity of LD and mitochondria promote FA degradation by beta-oxidation.

bacteria (Anand et al., 2012).

Proteins interact with LDs mainly through two types of domain: hydrophobic domains hairpin (Class I) or amphipathic helices (Class II) (Bersuker and Olzmann, 2017). LD-binding proteins of Class I, include proteins first localized at the ER membrane that relocate to the nascent LDs, such as GPAT4, DGAT2. In contrast, LD-binding proteins of Class II are cytosolic proteins containing amphipathic helices, a protein secondary structure that segregates hydrophobic residues and polar residues on two opposite face of the helix, which allows specific interaction with the LD monolayer. For example, Class II proteins include CTP: Phosphocholine Cytidylyltransferase 1 (CCT1) and perilipins (Dhiman et al., 2020). Perilipins are the most abundant LD-binding proteins. Perilipins act as a scaffold that maintains LD integrity and protects LDs from cytosolic lipases (treated in a separated

chapter). The class II also includes proteins that interact indirectly with LDs using lipid anchors or protein-protein interaction (Dhiman et al., 2020).

The protein content of LDs depends on the LD intrinsic properties such size, lipid composition and phospholipid packing but also the nature and abundance of proteins at the LD surface. Indeed, LD-binding proteins and phospholipids can act as surfactant and decrease LD surface tension (Figure 5). For instance, the packing of phospholipids on the LD, decreases the LD surface tension and limits the binding of proteins (Thiam et al., 2013a). Coat Protein complex I (COPI) act as a tension clamp that increases surface tension by reducing the phospholipids packing at the surface of LDs (Thiam et al., 2013a). In mammalian cells, the LD phospholipid monolayer contains more PC than PE, while in *Drosophila,* LDs contain more PE and less PC (Krahmer et al., 2011). The nature of the neutral lipids stored in the core of the droplet, sterol-esters or TAGs, also impacts the LD proteome (Chorlay and Thiam, 2020). Moreover, LD-binding proteins have different affinity for the LD surface and competition/crowding can decrease binding of weakly bound-proteins (Kory et al., 2015). Collectively these factors can impact the LD proteome within a same cell and contribute to LD heterogeneity.

In the following sections, I will discuss the most common LD-binding proteins and their functions in the regulation of LD growth and degradation, LD interaction with other organelles, and the degradation of LD-associated proteins.

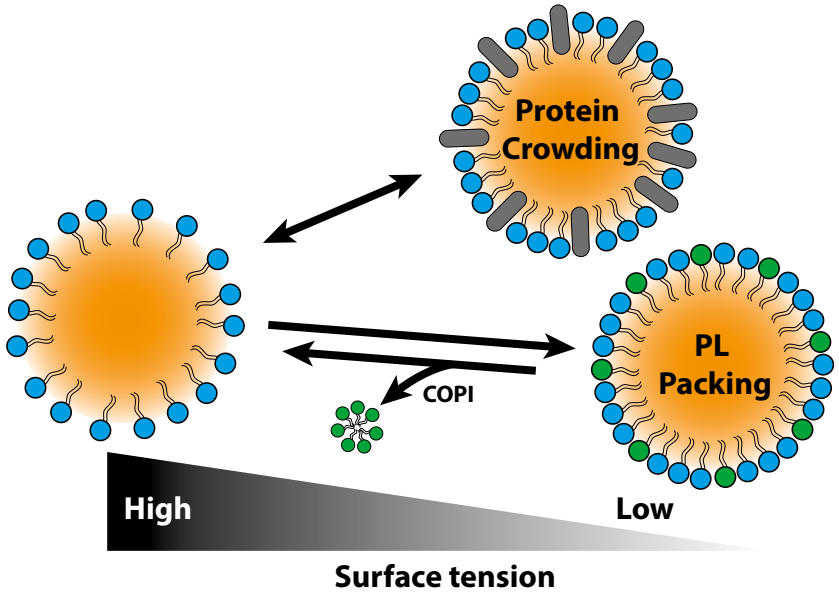

Figure 5. LD surface tension

The LD surface tension is regulated by phospholipid (PL) packing and protein abundance. A low surface tension allows LD-binding proteins to interact with LD surface. COPI, can promote the formation of nano-droplets, which decreases the phospholipid packing, and thus increases the LD surface tension, a state that favors the recruitment of LD-protein.

1.2.2. Local synthesis and LD fusion mediate LD growth

The growth of cytoplasmic LDs depends on the rate of neutral lipid accumulation and degradation. LD-binding proteins regulate two main mechanisms that are required for the growth of existing LDs: local lipid synthesis and LD fusion (Figure 6). Neutral lipids and phospholipids that are required for LD growth can be synthesized locally at the surface of LDs. The LD proteome reveals a number of proteins involved in TAG and phospholipid synthesis. For example, GPAT4, AGPAT3 and DGAT2 are isoforms of TAG synthesis enzymes found on the surface LDs (Wilfling et al., 2013). For continuous growth of the LD, the phospholipid monolayer must be extended as well, and enzymes that synthetize PC such as CCT1, and Lysophosphatidylcholine Acyltransferases 1 and 2 (LPCAT), are found on the LD surface (Krahmer et al., 2011; Moessinger et al., 2011). The lack of PC, in conditions such as knockdown of CCT1, increases LD surface tension and promotes LD coalescence and fusion (Krahmer et al., 2011; Thiam and Beller, 2017).

The cell death-inducing DFFA-like effector (CIDE) protein family includes CIDEA, CIDEB and CIDEC/Fsp27 promotes FA transfer from one LD to another. They are found on the LD surface and, CIDEA and CIDEC, accumulate at contact sites between adjacent LDs (Gong

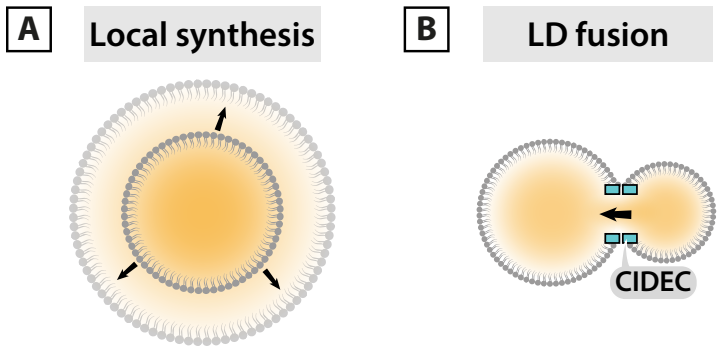

Figure 6. Mechanisms of LD growth

Two main mechanisms promote LD growth: local lipid synthesis and LD fusion. (A) Local lipid synthesis is mediated by a set of TAG synthesis enzymes localized at the surface of a subset of LDs (B) CIDE protein family such as CIDEC promote lipid transfer between LD in contact.

et al., 2011). Loss of CIDEC in mice adipocytes induces a phenotype with numerous small LDs in contrast with wild type adipocytes that contain a unique giant LD (Nishino et al., 2008).

1.2.3. The breakdown of LDs by lipolysis and lipophagy

Lipids can be remobilized from LDs by two main mechanisms: lipolysis mediated by cytosolic lipases and lipophagy (Zechner et al., 2012). The first mechanism involves cytoplasmic lipases, such as Adipose Triglyceride Lipase (ATGL/PNPLA2) and Hormone-

sensitive lipase (HSL), that bind the LD surface and insure hydrolysis of TAG and lipid remobilization (Lass et al., 2011; Sztalryd et al., 2003). TAG lipolysis is a sequential process initiated by ATGL that first hydrolyzes TAGs into DAGs, which are then hydrolyzed by HSL and finally Monoacylglycerol lipase (MAGL) that completes the remobilization of the esterified FAs (Figure 7). In mammalian and insect adipocytes, lipolysis is stimulated by hormonal signaling. The genome of *Drosophila* contains homologues of ATGL and HSL, known as Brummer (Bmm) and dHSL respectively (Grönke et al., 2005). Other putative intracellular lipases have been identified such as DDHD2 in mammals and its homolog PAPLA1 in *Drosophila* (Gáliková et al., 2017). PAPLA1 is a phospholipase A1 which primarily hydrolyzes phospholipids but could degrade TAGs as well in *Manduca sexta* (Arrese et al., 2006).

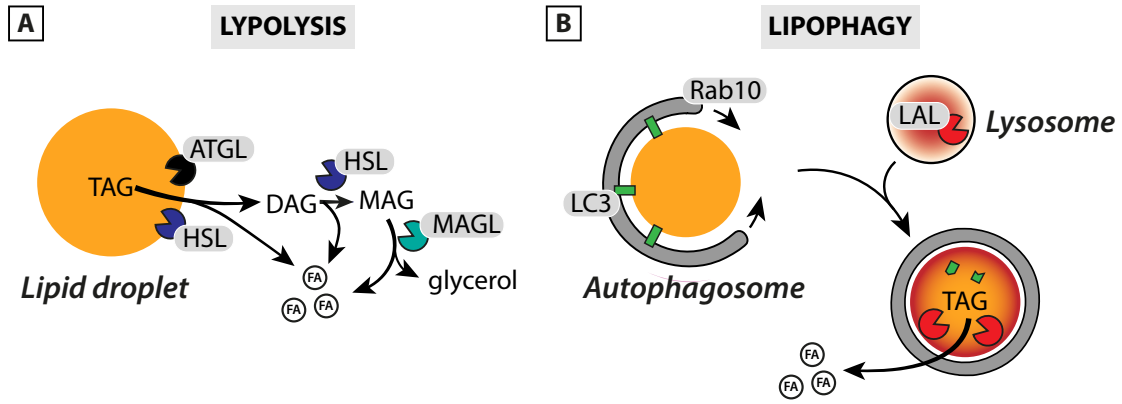

Figure 7. Mechanisms of LD degradation

LDs can be degraded by two main mechanisms. (A) Cytosolic lipases, such as ATGL and HSL, associate with LDs and promote TAG hydrolysis which generates FA and DAG. DAG can be further cleaved by HSL, and MAGL to liberate two more FA. (B) LDs can also be degraded by autophagy. LDs are recognized and engulfed by autophagosome, which then fuse to lysosomes. Lysosomes contain lysosomal acid lipases (LAL) that degrade the content of LDs.

LDs can also be degraded by a type of macro-autophagy called lipophagy. Entire LDs can be engulfed in autophagy vacuoles, which then fuse with lysosomes (Figure 7). Singh et al., demonstrated that LDs co-localize with the autophagosome reporter protein, microtubule-associated protein 1 light chain 3 (LC3) and lysosomal protein LAMP1, in hepatocytes (Singh et al., 2009). Lysosomes contain lysosomal acid lipases (LALs) that degrade neutral lipids at acidic pH. Lipophagy is particularly important in the liver, as autophagy deficient Atg7 knockout mice accumulate abnormal lipid levels in hepatocytes (Singh et al., 2009).

1.2.4. Regulation LD-protein abundance by the ubiquitin/proteasome system

Protein degradation is essential to maintain the composition of the LD proteome. Unnecessary or damaged proteins carrying ubiquitination sites are targeted to the proteasome for degradation. The protein composition of LDs is regulated by the ubiquitin-proteasome system (UPS). For example, the LD proteome contains proteins associated with the ER-associated Degradation (ERAD), such as UBX-domain containing protein 8 (UBXD8), Ancient Ubiquitous Protein 1 (AUP1) and VCP AAA ATPase (Bersuker et al., 2018). ATGL, DGAT2 and CIDEC are among the LD-proteins that can be degraded by the proteasome.

Additional evidence of LD-protein degradation by the UPS are found in plants. Indeed, a subset of LDs is associated with UBX family protein called the Plant UBX Domain-Containing Protein 10 (PUX10) in *Arabidopsis thaliana* seeds and tobacco pollen tubes (Deruyffelaere et al., 2018; Kretzschmar et al., 2018). PUX10 acts as an adaptor protein that recruits the AAA ATPase Cell Division Cycle 48 (CDC48A) at the LD surface (Deruyffelaere et al., 2018). CDC48A then extracts ubiquitinated proteins such as oleosins from the surface of LD for degradation by the proteasome (Deruyffelaere et al., 2018). Loss of PUX10, leads to accumulation of large LDs indicating that the UPS regulation of LD-protein abundance is required to maintain LD homeostasis (Kretzschmar et al., 2018).

1.2.5. Keeping in touch: the LD social network

LDs establish extensive contacts with most organelles including the ER, peroxisomes, mitochondria, the Golgi and lysosomes (Schuldiner and Bohnert, 2017; Valm et al., 2017). Valm et al. used multispectral time-lapse microscopy to investigate LD-organelle contacts in COS7 cells and found that the majority of LDs were in association with the ER (85%), mitochondria (25%) and finally peroxisomes and lysosomes (10%)(Valm et al., 2017). To establish contacts with other organelles, LDs require tether proteins, which interact with the target organelle itself or through a protein complex. Although some of these tether proteins have been identified for LDs in contacts with the ER and mitochondria, the mechanisms regulating LD-organelle contacts remain to be elucidated for the most part (Olzmannand Carvalho, 2019; Thiam and Dugail, 2019).

Maintaining contact between LDs and the ER is essential for nascent LDs. In yeast, Mdm1, is a tether protein that maintains ER-LD contacts and recruits enzymes such as ACSL3 homolog. Hariri et al., found that relocating Mdm1 artificially to the contact area between plasma membrane and ER is sufficient to change the localization of LD biogenesis in yeast (Hariri et al., 2019). Interestingly, the mammalian homolog of *Mdm1*, Sortin nexin protein 14 (*Snx14*) is also associated with LD-ER contacts (Datta et al., 2019). Loss of Snx14 leads to a phenotype reminiscent of Seipin mutant, with an heterogenous LD size. Snx14 could also be part of a LD-formation complex as it recruits the FA activation enzyme ACSL3 for

ER microdomain of LD formation (Datta et al., 2019; Kassan et al., 2013).

LDs are not static organelles and their association with microtubules is important for proper LD positioning and trafficking to other organelles. Several proteins in the LD proteome are associated with transport along microtubules. For example, in *Drosophila* embryos, the protein Klarschist, has been found to participate to LD mobility by interacting with LDs and kinesin molecular motors (Welte et al., 1998; Yu et al., 2011).

LDs physically associate with organelles that use FA as energy source, such as mitochondria and peroxisomes. This interaction promotes the efficient transfer of FA for use in ß-oxidation and prevents lipotoxicity associated with excessive FA leakage in cytoplasm. LDs associate with mitochondria in muscles, and brown adipocytes (Benador et al., 2018; Rambold et al., 2015). Proteins that are involved in the interaction between mitochondria and LDs include Plin5, a member of the Perilipin family (Wang et al., 2011a). Alternatively, LD-mitochondria association can promote LD expansion by providing ATP for TAG synthesis (Benador et al., 2018, 2019). Spastin has been shown to promote the association of LDs with peroxisomes (Chang et al., 2019).

The fact that the proteome of LDs can vary between different tissues strengthens the importance of studying tissue specific LD-binding proteins. One interesting candidate protein family are the perilipins.

1.3. Perilipins, guardians of LD integrity

1.3.1. Discovery and structure of mammalian perilipins

Perilipins are a family of LD-binding proteins that maintain LD integrity and promote lipid storage (Kimmel and Sztalryd, 2016). The founding member of the Perilipin protein family is PLIN1 (previously known as perilipin A), and was initially found by Londos et al. among the fraction of phosphorylated proteins in adipocytes (Greenberg et al., 1991). Immunostaining revealed that PLIN1 is visible around LDs as a hollow ring in cultured adipocytes. Four additional genes encoding related LD-binding proteins were then successively discovered in mammals: PLIN2 (also known as *a*dipose *d*ifferentiation-*r*elated *p*rotein [ADRP]), PLIN3 (also known as *t*ail-*i*nteracting *p*rotein of 47 kDa [TIP47]), PLIN4 (also known as S3-12) and PLIN5 (also known as MLDP, LSDP5 or OXPAT) (Dalen et al., 2007; Londos et al., 1999; Wolins et al., 2003). Perilipins are characterized by two N-terminal domains: a PAT domain, named after the three founding members of the family (perilipinA, ADRP, Tip47), and a domain encoding an amphipathic helix, which allows the binding to the LD surface (Kimmel et al., 2010). Perilipin amphipathic helices are constituted of a repeated patch of 11 amino acids (11-mer) containing hydrophobic and hydrophilic amino acids that segregate to opposite faces, as the helix folds. Unfolded in the cytosol, perilipins adopt an alpha helical conformation upon LD-binding at the interphase between aqueous cytosol and hydrophobic LD core (Rowe et al., 2016). Lipid

packing defects also promote the binding of perilipins at the surface of LDs. The length and hydrophobicity of the amphipathic helix as well, as well as the C-terminus domain control the affinity of perilipins for LDs (Ajjaji et al., 2019).

1.3.2. Perilipins: an evolutionary conserved family of LD-binding proteins

Functional perilipin proteins have been found in most eukaryotes examined so far including *Dictyostellium,* yeasts, *Drosophila, Caenorhabditis elegans* (*C. elegans*) and vertebrates, which suggest evolutionary conserved functions (Chughtai et al., 2015; Gao et al., 2017; Miura et al., 2002). As mentioned above, the Human genome contains 5 genes encoding perilipins: PLIN1-5. In contrast, *Drosophila* genome contains 2 genes coding PAT domain proteins, called *dPlin1* and *dPlin2* (also known as *Lsd-1* and *Lsd-2*) (Miura et al., 2002). *Drosophila* perilipins, like their mammalian counterparts are found on the LD surface and share similar functions in the regulation of LD structure and turnover (Beller et al., 2010; Bi et al., 2012; Grönke et al., 2003, 2005).

1.3.3. Perilipins tissue specificity

The Human perilipins appear to have different cellular specificity and functions. PLIN1 is mainly restricted to adipocytes. PLIN2 and PLIN3 are found ubiquitously and PLIN5 is found in oxidative tissue (muscle, heart, brown adipose tissue) (Itabe et al., 2017; Yamaguchi et al., 2006). PLIN4 is found in adipocytes, skeletal and heart muscles, and in the brain. Interestingly, the different distribution of perilipins in tissues indicates that perilipins are important for tissue-specific regulation and functions of LDs.

Drosophila perilipins have also a tissue-specific distribution. dPlin1 is mainly restricted to the fat body, while dPlin2 is expressed ubiquitously, at all stages of the fly life cycle: embryos, larvae and adults (Beller et al., 2010).

1.3.4. Perilipins functions at the LD

e. Regulation of basal and stimulated lipolysis

Perilipins are important regulators of basal and stimulated LD lipolysis (Figure 8). Perilipins form a protective coat around LDs that limits the access of cytosolic lipases to the neutral lipid core. In mammalian adipocytes, PLIN1, can prevent ATGL-mediated lipolysis by binding to an ATGL co-activator, named Comparative gene identification-58 (CGI-58, also known as ABDH5) (Brasaemle et al., 2000). Upon lipolytic stimulation, the of PLIN1 by Protein Kinase A (PKA) releases CGI-58 and allows ATGL mediated-lipolysis to proceed (Arrese et al., 2008; Brasaemle et al., 2000). PLIN1 can also promote HSL docking at the LD surface (Wang et al., 2009). PLIN1 knockout mice have a reduced adipose tissue and exhibit a higher rate of basal lipolysis. *plin1-/-* mutant adipocytes have reduced levels of stimulated lipolysis as well (Tansey et al., 2001).

PLIN2 and PLIN3 also regulate basal lipolysis and increase lipid storage when overexpressed in a variety of cell types (Listenberger et al., 2007). PLIN2 and PLIN3 do not appear to bind CGI-58, while PLIN5 contains binding sites for HSL, ATGL and CGI-58. In condition of increased nutrient demand, PLIN2 and PLIN3 are degraded by chaperone-mediated autophagy (CMA), which facilitates ATGL access to LDs and lipolysis in the liver of starved mice (Figure 8) (Kaushik and Cuervo, 2015). Collectively these results indicate that perilipins can limit lipolysis by two main mechanisms: 1) direct binding to lipases or

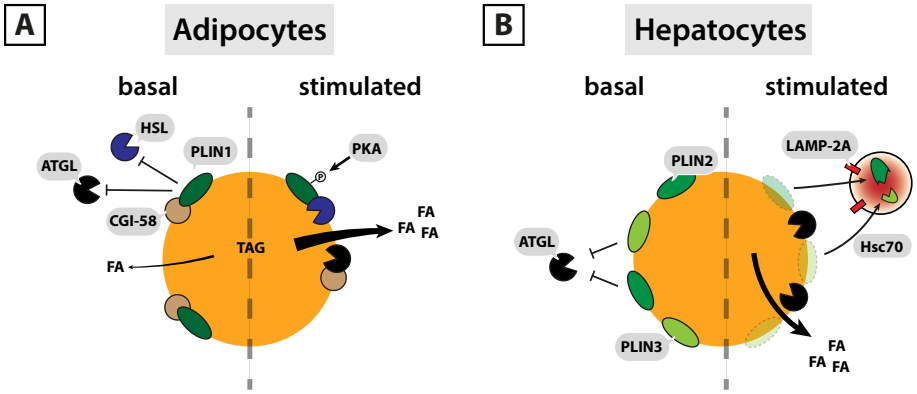

Figure 8. PLIN-mediated regulation of lipolysis

(A) In adipocytes, PLIN1 sequesters CGI-58, a co-activator of ATGL under basal condition. Upon stimulation, PKA phosphorylates PLIN1, which liberates CGI-58, and promotes ATGL-mediated lipolysis. dHSL can also been recruited by phosphorylated PLIN1. (B) In hepatocytes, LDs are covered by PLIN2 and PLIN3, which prevent ATGL binding to LDs and lipolysis. Upon stimulation, PLIN2 and PLIN3 are degraded by chaperone-mediated autophagy (CMA), which promotes ATGL binding to LD and lipolysis. CMA requires the chaperone Hsc70 and LAMP-2A on lysosomes.

lipase co-activators, 2) competition with lipases for binding at the LD-surface.

In *Drosophila*, dPlin1 and dPlin2, regulate lipolysis by mechanisms that share similarities with vertebrate perilipins. dPlin1 and dPlin2 modulate the lipolytic activity of the *Drosophila* ATGL ortholog, Bmm (Bmm) (Beller et al., 2010; Grönke et al., 2005). In addition, dPlin1 was associated with the recruitment of dHSL at the LDs in starved larvae (Bi et al., 2012). Furthermore, the stimulation of adipocytes by adipokinetic hormone (AKH) induces PKA-dependent phosphorylation of dPlin1, and increases lipolysis. Flies lacking both, dPlin1 and dPlin2 are lean but viable and can still mobilize fat upon starvation (Beller et al., 2010). dPlin1 expression levels correlate with body fat levels (Beller et al., 2010). dPlin1 null flies suffer from adult-onset obesity, and have reduced lipolysis (Beller et al., 2010). dPlin1 and dPlin2 are functionally redundant in wing disc (Bi et al., 2012; Fauny et al., 2005; Grönke et al., 2005; Teixeira et al., 2003). dPlin2 levels modulate TAG storage indeed, dPlin2 null mutant flies are lean and contain reduced levels of TAGs while flies overexpressing dPlin2 in fat body contain more TAGs (Grönke et al., 2003).

f. Stabilization of the LD structure

Perilipins are thought to act as scaffold proteins that maintain LD structure and integrity. For example, *Drosophila* fat body lacking dPlin1 contains one large unilocular LD instead of multiple smaller LDs, like in wild-type (Beller et al., 2010). This result indicates that perilipins association with LDs maintains LD morphology. Similarly, depletion of yeast Pet10, a putative gene encoding a PAT domain protein also leads to LD fusion (Gao et al., 2017). Interestingly, the binding of proteins to the LD surface, reduces the LD surface tension, which decreases LD fusion (Thiam et al., 2013b). Along those lines, PLIN4 which contains the largest amphipathic helix is an extreme example. Indeed, PLIN4 can coat LDs that are devoid of phospholipids and substitute for phospholipids by directly binding neutral lipids and stabilizing LDs (Čopič et al., 2018). Collectively, these results show that perilipins are involved in the stabilization of LD structure and the maintenance of LD integrity.

g. Other functions

Perilipins are also involved in the transport of LDs along microtubules: in *Drosophila* embryos dPlin2 interacts with Klarsicht, a regulator of kinesin-1 and dynein molecular motors (Welte et al., 2005).

1.4. LD, a dynamic organelle with multiple functions

LDs are important energy reserves but their content can also be used as precursor for the synthesis of membrane phospholipids or signaling molecules such as steroid hormones or lipid mediators of inflammation such as eicosanoids. In addition to these storage functions, LDs have emerged as important regulators of the cellular stress response (e.g. lipotoxicity,

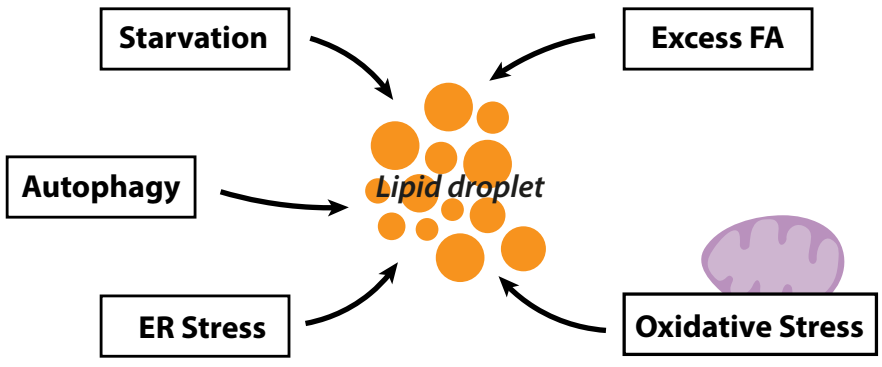

Figure 9. Cellular Stress inducing LDs

oxidative stress, ER stress) (Henne et al., 2018; Welte and Gould, 2017).

1.4.1. Storage of energy and lipid precursors

LDs contain large fat reserves that can be remobilized at any time in response to cellular context and the energy demand of the cell. In starved animals, FA stored in LDs of the adipose tissue are remobilized to provide energy. The lack of nutrients also increases the autophagy flux to produce nutrient from existing organelles, which paradoxically increases LD accumulation in Mouse Embryonic Fibroblasts (MEF) (Rambold et al., 2015). Indeed, in starved MEFs, LDs establish physical contacts with mitochondria to channel FAs resulting from lipolysis directly to the mitochondria for ß-oxidation (Rambold et al., 2015). Before reaching the mitochondria, FAs are modified by addition of carnitine and transported to the mitochondria matrix via Carnitine Palmitoyltransferase I and II (CPTI and CPTII).

LDs can also provide precursors for the synthesis of other lipid-based molecules such as steroid hormones and eicosanoids. In mammals, immune cells such as leukocytes can accumulate LDs, which are remobilized for the synthesis of lipids mediators of inflammation. For example, mast cells, a tissue-resident immune cell involved in the first steps of inflammation, can remobilized arachidonic acid contained in LDs, by ATGL-mediated lipolysis to provide precursor for the synthesis of eicosanoids, mediators of inflammation (Dichlberger et al., 2014).

1.4.2. A protective response against lipotoxicity

The accumulation of cytosolic FA in non-adipose tissues can have deleterious cellular consequences culminating with the dysfunctions of vital organs (Unger et al., 2010). For example, an excess cytosolic FA can disrupt mitochondrial membrane integrity, leading to oxidative stress, generation of toxic bioactive lipids (see 1.4.3), and ER stress (Chitraju et al., 2017; Nguyen et al., 2017). Therefore, the levels of free FAs must be controlled either by consuming or storing FAs inside LDs. The storage of FAs in LDs can be observed for example by treating cultured cells with exogenous FAs, such as oleic acid (OA). If the process of LD formation and TAG synthesis are inhibited, the exogenous lipid treatment becomes cytotoxic in *Dgat1*$^{-/-}$ fibroblasts (Listenberger et al., 2003). It also appears that the nature of FA has an impact on the cell ability to form LDs. For example, the treatment of cells with saturated FA, such as palmitic acid, induces LD formation less efficiently compared to OA, and triggers cellular demise. Interestingly, simultaneous treatment of cells with palmitic acid and OA promotes palmitate incorporation into LDs and reduces cytotoxicity indicating that saturated FA can also be incorporated in LDs but are less efficient at inducing their formation (Listenberger et al., 2003).

The importance of LDs in maintaining cellular FA homeostasis is best observed in condition of high autophagy. In response to starvation, autophagy is activated to break down existing organelle in order to produce metabolic fuel, such as FAs, which is required

to maintain cell viability. Interestingly, LDs accumulate in close proximity with highly-fused mitochondria in starved cells. In this context, LDs could act as intermediary step between the autophagy-dependent release of FA and mitochondrial ß-oxidation (Nguyen et al., 2017; Rambold et al., 2015). Mitochondria are then fueled by ATGL-mediated degradation of LD-stores (Rambold et al., 2015). Starved cells that fail to produce LDs, accumulate acyl-carnitine that cause mitochondria dysfunction (Nguyen et al., 2017). These results indicate that LD functions in lipotoxicity is to: 1) buffer the excessive FA production and 2) provide a safe passage for FA to be degraded without compromising the cell by physical association with mitochondria.

1.4.3. Resistance to oxidative stress

Recent evidences indicate that LDs accumulate in condition of oxidative stress such as hypoxia and mitochondria-associated disorders (Bailey et al., 2015; Liu et al., 2015). Oxidative stress is caused by an imbalance between the production of reactive oxygen species (ROS) by mitochondria and their elimination by antioxidant enzymes. Briefly, ROS are predominantly produced in the form of hydrogen peroxide (H_2O_2), which by reacting with ferrous iron liberates highly reactive hydroxyl radical in the Fenton reaction. These radicals can oxidize most organic molecules including FAs by a process called lipid peroxidation (Gaschler and Stockwell, 2017). In particular, the oxidation of unsaturated FAs results in the non-enzymatic cleavage of the acyl chain and the liberation of short aldehydes, such as 4 hydroxy-nonenal (4-HNE). This reaction results in: 1) the shortening of the acyl chain, which affects the properties of phospholipids and membrane integrity, 2) the generation of highly reactive short aldehydes that can damage nucleic acids and proteins. Short aldehydes, such as 4-HNE, can covalently modify proteins thus interfering with their normal functions and interaction (Hauck and Bernlohr, 2016).

LDs can act as antioxidant by protecting sensitive lipids from oxidative damages. In condition of hypoxia, a known-inducer of ROS, LDs accumulate in glial cells of the *Drosophila* larval nervous system (Bailey et al., 2015). Interestingly, the accumulation of LDs is associated with the relocation of polyunsaturated fatty acids (PUFAs) from membrane phospholipids to TAGs inside LDs. In this context, LDs do not contain oxidized lipids indicating that undamaged PUFAs are relocating in LDs (Bailey et al., 2015). Preventing LD accumulation leads to increased oxidative damages including lipid peroxidation and 4-HNE protein adducts (Bailey et al., 2015). Collectively these results indicate that LDs can protect PUFA from oxidation-induced damages.

The protective effects of LDs against oxidation have also been observed in cancer cells (Bensaad et al., 2014; Zhang et al., 2017). Tumors constitute a highly hypoxic environment, and cancer cells often accumulate LDs (Cruz et al., 2020). Zhang et al., found that the activation of hypoxia inducible factors (HIF) induces expression of Hypoxia-Inducible Gene 2 (HIG2), which inhibits ATGL, and increases LD accumulation in human cancer cell

lines Hela and HCT116 under hypoxia (Zhang et al., 2017). Inhibition of HIG2 reduces LD accumulation and leads to apoptosis of cancer cells in hypoxia (Zhang et al., 2017). This result suggests that the downregulation of lipid catabolism promotes LD accumulation and protect cells from excessive cytosolic free FA and oxidative stress-associated damages.

1.4.4. Resistance to ER stress

The ER is the major site of lipid and protein synthesis. However, excessive accumulation of lipids or unfolded proteins in the ER, can trigger ER stress and activate the pathways of the unfolded protein response (UPR) (Oakes and Papa, 2015; Pineau et al., 2009; Volmer and Ron, 2015). The formation of LDs has been proposed to act as an "escape hatch" mechanisms to relieve ER stress (Ploegh, 2007). For example, LD formation alleviates ER stress in a cellular model of hereditary spastic paraplegia. Expression of the mutated form of Seipin^{N88S}, leads to abnormal accumulation of misfolded Seipin in the ER and ER Stress in mouse motor-neuron cell line, NSC-34 (Hölttä-Vuori et al., 2013). Interestingly, LD accumulation could reduce ER stress by relocating abnormal seipin proteins to the LD surface (Hölttä-Vuori et al., 2013). These results support the hypothesis that LDs can act as an "escape hatch" to relieve the ER from overwhelming quantity of lipids or misfolded proteins (Ploegh, 2007).

1.5. The heterogeneity of LDs

Proteomic analysis of LDs extracted from different tissues revealed that LDs can vary in protein content from one tissue to the another (inter-cellular differences), but also within a single cell (intra-cellular differences)(Beller et al., 2020). This diversity reflects 1) differences in lipid metabolism between tissues (e.g. adipose tissue vs oxidative tissues), 2) differences in types of neutral lipid stored in the core of LDs (e.g. sterol-esters or TAG), 3) differences in the conditions in which LDs are generated (e.g. physiological or stress), 4) functionally distinct LD subpopulations.

1.5.1. Intra-cellular LD diversity

At the single cell level, differences in LD protein composition may reflect different stages of LD maturation but also functionally distinct LD subpopulations. Perilipins are one example of proteins that are differentially distributed at the surface of LDs. In mammalian cells, perilipins segregate to distinct LD populations depending of the nature of the neutral lipid core. Perilipins abundance is modulated by exogenous cholesterol or OA treatment in mouse adrenocortical cells, which express all five perilipin genes (Hsieh et al., 2012). While Plin1, 2 and 3 were increased by both types of lipid, Plin4 and Plin5 accumulated only upon treatment with cholesterol or OA, respectively (Hsieh et al., 2012). Interestingly, *Drosophila* perilipins, dPlin1 and dPlin2, also have different pattern of localization. While dPlin1 covers most LDs, dPlin2 is only found on smallest LDs in *Drosophila* fat body (Bi et al., 2012). A similar type of segregation for Plin1 and Plin2 is found in rodents, with Plin2

accumulating on small nascent LDs and Plin1 on large LDs of mice 3T3 adipocytes treated with OA (Wolins et al., 2003). These results indicate that different perilipins associate differentially with LDs depending on the LD maturation stage (nascent or mature).

Subpopulation of LDs are also defined by their capacity to grow. Indeed, growing LDs carry a specific set of proteins, such as GPAT4 in *Drosophila* and mammalian cells, but also Ldsdh1 in *Drosophila* fat body (Thul et al., 2017; Wilfling et al., 2013).

Finally, subpopulation of LDs can be defined by their subcellular localization. Ugrankar et al. found that, *Drosophila* adipocytes contain a subset of LD associated with the plasma membrane at the cell periphery (Ugrankar et al., 2019). These peripheral LDs are connected with the plasma membrane by a protein called Snazarus (Snz) and their formation requires Lipoprotein-derived lipids rather than fatty acid synthase 1 (FASN1) in contrast to medial LDs (Ugrankar et al., 2019).

In summary, different LD subpopulations co-exist inside the same cell. Little is known about these LD subsets but their functions and localization depends on a specific set of LD-associated proteins.

1.5.2. Inter-cellular LD heterogeneity

A large body of knowledge on LDs has been gathered from studies in adipocytes. It is clear that LDs can store different types of lipids and associate with different types of proteins depending on the tissue considered. For example, adipocytes require a particular set of proteins, such as PLIN1, to mediate storage and rapid mobilization of large quantity of FA. Cells can be specialized in the storage of different types of neutral lipids which may be sequestered in LDs containing different set of LD proteins. For example, sterol-esters in tissues producing steroid hormones such as *Drosophila* ring gland, or mammalian steroidogenic cells of the adrenal gland. In addition, tissue-specific LD mechanisms can be found such as LD-mitochondria coupling in cardiomyocytes or the predominant lipophagy in the hepatocytes (Beller et al., 2020).

While it is thought that all tissues can accumulate LDs, the mechanisms regulating LD homeostasis in the brain are not clear. Partly because it can be difficult to detect LDs in this lipid reach tissue. However, accumulating evidences indicate that LD homeostasis is impaired in neurodegenerative disorders. In the next chapter I will discuss LD-based lipid storage in the brain in health and disease.

2. LD in the brain in health and disease

The human brain is a lipid rich organ, with lipids representing more than half of the brain's dry weight (Hamilton et al., 2007). The brain is a complex, intricate network of about 100 billion interconnected neurons in close association with an equal number of supporting glial cells that includes astrocytes, oligodendrocytes, microglia, and ependymal cells (Allen and Lyons, 2018; von Bartheld, 2018; von Bartheld et al., 2016). Lipid homeostasis is crucial for the maintenance of neuronal membranes, synaptic structure, and neurotransmission (Montesinos et al., 2020). Lipids are also the principal component of myelin sheets, produced by oligodendrocytes, which wrap axons, and speed up signal transmission. Intriguingly, while little is known about lipid storage in the healthy brain, LD accumulation has been observed in an increasing number of neurodegenerative disorders including PD. The fact that LDs appear in different neurodegenerative disorders raises a lot of question about the contribution of LDs to these different pathologies and the importance of glia and neurons in the LD accumulation. In this section, I will discuss the current understanding of LDs in the healthy and pathological brain.

2.1. *Drosophila* central nervous system: a potent neurobiology model

Drosophila have a small, yet complex brain constituted of 100 000 interconnected neurons and supporting glial cells tightly packed in three fused bilateral ganglia: the paired visual protocerebrum, the paired deutocerebrum which processes sensory information from the antennae, and the central tritocerebrum which integrates information from other systems (Edwards and Meinertzhagen, 2010). Each ganglia is organized with neuronal cell bodies located in periphery in an area called the cortex and project towards the neuropil, a zone of dense synaptic connections (Ito et al., 2014). In similar fashion to its mammalian counterpart, the insect brain contains populations of specialized neurons expressing conserved neurotransmitter including dopamine, serotonin and gamma-aminobutyric acid (GABA) that controls a large array of complex behaviors such as locomotion, memory, and complex social interactions.

The *Drosophila* central nervous system (CNS) contains 5 major types of glial cells including: astrocyte-like, cortex, ensheathing, perineurial, and sub-perineurial glia that collectively recapitulate the morphological and functional features of mammalian glial cells (Figure 10)(Freeman, 2015; Kremer et al., 2017).

The cortex glia surrounds the neuronal cells bodies and provides energy substrates such as lactate for neuronal metabolism. Ensheathing and astrocyte glia are localized around the neuropil and maintain the synapses homeostasis. These subtypes of glia express the excitatory amino acid transporter 1 (Eaat1), glutamine synthetase and glutamate transaminase, which are necessary to take-up, and recycle the neurotransmitter glutamate to prevent neuronal excitotoxicity (Rival et al., 2004). In addition, ensheathing glia are

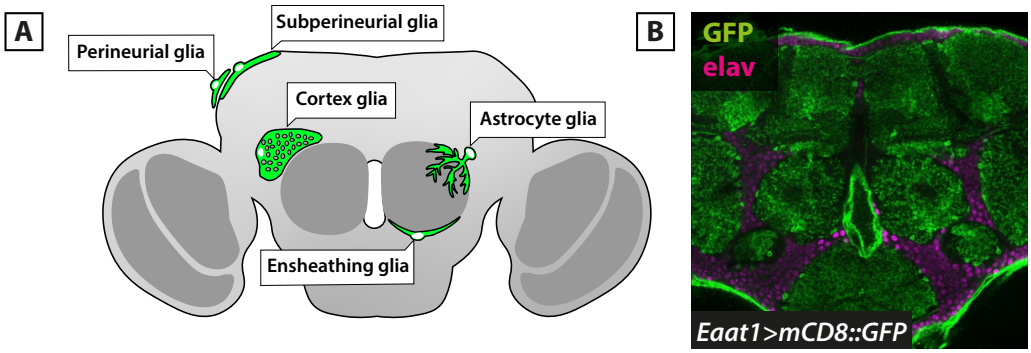

Figure 10. The *Drosophila* glial cell subtypes

(A). Schematic representation of adult *Drosophila* glial subtypes (green). Brain structure of the neuropils (dark grey) and cortex (light grey). (B). Localization of astrocyte-like glia in the *Drosophila* adult brain (Eaat1>mCD8::GFP). Neuron nuclei are visible in the cortex (magenta).

also associated with axons and peripheral nerves. Perineurial and sub-perineurial glia surround and isolate the brain from the circulating hemolymph, establishing a structure sharing functional similarities with the blood brain barrier (BBB) (Schirmeier and Klämbt, 2015; Schwabe et al., 2005). Interestingly, some *Drosophila* glial cells, including ensheathing glia, express Draper and SIMU, and like microglia in mammals can engulf axonal debris and dead cells (Doherty et al., 2009; Kurant et al., 2008).

During my thesis, I used *Drosophila* retina to investigate neuron-glia interactions. Indeed, the fly eye is composed of a repeated unit called ommatidia, which contains photoreceptor neurons, and retina pigment cells (known also inter-ommatidial cells) with glia-like functions. In this manuscript, I will therefore refer to pigment cells as retina glia (Figure 11)

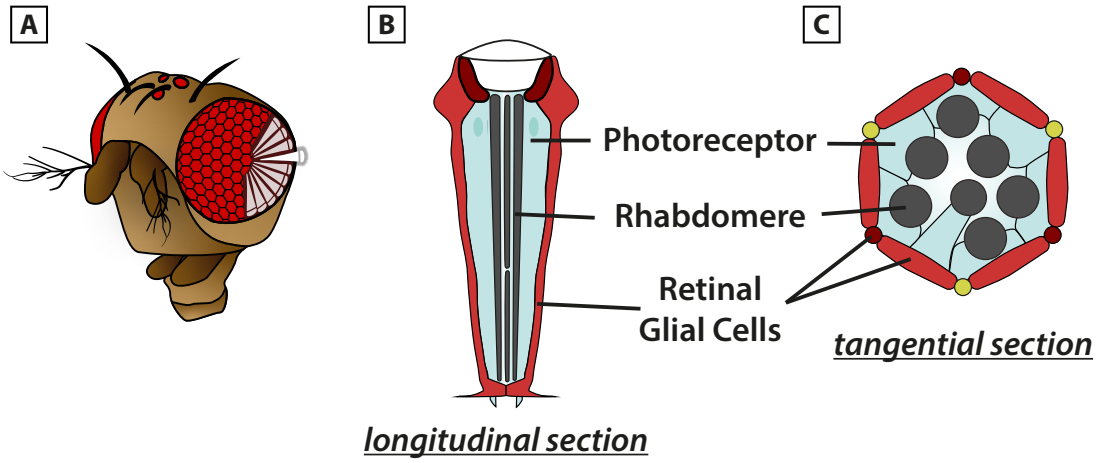

Figure 11. The structure of *Drosophila* retina

(A) Schematic of a *Drosophila* compound eye. The eye is composed of about 800 repeated units called ommatidia (hexagonal shapes). Longitudinal sections (shown in white) of the ommatidia

allows visualization of the retinal cells that span the entire width of the retina. (B) Schematic of a longitudinal section of one ommatidium. Each ommatidium is composed of 8 photoreceptor neurons (light blue), each containing one rhabdomere (dark gray), and 9 glial cells (also known as retinal pigment cells; red and maroon). (C) Schematic of a cross-section of one ommatidium. In addition to the 9 glial cells (6 secondary [red] and 3 tertiary [dark red]), each ommatidium contains 3 bristle cells (yellow) originating from the neuronal lineage.

2.2. How do lipids enter the brain

In vertebrates, neutral lipids, such as TAGs are transported to organs via the blood by low and very low density lipoprotein (LDL and VLDL), which are synthetized and secreted by the adipose tissue, the intestine and the liver. As the blood reaches the brain through thin capillaries, nutrient and other blood component are filtered through the Blood Brain Barrier (BBB) before being accessible by neurons in the CNS parenchyma. The BBB, isolates the brain from harmful blood substance, maintains the brain ions concentration and controls the supply of metabolites for neurons. To achieve these functions, the BBB is constituted of three cellular components: endothelial cells with tight junctions, pericytes, and astrocytes endfeet that connect neurons to all these cells types (Kysenius and Huttunen, 2016; Weiler et al., 2017). To cross the BBB, lipoproteins must be transported using specific transporters expressed by pericytes and astrocytes. Passive diffusion of FA through the BBB has also been reported and proteins important for the intracellular transport of FA such as FATP and fatty acid binding protein 7 (FABP7) are both expressed at the BBB. (Bruce et al., 2017; Hamilton and Brunaldi, 2007).

In *Drosophila*, a specialized type of glia called perineurial glia surrounds and isolates the brain from the hemolymph of the insect open circulatory system (Schwabe et al., 2005). This barrier, completed by sub-perineurial glial cells, acts as an equivalent of the vertebrate BBB. *Drosophila* BBB cells express a large array of transporters for metabolites, ions, and lipoproteins such as lipoprotein receptor 1 (LpR1) (Brankatschk and Eaton, 2010; DeSalvo et al., 2014). Lipids are transported in the hemolymph via three types of lipoprotein homologues of ApoB: lipophorin (Lpp), crossveinless d (Cv-d), and lipid transfer particle (LTP) (Palm et al., 2012). Lpp is the main fly lipoprotein, secreted by the fat body and loaded with lipids, mostly DAG, by the intestine (Palm et al., 2012). Lpp lipoproteins can cross the BBB and accumulate near neuron cell bodies and axons (Brankatschk and Eaton, 2010; Brankatschk et al., 2014). For example, LTP lipoproteins cross the BBB of the developing CNS, using the lipoprotein receptors LRp1 and Megalin, and accumulate near a specific subset of neurons involved in nutrient sensing called *Drosophila* insulin like peptide 2 (Dilp2)-recruiting neurons (DRN) (Brankatschk et al., 2014).

Finally, astrocytes also produce lipids *de novo* and transport them to neurons by secreting Apolipoprotein E (ApoE) lipoproteins (Wang and Eckel, 2014). Interestingly, the ApoE4 allele is a major AD risk factor (Farmer et al., 2019). Astrocytes also secrete high

levels of ApoE and ApoJ lipoproteins in the cerebrospinal fluid.

2.3. Fueling the brain with energy

Synaptic transmission is a process that requires a lot of energy (Harris et al., 2012; Yellen, 2018). Glutamate mediated neurotransmission may account for 80% of the energy expenditure and 80% of synapses belong to excitatory glutamatergic neurons (Bélanger et al., 2011). To maintain neuronal activity and synaptic transmission, the brain must be supplied at all time with metabolic fuel. For neurons, the fuel of choice is glucose rather than FA and energy in the form of ATP is provided mainly through oxidative phosphorylation (Schönfeld and Reiser, 2013). It is estimated that the brain is the largest energy consumer of the mammalian body and consumes alone 25% of ingested glucose and 20% of absorbed oxygen for only 2% of the total body mass (Schönfeld and Reiser, 2013). The energy supply must be maintained constant as neurons are thought to have very limited energy storage. Fuel supply is orchestrated by the tight metabolic coupling of neurons and supporting glial cells. Indeed, glucose reaches the brain through systemic circulation, and must cross the BBB to reach neurons (Desalvo et al., 2011; Featherstone, 2011). Astrocytes, which are in contact with neuronal synapses and the vascular system, act as metabolic hubs and are considered to be responsible for half of the brain glucose uptake (Bélanger et al., 2011). Astrocytes metabolize glucose through aerobic glycolysis and provide neurons with energy substrates such as lactate or alanine. This metabolic coupling between astrocytes and neurons is called the Astrocyte-Neuron lactate shuttle. Glial cells are mediating important functions regarding energy support and regulation of neuronal functions including glutamate uptake and recycling. Finally, astrocytes can also provide neurons with other energy substrates such as ketone bodies: ß-hydroxybutyrate and acetoacetate (Schönfeld and Reiser, 2013, 2017).

In *Drosophila*, the main source of carbohydrate is trehalose, a glucose disaccharide, and perineurial glial cells take up trehalose, through the specific trehalose transporter Tret1-1, and metabolize it for neurons (Volkenhoff et al., 2015). Volkenhoff et al. found also that loss of glycolysis enzymes in glia but not in neurons leads to severe neurodegeneration (Volkenhoff et al., 2015). Furthermore, *Drosophila* glial cells also express *chaski*, a monocarboxylate transporter (MCT) protein involved in transport of pyruvate/lactate indicating that, like in mammals, glial cells provide lactate to sustain neuronal energy demand (Delgado et al., 2018).

Whether brain cells use lipids as energy substrates remains a topic of debate. Lipids are not typically used as energy substrate by neurons. However, glial cells may use lipids as an energy source. Indeed, the glial knockdown of Carnitine-Palmitoyltransferase 2 (*CPT2*), the rate limiting enzyme of ß-oxidation, increases lipid storage in *Drosophila* glial cells (Schulz et al., 2015). This result indicates that FA, which should have been consumed through ß-oxidation, accumulate and are converted to TAG and LDs. *Drosophila* glial cells thus actively degrade FA through ß-oxidation and may by this mean provide neurons with energy substrates, is some particular conditions.

2.4. LD in the healthy brain

Glial cells can synthesize lipids and accumulate LDs. In contrast, LDs are rarely observed in healthy neurons. What are the functions of LDs in healthy glial cells? In this section, I will discuss the functions of LDs in the healthy brain (Lee et al., 2020).

During *Drosophila* CNS development, a specialized subset of glial cells accumulate LDs (Bailey et al., 2015; Kis et al., 2015). While these LDs are dispensable for neuroblast proliferation in normal environmental conditions, they provide an important antioxidant mechanism under condition of hypoxia (Bailey et al., 2015). Bailey et al. reported that LDs can protect PUFAs, contained in membranes phospholipids, from oxidative damages by relocating them to TAGs stored in LDs (Figure 12). Several molecular actors including Phospholipase D (PLD), Mdy, GPAT4, and dPlin2, are required, in glia, for PUFAs relocation to LDs, and protection against membrane lipid peroxidation (Bailey et al., 2015).

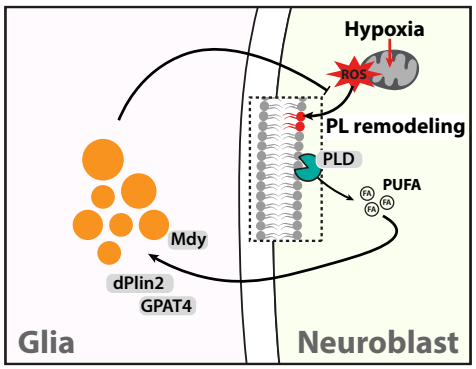

Figure 12. Hypoxia-induced LD in *Drosophila* developing CNS

In neuroblast under hypoxia, PUFA localized in membrane are remobilized by phospholipase D (PLD), relocated to glia, and incorporated to LDs by action of Mdy, GPAT4 and Plin2. This process prevents PUFA peroxidation, and supports neuroblast proliferation. See Bailey et al. 2015.

In adult *Drosophila*, cortex glia cells accumulate LDs under normal conditions, but it is yet to be demonstrated if these droplets have also an antioxidant function. Indeed, as I mentioned, a study showed that glial knockdown of *CPT2*, an important protein for the transfer of FA to mitochondria, is associated with increased lipid storage suggesting that ß-oxidation actively degrades FA in glia to produce energy (Schulz et al., 2015).

While the knowledge on LDs remains limited in the healthy mammalian glia, starvation or deficit in lipolysis can increase glial lipid storage suggesting that some glial cells degrade LDs rapidly in the brain. For example, the ependymal cells, which form the epithelial lining between brain ventricles and the cerebrospinal fluid (CSF), express high levels of ATGL (Etschmaier et al., 2011). LDs accumulate in ependymal cells of ATGL knockout mice (Etschmaier et al., 2011). Furthermore, a subset of ependymal cells located in hypothalamic area called tanycytes accumulate LDs upon palmitate treatment and degrade FA through ß-oxidation (Geller et al., 2019). These results suggest that LD turnover is rapid in brain

glial cells.

In contrast to glial cells, neurons rarely accumulate LDs in healthy animals (Pennetta and Welte, 2018). In culture, LDs were first observed in neurons isolated from *Aplysia californica*, a gastropod mollusk used in neurobiology for its giant neurons (Savage et al., 1987). In addition, treatment with OA induces LD formation in primary culture of hippocampal neurons (Ioannou et al., 2019). Mammalian neurons express enzymes required for TAG synthesis such as a specific isoforms of Lipin1 (Takeuchi and Reue, 2009; Wang et al., 2011b). Interestingly, a small number of LDs has been found in healthy photoreceptor neurons in the retina of one-day old *Drosophila* (Van Den Brink et al., 2018). These results suggest that neurons have the molecular tools required LD biogenesis but their accumulation in normal condition may be limited due to low uptake of fatty acid, or high levels of TAG lipolysis that would favor LD degradation rather than accumulation.

2.5. Lipid build-up in the aging brain

Aging is associated with accumulation of ectopic LDs in tissues such as liver in mammals and muscles in both mammals and insects (Greenberg and Coleman, 2011; Kirkland et al., 2002; Yan et al., 2017). Metabolism is less active with age which could contribute to the accumulation of fat in tissues with high metabolic turnover. The brain is not spared by this phenomenon and neurons and glial cells accumulating LDs with age have been reported in the brain cortical and striatal parenchyma, and in the optic nerve of aging mice (Nag and Wadhwa, 2012; Shimabukuro et al., 2016). Shimabukuro et al. showed that neurons, astrocytes, and microglia cells, accumulate LDs and PLIN1 with age (Shimabukuro et al., 2016). As aging is the most important risk factor associated with neurodegenerative disorders, we can hypothesize that age-induced fat accumulation may contribute to the age-dependent dysfunction of neuronal and glial cells.

Let's focus one more time on glial cells and their roles during aging in regard to LD accumulation and their functions of guard keeper of brain integrity. As I mention earlier, microglia are the brain resident macrophages, and can thus engulf cellular debris by phagocytosis. Interestingly, Marshallinger et al. found that microglia accumulate LDs in old mice (Marschallinger et al., 2020). These LD-containing microglia contain more ROS and are less efficient at phagocytosis (Marschallinger et al., 2020). Ependymal cells of aged mice also accumulate LDs in the sub ventricular zone of the lateral ventricles (Bouab et al., 2011; Capilla-Gonzalez et al., 2014). LD accumulation is associated with other morphological changes in ependymal cells that contribute to their malfunctions such as loss of cilia motility and impairment of their parenchyma/CSF barrier function. Interestingly, the expression of myristoylated alanine-rich protein kinase C substrate (MARCKS) decreases with age in ependymal cells and the phenotype of LD accumulation in ependymal cells of old 20-month-old mice is also recapitulated by the loss of MARCKS in young 2-month-old mice (Muthusamy et al., 2015; Ogrodnik et al., 2019). These results

highlight the critical function of MARCKS in the age-dependent LD accumulation in enpendymal cells.

Collectively these results indicate that LDs accumulate in both neurons and glial cells with age. This leads to impaired cellular functions and may contribute to age-dependent neurodegeneration.

2.6. LD in neurodegeneration

Neurodegenerative disorders are increasingly associated with LD accumulation. The lipid dysregulations observed in these diseases can be the direct consequence of mutation in genes involved in lipid metabolism (e.g. Hereditary Spastic Paraplegia [HSP], AD and PD). Lipid dysregulations can also be induced to other cellular deregulations such as mitochondria dysfunctions and ROS (Amyotrophic Lateral Sclerosis [ALS], Friedrich's Ataxia) or autophagy (Huntington's Disease [HD]). In this section, I will discuss the current knowledge on the brain cell types accumulating LDs in these disease (neuron or glia) and the consequences of LD accumulation on the progression of neurodegenerative disease.

2.6.1. Mitochondria dysfunctions induce glial LDs

The dysfunctions of mitochondria is particularly damaging in neurons as these rely heavily on mitochondria to produce energy through oxidative phosphorylation. In addition, impaired mitochondria respiration leads to accumulation of ROS which can damage lipids and proteins (see 1.4.3). In cellular and animal models of oxidative stress, LD accumulation in glial cells has emerged as an important regulator of the oxidative stress response (Henne et al., 2018). However, it remains unclear whether glial LDs protect or exacerbate neuronal demise in the context of neurodegenerative disorders.

Drosophila retina has become a model of choice to study the interaction of LDs and oxidative stress in the adult CNS. In newly hatched flies, LDs are transiently visible in retinal glial cells, before being degraded within 3 days (Van Den Brink et al., 2018). Liu et al., demonstrated that glial LD accumulation is exacerbated by mutations in mitochondrial genes involved in the respiratory chain complexes (*e.g sicily* [homolog of NDUFAF6, mitochondrial complex I chaperone] and *ND42* [complex I subunit]), mitochondria dynamics (*e.g. Marf* [homolog of mitochondrial fusion GTPase Mitofusin 1 and 2]), and mitochondrial DNA transcription and translation (*e.g. Aats-Met* [homolog of mitochondrial methionyl-tRNA synthetase 2, MARS2]) (Liu et al., 2015, 2017). As described previously, the fly retina is built on a repeated unit constituted of photoreceptor neurons and adjacent retina glial cells (also known as pigment cells). Interestingly, mitochondrial damages in photoreceptors were sufficient to trigger glial LD accumulation. This abnormal accumulation of LDs in glia is associated with the degeneration of photoreceptor neurons. Interestingly, preventing LD accumulation in glial cells by co-expression of ATGL ortholog Bmm lipase or knockdown of *dFatp* delayed photoreceptor degeneration indicating that

in these mutant lines LD accumulation could promote neurodegeneration (Liu et al., 2015; Van Den Brink et al., 2018). Interestingly, LDs accumulate also in astrocytes and microglia prior to degeneration in mitochondria complex I subunit *Ndufs4* knockout mice, indicating that glial LD accumulation upon oxidative stress is an evolutionary conserved mechanism (Liu et al., 2015).

Liu et al. identified several molecular actors required in neurons and glia for glia LD accumulation, using a cell-specific RNAi-mediated screen (Liu et al., 2017). Briefly, damaged mitochondria in photoreceptors lead to ROS production, which stimulate the neo-synthesis and transfer of lipids to the glial cell to promote LD formation. The authors suggested that, in condition of damaged mitochondria, lactate transferred from glia to neurons via MCTs (Silnoon, Outsider and Basigin) is used as substrate for *de-novo* lipid synthesis by enzymes such as enzymes Acetyl-CoA Carboxylase (ACC) (Figure 13) (Liu et al., 2017). This result indicate that lactate can be used to synthesize FA in neurons.

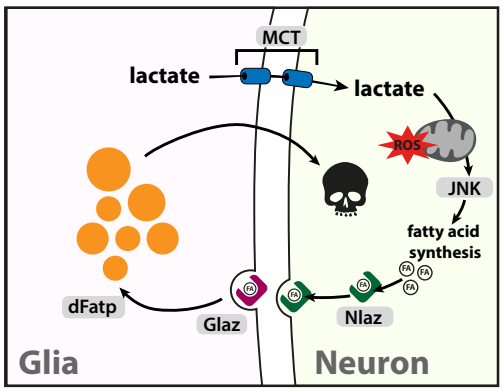

Figure 13. ROS-induced LD in *Drosophila Aats-Met* mutant retina

In *Aats-Met* mutant retina, photoreceptor mitochondria liberate ROS that activate the JNK pathway and promote the synthesis of lipids. Lactate derived from glia and transported using monocarboxylate transporters (MCTs), is required for lipid synthesis in neurons. Lipids are then transferred to glia by ApoD homologs Glaz and Nlaz, where they are incorporated into LDs. LD accumulation in glia precedes photoreceptor neurodegeneration. See Liu et al. 2015, 2017.

Furthermore, these lipids produced in neurons would be transported back to glia via lipoprotein transfer mediated by *Drosophila* ApoD homologues Neural lazarillo (Nlaz) and Glial lazarillo (Glaz) (Liu et al., 2017). Finally, these lipids would be integrated in TAGs in glia, using dFatp, and acyl-CoA ligase (Van Den Brink et al., 2018). Interestingly, replacing *Drosophila* ApoD homologs Glaz and Nlaz by human ApoE allelles revealed that while APOE2 and APOE3 can rescue *Drosophila* ApoD deficiency, APOE4 could not. ApoE4, which is associated with an increase Alzheimer's risk, is thus enable to transfer lipids between neuron and glia, under oxidative stress.

Mitochondrial damages in glia can also induce ROS and trigger LD accumulation

preceding photoreceptor demise. For example, loss of metalloprotease ADAM17 is associated with increased mitochondria ROS and LD accumulation in the *Drosophila* adult retina (Muliyil et al., 2020). LD accumulation also precedes the photoreceptors demise (Liu et al., 2015; Muliyil et al., 2020). In this study, the authors showed that the cleavage and liberation of Eiger, the *Drosophila* homolog of Tumor Necrosis Factor, by ADAM17, inhibits oxidative stress by an unknown mechanism (Muliyil et al., 2020). In this model, the glial specific expression of the Bmm lipase prevented photoreceptor degeneration in a similar fashion to what is observed in *Aats-Met* mutant retina, (Liu et al., 2015; Muliyil et al., 2020). In contrast to *Aats-Met* mutant, loss of ADAM-17 leads to mitochondria-induced ROS in glia (Figure 14). This indicates that glial LDs accumulate in response to neuronal but also glial ROS. Likewise, LDs accumulate in the cortex and neuropil glia in the glial knockdown of *ND23, a* Complex I subunit homolog of NDUFS8 associated with a neurodegenerative disease called Leigh syndrome (Cabirol-Pol et al., 2018). Collectively these results indicate that mitochondrial damages in glia, also lead to LD accumulation in both *Drosophila* retina and brain glial cells.

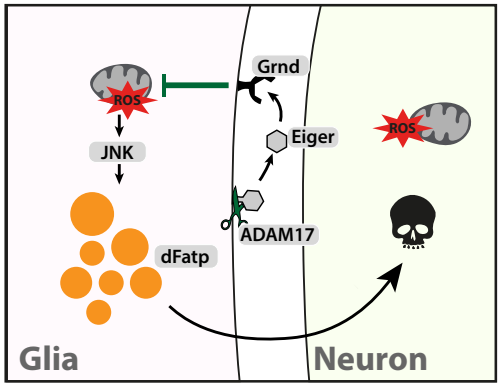

Figure 14. Loss of ADAM17 induce ROS and LDs in *Drosophila* retina

ADAM-17 is a metalloprotease that cleaves and liberates Eiger, the Drosophila ortholog of TNF. Eiger binds to its receptor Grindelwald (Gr) and limits ROS production by an unknown mechanism. In ADAM-17 mutant, ROS increase in glia, activate the JNK pathways which promotes LD accumulation by a mechanism that requires dFatp. LD accumulation in glia precedes the demise of photoreceptors. See Muliyil et al. 2020.

Mitochondria dysfunction and lipid storage dysregulation have also been observed in Friedrich's Ataxia (FRDA), a neurodegenerative disorder (spino-cerebellar ataxia) that leads to large sensory neurons degeneration. FRDA is caused by mutation of the gene encoding frataxin, a mitochondrial protein that is involved in the assembly Fe-S cluster associated with the mitochondria respiratory chain complexes (Campuzano et al., 1997). Interestingly, loss of frataxin leads to LD accumulation in *Drosophila* glial cells and to an increased sensitivity to oxidative stress (Navarro et al., 2010). Similar to Liu et al.'s study,

expression of ApoD homolog, Glaz, can rescue lipid-associated defects indicating that lipid export via lipoprotein could reduce lipotoxicity in glia (Liu et al., 2017; Navarro et al., 2010).

Chorea Acanthocytosis (ChAc) is a neurodegenerative disorder, caused by loss of function mutation in vacuolar protein sorting 13 homolog A (VPS13A), which has recently been associated with mitochondria damages and LDs. VPS13A is found on mitochondria, ER, and LDs, and knockout of VPS13A leads to impaired mitochondria elongation, defective mitophagy and increased LD accumulation in mammalian cells (Yeshaw et al., 2019) Interestingly, the loss of Vps13, *Drosophila* homolog of VPS13A, leads to age-dependent locomotion impairment, premature death and LD accumulation in retina glial cells (Vonk et al., 2017; Yeshaw et al., 2019). At this point, it remains however unclear whether LD accumulation in Vps13 mutant flies is the consequence of mitochondria damages only, or impaired Vps13 LD-related function.

Collectively these results show that the accumulation of LDs in glial cells is an evolutionary conserved response to mitochondria damages and oxidative stress in the CNS. The function of such a response is however incompletely understood. On one hand, LD formation protects from oxidative damages sensitive lipids such as PUFA in *Drosophila* developing nervous system (Bailey et al., 2015). On the other hand, preventing LD accumulation by knockdown of *dFatp* or overexpression Bmm lipase in *Aats-Met* or *ADAM17* mutant flies delays neurodegeneration. This raises the possibility that glial LDs could be detrimental in condition of high ROS (Liu et al., 2015; Muliyil et al., 2020; Van Den Brink et al., 2018). Additional evidences for a detrimental role of LDs are provided in experiments in which mice primary microglia accumulate LDs and ROS in response to LPS (Khatchadourian et al., 2012; Marschallinger et al., 2020). Interestingly, treatment with Triacin C, an inhibitor of long-chain acyl-CoA synthetase, reduces LD accumulation and ROS suggesting that LDs could promote ROS production in this context (Marschallinger et al., 2020).

2.6.2. LDs in protein misfolding disorders

HD and AD are neurodegenerative disorders associated with protein misfolding and formation of protein aggregates. Interestingly, several studies indicate the presence of LDs in post-mortem human brain which suggest that dysregulation of LD homeostasis may be a contributing factor in HD and AD(Gómez-Ramos and Asunción Morán, 2007; Martinez-Vicente et al., 2010).

HD is a genetic disorder associated with mutations in the gene encoding Huntingtin (Htt) that lead to an abnormal Htt proteins containing expanded poly-glutamine tract prone to form aggregate in neurons. Interestingly, LDs are observed in primary striatal neurons of ^{111}Q-Htt knock-in mice and in brain sections of HD patients (Martinez-Vicente et al., 2010). In this study, Martinez-Vicente et al., suggest that LDs accumulate because of an impaired degradation by autophagy.

AD is the most common form of dementia, and has been associated with including protein aggregates (amyloid plaques and neurofibrillary tangles) and lipid deposition in glia since its earliest description by Alois Alzheimer (Foley, 2010). In AD, protein aggregates contain abnormally phosphorylated tau and amyloid-ß peptides, a pathogenic cleaved form of Amyloid Precursor Protein (APP) resulting from processing by beta and gamma-secretase. One post-mortem analysis of AD patient brain tissue revealed the presence of neuronal LDs in close proximity with immunostaining of Aß-peptides in neurons (Gómez-Ramos and Asunción Morán, 2007). LDs were also observed along brain/CSF interface in ependymal cells of the subventricular zone in 2-month-old -AD mice, carrying a triple AD mutation (Hamilton et al., 2015). Interestingly, the most important risk factor to develop AD is to carry a particular allele of the gene encoding the apolipoprotein E called ApoE4 (Corder et al., 1993). As mentioned above Apolipoprotein E is the major lipid carrier in the human brain (Verghese et al., 2011). ApoE lipoprotein are secreted by neurons in a model of N-methyl-D-aspartate (NMDA)- induced excitotoxicity. In this models, lipids carried by ApoE lipoprotein are transferred to glia where they accumulate as lipid droplets (Ioannou et al., 2019). Interestingly, the transfer of lipids from neuron to glia is hindered in humanized flies expressing ApoE4, or in neuron-astrocyte co-culture derived from *Apoe-/-* mice, suggesting that ApoE4 is ineffective in lipid transfer (Liu et al., 2017). These result support that failure to export lipids via ApoE may contribute to LD accumulation in AD neurons.

2.6.3. Motor-Neuron Diseases: Hereditary Spastic Paraplegia

The Hereditary Spastic Paraplegia (HSP) are a group of inherited neurodegenerative disorders that affect primarily the upper motor neurons of the spinal cord. HSPs are characterized by a progressive lower limb spasticity and weakness that can be associated with various other symptoms such as intellectual disabilities and motor-symptoms reminiscent of PD. HSPs are associated with mutations affecting more than 76 different genes (Spastic Paraplegia Genes [SPG1-76]). Interestingly, the most common forms of autosomal dominant HSP affect genes associated with LD biology including Receptor Expression-Enhancing Protein 1 (REEP1 or SPG31), spastin (SPAST or SPG4), Atlastin-1 (SPG3A), and spartin (SPART or SPG20) (Figure 15)(Pennetta and Welte, 2018).

REEP1, atlastin and spastin interacts together and maintain the ER tubular morphology (Falk et al., 2014; Renvoisé et al., 2016). Renvoisé et al., found that *reep1-/-* mice have a severe reduction in adipose tissue, and a reduction of LD number in neurons of the cerebral cortex of mice (Renvoisé et al., 2016). In addition, *reep1-/-* Mouse Embryonic Fibroblasts (MEF) fail to accumulate LDs upon oleic acid treatment. Co-overexpression of Reep1 and Atlastin-1 induce LD accumulation in NIH-3T3, COS7 and Hela cells (Falk et al., 2014; Renvoisé et al., 2016). Reep1 is normally anchored at the ER by an N-term hydrophobic hairpin. Interestingly, missense mutations found in HSP patient affecting

Reep1 N-term, lead to a relocalization of Reep1 to the surface of LDs (Falk et al., 2014). The exact mechanism by which Reep1 could mediate LD accumulation is unclear. Interestingly, Reep1 can also bind to Seipin in 3T3 cells (Renvoisé et al., 2016). As described previously, Seipin in an important contributor to LD formation (see 1.1.2). Interestingly, mutation of Seipin is also associated with a form of HSP (SPG17) (Musacchio et al., 2017; Windpassinger et al., 2004). Collectively these results suggest that control of LD biogenesis is an important contributor of motor-neuron survival.

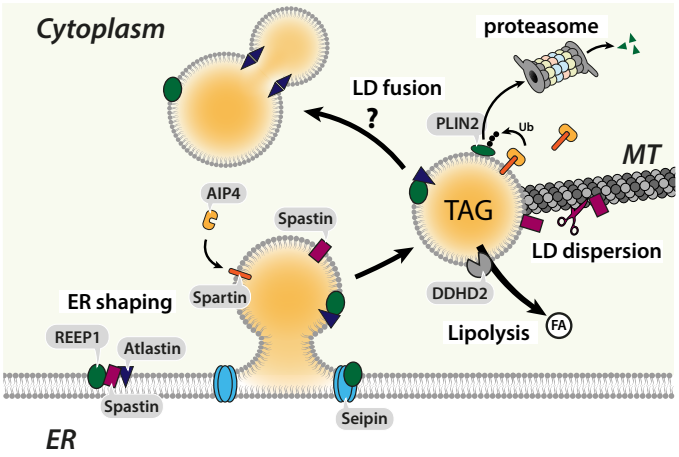

Figure 15. LD-related proteins involved in HSPs

Schematic representation of the main genes involved in HSP and their LD-related functions. REEP1 associates with Spastin and Atlastin at the ER, and could promote Atlastin localization to LD. Spastin is a microtubule-severing protein which promote LD dispersion. Atlastin is a LD protein that may promote LD fusion. DDHD2 is a TAG lipase found in neurons. Spartin is an adaptor protein, that recruits the ubiquitin ligase AIP4 at the surface of LD, which targets PLIN2 for proteasome degradation. Seipin is involved in LD formation at the ER.

Atlastin-1, is a membrane-bound GTPase of the dynein family, which is also associated with HSP (Klemm et al., 2013). Atlastin modulates membrane fusion, and could increase LD size by promoting LD fusion in COS7 cells. Depletion of the *Drosophila* Atlastin (*Atl*) leads to smaller LDs in larvae fat body.

SPAST is a microtubule (MT)-severing protein found at the ER membrane. Spastin binds LDs in Hela cells, and (Papadopoulos et al., 2015). Interestingly, knockdown of *Drosophila* Spastin (*dSpastin)* increases TAG levels, LD size and number in larval fat body, muscle and nerve cells (Papadopoulos et al., 2015). Neural specific knockdown of *dSpastin* leads to neurodegeneration and impaired locomotion. Arribat et al. found that Spastin is involved in LD dispersion by shaping the ER membrane along MTs (Arribat et al., 2020).

One rare form of recessive autosomal HSP involves mutation encoding a TAG lipase called *DDHD Domain Containing 2* (*DDHD2*, SPG54). Mice lacking DDHD2, recapitulates

key phenotypes of HSP including locomotor and cognitive impairment, progressive loss of motor neurons in the spinal cord (Inloes et al., 2014; Maruyama et al., 2018). In addition, DDHD2$^{-/-}$ mice have higher TAG levels in the brain and electronic microscopy analysis revealed an accumulation of large LDs in neurons of but not in glial cells (Inloes et al., 2014). This result reinforces the idea that TAG lipolysis is regulated by different actors depending on the tissue (Inloes et al., 2014, 2018). These results suggest that active neuronal lipolysis is important for neuronal survival.

The fact that mutations in multiple genes involved LD biogenesis are associated with HSPs, and that animal models of HSPs show sign of LD dysregulations in neurons support the idea that impaired neuronal LD homeostasis is a contributing factor of neurodegeneration.

3. Parkinson's Disease, Alpha-synuclein, and Lipids

3.1. Generalities about PD

3.1.1. Epidemiology of PD: a rising pandemic

PD is the neurodegenerative disorder with the fastest growing incidence and a concern worldwide as both world population and life expectancy increase (Dorsey et al., 2018). In 2016, 6.1 million people were living with PD worldwide, which was more than the double of the number of affected people in 1990 and by 2040, and it is estimated that 12 to 17 million people will be living with PD (Dorsey et al., 2018). The increase in life-expectancy alone cannot explain the steep rise in PD incidence indicating the contribution of environmental and societal factors. In France, the number of people living with PD is projected to increase by 65% between 2010 and 2030 (Wanneveich et al., 2018).

In addition to be a social burden for patients, which often have a reduced quality of life and cannot work anymore; PD represents an important financial burden for the society. Indeed, PD patients often need caregiver's help for their daily life when the disease is progressing and the motor symptoms are rising. The cost for therapy is quite heavy as well. Even if there is no available treatment to stop or to slow the progression of the dopaminergic neuron's degeneration, dopamine replacement therapy can be used to relieve motor symptoms. Indeed, dopamine agonists and levodopa are widely use as symptoms relieving therapies. Regarding the cost of the disease, in the United states, the disease-related medical costs per PD patient per year ranges from $10,378 to $14,400 and the total annual PD economical cost was $51.9 billion in 2017 (medical and non-medical) and is projected to reach $79 billions by 2032 (Rossi et al., 2018; Yang et al., 2020). As the global impact of PD will continue to rise, it is crucial to understand the underlying mechanisms of neurodegenerative processes associated with PD to find new ways to prevent its progression (Kalia and Lang, 2015).

3.1.2. An historical perspective: from the clinical to the cellular description of PD

200 years ago, James Parkinson, described "a new type of Shaking Plasya" (1817) characterized by locomotion and movement impairment with symptoms including slowness of movement (bradykinesia), postural instability, and resting tremor(Goedert and Compston, 2018). The description of the clinical manifestation of what is now called PD, has become more complex with the years. In particular, a large variety of non-motor symptoms are known to precede the motor phase of the disease: intestinal perturbation, visual troubles, and depression(Barone et al., 2017). In the late stage of the disease, PD patients can also develop dementia.

PD is associated with the progressive loss of dopaminergic neurons that are for most

part located in the *substantia nigra pars compacta,* project to the striatum, and are involved in the control of movements (Poewe et al., 2017). The main cellular hallmark of PD is the presence of large protein aggregates in the cytoplasm and neurites of affected neurons known as Lewy Bodies and Lewy Neurites respectively, named after Friedrich Lewy who first described them in 1912. These structures are constituted of a protein called alpha-synuclein (aSyn) (Spillantini et al., 1997). However, lipid stainings and recent correlative high resolution imaging on brain tissues from PD brain donors revealed that the composition of the Lewy Bodies is more complex than previously anticipated and contains organelle membranes and vesicular structures (Gai et al., 2000; den Jager, 1969; Shahmoradian et al., 2019). Lewy Bodies are found initially in the olfactory bulb and/or the medulla (dorsal motor nucleus of the glossopharyngeal and vagal nerves); and progressively invade other neuronal and glial cells throughout the brain with time including the dopaminergic neurons of the *substantia nigra* (Braak et al., 2003). The progressive spreading of Lewy Body is correlated with the severity of the disease and follow a stereotypical pattern(Braak et al., 2003). Braak et al., used this pattern to define six PD stages. Of note, due to difficulties with identifying PD at early stages, PD is often diagnosed at the late stage of the disease when motor symptoms are appearing (Braak et al., 2003).

The identification of familial forms of PD and concomitant rise of the molecular genetics, have greatly contributed to the identification of genes and cellular pathways affected in PD.

3.1.3. A polyfactorial disease: Genetic and environmental clues

PD is a multifactorial disorder that involves complex interactions between environmental and genetic factors. In 10% of cases, PD is due to a mutation in a particular gene transmissible to the offspring, collectively referred as familial forms. Although these cases are rare, the identification of these mutated genes and their functions is crucial for understanding the pathological mechanisms involved in PD. So far, 20 genes, including aSyn have been associated with mutation causing familial forms of PD (Figure 16) (Poewe et al., 2017; Polymeropoulos et al., 1997). Most of these genes are involved in protein homeostasis (e.g. SNCA, GBA), mitochondria functions (e.g. PTEN-induced kinase 1 [Pink1], parkin and DJ-1), intracellular trafficking (e.g. VPS35, LRKK2, GBA) as well as oxidative stress and neuroinflammation (Abeliovich and Gitler, 2016).

In the large majority of cases, PD is sporadic (90%), and is not associated with the identification of any genetic mutation. The main risk factor for PD is age, as indicated by the steep increase in PD prevalence for people over 65 years old. Environmental factors such as exposure to toxic substances, or pesticides can also increase the risk to develop PD (Tanner et al., 2011). For example, in 1998, heroin addicts that accidently inoculated heroin contaminated with MPTP (1-methyl-4-phenyl-1,2,5,6-tetrahydropyridine) rapidly

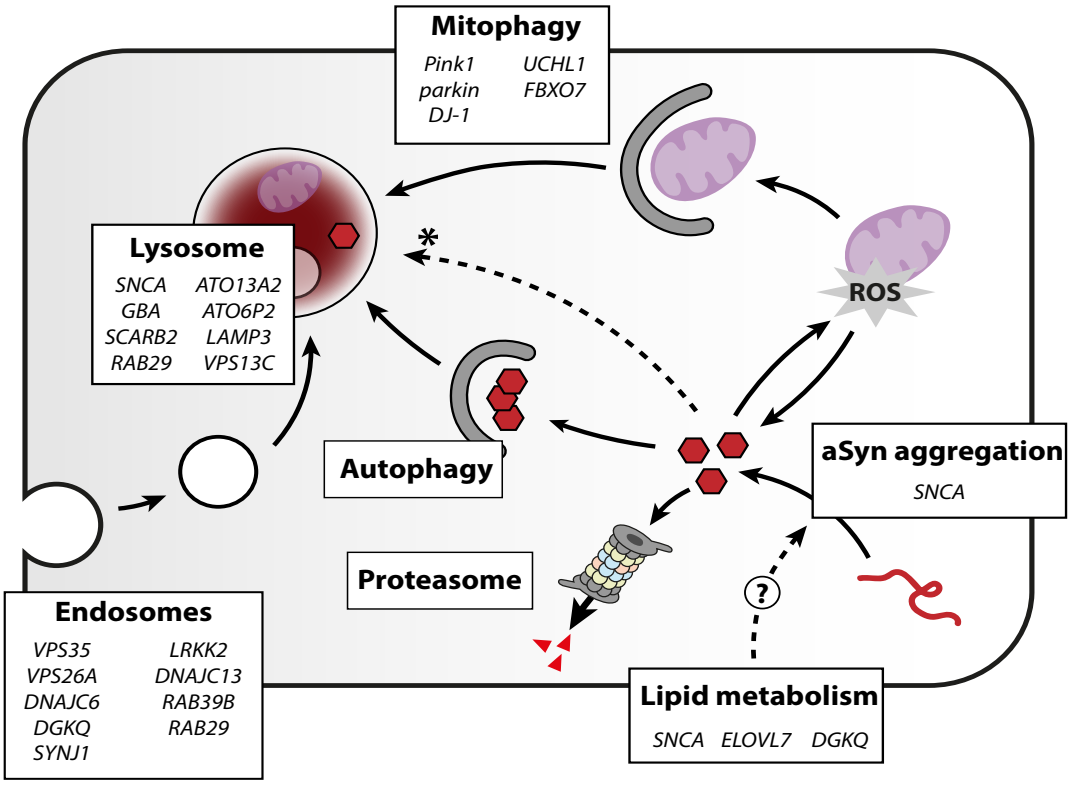

Figure 16. Genes and main cellular pathways involved in PD

Most genes associated with common sporadic and familial forms of PD, affect trafficking to the lysosome in the context of late endosome-to-lysosome pathways, clathrin-dependent endocytosis, macroautophagy or mitophagy. Wild-type α-synuclein (red) can also enter lysosomes through chaperone-mediated autophagy (asterisk). Scheme adapted from (Abeliovich and Gitler, 2016).

developed PD symptoms (Davis et al., 1979; Langston et al., 1983). Another example of toxic substance inducing PD is paraquat (1,1′-dimethyl-4–4′-bipyridinium), a pesticide closely related to MPTP, that has been widely used in agriculture and associated with PD contracted by European farmers (Baldi et al., 2003; Langston et al., 1983; Lee et al., 2012; Tanner et al., 2011). Both MPTP, and Paraquat inhibits the mitochondrial respiratory chain complex I highlighting the importance of mitochondria defects in PD. In addition, while not directly causing PD, a number of genetics variants, including in the aSyn loci, that increase the risks to develop PD were identified by Genetic Genome Wide Association Studies (GWAS). These studies thus highlight the contribution of a permissive genetic background to the development of sporadic PD(Klemann et al., 2017).

3.1.4. aSyn structure and conservation

Mutations and polymorphisms in the aSyn gene are associated with both familial and sporadic forms of PD. In the late nineties, aSyn was the first gene to be identified in association with familial forms of PD (Polymeropoulos et al., 1997). Indeed, missense

mutations, duplication or triplication of the gene encoding aSyn (SNCA) lead to familial forms of PD (Chartier-Harlin et al., 2004; Ibáñez et al., 2009; Singleton et al., 2003). In addition, polymorphisms of the SNCA locus are associated with increased risk of developing sporadic forms of PD (Klemann et al., 2017). Expression of human wild-type and mutated forms aSyn is sufficient to induce PD-like symptoms such as dopaminergic loss and locomotion impairment in *Drosophila* and in rodents (Feany and Bender, 2000; Tofaris et al., 2006). Finally, aSyn accumulation as aggregates is not unique to PD but is also associated with other disorders classified as synucleinopathies including dementia with Lewy Body (DLB) and Multiple System Atrophy (MSA). Note that MSA is associated with glial cytoplasmic inclusions of aSyn. Collectively these results indicate that aSyn is a central element in PD pathology but the precise mechanism underlying aSyn neurotoxicity remains unclear.

aSyn is a 14kD protein, highly expressed in the brain, originally, discovered in the electric ray *Torpedo califonica* as a protein localized in both synapses and nuclei (Maroteaux et al., 1988). If aSyn is enriched at synaptic terminals, it is also observed at different subcellular compartments including the plasma membrane, mitochondria, and LDs (Cole et al., 2002; Martinez-Vicente et al., 2010; Outeiro and Lindquist, 2003; Thiam et al., 2013a).

aSyn is only found in the vertebrate lineage (Siddiqui et al., 2016), no synuclein orthologue has been identified in *Drosophila*. The Human genome encodes 2 other genes of the synuclein family: beta, and gamma-synuclein (Surguchov, 2008). The physiological

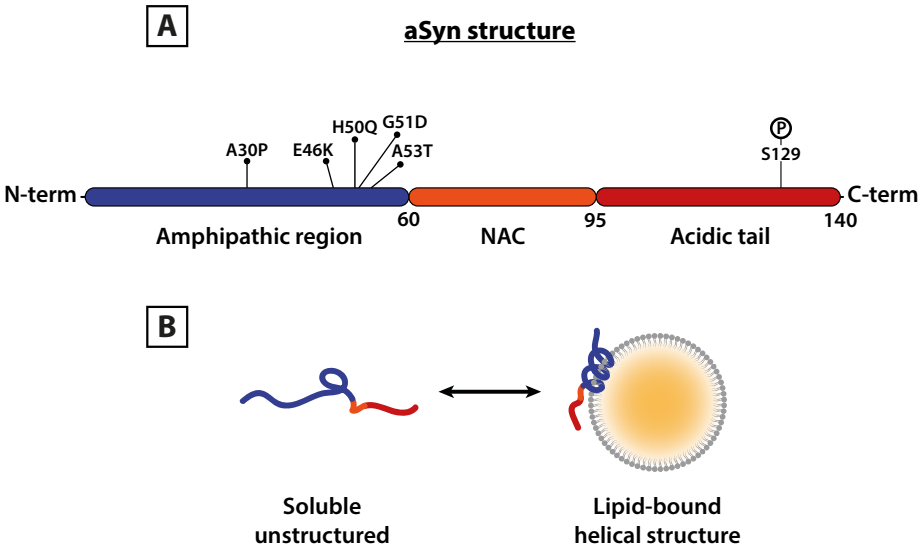

Figure 17. Scheme of aSyn structure

(A) aSyn structure is constituted of an N-term amphipathic helix with the capacity to bind lipids, the NAC domain, and the C-term domain. aSyn familial mutations are all located in the amphipathic domain. aSyn phosphorylation in S129 is associated with increased toxicity (B) Upon biding to membrane or LD aSyn structure is converted from random coil to alpha-helical.

function of aSyn is still matter of debate but evidences point to a role in synaptic vesicles and neurotransmitters release (Selkoe, 2017). Knockout of aSyn and triple knockout of alpha, beta, gamma synuclein cause alteration of synaptic structure including reduction in size of presynaptic button (Abeliovich et al., 2000; Bendor et al., 2013; Chandra et al., 2004; Greten-Harrison et al., 2010; Logan et al., 2017).

aSyn contains 3 main structural domains (Figure 17). (1) a N-terminal domain containing 11-amino acid repeats containing KTKEGV motifs typical of amphipathic helix found in lipid binding protein such as Perilipins, (2) a central hydrophobic domain called the Non-Amyloid ß Component (NAC) domain and (3) an acidic C-term containing aspartate and glutamate that can be phosphorylated (Bisaglia et al., 2006; Bussell and Eliezer, 2003).

To date, six aSyn mutations causing monogenic forms of PD have been identified (A30P, A53T, E46K, H50Q, G51D, A53E). These forms are thought to increase aSyn aggregation by inhibiting aSyn degradation (Cuervo et al., 2004). In addition, it is interesting to note that all these mutations affect the lipid-binding domain of aSyn, suggesting a particular importance for lipid binding in PD pathology.

3.1.5. *Drosophila* as a model organism to investigate PD pathology

For the last 20 years, *Drosophila* has been widely used to study the mechanisms of neurodegenerative disorders including PD (Feany and Bender, 2000). Three main models exist including heterologous expression of human genes using the UAS/GAL4 system, flies carrying mutation in PD-genes homologs or flies treated with pesticides to model sporadic PD. have been generated to investigate the pathogenic mechanisms associated with the genetic components associated with PD such as aSyn, Pink1 and Parkin.

The brain of *Drosophila* and mammals shares key similarities in structure and functions (see section 2.1). Among the advantages of *Drosophila* for the study of neurodegeneration, we can mention the binary expression system UAS/GAL4 system, which has been instrumental for the heterologous expression of human genes such as aSyn(Brand and Perrimon, 1993; Feany and Bender, 2000). The first example of such models, published by Feany and Bender in 2000, established that expression of human wild-type or mutated aSyn in *Drosophila* neurons promotes neurodegeneration (Feany and Bender, 2000). Flies expressing aSyn show several phenotypes reminiscent of PD including progressive age-dependent locomotor dysfunction, loss of dopaminergic neurons and intracellular accumulation of aggregated forms of aSyn (Auluck et al., 2002; Chen and Feany, 2005; Cooper et al., 2006; Feany and Bender, 2000; Periquet et al., 2007). The severity of the phenotype remains variable from one study to the other and aSyn expression levels may be in part responsible for this discrepancy (Navarro et al., 2014).

Major work has also been conducted using *Drosophila* retina, a non-essential neuronal tissue, that is quite useful to study neuron-glia interaction (Chouhan et al., 2016). For example, a transgenic *Drosophila* carrying an aSyn optimized for insect expression,

which leads to 20 times higher aSyn level than regular transgenic, is associated with an exacerbated phenotype including progressive retina degeneration (Chouhan et al., 2016; Ordonez et al., 2018; Pocas et al., 2015).

Drosophila is also a model of choice to investigate the functions of genes associated with PD, as 75% of human genes involved in disease have homologs in *Drosophila* (Bier, 2005). The analysis of *Drosophila* carrying mutations in PD associated genes is crucial to understand the underlying pathological mechanisms associated with PD (Lessing and Bonini, 2009). For example, the discovery of a link between the parkin E3 ubiquitin ligase and the serine/threonine kinase Pink1 in mitochondria homeostasis was made using *Drosophila* (Greene et al., 2003). Indeed, loss of function of parkin or Pink1, both lead to severely impaired mitochondria morphology in *Drosophila* flight muscles and Parkin overexpression rescues mitochondria defects of Pink1 mutant flies (Clark et al., 2006; Greene et al., 2003; Park et al., 2006).

Finally, *Drosophila* has also been used to investigate the contribution of environmental factors with chemical-induced models of PD (Nagoshi, 2018). *Drosophila* fed with pesticides such as Paraquat or Rotenone, which inhibits mitochondria complex I, are associated with progressive dopaminergic neuron cell death, loss of locomotion and premature death (Cassar et al., 2015; Coulom and Birman, 2004).

3.2. aSyn aggregation

aSyn aggregation is a progressive multi-step process central in the pathogenesis of PD. In physiological conditions, different conformations of aSyn co-exist, including soluble monomers, oligomeric forms such as tetramers and membrane-bound alpha-helical monomers and multimers. However, the physiological functions and pathological relevance of these different aSyn conformational forms are far from understood (Bartels et al., 2011; Burré et al., 2014; Dettmer et al., 2013, 2017; Gould et al., 2014). In PD, the pathological misfolding of aSyn contributes to the formation of abnormal oligomers, aggregates and fibrillary structures as found in Lewy Body (Spillantini et al., 1998). The mechanisms mediating the conversion of physiological to pathological forms of aSyn are under deep scrutiny in both *in vitro* systems and animal models. In this section, I will discuss the steps of the aggregation model and how lipids can contribute to aSyn oligomerization and aggregation.

3.2.1. A multi-step process

The initiation of the aSyn aggregation process is a random event, which occurs more frequently as the organism age. This may be due to the fact that the «cleaning» mechanisms that control the degradation of misfolded and damaged protein, the Autophagosomal–lysosomal system and the Proteasome-ubiquitin are less efficient during aging (Hipp et al., 2019). When those cleaning machineries are impaired, misfolded aSyn accumulate and

eventually assemble to form abnormal degradation resistant oligomers after a primary nucleation step (Cremades et al., 2012). would then grow by incorporating more aSyn monomers and assemble as ß-sheets rich fibrils that are toxic for cells (Figure 18) (Buell et al., 2014). Finally, fibril fragmentation, could create seeds that would amplify the process by generating secondary nucleation event contributing to the formation of the large amyloid fibrils found in Lewy Bodies (Knowles et al., 2009).

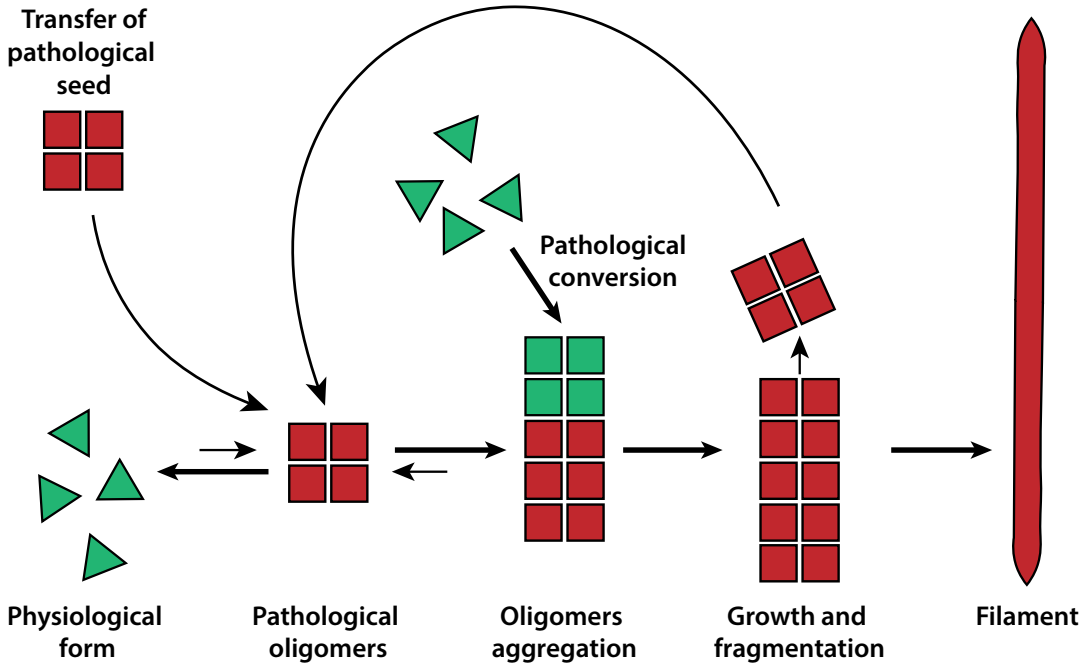

Figure 18. The steps of aSyn aggregation

The formation of pathological aSyn oligomer is a rare event. These abnormal oligomers can then grow by incorporating more aSyn monomers to form fibrillary aggregates. Fragmentation generates seeds, that accelerate the formation of aggregates and can spread to nearby neurons. Filaments are the principal component of Lewy Bodies. Schematic adapted from (Goedert, 2015).

If the aggregation process is random and rare event, one could wonder how it is possible that the whole brain is affected in PD. One hypothesis, inspired by prion diseases, is that abnormal aSyn oligomers and seeds generated in a small number of neurons could transfer from one cell to another and convert physiological aSyn into pathological forms and generate new fibrils (Goedert, 2015). Fragmentation of the new fibrils would repeat the cycle and contribute to the progressive spreading of PD pathology throughout the brain (Goedert, 2015). In line with this hypothesis, intra-cerebral injections of artificially generated aSyn preformed fibrils (PFF), or brain extracts from symptomatic mice triggers aSyn pathology in wild-type mice (Luk et al., 2012; Mougenot et al., 2012).

Finally, the question which aSyn pathological form is the more toxic between misfolded monomers, abnormal oligomers or large fibrils remains debated. The formation of large

aggregate could be a protective mechanism (Arrasate et al., 2004; Lázaro et al., 2014). The formation of large inclusion was associated with neuron survival in primary culture of rat striatal neurons expressing Htt (Arrasate et al., 2004).

3.2.2. Impact of lipids on synuclein aggregation

Research is now showing that these early steps of conformation, oligomerization and aggregation can be influenced by lipids and other factor such as ROS or mutations. The levels and nature of specific lipids can trigger and modulate the kinetic of aSyn oligomer and fibrils formation *in vitro* (Galvagnion, 2017). Upon binding to negatively charged phospholipids and PUFAs, the structure of aSyn is converted from random coil to alpha-helical (Davidson et al., 1998; Sharon et al., 2001). Furthermore, aSyn oligomer and fibril formation is triggered by exposure monounsaturated fatty acids (MUFAs, e.g. Oleic Acid [OA, C18:1]) or some PUFAs (Arachidonic Acid [AA, C20:4] and Docosahexaenoic acid [DHA, C22:6]) in artificial aggregation experiments using recombinant aSyn and in cellular models (Broersen et al., 2006; Davidson et al., 1998; De Franceschi et al., 2011; Fecchio et al., 2018; Sharon et al., 2001, 2003). For example, prolonged exposure to DHA promotes the formation of toxic oligomers and fibrils *in vitro*, detected by Thioflavin T fluorescence. Collectively these studies, indicate that lipid nature (unsaturation and carbon chain length) but also the relative lipid quantity (lipid:protein ratio) are key contributing factors in the initiation of aSyn aggregation process.

The role of sphingolipids in aSyn aggregation has been well documented as well. Mutations in *Glucosylcerebrosidase 1* (*GBA1)* is a main genetic risk factor in sporadic PD (Clark et al., 2007). *GBA1* encodes a lysosomal enzyme responsible for the hydrolysis of sphingolipids, such as Glucosylceramide (GlcCer) and Glucosylsphingosine (GlcSph). Loss of GBA1 activity leads to accumulation of GlcCer in lysosomes, abnormal clearance of aSyn oligomers and increase the likelihood of aSyn aggregation (Mazzulli et al., 2011). Suzuki and al. showed that loss of *Drosophila GBA1* (*dGBA1*) in flies expressing human aSyn, exacerbates aSyn neurotoxicity (Suzuki et al., 2015). Furthermore, accumulation of GlcCer was associated with increase in aSyn proteinase K resistant forms in both *Drosophila* and *in vitro* aggregation assays (Suzuki et al., 2015).

The fact that all known aSyn mutations associated with familial forms of PD affect aSyn lipid-binding domain and that lipids can trigger aSyn aggregation, strengthen the idea that lipids are major contributor in PD. In line with this idea, familial mutations of *SNCA* modulate aSyn binding affinity for negatively charged membrane phospholipids, impair the formation of physiological tetramer and increase formation of f insoluble fibrils (Dettmer et al., 2015; Flagmeier et al., 2016; Lázaro et al., 2014; Rovere et al., 2019; Volles and Lansbury, 2007). For example, the A30P mutation decreases, while E46K and A53T increases, the formation of cytoplasmic inclusion when co-expressed with synphilin-1 in human neuroglioma cells (Lázaro et al., 2014). Furthermore, mutations that aSyn charge

such as E46K enhance aSyn binding to lipid and propensity to aggregate *in vitro* (Rovere et al., 2019). The association of aSyn with membrane is even exacerbated in the artificially engineered "aSyn-3K" (E35K-E46K-E61K). Indeed, aSyn-3K increased association with membrane lipids is associated with a shift of aSyn conformation towards proteinase-K resistant monomers and formation of cytoplasmic inclusions (Dettmer et al., 2015). Mice expressing aSyn-3K, develop a stronger PD-phenotype than mice expressing aSyn wild type including progressive locomotion impairment, loss of dopaminergic neurons and proteinase K resistant inclusions(Nuber et al., 2018). Collectively these results strongly suggest that the modulation of lipid binding by increasing lipid levels or modulating aSyn affinity for lipids may promote the conversion of aSyn to forms prone to aggregate.

3.3. aSyn and LDs: friends or foes?

In parallel to the link between aSyn and lipids on a molecular level (described above), there is now also accumulating evidence that points to systemic dysregulation of lipid metabolism in PD. Lipids levels are modified in the brain of PD patients and animal models of PD (Bosco et al., 2006; Sharon et al., 2003). In addition, mutations in genes involved in lipid metabolism such as *GBA1* (see 3.1.5), the *fatty acid elongase 7* (*ELOVL7*) and a diacylglycerol kinase (*DGKQ*) have been associated with increased risk of PD by multiple GWAS studies (Chang et al., 2017; Klemann et al., 2017; Nalls et al., 2014). Diacylglycerol kinase controls the transformation of DAG into PA (Qiu et al., 2016). Four major lines of evidence indicate an association between aSyn and LDs in PD. First, aSyn can bind LDs in Hela cells and synthetic LDs (Cole et al., 2002; Thiam et al., 2013a). Second, expression of wild type and mutated forms of aSyn leads to LD accumulation in yeast and rat dopaminergic neuronal cell line, N27 cells (Fanning et al., 2019; Outeiro and Lindquist, 2003; Sánchez Campos et al., 2018; Soste et al., 2019). Third, aSyn is also also associated with increased TAG levels in cell culture and animal models (Fanning et al., 2019). Fourth, mutations in genes involved in LD biogenesis such as *Seipin* increase aSyn toxicity (Wang et al., 2018). Collectively, these results strongly suggest that aSyn is interfering with LD homeostasis, and *vice-versa* but the exact mechanism involved and their relevance for PD remain unclear. In yeast, the phenotype of aSyn-induced LDs is associated with elevated levels of intracellular unsaturated FA (Fanning et al., 2019). Interestingly, inhibition of stearoyl CoA desaturase 1 (SCD1), the rate-limiting enzyme of saturated to monounsaturated FA conversion, reduces aSyn toxicity in yeast and in human induced Pluripotent Stem Cells (iPSC) (Fanning et al., 2019; Imberdis et al., 2019). However, the connection between aSyn expression and SCD1 increased desaturase activity has not been explored. Furthermore, this model does not account for a putative direct action of aSyn at the LD surface. Indeed, aSyn binding to LDs delayed lipid remobilization, a function reminiscent of perilipins, in Hela cells loaded with OA (Cole et al., 2002). Interestingly, the close aSyn paralog, gamma-synuclein is expressed in adipocytes, and may limit ATGL-mediated lipolysis (Dunn et al.,

2015; Millership et al., 2012). Collectively these data raise the possibility that the direct association of aSyn and LD could promote LD accumulation in neurons.

4. Objectives

During my thesis, I investigated the mechanisms of formation and contribution of LDs in both neuron and glia in two genetic and pesticide-induced *Drosophila* models of PD.

Firstly, I used flies expressing wild-type and mutated forms of aSyn in *Drosophila* retina as a model to investigate the formation of aSyn-induced LDs in neurons and the contribution of LDs to PD associated phenotypes.

Secondly, I used exposure to Paraquat as a model of sporadic PD. Using this model, I tested the contribution of glial LD homeostasis for the resistance against paraquat-induced neurotoxicity.

Neuronal lipid droplets promote a pathological conversion in alpha-synuclein via a feed-forward mechanism

Victor Girard[1], Florence Jollivet[1], Oskar Knittelfelder[2], Jean-Noel Arsac[3], Gilles Chatelain[1], Daan M. Van den Brink[1,4], Thierry Baron[3], Andrej Shevchenko[2], Nathalie Davoust-Nataf[1,*], Bertrand Mollereau[1,*]

[1] Laboratory of Biology and Modelling of the Cell, UMR5239 CNRS/ENS de Lyon, INSERM U1210, UMS 3444 Biosciences Lyon Gerland, University of Lyon, F-69342, Lyon, France.
[2] Max-Planck-Institute of Molecular Cell Biology and Genetics, Pfotenhauerstraße 108, 01307 Dresden, Germany.
[3] Neurodegenerative Disease Unit; French Agency for Food, Environmental and Occupational Health & Safety (Anses) Laboratory of Lyon, Université de Lyon, Lyon, France.
[4] Plant Systems Physiology, Institute for Water and Wetland Research, Radboud University, PO Box 9010, 6500 GL Nijmegen, The Netherlands.

*Co-senior and co-corresponding authors: nathalie.davoust-nataf@ens-lyon.fr and bertrand.mollereau@ens-lyon.fr

Abstract

Parkinson's disease is a neurodegenerative disorder characterized by accumulation of alpha-synuclein (αSyn) aggregates and by abnormalities in lipid storage. To investigate the potential pathophysiological consequences of interactions between αSyn and proteins that regulate the homeostasis of intracellular lipid droplets (LDs), we employed a transgenic *Drosophila* model of PD in which human αSyn is specifically expressed in photoreceptor neurons. We found that overexpression of the LD-coating proteins perilipin 1 and 2 (dPlin1/2) markedly increased LD accumulation in the neurons. Perilipins also co-localized with αSyn at the LD surface in both *Drosophila* photoreceptor neurons (dPlin2) and human neuroblastoma cells (PLIN3). Co-expression of αSyn and dPlin2 in photoreceptor neurons synergistically amplified LD content through a mechanism involving LD stabilization, independently of *Brummer*-mediated lipolysis or *de novo* synthesis of triacylglycerols. Accumulation of LDs also increased the resistance of αSyn to proteolytic digestion, a phenomenon associated with αSyn aggregation in human neurons. Our results suggest that binding of αSyn to PLIN-coated LDs stabilizes the LD structure and may contribute to the pathogenic misfolding and aggregation of αSyn in neurons.

Introduction

Lipids play crucial roles in many essential cellular functions, including membrane formation, energy production, intracellular and intercellular signal transduction, and regulation of cell death. Fatty acids (FAs) taken up into or synthesized within cells are stored in discrete organelles known as lipid droplets (LDs), which consist of a core of neutral lipids (predominantly triacylglycerols [TGs] and sterol esters), surrounded by a monolayer of phospholipids containing numerous peridroplet proteins (1). Maintenance of LD homeostasis in adipose tissue and the central nervous system, among other tissues, has emerged as a central process for organismal health, and its dysregulation contributes to many human diseases, such as obesity, atherosclerosis, fatty liver disease, and neurodegenerative disorders such as Parkinson's disease (PD) (2–5).

Several peridroplet proteins regulate the homeostasis and abundance of LDs by controlling their biogenesis, degradation, and/or structural stabilization (1). LD biogenesis is initiated at the endoplasmic reticulum membrane, where key lipid metabolic enzymes such as diacylglycerol acyltransferase 1 and 2 (DGAT1, DGAT2) and FA transport protein 1 (FATP1) are recruited. These enzymes synthesize TGs that are incorporated into the LD (6–8). LD degradation is mediated by lipases such as adipose triglyceride lipase (ATGL) and hormone-sensitive lipase (9). In turn, lipase activity is controlled by a family of peridroplet proteins called perilipins (PLINs) that play different roles in LD homeostasis, including maintaining LD integrity, limiting basal lipolysis, and interacting with mitochondria (10). The human genome encodes five PLIN proteins, PLIN1–5 (10), whereas the *Drosophila* genome encodes two PLINs, Lsd-1 and Lsd-2 (hereafter named dPlin1 and dPlin2) (11), that have redundant functions in controlling lipolysis (12,13). *dPlin1* expression, like that of human *PLIN1*, is restricted to adipose tissue, while *dPlin2* and human *PLIN2* and *3* are expressed ubiquitously (14). Although LDs are present in all cells, relatively few types are particularly prone to LD accumulation (15). These include adipocytes and glial cells, which have a higher rate of FA synthesis and express tissue-specific peridroplet proteins that promote the biogenesis or stabilization of LDs or inhibit their lipolytic degradation. About 200 peridroplet proteins have been identified to date (1,16,17), but their cellular specificity and precise involvement in the regulation of LD biogenesis, stabilization, and degradation are largely unknown.

The mechanisms by which fat is stored and remobilized in LDs in adipose tissue are relatively well understood (11); in contrast, less is known about the non-lipid storage functions

of LDs, such as their involvement in the regulation of cellular stress and protein handling, folding, and turnover (1,18). This situation has improved in the last few years; for example, studies with *Drosophila* and vertebrate cellular models have begun to unravel the pathophysiological roles of LDs in regulating stress in cells of the nervous system. Oxidative stress exposure or excitotoxicity induces LD accumulation in developing or adult *Drosophila* and in mouse glial cells co-cultured with neurons (19–23). In *Drosophila* larvae subjected to hypoxia, LD accumulation in glial cells is thought to play a neuroprotective role by enabling relocation of lipids sensitive to peroxidation, such as polyunsaturated FAs, from membrane phospholipids to TGs in the LD core (19). While LDs are abundant in glial cells, they are rarely detected in neurons and little is known about their potential pathophysiological relevance to neurological diseases (24).

PD is characterized by the neuronal accumulation of misfolded proteins, including α-synuclein (αSyn), in cytoplasmic aggregates known as Lewy bodies (25,26). αSyn is a vertebrate-specific 14-kDa presynaptic protein and contains an N-terminal domain consisting of repeated sequences of 11 amino acids that fold into an amphipathic helix upon lipid binding (27). Although the physiological function of αSyn is still unclear, several lines of evidence indicate that αSyn binding to phospholipid membranes is important for vesicle dynamics at the synapse (28). Importantly, αSyn has been shown to bind to LDs and to contribute to LD homeostasis (29,30). However, the underlying molecular mechanisms and the pathological consequences of this interaction are unclear.

We used a Drosophila model in which the neuronal expression of human αSyn has proven useful to study the pathological mechanisms of PD (31–33). We investigated the effects of PLIN and αSyn expression on LD formation in photoreceptor neurons; the subcellular co-localization of αSyn with LDs; the potential contribution of αSyn/PLINs to LD homeostasis via regulation of LD formation, stabilization, and/or degradation; and the potential effects of αSyn–LD binding on the susceptibility of αSyn to misfolding in the context of PD.

Results

αSyn synergizes with PLIN proteins to induce LD accumulation in neurons

Several studies have reported that expression of human αSyn dysregulates TG metabolism and LD homeostasis in cellular and rodent models of PD (29,30,34–36). As noted above, LD homeostasis crucially relies on peridroplet proteins. To determine whether the function of PLINs in LD homeostasis is influenced by αSyn expression, we first established the dynamics of LD homeostasis in *Drosophila* neurons. The *Drosophila* compound eye is composed of 800 ommatidia, each containing six outer and two inner photoreceptor neurons surrounded by nine retina pigment/glial cells (Figure S1) (37). *dPlin1::GFP* (12) and *dPlin2::GFP* (38) were expressed specifically in outer photoreceptor neurons of flies using a rhodopsin 1 (*Rh1*) driver, and the abundance of LDs was assessed by co-labeling of whole-mount retinas with the lipophilic fluorophore Bodipy to label LDs. This analysis revealed that, while LDs were virtually undetectable in the retina of 20-day-old control flies, *dPlin1::GFP* or *dPlin2::GFP* overexpression led to accumulation of LDs (measured as the percentage of the retina area stained with Bodipy, Figure 1A, B). Next, we determined whether this effect of dPlin expression was specific to neurons or also observed in surrounding glial cells, we immunostained the retina for the Na^+/K^+ ATPase α subunit, a marker of the photoreceptor plasma membrane (39). As shown in Figure 1C, *dPlin1::GFP* and *dPlin2::GFP* labeling was visible as rings, characteristic of peridroplet proteins, located within the cytoplasm of photoreceptors but not in the adjacent glial cells. These results indicate that *Rh1*-driven PLIN overexpression leads to accumulation of LDs only in photoreceptor neurons, and not in adjacent glial cells.

Having established that PLIN levels regulate LD accumulation, we next determined whether αSyn co-expression affected LD accumulation in photoreceptor neurons. For this, we employed transgenic *Drosophila* lines expressing wild-type human αSyn^{WT} (31–33,40–42) together with *dPlin2::GFP*; these flies harbor a relatively low level of LDs, thereby enabling the effects of αSyn to be detected (Figure 1D). Notably, while photoreceptor neuron-specific expression of αSyn^{WT} induced a small but insignificant increase in LD accumulation compared with control (LacZ) flies, concomitant expression of αSyn^{WT} and *dPlin2::GFP* resulted in a striking synergistic effect, more than tripling the abundance of LDs compared with either *αSyn* or *dPlin2::GFP* expression alone (Figure 1D and 1E). This result was confirmed using

independent fly lines carrying *UAS-dPlin2::GFP* and *UAS-αSyn^{WT}* transgenes inserted at a different chromosomal localization (Figure S2). Thus, these results indicate that *Drosophila* photoreceptor neurons contain few LDs under normal physiological conditions, and that LD content is significantly increased in a synergistic manner by co-expression of *dPlin2* and *αSyn*.

αSyn and PLINs co-localize at the LD surface in *Drosophila* photoreceptor neurons and in human neuroblastoma cells

Because PLINs are LD membrane-associated proteins, we hypothesized that the synergistic effect of αSyn and PLINs on LD accumulation in neurons might involve co-localization of the proteins at the LD surface. Indeed, immunostaining of αSyn in flies with photoreceptor neuron-specific expression of *dPlin2::GFP* revealed co-localization of the αSyn^{WT} and dPlin2 at the LD surface (Figure 2A). In addition, we examined protein co-localization in the human neuroblastoma cell line SH-SY5Y (43), which expresses *αSyn* at very low levels and was therefore transfected with *αSyn^{WT}*. In these cells, PLIN3 (also known as TIP47), which is broadly expressed in human brain cells (44), co-localized with αSyn^{WT} around circular vesicles, as detected using high-resolution Airyscan microscopy (Figure 2B). To confirm this finding, we performed proximity ligation assays (PLA), in which oligonucleotide-coupled secondary antibodies generate a fluorescent signal when the two target protein-bound primary antibodies are in close proximity (45). Confocal microscopy of SH-SY5Y cells co-labeled with Bodipy and primary antibodies against αSyn^{WT} and PLIN3 revealed PLA signals on the surface of LDs (Figure 2C). Taken together, these experiments confirm that αSyn^{WT} co-localizes with the LD-binding protein dPlin2 in *Drosophila* photoreceptor neurons and with PLIN3 in human neuroblastoma cells.

PLINs promote LD accumulation in neurons by stabilizing LDs, and not by modulating LD formation or Brummer-mediated lipolysis

The mechanism(s) by which αSyn and PLINs might cooperate to promote LD accumulation could be mediated through effects on the formation, stabilization, or degradation of LDs. Indeed, PLINs are known to maintain the structure of LDs and protect

them from lipolysis (46). We first examined how LDs might be degraded in photoreceptor neurons by RNAi interference-mediated depletion of the main TG lipase *Brummer* (Bmm), the *Drosophila* ATGL ortholog (47) using either a pan-retinal (*GMR-GAL4*) or photoreceptor-specific *(Rh1-GAL4*) driver. Knockdown of *Bmm* using *GMR-GAL4* resulted in LD accumulation between adjacent photoreceptor membranes (Na^+/K^+ ATPase α subunit-positive), indicating that prevention of Bmm-mediated lipolysis increased LD accumulation in glial cells (Figure 3A, B). In striking contrast, photoreceptor-specific knockdown of *Bmm* did not increase LD abundance, indicating that Bmm-mediated lipolysis does not influence LD homeostasis in photoreceptor neurons (Figure 3A). The fact that LD degradation in *Drosophila* photoreceptor neurons does not involve Bmm, the main *Drosophila* lipase, is in contrast with what is observed in other tissues (47). It also suggests that αSyn and dPlin1/2 could not induce LD degradation through a mechanism involving lipolysis.

We next asked whether dPlins can enhance LD accumulation by promoting the activity of two canonical enzymes of TG synthesis; dFatp and midway (Mdy). Mdy is a diacylglycerol acyltransferase that is structurally related to mammalian DGAT1 (48). For these experiments, we used *dPlin1:GFP* flies because they produce large easily quantified LDs in photoreceptors (Figure 1C). Whereas pan-retinal knockdown of *dFatp* or *Mdy* reduced the accumulation of LDs in glial cells induced by *Bmm* knockdown (Figure S3), photoreceptor neuron-specific knockdown of either *dFatp* or *Mdy* had no effect on LD accumulation in *dPlin1::GFP*-expressing flies (Figure 3C and 3D).These results indicate that PLIN-induced LD accumulation in photoreceptor neurons probably occurs through a mechanism independent of Bmm inhibition or *de novo* TG synthesis, and is thus distinct from the mechanism of LD accumulation in glial cells.

We then considered that PLINs may stabilize the LD structure, as previously proposed in yeast and *Drosophila* fat cells (12,49). Therefore, we asked whether additional LD-binding proteins might have effects similar to PLIN overexpression. We examined *Drosophila* expressing a fusion protein of GFP bound to the LD-binding domain (LD^{BD}-GFP) of the protein Klarsicht, that is required for the intracellular transport of LDs in *Drosophila* embryos (50,51). Additionally, we tested flies overexpressing *CG7900*, the *Drosophila* ortholog of FA amide hydrolase *FAAH2*, which contains a functional LD-binding domain (52). Notably, photoreceptor-specific expression of *LD^{BD}-GFP* or *CG7900* (using EP-[UAS] insertion) induced an accumulation of LDs (Figure 3E, 3F, S4) similar to that observed with dPlin overexpression.

Taken together, these results show that overexpression of an LD-binding protein is sufficient to promote LD accumulation in *Drosophila* photoreceptor neurons, thus suggesting that PLIN expression induces LD accumulation by stabilizing the LD structure, at least in part.

Co-expression of αSyn^{A53T} and CG7900 proteins induces LD accumulation in *Drosophila* photoreceptor neurons

Given the crucial role of αSyn aggregates in PD and our demonstration of a link between αSyn and LD accumulation in *Drosophila* neurons, we hypothesized that αSyn–LD interactions might have relevance to PD. To test this, we employed the *GMR>αSyn^{A53T}-CG7900* *Drosophila* line, which expresses a mutant form of αSyn that is not only associated with familial PD but also, like αSyn^{WT}, binds to LDs in HeLa cells and cultured mouse hippocampal neurons (29). In the *UAS-αSyn^{A53T}* transgenic line, the insertion occurs in the promoter region of *CG7900* (Figure 4A, chromosomal position 3R-48; see Materials and Methods). GAL4-mediated transcription of *UAS-αSyn^{A53T}* using the *GMR-GAL4* driver resulted in overexpression of both *CG7900* and *αSyn^{A53T}* (Figure 4A and 4B) and induced the accumulation of LDs, as visualized by Bodipy staining in longitudinal retinal sections (Figure 4C). Electronic microscopy of retina tangential sections of these flies also revealed that LDs accumulated in the cytoplasm of photoreceptors (Figure 4D). Expression of RNAi targeting *CG7900* in the *αSyn^{A53T}-CG7900* transgenic line abolished the accumulation of LDs (Figure S5), indicating that expression of an LD-binding protein was essential to observe the increase in LD accumulation in response to αSyn^{A53T} in photoreceptor neurons, as was also observed for αSyn^{WT}-expressing flies.

Interestingly, lipidomic analyses of retinas revealed that the lipid content of LDs was identical in flies with photoreceptor neuron-specific expression of *αSyn^{A53T}-CG7900* and *αSyn^{WT}* with the exception of TGs, which were enriched in *αSyn^{A53T}-CG7900* -expressing flies (Figure S6). Consistent with this, Bodipy staining was abolished by overexpressing the TG lipase *Bmm* in *αSyn^{A53T}- CG7900* expressing flies (Figure 4E). These results demonstrate that TG is the major lipid in ectopic LD-induced by CG7900.

LDs promote αSyn resistance to proteinase K

In human neurons, αSyn aggregation is a multi-step process involving accumulation of misfolded αSyn, a process that renders αSyn resistant to mild proteolysis using proteinase K

(53,54). Therefore, we determined whether αSyn–LD interactions might influence the physical state/structure of αSyn in *Drosophila* photoreceptor neurons. αSyn resistance to proteinase K was evaluated by western blot analysis of protein extracts from flies overexpressing *αSyn^{A53T}-CG7900*, which accumulate LDs as noted above. αSyn^{A53T} from 30-day-old transgenic flies was more resistant to proteinase K digestion compared with αSyn^{A53T} from 6-day-old flies (Figure 5A and 5B), consistent with an age-dependent conversion of αSyn to misfolded forms. Because LDs also accumulate with advancing age, we examined αSyn resistance in *αSyn^{A53T}-CG7900* flies depleted of LDs by co-expression of Bmm lipase in photoreceptor neurons. Indeed, depletion of LDs abolished the age-related difference in αSyn^{A53T} resistance to proteinase K digestion (Figure 5A and 5B), providing a direct link between LD abundance and aberrant αSyn folding and/or aggregation. To confirm this link, we performed proteinase K-resistance assays on αSyn^{WT} from 6- and 30-day-old flies in which LD accumulation is increased by *dPlin2* and *αSyn^{WT}* co-expression. We observed that proteinase K-resistance was increased when LD abundance was synergistically increased by expression of both *αSyn^{WT}* and *dPlin2* compared to *αSyn^{WT}* alone in 6-day-old flies (Figure S7A and S7B). This indicates that LD abundance had a crucial influence on αSyn^{WT} proteinase K-resistance. Taken together, these results substantiate our conclusion that LD accumulation enhances the resistance of αSyn to proteinase K.

Discussion

In this study, we investigated the mechanisms that regulate LD homeostasis in neurons, the contribution of αSyn to LD homeostasis, and whether αSyn–LD binding influences the pathogenic potential of αSyn. We found that expression of the perilipins dPlin1 and dPlin2 in *Drosophila* photoreceptor neurons increased LD accumulation and that this was amplified by co-expression of the PD-associated protein αSyn with dPlin2. αSyn co-localized with PLINs on the LD surface in both *Drosophila* photoreceptor neurons and human neuroblastoma cells, as demonstrated by confocal microscopy and PLA assays. PLIN-induced LD accumulation was not dependent on inhibition of ATGL/Bmm or on TG synthesis, suggesting that PLINs act to stabilize existing LDs, rather than to promote their formation or degradation. Finally, we observed that LD accumulation in photoreceptor neurons was associated with an increase in the resistance of αSyn to proteinase K, suggesting that an increase in LDs might promote αSyn misfolding, an important step in the progression to PD. Thus, we have uncovered a potential novel role for LDs and PLINs in the pathogenicity of αSyn in PD.

Our understanding of the mechanisms of LD homeostasis in neurons under physiological or pathological conditions is far from complete. Neurons predominantly synthesize ATP through aerobic metabolism of glucose, rather than through FA β-oxidation, which likely explains the relative scarcity of LDs in neurons compared with glial cells (55). Nevertheless, LD accumulation has been observed in cultured primary rat cortical neurons, rat dopaminergic N27 cells expressing αSyn, and SH-SY5Y cells exposed to 1-methyl-4-phenyl-1,2,3,6-tetrahydropyridine, a dopaminergic neurotoxin prodrug that causes PD-like symptoms in animal models (34–36). Our results indicating that PLIN expression enhances LD content independently of Bmm lipase activity is consistent with previous data showing that neurons from ATGL-mutant mice do not accumulate LDs (56). Moreover, our observation that overexpression of Klarsicht lipid-binding domain or CG7900 phenocopied the effect of PLINs on LD accumulation, supports the possibility that PLINs serve to stabilize LDs, rather than promote their degradation or synthesis. Stabilization of LDs could well be an ancestral function of PLINs, as reported for yeast and *Drosophila* adipose tissue (12,49,57). However, we cannot exclude the possibility that an additional lipase(s) may regulate LD homeostasis in *Drosophila* photoreceptor neurons.

Earlier studies in yeast, rat dopaminergic neurons, and human induced pluripotent stem cells have proposed that αSyn expression induces lipid dysregulation and LD accumulation, but the underlying mechanisms were unclear (30,34,36). Low levels of αSyn accumulation were thought to perturb lipid homeostasis by enhancing unsaturated FA synthesis and the subsequent accumulation of diacylglycerols (DGs) and TGs. In the present study, we showed that αSyn expression alone did not enhance the accumulation of LDs but instead required concomitant overexpression of PLINs. Moreover, αSyn^{WT} expression alone had no effect on DG, TG, or LD content in *Drosophila* photoreceptor neurons. Given that αSyn and PLINs co-localized at the LD surface in both *Drosophila* photoreceptor neurons and human neuroblastoma cells, our results suggest the possibility that LD-associated αSyn could have a direct role in promoting neutral lipid accumulation by stabilizing LDs. Age-related accumulation of PLIN-bound LDs has been observed in fly muscles (58); however, further analyses will be required to determine whether this occurs in neurons and/or whether it is enhanced by αSyn.

The role of LDs in the evolution of PD pathology is the subject of intense scrutiny. LDs have been proposed to protect cells from lipotoxicity. Selkoe and colleagues showed that LD accumulation in yeast cells required TG synthesis, protected against elevated levels of oleic acid or DGs, and prevented αSyn toxicity (34). The results of the present study suggest an alternative but not mutually exclusive role for LDs in promoting αSyn misfolding and conversion to a proteinase K-resistant form. Indeed, increased LD surface could provide a physical platform for αSyn deposition and conversion. In support of this hypothesis, it was previously proposed that αSyn aggregation is facilitated in the presence of synthetic phospholipid vesicles (59). Based on a combination of our results and these observations, we propose a model of LD homeostasis in healthy and diseased neurons (Figure 6). In healthy neurons, relatively few LDs are detected due to a combination of low basal rate of TG synthesis and low expression of peridroplet proteins that promote LD stabilization. In pathological conditions such as PD, possibly in combination with age-dependent accumulation of fat and PLINs (58,60), αSyn and PLINs could cooperate to promote the stabilization and accumulation of LDs in neurons. In this case, a pathogenic feed-forward mechanism is created in which αSyn enhances PLIN-dependent LD stabilization, which, in turn, increases αSyn conversion to a proteinase K-resistant form, culminating in αSyn aggregation and formation of cytoplasmic

inclusion bodies. Collectively, our results raise the possibility that αSyn binding to LDs could be an important step in the pathogenesis of PD.

Material and Methods

Fly Stocks

All flies used for this study were raised on regular yeast medium at 25°C on a 12h light/dark cycle. The fly stocks were obtained as follows. *UAS-αSyn^{WT}* (BL8146), *UAS-αSyn^{A53T}* (BL8148), *UAS-Mdy-RNAi* (BL65963), *UAS-Bmm-RNAi* (BL25926), *UAS-GFP-shRNA* (BL41555), *sGMR-GAL4*, *Rh1-GAL4* (BL8688), *TH-GAL4* (Alex Whitworth/Léo Pallanck), *UAS-CG7900* (EY10020, BL17633), *UAS-LacZ* (BL1777) were from Bloomington *Drosophila* Stock Center. *UAS-dFatp-RNAi* (100124), *UAS-LacZ-RNAi* (51446) and *UAS-CG7900-RNAi* (101025) were from Vienna *Drosophila* Resource Center. *UAS-dPlin1::GFP* (12), *UAS-dPlin2::GFP* (38) (second and third chromosome insertions), and *UAS-Bmm* were kindly provided by R.P. Kuhnlein (University of Graz); *UAS-LD^{BD}-GFP* was provided by M. Welte (51); and *UAS-αSyn^{WT}* (second chromosome insertion) was provided by M.B. Feany.

Cell Culture

The human neuroblastoma cell line SH-SY5Y was obtained from T. Baron (ANSES, Lyon, France) and transfected with 1 µg of a pcDNA3.1 vector containing human αSyn^{WT} cDNA (provided by T. Baron, Anses, Lyon, France) using Effecten transfection reagent (Qiagen). Positive clones were selected using geneticin and cultured in Dulbecco's modified Eagle's medium (DMEM/F-12, Gibco) supplemented with 4.5 g/L D-glucose, 10% fetal bovine serum, 100 U/mL penicillin, and 100 g/mL streptomycin at 37°C. Cells were passaged when they reached 70–80% confluence.

Bodipy Staining

Unless otherwise stated, experiments were performed using 20-day-old female flies. Flies were sedated on ice, decapitated, and the retinas were dissected in a drop of HL3 medium (61). Whole-mount retinas were fixed in 4% paraformaldehyde (PFA), briefly washed in PBS supplemented with 0.1% Triton X-100 (PBS-T), and incubated overnight at 4°C in Bodipy 493/503 (D3922, Molecular Probes) diluted in PBS-T supplemented with 1:400 phalloidin-rhodamine (R415, Molecular Probes). The retinas were rinsed once in PBS-T and then mounted on a bridged slide in Vectashield medium. Samples were examined on a Zeiss LSM800 at the LYMIC-PLATIM – Imaging and Microscopy Core Facility of SFR Biosciences (UMS3444), Lyon, France.

Bodipy Quantification

Retina images were acquired on a Zeiss LSM800 confocal microscope as 16-bit stacks and processed for quantification using ImageJ software (62). Images were first filtered for noise using Gaussian Blur 3D (σ = 1) and projected along the Z-axis. LDs were identified using the Otsu thresholding algorithm. The area of Bodipy staining was measured and divided by the total retinal area as previously described (23).

Immunohistochemistry

Flies were sedated on ice, decapitated, and retinas were dissected in a drop of HL3 medium (61) supplemented with D-glucose (120 mM). Whole-mount retinas were fixed in 4% PFA and permeabilized in PBS supplemented with 0.5% Triton X-100 and 5 mg/mL BSA. Mouse anti-Na+/K+ ATPase α-subunit (a5, DSHB), rabbit anti-GFP (A6455, Invitrogen), mouse anti-αSyn (sc-12767, Santa Cruz Biotechnology), or rabbit anti-dPlin2 (38) a gift from R.P. Kuhnlein) primary antibodies were diluted in blocking solution and incubated with the retinas overnight at 4°C. The samples were then washed and incubated overnight at 4°C in blocking solution containing Alexa Fluor-conjugated anti-mouse Alexa488, anti-rabbit Alexa488, or anti-mouse Alexa647 secondary antibodies together with phalloidin-rhodamine to label F-actin.

SH-SY5Y cells were fixed with 4% PFA for 15 min and permeabilized with PBS containing 5% BSA and 0.05% saponin for 15 min. Cells were then incubated with mouse anti-αSyn (1:2000, sc-12767, Santa Cruz Biotechnology) and rabbit anti-PLIN3 (1:500, NB110, Novus Biologicals) primary antibodies at room temperature for 1 h. The cells were then washed and incubated with Bodipy 493/503 (D3922, Molecular Probes) and Alexa Fluor-conjugated anti-rabbit Alexa488/Alexa546 or anti-mouse Alexa647 secondary antibodies. Nuclei were counterstained with 1 μg/mL DAPI. Slides were mounted in Mowiol 4-88 (Sigma-Aldrich) and imaged with a Zeiss LSM800 confocal microscope.

Proximity Ligation Assay (PLA)

PLAs were performed using Duolink® PLA kits (Sigma) according to the manufacturer's instructions. Briefly, cells were fixed in 4% PFA and incubated with mouse anti-αSyn (1:2000, sc-12767, Santa Cruz Biotechnology) and rabbit anti-PLIN3 (1:500, NB110, Novus Biologicals)

antibodies diluted in PBS containing 5% BSA and 0.05% saponin. The cells were then incubated with Duolink probes (anti-rabbit plus, DIO88002 and anti-mouse minus DIO82004).The PLA signal was revealed using the red Duolink In Situ Detection Reagent (DUO92008) and the cells were stained with Bodipy 493/503 (D3922, Molecular Probes). Nuclei were counterstained with DAPI in Mowiol mounting medium.

Mapping of *UAS-αSyn^{A53T}* Insertion Site

UAS-αSyn^{A53T} genomic localization was mapped using the Splinkerette protocol for mapping of transposable elements in *Drosophila* (63). Briefly, genomic DNA was isolated from one fly (stock BL8148) and digested using BstYI. DNA fragments containing the P-element flanking regions were then amplified using primers specific for pCaSpeR based P-element. The resulting DNA fragments were sequenced and mapped to the *Drosophila* genome using the BLAST platform.

Transmission Electron Microscopy (TEM) of *Drosophila* Eyes

TEM sample preparation was performed as previously described (23). Briefly, *Drosophila* eyes were fixed in 0.1 M cacodylate buffer supplemented with 2.5% glutaraldehyde and 2 mM $CaCl_2$ for 16 h at 4°C. After rinsing with 0.1 M cacodylate, the tissues were contrasted by incubation in 1% OsO_4 in 0.1 M cacodylate buffer for 2 h at room temperature. Tissues were then dehydrated in acetone and mounted in 100% epoxy resin (Epon 812). After resin polymerization, samples were sliced into 60 nm sections, stained with lead citrate, and examined with a Philips CM120 TEM operating at 80 kV.

Lipid Extraction and Quantification by Shotgun Mass Spectrometry

Ten retinas per biological sample were homogenized twice for 5 min each with 1 mm zirconia beads in 300 µl isopropanol using a cooled Tissuelyzer II at 30 Hz. The homogenate was evaporated in a vacuum desiccator to complete dryness, and lipids were extracted as described (64,65). After evaporation, the samples were reconstituted in 300 µL 1:2 $CHCl_3$:MeOH. To quantify sterols, 200 µL aliquots of lipid extracts were evaporated and acetylated with 300 µL 2:1 $CHCl_3$:acetyl chloride for 1 h at room temperature (method modified from (66)). After evaporation, sterol samples were reconstituted in 200 µL 4:2:1

isopropanol:MeOH:$CHCl_3$ with 7.5 mM ammonium formate (spray solution). For sterol and lipidome measurements, samples were diluted 1:1 with spray solution. Mass spectrometric analysis was performed as described (64).

RNA Extraction and qRT-PCR

Total RNA was extracted from three sets of 10 *Drosophila* heads using TRI-Reagent (T9424, Sigma) and RNA was reverse transcribed using an iScript cDNA Synthesis Kit (Bio-Rad) according to the manufacturers' instructions. Quantitative PCR reactions were carried out using FastStart Universal SYBER Green Master mix (Roche Applied Science) on a StepOnePlus system (Applied Biosystems). Primer efficiency (E) was assessed using serial dilutions of cDNA preparations. Standard curves were used to determine the relationship between PCR cycle number (Ct) and mRNA abundance. Relative mRNA quantity (Qr) was calculated as: Qr = $E^{\wedge}Ct_{Rp49}$-Ct_{target}. Qr values were then normalized to control genotype. Experiments were performed using the following primers: *CG7900*: 5′-CTGCTCACTCTCAGCGTTCAG-3′ and 5′-ATATGTGCGAACCAACTCCAC-3′; *Rp49*: 5′-ATCGTGAAGAAGCGCACCAAG-3′ and 5′-ACCAGGAACTTCTTGAATCCG-3′.

Proteinase K-Resistance Assay

Fly heads were homogenized in lysis buffer (50 mM Tris-HCl pH 7.5, 5 mM EDTA, 0.1% NP40, 1 mM DTT, and 1% Protease Inhibitor Cocktail), incubated for 1 h at 25°C, and centrifuged at 13,000 rpm for 1 min. Supernatants were collected and incubated for 30 min at 25°C with proteinase K (0, 0.5, 1, 1.5, or 2 µg/mL). Denaturing buffer TD4215 4X was added to each sample, and proteins were separated in 4%–15% gradient acrylamide gels (Bio-Rad) and transferred to PVDF membranes (Millipore). PVDF membranes were fixed in 4% PFA and 0.01% glutaraldehyde in PBS for 30 min and then blocked in 3% BSA/0.1% Tween/PBS for XX h. Membranes were incubated with rabbit anti-α-Syn (MJFR1, ab138501, Abcam; 1:1000) or mouse anti-β-tubulin (T 6199, Sigma, 1:1000) primary antibodies overnight at 4°C, washed, and incubated with horseradish peroxidase-conjugated anti-mouse IgG or anti-rabbit IgG (both from Pierce, 1:1000). After washing, membranes were incubated with SuperSignal West Dura Chemiluminescence Substrate (Thermo Scientific), and images were acquired using a ChemiDoc MP system (Bio-Rad).

Statistical Analysis

Data are presented as the means ± standard deviation (SD) of three experiments unless noted. Statistical analyses were performed using R software. Differences between groups were analyzed by t-test or ANOVA and Tukey's HSD paired sample comparison test depending on the number of groups, as specified in the figure legends.

Acknowledgements

We thank the ARTHRO-TOOLS and PLATIM microscopy platforms of SFR Biosciences (UMS3444/CNRS, US8/INSERM, ENS de Lyon, UCBL) and the Centre Technologique des Microstructures CTμ at Lyon 1 University. This work was supported by a grant from ENS Fond Recherche to BM. VG was supported by the Laboratory of Modelling and Biology of the Cell, Servier Research Institute, a PhD fellowship from Fondation pour la Recherche Medicale, and salary support from ENS Fond Recherche. Work in the Shevchenko laboratory was supported by Deutsche Forschungsgemeinschaft (grant FOR 2682).

Author Contributions

V.G., N.D. and B.M. designed the experiments. BM obtained funding to support this research. F.J performed the mammalian cell experiments with the help of V.G. G.C. performed the electronic microscopy. V.G. performed the proteinase K resistance assay with the help of J.N.A in T.B.'s laboratory. O.K. performed the mass spectrometry lipidomic analysis in A.S.'s laboratory. V.G. performed all statistical analysis. V.G. prepared the figures and drawings. V.G., B.M. and N.D. wrote the first draft of the manuscript. V.G, N.D. and BM revised the manuscript for critical content.

Conflicts of Interest

The authors declare that they have no competing interests.

Figure Legends

Figure 1. αSyn enhances dPlin2-induced LD accumulation in *Drosophila* photoreceptor neurons.

(A) Longitudinal optical sections of whole-mount retinas from flies expressing *GFP* (control), *dPlin1::GFP*, or *dPlin2::GFP* in photoreceptor neurons (*Rh1-GAL4*). LDs are labeled green (lipophilic dye Bodipy D3922) and photoreceptor rhabdomeres are in magenta (phalloidin-rhodamine labeling of F-actin). Scale bar, 10 μm.

(B) Quantification of LD area expressed as % of total retinal area. Data are from the images shown in (A). Mean ± SD. ***p<0.001 by ANOVA with Tukey's HSD test.

(C) Longitudinal optical sections of whole-mount retinas from flies expressing *dPlin1::GFP* or *dPlin2::GFP* in photoreceptor neurons (*Rh1-GAL4*). Photoreceptor plasma membranes are in cyan (anti-Na^+/K^+ ATPase immunostaining) and rhabdomeres are in magenta(phalloidin-rhodamine labeling of F-actin). dPlin1 and dPlin2 are visible as ring shapes in the photoreceptor cytoplasm (yellow arrowheads). Scale bar, 10 μm.

(D) Longitudinal optical sections of whole-mount retinas from flies expressing LacZ (control) or human αSyn^{WT} alone or in conjunction with *dPlin2::GFP* in photoreceptor neurons (*Rh1-GAL4*). LDs are in green (Bodipy) and photoreceptor rhabdomeres are in magenta phalloidin-rhodamine labeling of F-actin). Scale bar, 10 μm.

(E) Quantification of LD area from the images shown in (D). Mean ± SD. ***p<0.001, ** p<0.05 by ANOVA with Tukey's HSD test.

Figure 2. αSyn co-localizes with PLINs at the surface of LDs in *Drosophila* photoreceptor neurons and human neuroblastoma cells.

(A) Longitudinal optical sections of whole-mount retinas from flies expressing αSyn^{WT} and *dPlin2::GFP* in photoreceptor neurons (*Rh1-GAL4*). αSyn is in magenta (immunostaining) and photoreceptor rhabdomeres are in red (phalloidin-rhodamine labeling of F-actin). White arrowheads indicate co-localization of αSyn and dPlin2 at LDs. Scale bar, 5 μm.

(B) High-resolution Airyscan micrograph of SH-SY5Y neuroblastoma cells transfected with αSyn^{WT}. αSyn and endogenous PLIN3 immunostaining are shown in magenta and green, respectively. Nuclei are counterstained with DAPI (cyan). Arrowheads indicate co-localization of αSyn and PLIN3 staining on LDs. Scale bar, 5 μm.

(C) Proximity ligation assay between αSyn and PLIN3 in SH-SY5Y cells transfected with human αSyn^{WT}. The PLA signal generated by close proximity of the two protein-bound primary antibodies is shown in magenta, LDs are in green (Bodipy), and nuclei are counterstained with DAPI (cyan). Scale bars, 5 μm.

Figure 3. LD abundance in photoreceptor neurons is not affected by knockdown of enzymes involved in TG synthesis (*Fatp*, *Mdy*) or degradation (*Bmm*).

(A) Longitudinal optical sections of whole-mount retinas from flies expressing RNAi targeting *Bmm* lipase under the control of the pan-retinal driver *GMR-GAL4* or the photoreceptor-specific driver *Rh1-GAL4*. LDs are visible in green (Bodipy) and photoreceptor rhabdomeres are in magenta (phalloidin-rhodamine labeling of F-actin). Pan-retinal *Bmm* knockdown leads to LD accumulation in retinal glial cells between photoreceptor cells (left panel), but LDs are not detected in flies with photoreceptor neuron-specific Bmm knockdown (right panel). Scale bar, 10 μm.

(B) Longitudinal optical sections of whole-mount retinas from flies with pan-retinal knockdown of *Bmm* lipase. dPlin2 is shown in green (immunostaining), photoreceptor plasma membrane is in cyan (Na^+/K^+ ATPase immunostaining), and photoreceptor rhabdomeres are in magenta (phalloidin-rhodamine labeling of F-actin). White arrowheads indicate LDs in glial cells, juxtaposed between the plasma membrane and rhabdomeres. Scale bar, 10 μm.

(C) Longitudinal optical sections of whole-mount retina from flies with photoreceptor neuron-specific expression of *dPlin1::GFP* and *LacZ-RNAi* (control), *dFatp-RNAi,* or *Mdy-RNAi*. LDs are in green (Bodipy) and photoreceptor rhabdomeres are in magenta (phalloidin-rhodamine labeling of F-actin). Scale bar, 10 μm.

(D) Quantification of LD area from the images shown in (C). Mean ± SD. ns, not significant, *p<0.05, by ANOVA with Tukey's HSD test.

(E) Longitudinal optical sections of whole-mount retina from flies with photoreceptor neuron-specific expression of *LacZ* (control), Klarsicht lipid-binding domain (LD^{BD}-GFP), or the *FAAH2* ortholog *CG7900*. LDs are shown in green (Bodipy) and photoreceptor rhabdomeres in magenta (phalloidin-rhodamine labeling of F-actin). Scale bar, 10 μm.

(F) Quantification of LD area from the images shown in (E). Mean ± SD. ***p<0.001 by ANOVA with Tukey's HSD test.

Figure 4. Characterization of the *P{UAS-αSyn^{A53T}}CG7900* transgenic line promoting LD accumulation in photoreceptors

(A) Schematic illustration of the genomic localization of the *P{UAS-αSyn^{A53T}}* transgene mapped using the Splinkerette protocol. The P element carrying the yeast minimal promoter UAS upstream of the coding sequence of human *αSyn^{A53T}* is inserted in the promoter region of *CG7900*.

(B) qRT-PCR analysis of *CG7900* mRNA in whole flies expressing *LacZ, αSyn^{A53T}-CG7900,* or *CG7900* (EP-[UAS] insertion, EY10020) under the control of the pan-retinal driver *GMR-GAL4*. mRNA levels are expressed as the mean ± SD of triplicates relative to the level in control (*GMR>LacZ*) flies.

(C) Longitudinal optical sections of whole-mount retinas from flies with pan-retinal expression of *GFP* or *αSyn^{A53T}-CG7900*. LDs are shown in green (Bodipy) and photoreceptor rhabdomeres are in magenta (phalloidin-rhodamine labeling of F-actin). Scale bar, 20 μm.

(D) TEM images of ommatidia cross-sections from 60-day-old flies with pan-retinal expression of *GFP* (top panel) or *αSyn^{A53T}-CG7900* (bottom panel). Each panel shows a representative cross-section of one ommatidium containing seven photoreceptors (false-colored blue) with central rhabdomeres (R) surrounded by retinal glial cells (false-colored orange). Yellow asterisks indicate LDs accumulating in the photoreceptor cytoplasm of flies expressing *αSyn^{A53T}-CG7900*. Scale bar, 2 μm.

(E) Longitudinal optical sections of whole-mount retinas from flies expressing *αSyn^{A53T}-CG7900* alone or in conjunction with Bmm in photoreceptors (*Rh1-GAL4*). LDs are shown in green (Bodipy) and photoreceptor rhabdomeres are in magenta (phalloidin-rhodamine labeling of F-actin). Scale bar, 20 μm.

(F). Quantification of LD area from the images shown in (E). Mean ± SD. ***p<0.001 by t-test.

Figure 5. LD depletion by expression of *Bmm* lipase reduces αSyn resistance to proteinase K.

(A) αSyn proteinase K-resistance assay. Lysates of the heads of 6- and 30-day-old flies with photoreceptor neuron-specific expression of *αSyn^{A53T}-CG7900* and either *LacZ* (control) or *Bmm* lipase were digested with the indicated concentrations of proteinase K and then immunoblotted for αSyn or β-tubulin (loading control).

(B) Quantification of proteinase K-resistant αSyn, as analyzed in (A). Resistance is expressed as the ratio of undigested αSyn remaining after treatment with 2 μg/mL of proteinase K relative to the untreated sample.

Figure 6. Model of the contribution of αSyn to LD accumulation in PD.

Under normal physiological conditions, neurons contain relatively few LDs. We propose the following scenario under pathological conditions associated with elevated levels of αSyn and dPlin2: **(1)** LDs are stabilized by the increase dPlin2; **(2)** αSyn binds to the expanding dPlin2-positive LDs, which further increases LD accumulation; **(3)** αSyn is converted to a proteinase K-resistant form(s) on the surface of LDs; and **(4)** the aberrant form of αSyn may aggregate at the surface of or in close proximity to LDs, leading to formation of cytoplasmic inclusion bodies (67).

Bibliography

1. Olzmann JA, Carvalho P. Dynamics and functions of lipid droplets. Nat Rev Mol Cell Biol. 2019;20(3):137-**55.**
2. Fanning S, Selkoe D, Dettmer U. Parkinson's disease: proteinopathy or lipidopathy? NPJ Park Dis. 2020;6:3.
3. Farmer BC, Walsh AE, Kluemper JC, Johnson LA. Lipid Droplets in Neurodegenerative Disorders. Front Neurosci. 2020;14:742.
4. Krahmer N, Farese RV, Walther TC. Balancing the fat: lipid droplets and human disease. EMBO Mol Med. juill 2013;5(7):973-83.
5. Pennetta G, Welte MA. Emerging Links between Lipid Droplets and Motor Neuron Diseases. Dev Cell. 21 2018;45(4):427-32.
6. Dourlen P, Sujkowski A, Wessells R, Mollereau B. Fatty acid transport proteins in disease: New insights from invertebrate models. Prog Lipid Res. oct 2015;60:30-40.
7. Thiam AR, Beller M. The why, when and how of lipid droplet diversity. J Cell Sci. 15 2017;130(2):315-24.
8. Walther TC, Chung J, Farese RV. Lipid Droplet Biogenesis. Annu Rev Cell Dev Biol. 06 2017;33:491-510.
9. Zechner R, Zimmermann R, Eichmann TO, Kohlwein SD, Haemmerle G, Lass A, et al. FAT SIGNALS--lipases and lipolysis in lipid metabolism and signaling. Cell Metab. 7 mars 2012;15(3):279-91.
10. Kimmel AR, Sztalryd C. The Perilipins: Major Cytosolic Lipid Droplet-Associated Proteins and Their Roles in Cellular Lipid Storage, Mobilization, and Systemic Homeostasis. Annu Rev Nutr. 17 2016;36:471-509.
11. Heier C, Kühnlein RP. Triacylglycerol Metabolism in Drosophila melanogaster. Genetics. 2018;210(4):1163-84.
12. Beller M, Bulankina AV, Hsiao H-H, Urlaub H, Jäckle H, Kühnlein RP. PERILIPIN-Dependent Control of Lipid Droplet Structure and Fat Storage in Drosophila. Cell Metab. nov 2010;12(5):521-32.
13. Bi J, Xiang Y, Chen H, Liu Z, Grönke S, Kühnlein RP, et al. Opposite and redundant roles of the two Drosophila perilipins in lipid mobilization. J Cell Sci. 1 août 2012;125(Pt 15):3568-77.
14. Itabe H, Yamaguchi T, Nimura S, Sasabe N. Perilipins: a diversity of intracellular lipid droplet proteins. Lipids Health Dis. 28 avr 2017;16(1):83.
15. Beller M, Herker E, Füllekrug J. Grease on—Perspectives in lipid droplet biology. Semin Cell Dev Biol [Internet]. 4 juill 2020 [cité 19 juill 2020]; Disponible sur: http://www.sciencedirect.com/science/article/pii/S108495212030118X
16. Bersuker K, Olzmann JA. Establishing the lipid droplet proteome: Mechanisms of lipid droplet protein targeting and degradation. Biochim Biophys Acta BBA - Mol Cell Biol Lipids. oct 2017;1862(10):1166-77.
17. Bersuker K, Peterson CWH, To M, Sahl SJ, Savikhin V, Grossman EA, et al. A Proximity Labeling Strategy Provides Insights into the Composition and Dynamics of Lipid Droplet Proteomes. Dev Cell. 08 2018;44(1):97-112.e7.
18. Welte MA, Gould AP. Lipid droplet functions beyond energy storage. Biochim Biophys Acta. oct 2017;1862(10 Pt B):1260-72.
19. Bailey AP, Koster G, Guillermier C, Hirst EMA, MacRae JI, Lechene CP, et al. Antioxidant Role for Lipid Droplets in a Stem Cell Niche of Drosophila. Cell. oct 2015;163(2):340-53.

20. Ioannou MS, Jackson J, Sheu S-H, Chang C-L, Weigel AV, Liu H, et al. Neuron-Astrocyte Metabolic Coupling Protects against Activity-Induced Fatty Acid Toxicity. Cell. mai 2019;177(6):1522-1535.e14.
21. Liu L, Zhang K, Sandoval H, Yamamoto S, Jaiswal M, Sanz E, et al. Glial Lipid Droplets and ROS Induced by Mitochondrial Defects Promote Neurodegeneration. Cell. janv 2015;160(1-2):177-90.
22. Liu L, MacKenzie KR, Putluri N, Maletić-Savatić M, Bellen HJ. The Glia-Neuron Lactate Shuttle and Elevated ROS Promote Lipid Synthesis in Neurons and Lipid Droplet Accumulation in Glia via APOE/D. Cell Metab. nov 2017;26(5):719-737.e6.
23. Van Den Brink DM, Cubizolle A, Chatelain G, Davoust N, Girard V, Johansen S, et al. Physiological and pathological roles of FATP-mediated lipid droplets in Drosophila and mice retina. Tennessen JM, éditeur. PLOS Genet. 10 sept 2018;14(9):e1007627.
24. Welte MA. Expanding Roles for Lipid Droplets. Curr Biol. juin 2015;25(11):R470-81.
25. Poewe W, Seppi K, Tanner CM, Halliday GM, Brundin P, Volkmann J, et al. Parkinson disease. Nat Rev Dis Primer. 23 mars 2017;3:17013.
26. Shahmoradian SH, Lewis AJ, Genoud C, Hench J, Moors TE, Navarro PP, et al. Lewy pathology in Parkinson's disease consists of crowded organelles and lipid membranes. Nat Neurosci. juill 2019;22(7):1099-109.
27. Bussell R, Eliezer D. A Structural and Functional Role for 11-mer Repeats in α-Synuclein and Other Exchangeable Lipid Binding Proteins. J Mol Biol. juin 2003;329(4):763-78.
28. Auluck PK, Caraveo G, Lindquist S. α-Synuclein: membrane interactions and toxicity in Parkinson's disease. Annu Rev Cell Dev Biol. 2010;26:211-33.
29. Cole NB, Murphy DD, Grider T, Rueter S, Brasaemle D, Nussbaum RL. Lipid droplet binding and oligomerization properties of the Parkinson's disease protein alpha-synuclein. J Biol Chem. 22 févr 2002;277(8):6344-52.
30. Outeiro TF, Lindquist S. Yeast cells provide insight into alpha-synuclein biology and pathobiology. Science. 5 déc 2003;302(5651):1772-5.
31. Auluck PK, Chan HYE, Trojanowski JQ, Lee VM-Y, Bonini NM. Chaperone Suppression of a-Synuclein Toxicity in a Drosophila Model for Parkinson's Disease. Science. 2002;295(5556):862–865.
32. Feany MB, Bender WW. A Drosophila model of Parkinson's disease. Nature. mars 2000;404(6776):394-8.
33. Ordonez DG, Lee MK, Feany MB. α-synuclein Induces Mitochondrial Dysfunction through Spectrin and the Actin Cytoskeleton. Neuron. janv 2018;97(1):108-124.e6.
34. Fanning S, Haque A, Imberdis T, Baru V, Barrasa MI, Nuber S, et al. Lipidomic Analysis of α-Synuclein Neurotoxicity Identifies Stearoyl CoA Desaturase as a Target for Parkinson Treatment. Mol Cell. mars 2019;73(5):1001-1014.e8.
35. Han X, Zhu J, Zhang X, Song Q, Ding J, Lu M, et al. Plin4-Dependent Lipid Droplets Hamper Neuronal Mitophagy in the MPTP/p-Induced Mouse Model of Parkinson's Disease. Front Neurosci. 2018;12:397.
36. Sánchez Campos S, Alza NP, Salvador GA. Lipid metabolism alterations in the neuronal response to A53T α-synuclein and Fe-induced injury. Arch Biochem Biophys. 1 oct 2018;655:43-54.
37. Mollereau B, Domingos PM. Photoreceptor differentiation in Drosophila: from immature neurons to functional photoreceptors. Dev Dyn Off Publ Am Assoc Anat. mars 2005;232(3):585-92.

38. Grönke S, Beller M, Fellert S, Ramakrishnan H, Jäckle H, Kühnlein RP. Control of fat storage by a Drosophila PAT domain protein. Curr Biol CB. 1 avr 2003;13(7):603-6.
39. Yasuhara JC, Baumann O, Takeyasu K. Localization of Na/K-ATPase in developing and adult Drosophila melanogaster photoreceptors. Cell Tissue Res. mai 2000;300(2):239-49.
40. Chouhan AK, Guo C, Hsieh Y-C, Ye H, Senturk M, Zuo Z, et al. Uncoupling neuronal death and dysfunction in Drosophila models of neurodegenerative disease. Acta Neuropathol Commun [Internet]. déc 2016 [cité 30 nov 2016];4(1). Disponible sur: http://actaneurocomms.biomedcentral.com/articles/10.1186/s40478-016-0333-4
41. Cooper AA, Gitler AD, Cashikar A, Haynes CM, Hill KJ, Bhullar B, et al. α-Synuclein Blocks ER-Golgi Traffic and Rab1 Rescues Neuron Loss in Parkinson's Models. Science. 21 juill 2006;313(5785):324-8.
42. Lessing D, Bonini NM. Maintaining the brain: insight into human neurodegeneration from Drosophila melanogaster mutants. Nat Rev Genet. juin 2009;10(6):359-70.
43. Ryu EJ, Harding HP, Angelastro JM, Vitolo OV, Ron D, Greene LA. Endoplasmic reticulum stress and the unfolded protein response in cellular models of Parkinson's disease. J Neurosci Off J Soc Neurosci. 15 déc 2002;22(24):10690-8.
44. Sjöstedt E, Zhong W, Fagerberg L, Karlsson M, Mitsios N, Adori C, et al. An atlas of the protein-coding genes in the human, pig, and mouse brain. Science. 06 2020;367(6482).
45. Wang S, Yoo S, Kim H-Y, Wang M, Zheng C, Parkhouse W, et al. Detection of in situ protein-protein complexes at the Drosophila larval neuromuscular junction using proximity ligation assay. J Vis Exp JoVE. 20 janv 2015;(95):52139.
46. Brasaemle DL. Thematic review series: adipocyte biology. The perilipin family of structural lipid droplet proteins: stabilization of lipid droplets and control of lipolysis. J Lipid Res. déc 2007;48(12):2547-59.
47. Grönke S, Mildner A, Fellert S, Tennagels N, Petry S, Müller G, et al. Brummer lipase is an evolutionary conserved fat storage regulator in Drosophila. Cell Metab. mai 2005;1(5):323-30.
48. Buszczak M, Lu X, Segraves WA, Chang TY, Cooley L. Mutations in the midway gene disrupt a Drosophila acyl coenzyme A: diacylglycerol acyltransferase. Genetics. avr 2002;160(4):1511-8.
49. Gao Q, Binns DD, Kinch LN, Grishin NV, Ortiz N, Chen X, et al. Pet10p is a yeast perilipin that stabilizes lipid droplets and promotes their assembly. J Cell Biol. 02 2017;216(10):3199-217.
50. Welte MA, Gross SP, Postner M, Block SM, Wieschaus EF. Developmental Regulation of Vesicle Transport in Drosophila Embryos: Forces and Kinetics. Cell. 20 févr 1998;92(4):547-57.
51. Yu YV, Li Z, Rizzo NP, Einstein J, Welte MA. Targeting the motor regulator Klar to lipid droplets. BMC Cell Biol. 24 févr 2011;12:9.
52. Kaczocha M, Glaser ST, Chae J, Brown DA, Deutsch DG. Lipid droplets are novel sites of N-acylethanolamine inactivation by fatty acid amide hydrolase-2. J Biol Chem. 22 janv 2010;285(4):2796-806.
53. Cremades N, Cohen SIA, Deas E, Abramov AY, Chen AY, Orte A, et al. Direct Observation of the Interconversion of Normal and Toxic Forms of α-Synuclein. Cell. 25 mai 2012;149(5):1048-59.
54. Suzuki M, Fujikake N, Takeuchi T, Kohyama-Koganeya A, Nakajima K, Hirabayashi Y, et al. Glucocerebrosidase deficiency accelerates the accumulation of proteinase K-resistant α-

synuclein and aggravates neurodegeneration in a *Drosophila* model of Parkinson's disease. Hum Mol Genet. 1 déc 2015;24(23):6675-86.
55. Schönfeld P, Reiser G. Why does brain metabolism not favor burning of fatty acids to provide energy? Reflections on disadvantages of the use of free fatty acids as fuel for brain. J Cereb Blood Flow Metab Off J Int Soc Cereb Blood Flow Metab. oct 2013;33(10):1493-9.
56. Etschmaier K, Becker T, Eichmann TO, Schweinzer C, Scholler M, Tam-Amersdorfer C, et al. Adipose triglyceride lipase affects triacylglycerol metabolism at brain barriers. J Neurochem. déc 2011;119(5):1016-28.
57. Čopič A, Antoine-Bally S, Giménez-Andrés M, La Torre Garay C, Antonny B, Manni MM, et al. A giant amphipathic helix from a perilipin that is adapted for coating lipid droplets. Nat Commun [Internet]. 6 avr 2018 [cité 23 avr 2020];9. Disponible sur: https://www.ncbi.nlm.nih.gov/pmc/articles/PMC5889406/
58. Yan Y, Wang H, Hu M, Jiang L, Wang Y, Liu P, et al. HDAC6 Suppresses Age-Dependent Ectopic Fat Accumulation by Maintaining the Proteostasis of PLIN2 in Drosophila. Dev Cell. 9 oct 2017;43(1):99-111.e5.
59. Galvagnion C, Buell AK, Meisl G, Michaels TCT, Vendruscolo M, Knowles TPJ, et al. Lipid vesicles trigger α-synuclein aggregation by stimulating primary nucleation. Nat Chem Biol. mars 2015;11(3):229-34.
60. Conte M, Martucci M, Sandri M, Franceschi C, Salvioli S. The Dual Role of the Pervasive « Fattish » Tissue Remodeling With Age. Front Endocrinol. 2019;10:114.
61. Stewart BA, Atwood HL, Renger JJ, Wang J, Wu CF. Improved stability of Drosophila larval neuromuscular preparations in haemolymph-like physiological solutions. J Comp Physiol [A]. août 1994;175(2):179-91.
62. Schneider CA, Rasband WS, Eliceiri KW. NIH Image to ImageJ: 25 years of Image Analysis. Nat Methods. juill 2012;9(7):671-5.
63. Potter CJ, Luo L. Splinkerette PCR for Mapping Transposable Elements in Drosophila. Callaerts P, éditeur. PLoS ONE. 13 avr 2010;5(4):e10168.
64. Knittelfelder O, Prince E, Sales S, Fritzsche E, Wöhner T, Brankatschk M, et al. Sterols as dietary markers for Drosophila melanogaster. Biochim Biophys Acta Mol Cell Biol Lipids. juill 2020;1865(7):158683.
65. Sales S, Knittelfelder O, Shevchenko A. Lipidomics of Human Blood Plasma by High-Resolution Shotgun Mass Spectrometry. In: Methods in Molecular Biology. 2017. p. 203-12.
66. Liebisch G, Binder M, Schifferer R, Langmann T, Schulz B, Schmitz G. High throughput quantification of cholesterol and cholesteryl ester by electrospray ionization tandem mass spectrometry (ESI-MS/MS). Biochim Biophys Acta. janv 2006;1761(1):121-8.
67. Dettmer U, Ramalingam N, von Saucken VE, Kim T-E, Newman AJ, Terry-Kantor E, et al. Loss of native α-synuclein multimerization by strategically mutating its amphipathic helix causes abnormal vesicle interactions in neuronal cells. Hum Mol Genet. 15 2017;26(18):3466-81.

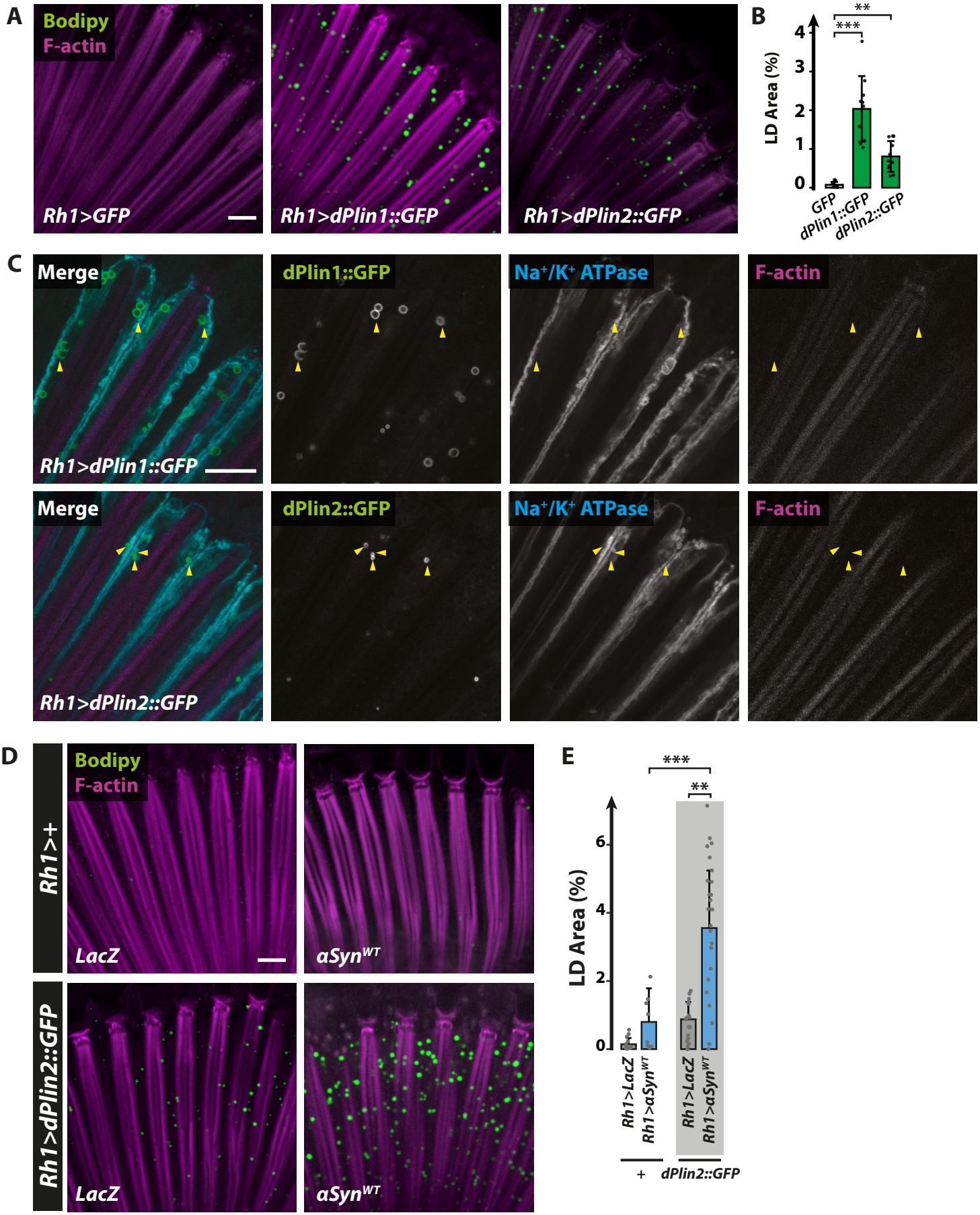
A
Bodipy
F-actin
Rh1>GFP
Rh1>dPlin1::GFP
Rh1>dPlin2::GFP
B
LD Area (%)
0
1
2
3
4
**
***
GFP
dPlin1::GFP
dPlin2::GFP
C
Merge
dPlin1::GFP
Na+/K+ ATPase
F-actin
Rh1>dPlin1::GFP
Merge
dPlin2::GFP
Na+/K+ ATPase
F-actin
Rh1>dPlin2::GFP
D
Rh1>+
Bodipy
F-actin
LacZ
αSynWT
Rh1>dPlin2::GFP
LacZ
αSynWT
E
LD Area (%)
0
2
4
6
***
**
Rh1>LacZ
Rh1>αSynWT
Rh1>LacZ
Rh1>αSynWT
+
dPlin2::GFP

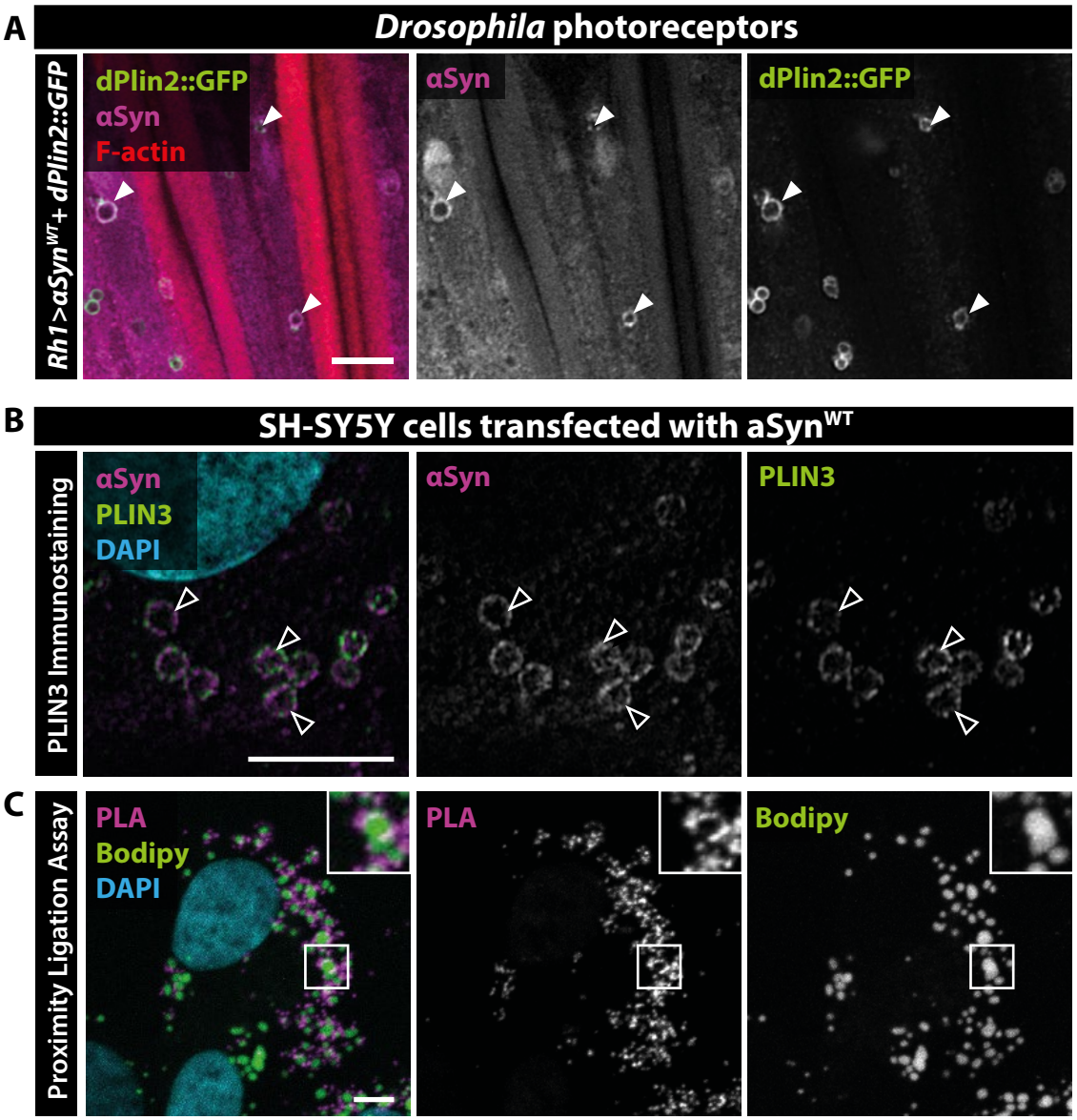
A
Drosophila photoreceptors
Rh1>αSyn^WT+ dPlin2::GFP
dPlin2::GFP
αSyn
F-actin
αSyn
dPlin2::GFP
B
SH-SY5Y cells transfected with aSyn^WT
PLIN3 Immunostaining
αSyn
PLIN3
DAPI
αSyn
PLIN3
C
Proximity Ligation Assay
PLA
Bodipy
DAPI
PLA
Bodipy

Girard et al. Figure 3

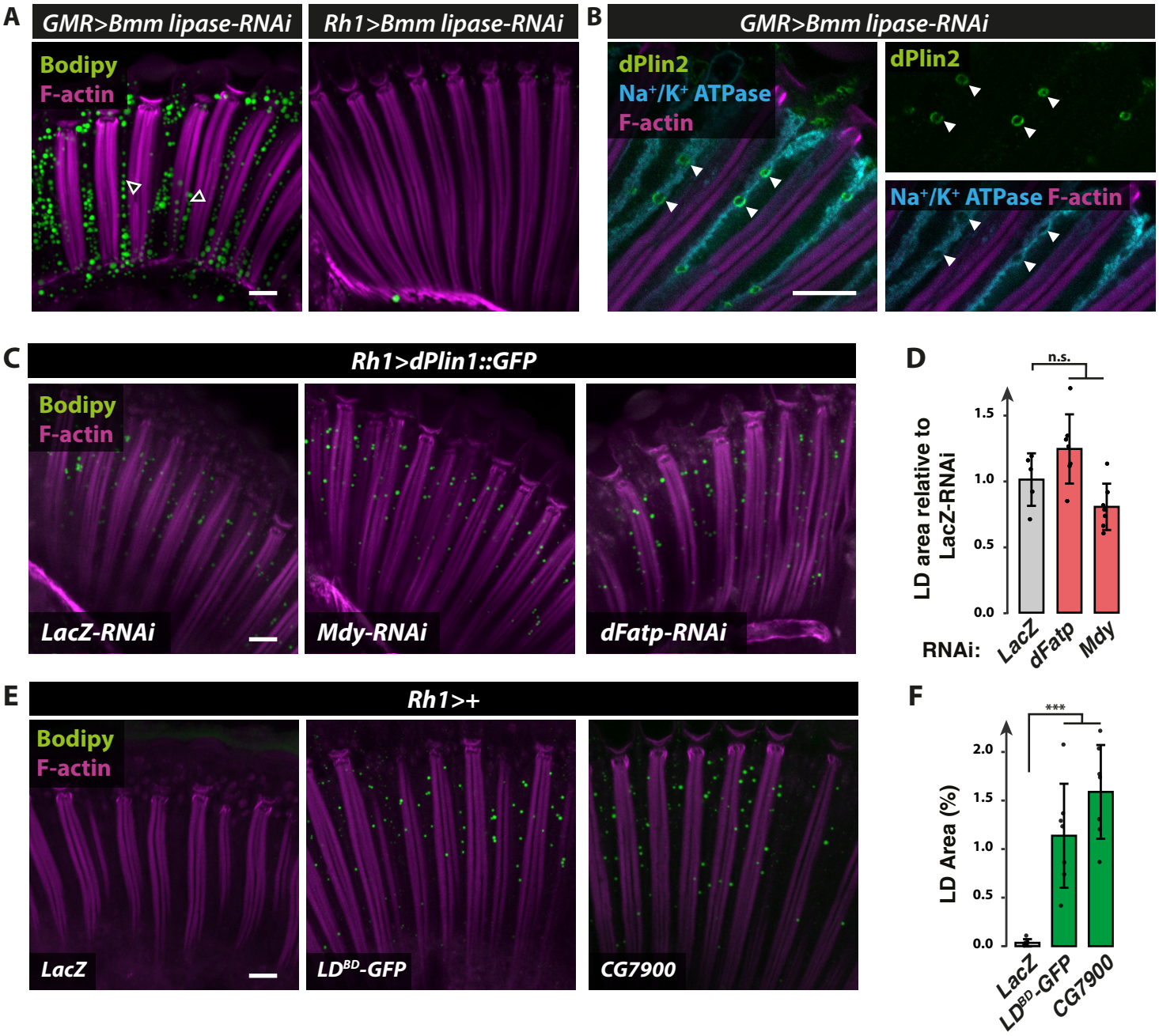

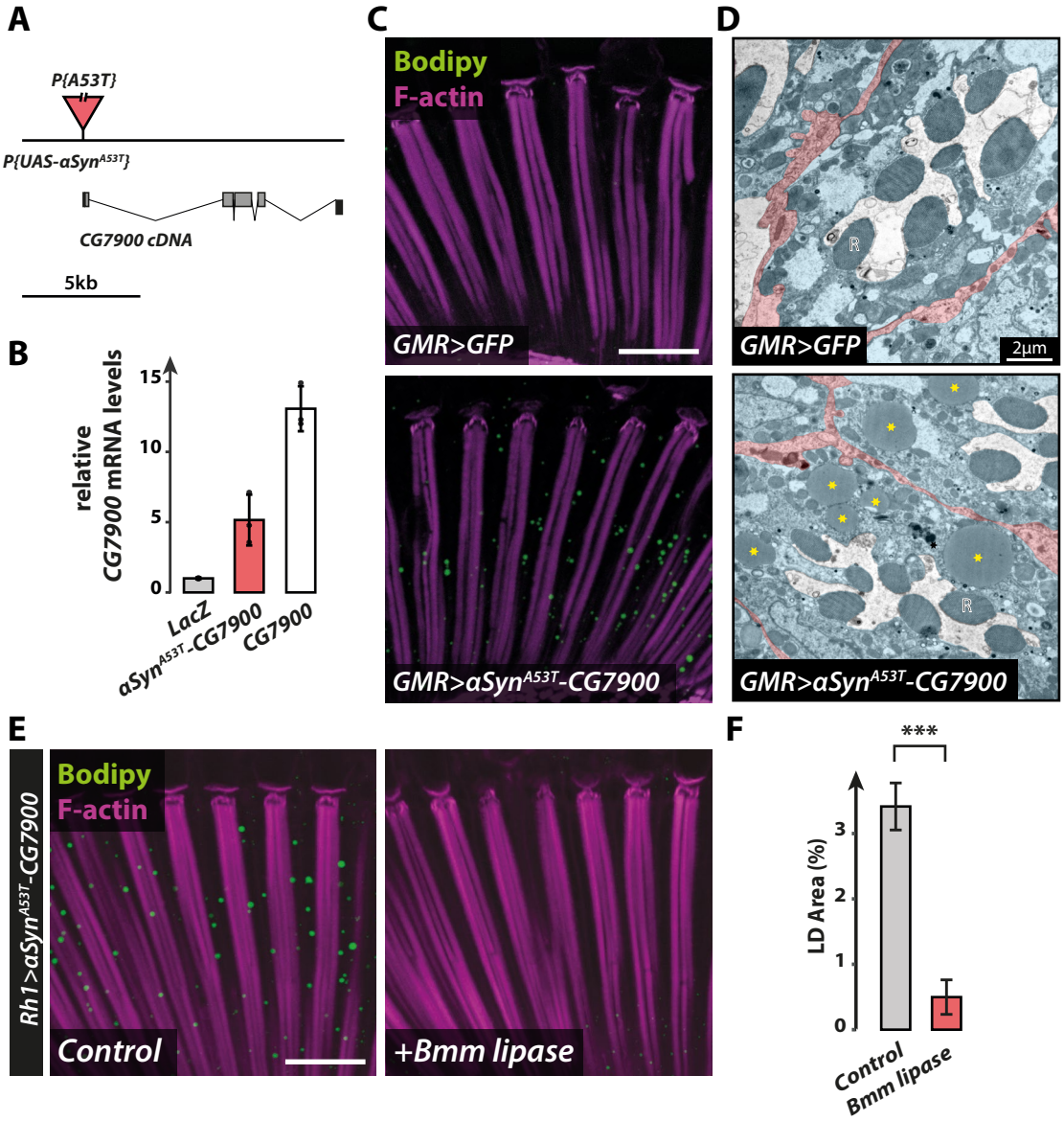
A
P{A53T}
P{UAS-αSyn^A53T}
CG7900 cDNA
5kb
B
relative CG7900 mRNA levels
15
10
5
0
LacZ
αSyn^A53T-CG7900
CG7900
C
Bodipy
F-actin
GMR>GFP
GMR>αSyn^A53T-CG7900
D
GMR>GFP
2µm
GMR>αSyn^A53T-CG7900
E
Rh1>αSyn^A53T-CG7900
Bodipy
F-actin
Control
+Bmm lipase
F
***
LD Area (%)
3
2
1
0
Control
Bmm lipase

Girard et al. Figure 5

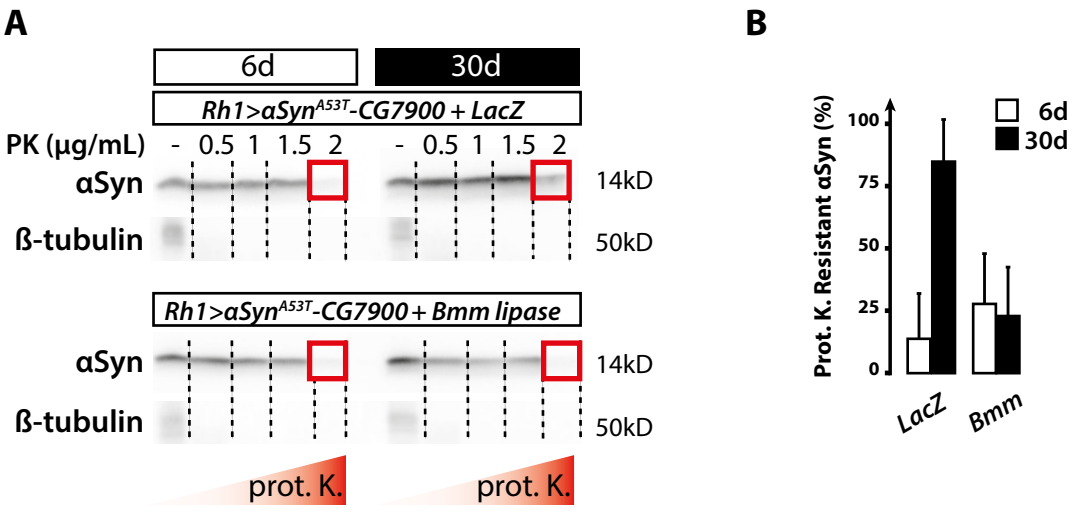

Girard et al. Figure 6

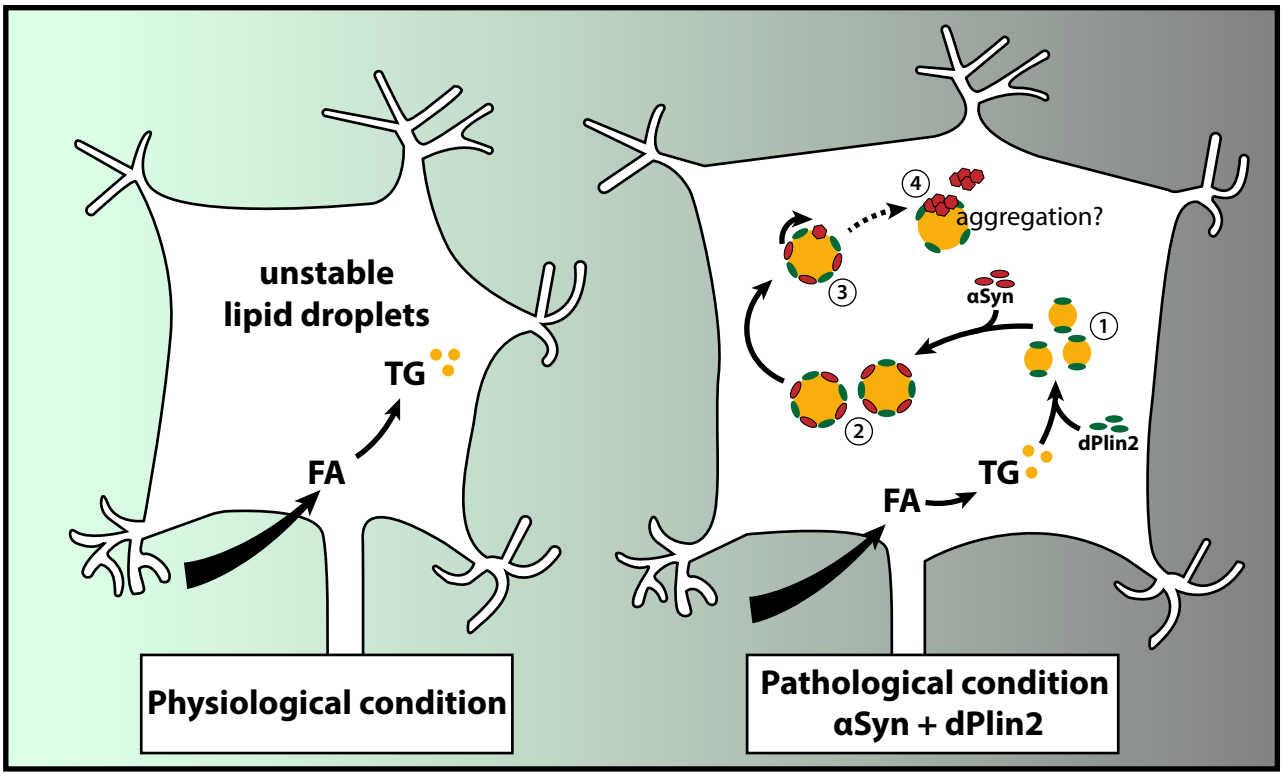

Supplemental Figures

Figure S1. *Drosophila* retinal structure.

(A) Schematic of a *Drosophila* compound eye. The eye is composed of about 800 repeated units called ommatidia (hexagonal shapes). Longitudinal sections (shown in white) of the ommatidia allow visualization of the retinal cells that span the entire width of the retina.

(B) Schematic of a longitudinal section of one ommatidium. Each ommatidium is composed of 8 photoreceptor neurons (light blue), each containing one rhabdomere (dark gray), and 9 glial cells (also known as retinal pigment cells; red and maroon).

(C) Schematic of a cross-section of one ommatidium. In addition to the 9 glial cells (6 secondary [red] and 3 tertiary [maroon]), each ommatidium contains 3 bristle cells (yellow) originating from the neuronal lineage.

Figure S2. αSyn and dPlin2 synergize to induce LD accumulation in photoreceptor neurons.

(A) Longitudinal optical section of whole-mount retinas from flies with photoreceptor neuron-specific expression of *LacZ* (control) or αSyn^{WT} (two independent lines located on second and third chromosome, see Figure 1) alone or in conjunction with *dPlin2::GFP* (independent line inserted on third chromosome). LDs are shown in green (Bodipy) and photoreceptor rhabdomeres are shown in magenta (phalloidin-rhodamine labeling of F-actin). Scale bar, 20 μm.

(B) Quantification of LD area from the images shown in (A). Mean ± SD. ***p<0.001, **p<0.01 by ANOVA with Tukey's HSD test.

Figure S3. *dFatp* or *Mdy* knockdown prevents LD accumulation in glial cells.

(A) Longitudinal optical sections of whole-mount retinas from flies with pan-retinal expression of *UAS-Bmm-RNAi* in conjunction with *GFP*-RNAi (control), *dFatp*-RNAi, or *Mdy*-RNAi. LDs are shown in green (Bodipy) and photoreceptor rhabdomeres are in magenta (phalloidin-rhodamine labeling of F-actin). Scale bar, 20 μm.

(B) Quantification of LD area from images shown in (A). Mean ± SD. ***p<0.001 by ANOVA with Tukey's HSD test.

Figure S4. Expression of GFP-tagged Klarsicht lipid-binding domain induces LD accumulation in photoreceptor neurons.

Longitudinal optical sections of whole-mount retinas from flies with photoreceptor neuron-specific expression of the minimal lipid-binding domain of Klarsicht fused to GFP (*UAS-LD^{BD}-GFP*) (Yu et al., 2011). GFP localizes to the ring-shaped structures (yellow arrowheads) located between photoreceptor plasma membranes (Na^+/K^+ ATPase immunostaining, cyan) and rhabdomere (phalloidin-rhodamine labeling of F-actin, magenta). Scale bar, 10 µm.

Figure S5. Knockdown of *CG7900* prevents LD accumulation in *Drosophila* photoreceptor neurons expressing *αSyn^{A53T}*.

(A) Longitudinal optical sections of whole-mount retinas from flies with pan-retinal expression of *αSyn^{A53T}-CG7900* in conjunction with *GFP-RNAi* (control) or *CG7900-RNAi*. LDs are shown in green (Bodipy) and photoreceptor rhabdomeres are in magenta (phalloidin-rhodamine labeling of F-actin). Scale bar, 20 µm.

(B) Quantification of LD area from the images in (A). Mean ± SD. ***p<0.001 by t-test.

Figure S6. Expression of αSyn^{A53T}-CG7900 induces TG accumulation in *Drosophila* retina.

Main lipid classes detected by shotgun mass spectrometric analysis of retinas from 20-day-old flies with pan-retinal expression of *LacZ* (control, gray bars), *αSyn^{WT}* (blue bars), or αSyn^{A53T}-*CG7900* (red bars). Lipids quantities are expressed as mole % within each species. Data show the mean ± SD of five biological replicates. Expression of *αSyn^{A53T}-CG7900* induces a significant accumulation of triacylglycerols (TG) in *Drosophila* retina. PC, phosphatidylcholine; PE, phosphatidylethanolamine; PA, phosphatidic acid; PI, phosphatidylinositol; PS, phosphatidyl serine; DG, diacylglycerol.

Figure S7. LD accumulation induced by αSyn and dPlin2 co-expression enhances αSyn resistance to proteinase K in *Drosophila* photoreceptor neurons.

(A). Lysates of the heads of 6- and 30-day-old flies with photoreceptor neuron-specific expression of *αSyn^{WT}* and either *LacZ* (control) or *dPlin2::GFP* were treated with the indicated concentrations of proteinase K and then immunoblotted for αSyn or β-tubulin (loading control).

(B) Quantification of proteinase K-resistant αSyn expressed as the ratio of undigested αSyn remaining after treatment with 1.5 µg/mL of proteinase K relative to the untreated sample.

Girard et al. Figure Supplemental 1

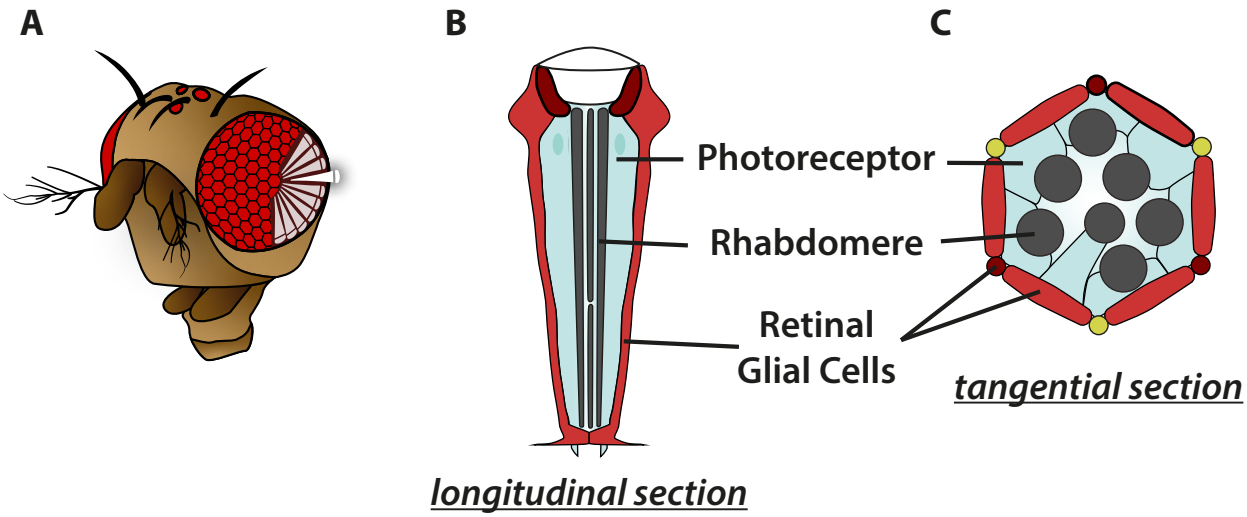

Girard et al. Figure Supplemental 2

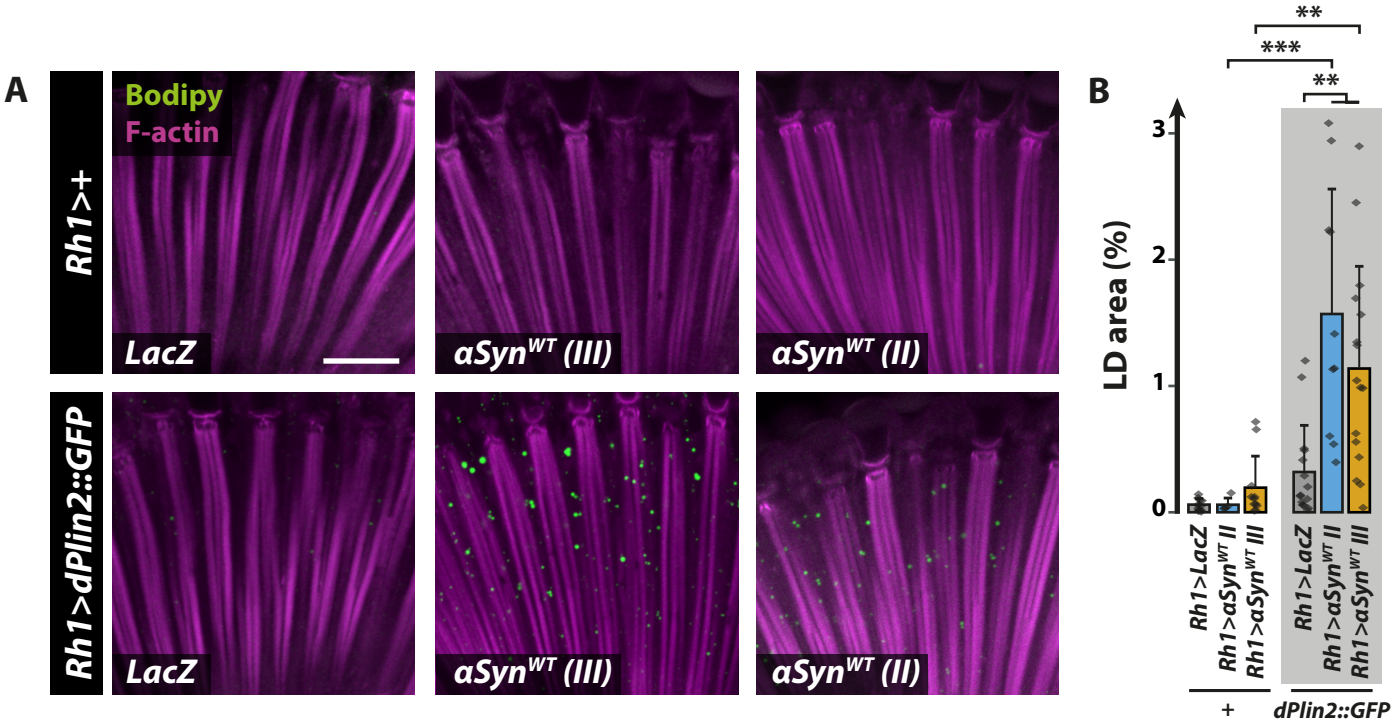

Girard et al. Figure Supplemental 3

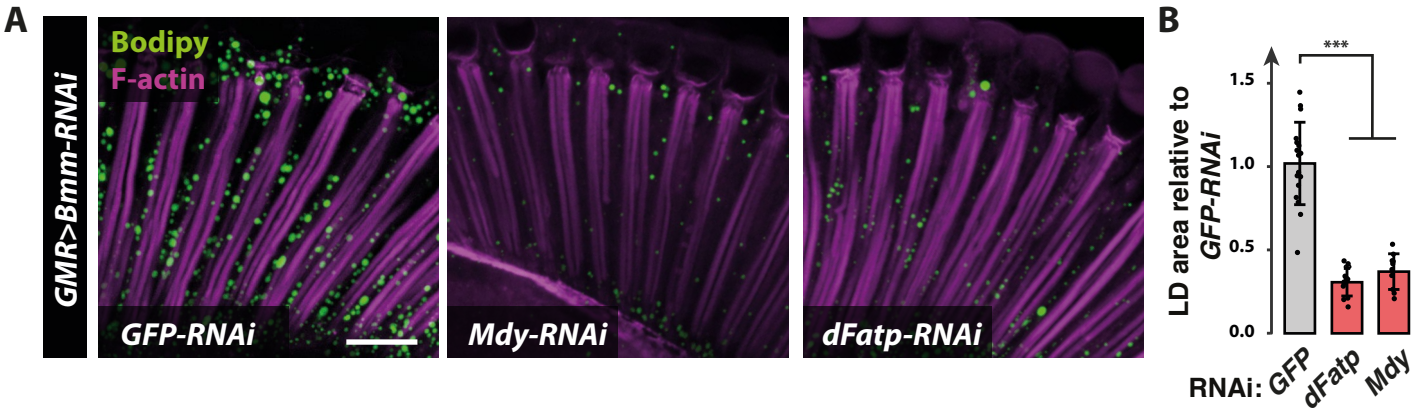

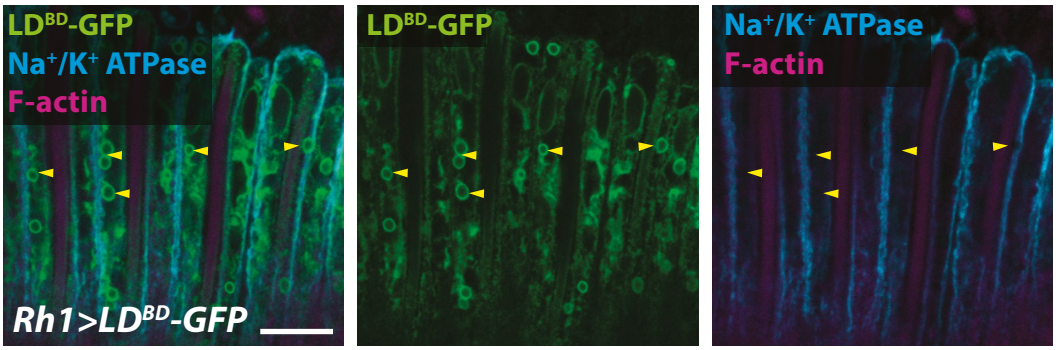
LD^BD-GFP
Na+/K+ ATPase
F-actin
Rh1>LD^BD-GFP
LD^BD-GFP
Na+/K+ ATPase
F-actin

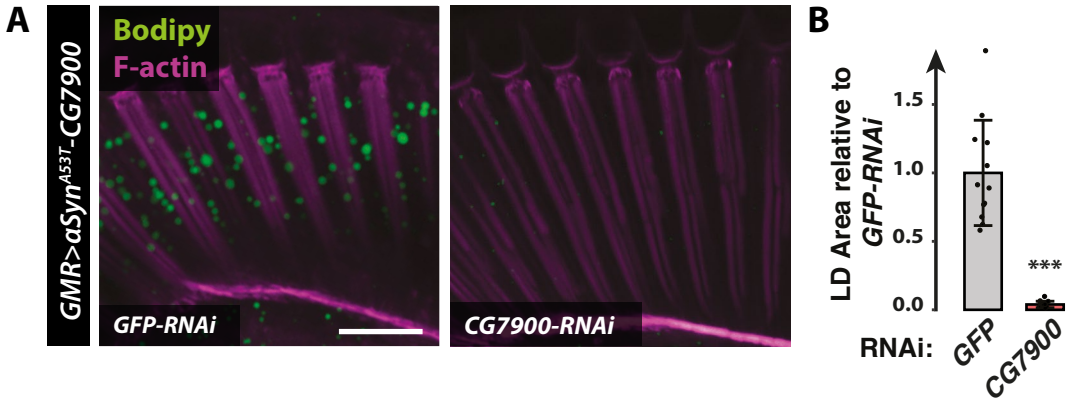
A
GMR>αSyn^A53T-CG7900
Bodipy
F-actin
GFP-RNAi
CG7900-RNAi
B
LD Area relative to GFP-RNAi
1.5
1.0
0.5
0.0
***
RNAi:
GFP
CG7900

Girard et al. Figure Supplemental 6

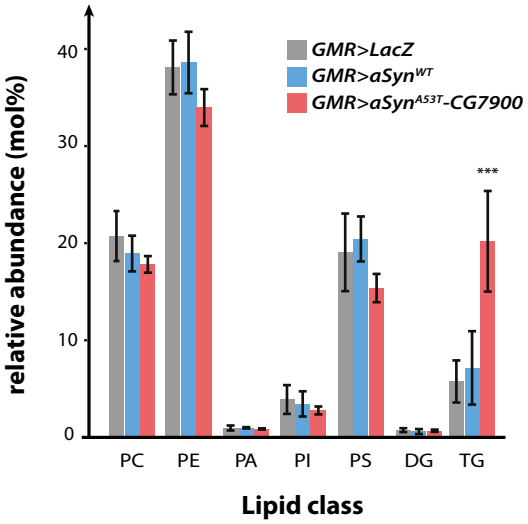

Girard et al. Figure Supplemental 7

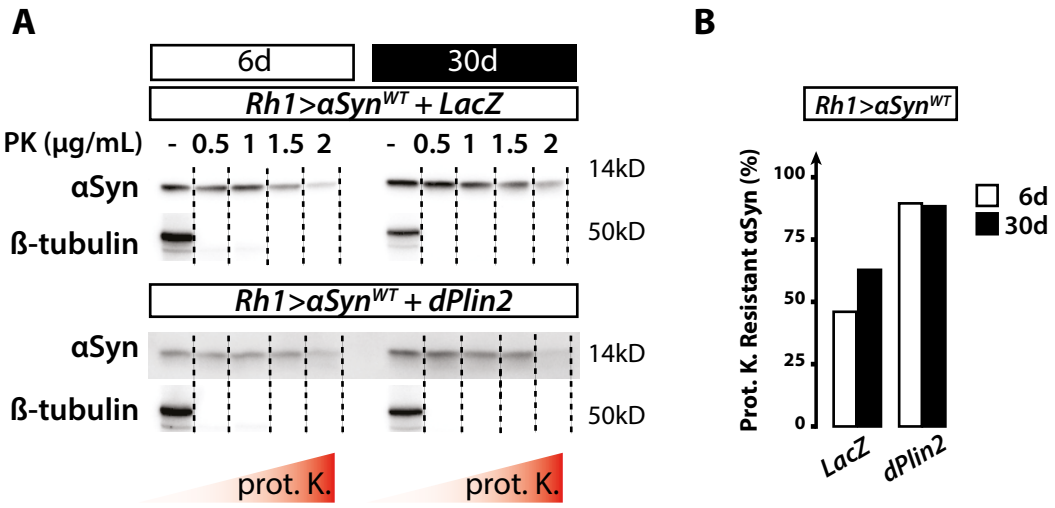

RESULTS

1. Neuronal lipid droplets promote a pathological conversion in alpha-synuclein via a feed-forward mechanism

1.1. Girard et al. (1)

At the beginning of this project, in 2016, the putative physical or functional associations between aSyn and LDs was only investigated in few studies that reported that: 1) aSyn interacts with LDs in mammalian Hela cells (Cole et al., 2002), 2) the expression of wild-type and familial forms of aSyn (A30P and A53T) induces LD accumulation in the yeast *Saccharomyces cerevisiae* (Outeiro and Lindquist, 2003). However, the relevance of these mechanisms for PD pathology remained unclear. In order to investigate the functional association between alpha-synuclein and LDs in neurons, *in vivo*, I used *Drosophila* as a model organism. Expressing human aSyn in *Drosophila* is particularly relevant model because it has previously been shown to recapitulates major features of PD pathology and contains evolutionary conserved genes involved in lipid metabolism and LD formation (Auluck et al., 2002; Feany and Bender, 2000; Heier and Kühnlein, 2018). In particular, *Drosophila* retina has recently become a model of choice to study LD formation in the nervous system (Liu et al., 2015, 2017; Muliyil et al., 2020; Van Den Brink et al., 2018). I thus decided to investigate whether the expression of human aSyn in combination with LD-binding proteins including perilipins could promote the formation of LDs in *Drosophila* photoreceptor neurons from the retina. I first found that expression of LD-binding proteins including *Drosophila* perilipins dPlin1, and dPlin2 was sufficient to induce LD accumulation in photoreceptor neurons. Perilipins-induced LD formation in photoreceptor neurons did not require many of the genes necessary for formation of LDs in *Drosophila* glial cells. I thus hypothesized that binding of proteins to unstable LDs in neurons contributed to LD stabilization and accumulation. Interestingly, simultaneous expression of aSyn and dPlin2, had a synergistic effect on LD accumulation and aSyn and perilipins were colocalized at the LD surface in *Drosophila* photoreceptors and human neuroblastoma cells. Finally, the presence of LDs in photoreceptors increased aSyn resistance to proteinase K suggesting that LDs are involved in the conversion of aSyn to pathological forms, *i.e.* aSyn aggregates resistant to proteinase K enzymatic digestion. I propose that aSyn pathological conversion and LD cytoplasmic accumulation might be linked by a feed-forward mechanism, in which: 1) aSyn promotes LD accumulation in neurons and 2) LDs provide a platform for the conversion of aSyn to proteinase K resistant forms. Collectively these results suggest that neuronal LDs contribute to aSyn pathological conversion and the progression of PD.

1.2. Additional results not included in Girard et al. (1)

We showed in Girard et al. (1) that expression of a set of different LD-binding proteins including dPlin1, dPlin2, CG7900 and Klarsicht LD-binding domain (LD^{BD}-GFP) induce a similar phenotype of LD accumulation in photoreceptor neurons of 20 day-old flies. We found that the accumulation of dPlin1-induced LDs does not require dFatp or Mdy in contrast with what is observed in glial cell accumulating LDs. In addition, we found that the knockdown of Bmm, the homolog of ATGL lipase, which leads to LD accumulation phenotype in glial cells did not lead to LDs in photoreceptors. This suggests that in neurons, dPlin-induced LDs did not result from inhibition of Bmm and that other lipases could be playing this role. We finally describe a *Drosophila* transgenic line co-expressing aSynA53T and CG7900 that induces LDs in photoreceptors. In this section of the thesis manuscript, I will provide additional results regarding the putative mechanisms of accumulation of LDs in the *CG7900-aSynA53T* transgenic line (Girard et al. (1) - Figure 4). I also describe the association between LDs induced by *CG7900-aSynA53T* and mitochondria in photoreceptors. Finally, I show that *Drosophila* dopaminergic neurons expressing dPlin2 also contain LDs.

1.2.1. CG7900, the ortholog of human FAAH-2 is a new LD-binding protein

In mammals, Fatty Acid Amide Hydrolases 1 (FAAH-1) and FAAH-2, hydrolyze and inactivate bioactive endocannabinoids such as N-acylethanolamines (Khaliullina et al., 2015). Interestingly, FAAH-2, contains an amphipathic helix and has been shown to bind LDs in mammalian cells (Kaczocha et al., 2010). We found that expression of CG7900 results in LD accumulation in *Drosophila* photoreceptor neurons much like over-expression of other LD-binding proteins, Perilipins or the LD-binding domain LD^{BD}-GFP. Interestingly, *Drosophila* genome contains 5 predicted FAAH-2 homologs: *CG5112*, *CG5191*, *CG7900*, *CG7910,* and, *CG8839* that share extensive sequence similarities with each other. Two of these genes, CG8839 and CG5112, were found in LD proteomes, of both embryos and S2 cells (Cermelli et al., 2006; Krahmer et al., 2013). FAAH-2 homologs are predicted to catalyze the hydrolysis of a broad range of bioactive lipids, including those from the three main classes of fatty acid amides; N-acylethanolamines, fatty acid primary amides and N-acyl amino acids. Most intriguingly, micromolar amounts of endocannabinoids including N-acylethanolamines have been found in *Drosophila* hemolymph by mass spectrometry (Khaliullina et al., 2015). This indicates that CG7900 and other FAAH family members may be LD binding proteins in *Drosophila* but their tissue specific expression or functions remain to be studied.

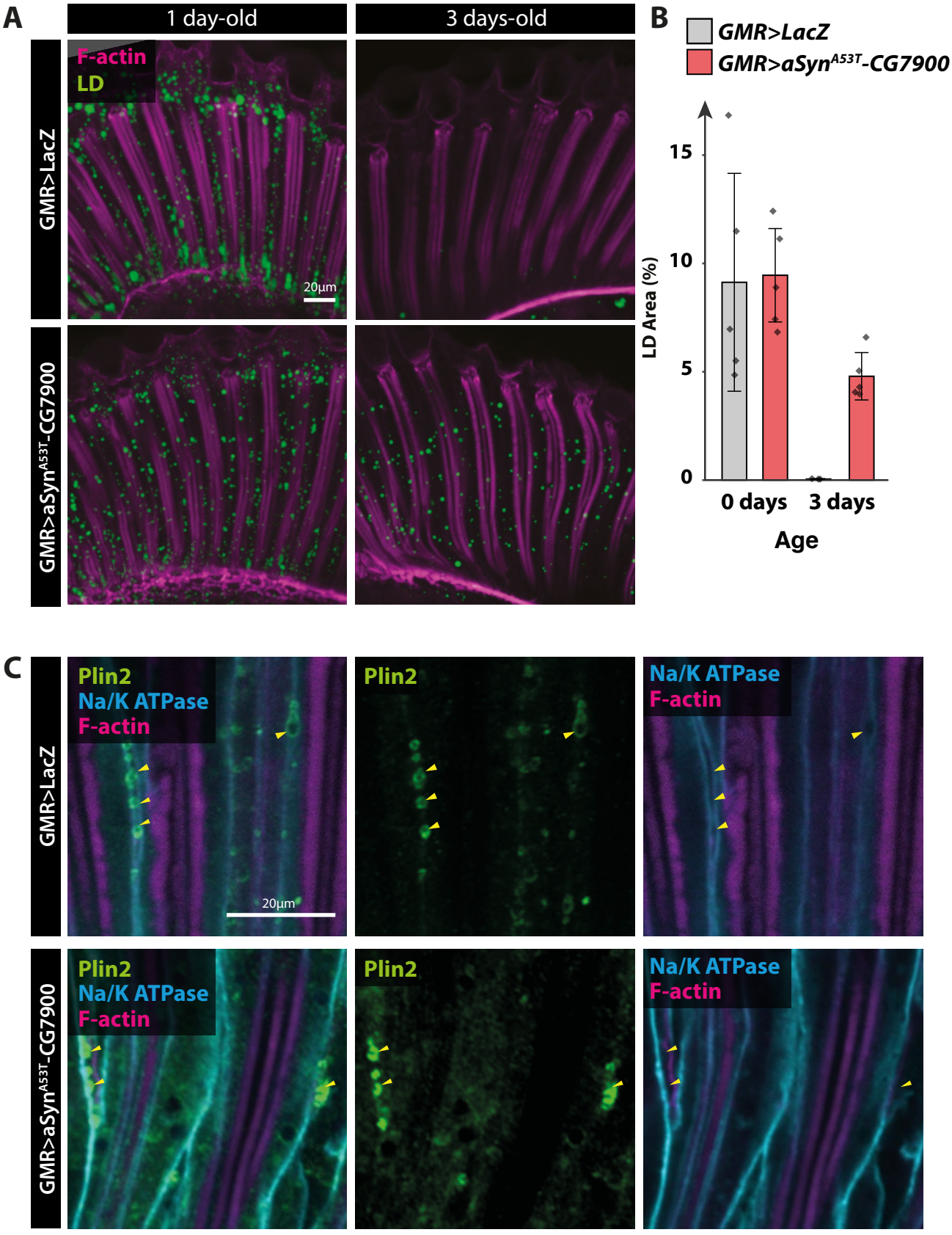
A
1 day-old
3 days-old
GMR>LacZ
GMR>aSyn^A53T-CG7900
F-actin
LD
20µm
B
GMR>LacZ
GMR>aSyn^A53T-CG7900
LD Area (%)
15
10
5
0
0 days
3 days
Age
C
GMR>LacZ
GMR>aSyn^A53T-CG7900
Plin2
Na/K ATPase
F-actin
20µm

Figure 19. *aSynA53T-CG7900* expression does not impact glial LD accumulation in one day-old flies.

(A) Longitudinal optical sections of whole-mount retinas from one and three day-old flies expressing *LacZ* (control) or *aSynA53T-CG7900* using a pan-retinal driver (*GMR-GAL4*). LDs are labeled green (lipophilic dye Bodipy D3922) and photoreceptor rhabdomeres are in magenta (phalloidin-rhodamine labeling of F-actin). Scale bar, 10 µm. (B) Quantification of LD area expressed as % of total retinal area. Data are from the images shown in (A), *GMR>LacZ* (grey) and *GMR>aSynA53T-CG7900* (red). Mean ± SD. ***p<0.001 by ANOVA with Tukey's HSD test. (C) Longitudinal optical sections of whole-mount retinas from one-day old flies expressing *LacZ* or *aSynA53T-CG7900* in photoreceptor neurons and retina glia (*GMR-GAL4*). LDs are labelled green (endogenous dPlin2 immunolabeling), photoreceptor plasma membranes are in cyan (anti-Na^+/K^+ ATPase immunostaining) and rhabdomeres are in magenta (phalloidin-rhodamine labeling of F-actin). dPlin2 is visible as ring shapes in glia cells between the plasma membrane of adjacent photoreceptor neurons (yellow arrowheads). Scale bar, 10 µm.

We previously reported that healthy one day-old flies accumulate LDs in retina glia and to a lesser extend in photoreceptors neurons (Van Den Brink et al., 2018). This phenotype was transient, and by three days, LDs could not be detected anymore in control flies (Figure 19 A, B). In Girard et al. (1), we found that simultaneous expression of *CG7900* and *aSynA53T* using the *aSynA53T-CG7900 Drosophila* transgenic line induced LD accumulation in photoreceptor neurons of 20 day-old flies. I wondered whether the expression of *aSynA53T-CG7900* could modulate the physiological accumulation of LDs in glial cells. I thus stained with Bodipy the retina of one day-old flies expressing *aSynA53T-CG7900* using a pan-retinal driver (*GMR-GAL4*). LDs accumulated to similar levels in one-day old flies expressing LacZ or *aSynA53T-CG7900* ((Figure 19 A, B). This suggests that the expression of *aSynA53T-CG7900* does not impact LD accumulation in glial cells. Moreover, immunostaining of endogenous dPlin2 was visible as ring shapes in retina glia between plasma membranes of adjacent photoreceptors, in one-day old control and flies expressing *aSynA53T-CG7900* in flies (Figure 19 C). This result indicates that expression of *aSynA53T-CG7900* does not impact the transient accumulation of glial LD in one day-old flies.

in cytoplasm of photoreceptor expressing *aSynA53T-CG7900* (white asterisks). Scale bar, 10 µm.

1.2.2. Lipid metabolism genes involved in glial LD accumulation are not required for photoreceptors LD accumulation in of flies expressing *CG7900-aSynA53T*.

In an attempt to characterize the mechanisms of LD formation in photoreceptors of flies expressing *CG7900-aSynA53T*, I performed a RNA-mediated interference screen targeting candidate genes required for LD accumulation in retinal glial cells (Figure 20 A)(Liu et al.,

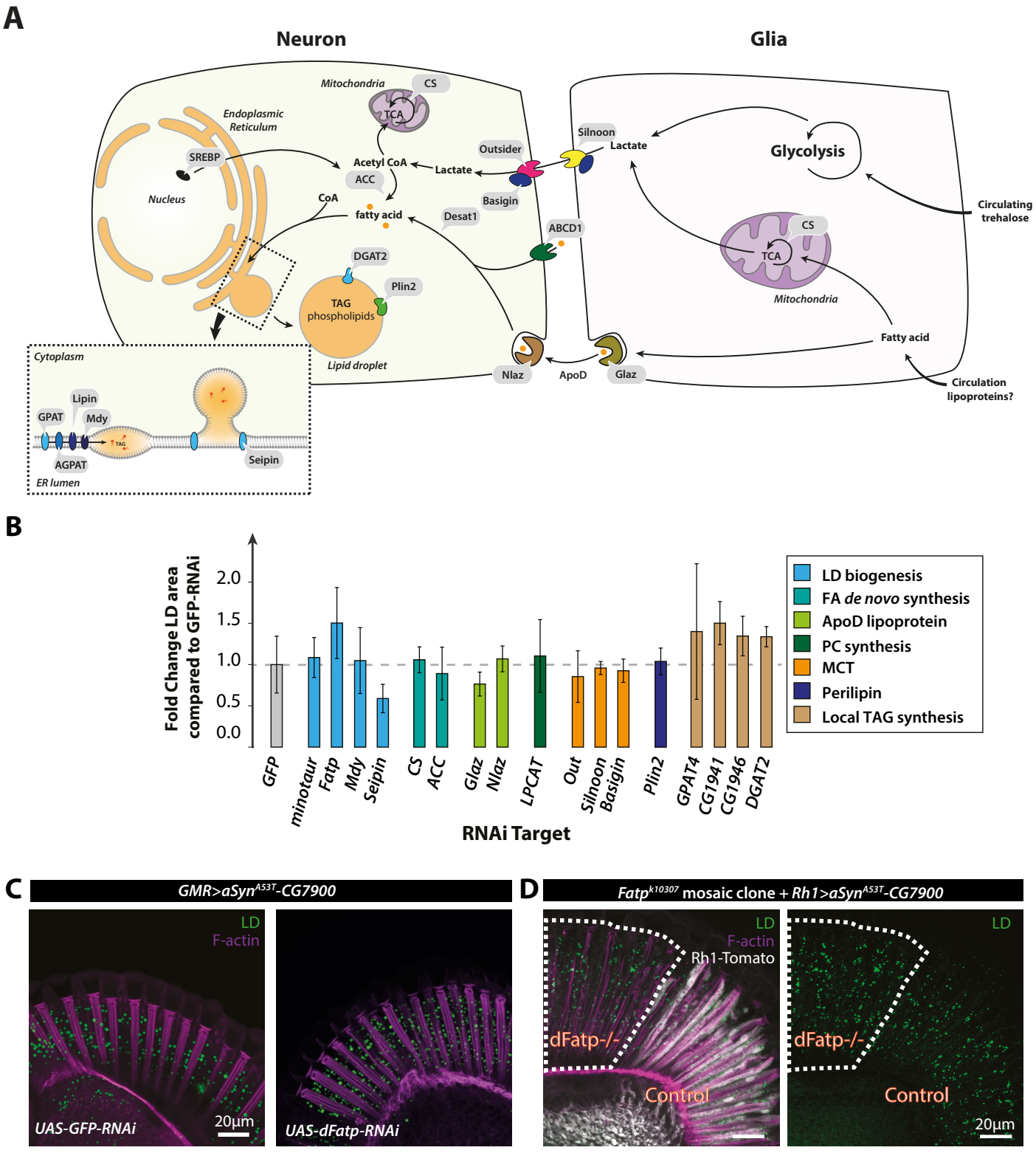

Figure 20. ***aSynA53T-CG7900*** **expression induces LD in photoreceptors independently the main LD biogenesis actors.**

(A) Schematic illustration of possible genes required for LD accumulation in photoreceptor neurons based on actors required for glia LD formation in *Drosophila* retina (Liu et al., 2017; Van Den Brink et al., 2018) and additional important genes. (B) Quantification of LD area relative to control (*GMR>aSynA53T-CG7900 + GFP-RNAi*). Flies expressing *aSynA53T-CG7900* in conjunction

with RNAi targeting gene identified in the schematic illustration in (A). Mean ± SD. Not significant, P>0.05 by ANOVA with Tukey's HSD test. (C) Longitudinal optical sections of whole-mount retinas from flies expressing *aSynA53T-CG7900* in conjunction with *GFP-RNAi* (control) or *dFatp-RNAi* using a pan-retinal driver (*GMR-GAL4*). LDs are labeled green (lipophilic dye Bodipy D3922) and photoreceptor rhabdomeres are in magenta (phalloidin-rhodamine labeling of F-actin). Scale bar, 20 µm. (D) Longitudinal optical sections of whole-mount retinas from flip-out mediated dFatp mutant clone in conjunction with expression of *aSynA53T-CG7900* using pan-retinal driver (*GMR-GAL4*). LDs are labeled green (lipophilic dye Bodipy D3922), wild type photoreceptors are in grey (*FRT40A-Tomato*) and rhabdomeres are in magenta (phalloidin-rhodamine labeling of F-actin). LDs are visible in photorecptors lacking dFatp (mutant clone surrounded by dashed line). Scale bar, 20 µm.

2015, 2017; Van Den Brink et al., 2018). I reasoned that genes including: the canonical TAG synthesis enzyme at the ER (dFatp, GPAT, AGPAT, Mdy, DGAT2, Seipin), Monocarboxylate transporter (Silnoon, Outsiders), and, ApoD homologs, Glial lazarillo (Glaz) and Neural lazarillo (Nlaz) could be required for the formation of LDs in photoreceptor neurons. Surprisingly, none of the genes tested (indicated in the schematic view) reduced significantly the amount of LD accumulating in flies expressing *aSynA53T-CG7900* (Figure 20 A, B, C). In addition, I also expressed *aSynA53T-CG7900* in mosaic clones for *dFatp* mutant generated using *FLP-mediated FRT* recombination, in which *dFatp* mutant clones are recognized by the lack of Rh1-tomato (Figure 20 D). LDs were detected in both wild type and homozygous dFatp mutant clones supporting that dFatp is not required for LD accumulation in photoreceptor. Collectively these results indicate that CG7900 expression, like dPlin1, does not require dFatp or Mdy to induce LDs in photoreceptors. Furthermore, the silencing of genes involved in lactate (Silnoon, Outsiders, and Basigin) and ApoD-dependent lipid transport (Glaz and Nlaz) did not affect the Bodipy labelling induced by *aSynA53T-CG7900,* suggesting that neuronal LD accumulation was not dependent on the traffic of lactate or lipids between glia and neurons.

1.2.3. Knockdown of known lipase in photoreceptor does not recapitulate dPlin1-induced LD in photoreceptor

As the best described function of Perilipins is to regulate lipolysis, we hypothesized that the LD accumulation observed in the retina of flies expressing perilipins may be due to a reduced activity of cytosolic lipases. We found in Girard et al. (1) that knockdown of Bmm using a pan-retinal driver led to LD accumulation in retina glial cells but not in neurons (Girard et al. (1) – Figure 3). This result indicates that dPlin-induced LDs in photoreceptor do not result from Bmm inhibition. One possibility is that LD lipolysis depends on another lipase or a combination of lipases. To test this possibility, we also investigated dHSL mutant but we did not observe any LD accumulation (Figure 21, A). Finally, we knockdown several

other lipases predicted to be expressed in the eye such as PAPLA1, the homolog of DDHD1/DDHD2 and InaE, the homolog of DAGLA (Gáliková et al., 2017; Leung et al., 2008). In both cases, the lipase knockdown did not lead to LD accumulation (Figure 21, B). The fact that lipase knockdown did not recapitulate dPlin-induced LD accumulation observed in photoreceptor suggests that dPlin may induce LDs by a mechanism independent of lipase inhibition, or alternatively dPlin may protect LDs from the redundant activity of several cytosolic lipases.

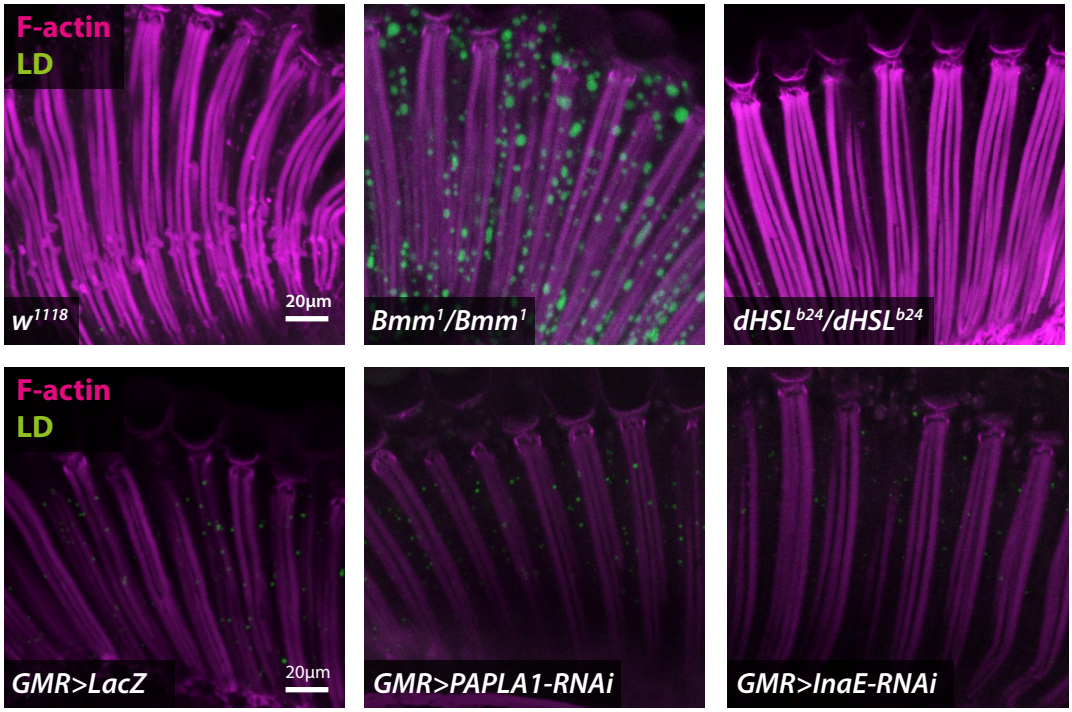

Figure 21. Lipase inhibition is not sufficient to induce LD accumulation in *Drosophila* photoreceptors

(A) Longitudinal optical sections of whole-mount retinas from flies carrying homozygous loss of function mutation in *white*^{1118}, Bmm^{1} lipase and dHSL^{b24} LDs are labeled green (lipophilic dye Bodipy D3922) and photoreceptor rhabdomeres are in magenta (phalloidin-rhodamine labeling of F-actin). Scale bar, 20 µm. (B) Longitudinal optical sections of whole-mount retinas from flies expressing *RNAi* targeting *LacZ, PAPLA1 (homolog of DDHD1/DDHD2 lipase) or inaE (homolog of DAGLA)* under the control of a pan-retinal driver (*GMR-GAL4*). LDs are labeled green (lipophilic dye Bodipy D3922) and photoreceptor rhabdomeres are in magenta (phalloidin-rhodamine labeling of F-actin). Scale bar, 20 µm.

1.2.4. Expression of the catalytically inactive BmmS38A promote LD accumulation in photoreceptor

We described that several LD binding proteins, dPlin1, dPlin2, CG7900 and the Klarsicht LD-binding domain (LD^{BD}-GFP), all lead to a similar LD accumulation when expressed with a neuronal driver in photoreceptors (Girard et al. (1) - Figure1 and 3). This result suggests

that these LD-binding proteins could stabilize unstable LDs resulting in their accumulation in photoreceptors. The Bmm lipase is also a LD-binding protein, which has been found at the surface of LDs, in LD proteome and in *Drosophila* tissues (Beller et al., 2010; Grönke et al., 2005). Interestingly, the Bmm catalytic center mutant (BmmS38A) that lost its ability to degrade LDs by lipolysis retains its ability to bind LDs. I thus hypothesize that if BmmS38A still binds LDs it may be sufficient to stabilize LDs in photoreceptors. Indeed, expression of BmmS38A::GFP, using pan-retinal or and photoreceptor specific drivers led both to LD accumulation (Figure 22). This result strengthens the idea that homeostasis of LD-binding protein is important to maintain healthy levels of LDs. Furthermore, BmmS38A::GFP provides an interesting tool to study lipolysis in photoreceptor neurons. For example, to determine whether simultaneous expression of aSyn and BmmS38A can affect the localization of Bmm at the LDs.

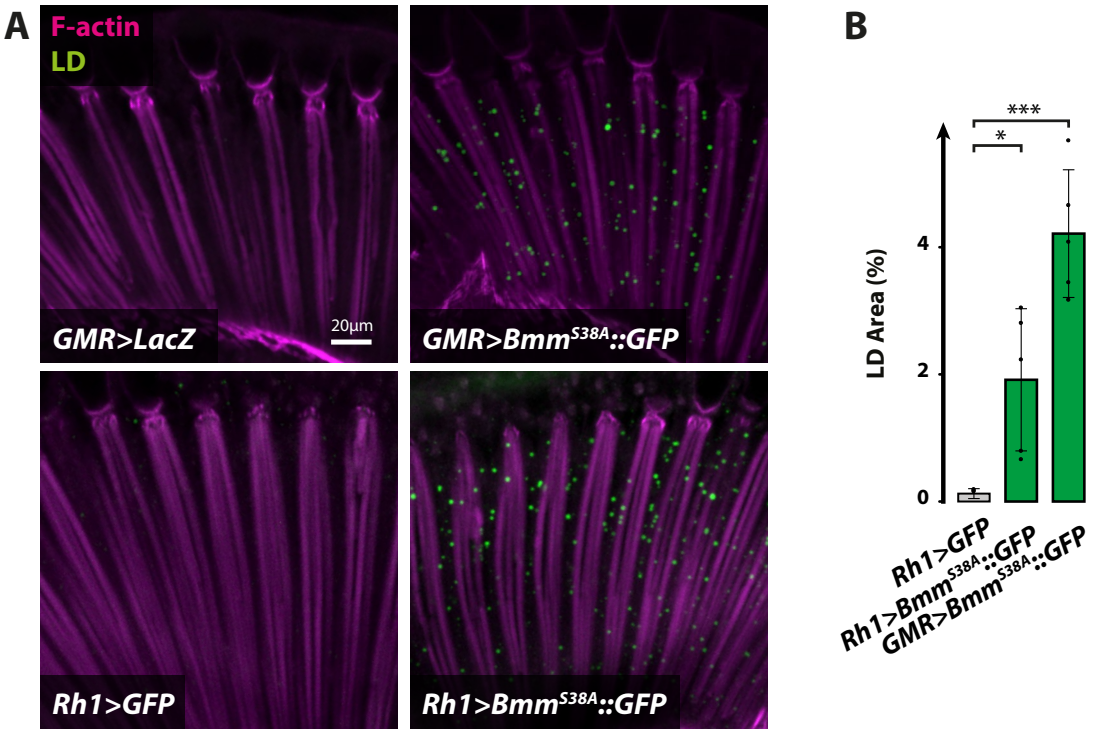

Figure 22. Expression of catalytic inactive *Bmm^{S38A}* induces LDs in photoreceptor neurons.

(A) Longitudinal optical sections of whole-mount retinas from flies expressing *LacZ* (control) or *BmmS38A::GFP* using pan-retinal (*GMR-GAL4*) or photoreceptor specific driver (*Rh1-GAL4*). LDs are labeled green (lipophilic dye Bodipy D3922) and photoreceptor rhabdomeres in magenta (phalloidin-rhodamine labeling of F-actin). Scale bar, 10 µm. (B) Quantification of LD area expressed as % of total retinal area. Data are from the images shown in (A), *GMR>LacZ* (grey) and *GMR>aSynA53T-CG7900* (red). Mean ± SD. ***p<0.001 by ANOVA with Tukey's HSD test.

1.2.5. Mitochondria are in close proximity with LD in *Drosophila* photoreceptor neurons

Although the ER is the main organelle that contacts LDs, mitochondria are also often in contact with LDs. For example, as described in this manuscript (Introduction section), the physical interaction between mitochondria and LDs is important to control lipid shuttling and ß-oxidation in condition of nutrient starvation (Rambold et al., 2015). Alternatively, mitochondria can also promote LD expansion by providing extra ATP for TAG synthesis

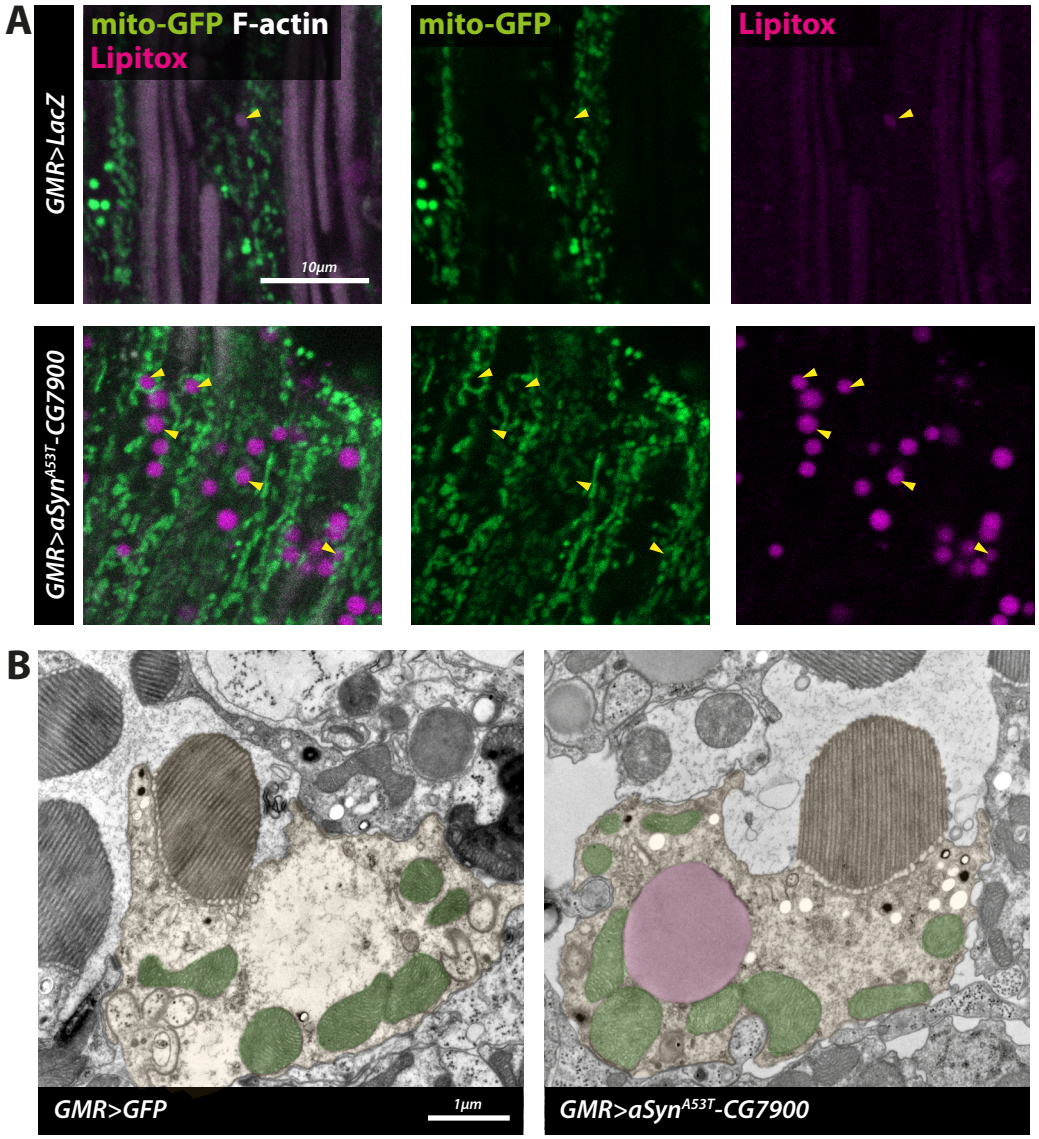

Figure 23. LDs are in close proximity with mitochondria in photoreceptor neurons
(A) Longitudinal optical sections of whole-mount retinas from flies expressing mito-GFP in conjunction with *LacZ* (control) or *aSynA53T-CG7900* using pan-retinal driver (*GMR-GAL4*). Mitochondria are labeled green (mito-GFP), LDs are labeled magenta (lipophilic dye Lipidtox 633) and photoreceptor rhabdomeres are in grey (phalloidin-rhodamine labeling of F-actin). Scale bar, 10 µm. (B) TEM images of a photoreceptor cross-sections from 30-day-old flies

with pan-retinal expression of *GFP* (left panel) or a*Syn^{A53T}-CG7900* (right panel). Each panel shows a representative cross-section of one photoreceptor (false-colored orange) with central rhabdomeres (R). Mitochondria (false-colored greed) are in close proximity to LDs (false-color magenta) accumulating in the photoreceptor cytoplasm of flies expressing a*Syn^{A53T}-CG7900*. Scale bar, 1 μm.

(Benador et al., 2018). I observed that LD accumulation was independent of most TAG synthesis actors, and reasoned that defects in mitochondria dependent lipid catabolism such as a decrease in ß-oxidation may also lead to lipid build-up in neurons. To this end, I first tested whether mitochondria were in contacts with LDs in photoreceptor neurons, using *Drosophila* expressing a genetically encoded mitochondrial fluorescent reporter mito-GFP, stained with lipidtox. Although broad mitochondrial morphology did not seem altered, mitochondria were detected surrounding LDs in flies expressing *aSynA53T-CG7900* (Figure 23, A). Mitochondria were also observed juxtaposed to LDs in retina tangential section using electronic microscopy in flies expressing *aSynA53T-CG7900* (Figure 23, B).

Although neurons, are not known to use lipid as an energy substrate one possible explanation for the proximity of LDs and mitochondria is that photoreceptor mitochondria can use lipid through ß-oxidation to produce energy. I reasoned that if mitochondria function is impaired, failure to consume lipids could lead to LD accumulation. To test this hypothesis, I knocked-down the rate limiting ß-oxidation enzyme *Carnitine Palmitoyltransferase 2* (*CPT2*), using either a pan-retinal, or photoreceptor specific driver. While lack of *CPT2* solely in photoreceptor had no effect on LD accumulation, pan-retinal *CPT2* knockdown led to LD accumulation, in a pattern reminiscent of glial LDs also seen with the Bmm lipase knockdown (Figure 24 A-B, Girard et al. (1)-Figure 3). Examination of retina stained with dPlin2 antibody and ATPase staining confirmed the glial localization of

Figure 24. Knockdown of *CPT2* induces LD accumulation in glia but not in photoreceptors. (A) Longitudinal optical sections of whole-mount retinas from flies expressing RNAi targeting *CPT2* under the control of the pan-retinal driver *GMR-GAL4* or the photoreceptor-specific driver *Rh1-GAL4*. LDs are visible in green (Bodipy) and photoreceptor rhabdomeres are in magenta (phalloidin-rhodamine labeling of F-actin). Pan-retinal *CPT2* knockdown leads to LD accumulation in retinal glial cells between photoreceptor cells (top panel), but LDs are not detected in flies with photoreceptor neuron-specific *CPT2* knockdown (bottom panel). Scale bar, 10 μm. (B) Quantification of LD area expressed as % of total retinal area. Data are from the images shown in (A). Mean ± SD. ***p<0.001 by ANOVA with Tukey's HSD test. (C) Longitudinal optical sections of whole-mount retinas from flies with pan-retinal knockdown of *CPT2*. dPlin2 is shown in green (immunostaining), photoreceptor plasma membrane is in cyan (Na^+/K^+ ATPase immunostaining), and photoreceptor rhabdomeres are in magenta (phalloidin-rhodamine labeling of F-actin). Yellow arrowheads indicate LDs in glial cells, between plasma membrane of adjacent photoreceptors. Scale bar, 10 μm.

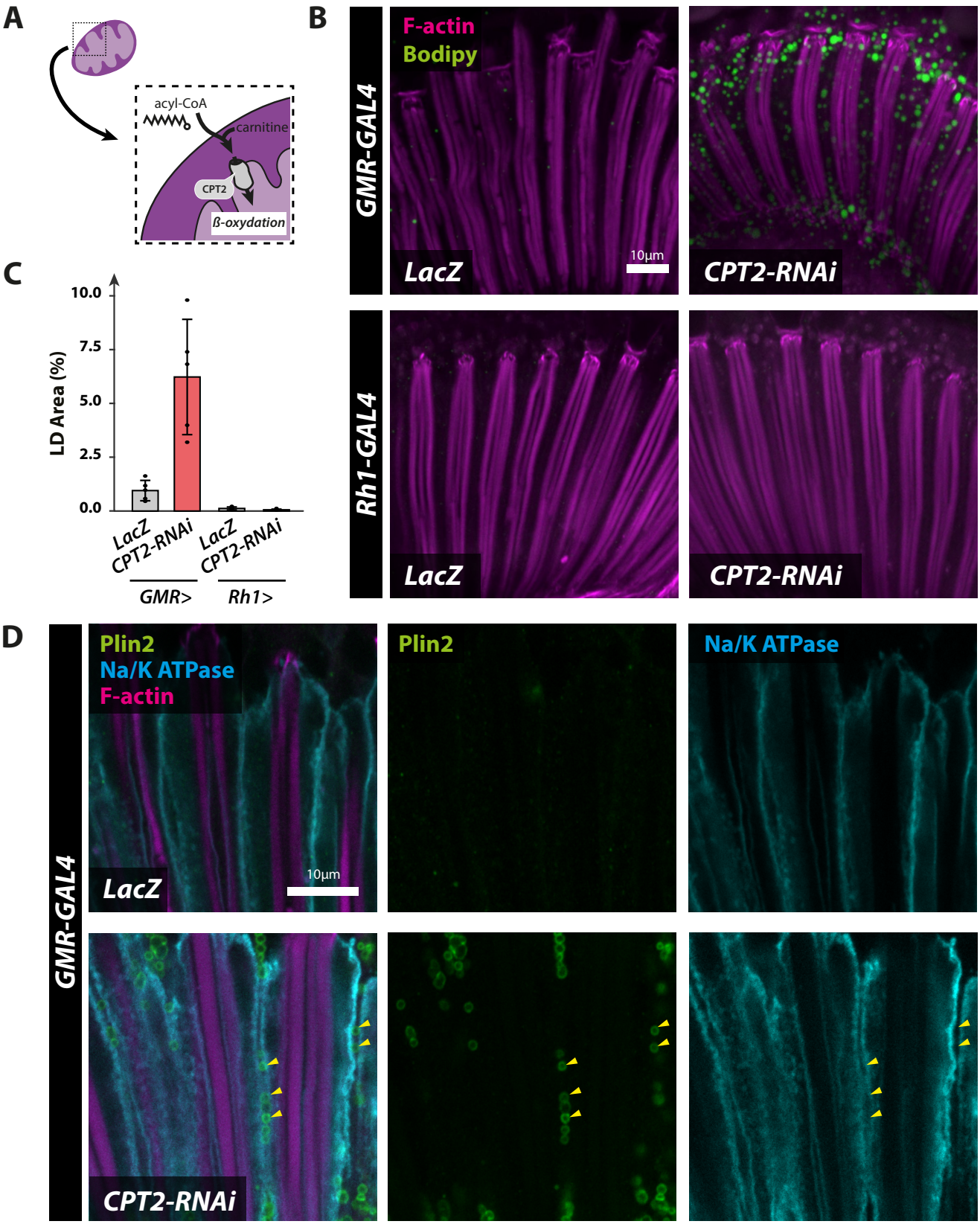
A
acyl-CoA
carnitine
CPT2
ß-oxydation
B
GMR-GAL4
F-actin
Bodipy
LacZ
10µm
CPT2-RNAi
Rh1-GAL4
LacZ
CPT2-RNAi
C
LD Area (%)
10.0
7.5
5.0
2.5
0.0
LacZ
CPT2-RNAi
LacZ
CPT2-RNAi
GMR>
Rh1>
D
GMR-GAL4
Plin2
Na/K ATPase
F-actin
LacZ
10µm
Plin2
Na/K ATPase
CPT2-RNAi

LDs (Girard et al. (1)-Figure3; Figure 24 C). These results suggest that retina glia, actively degrade LDs using Bmm to produce FA that are transferred to the mitochondria through CPT2 to potentially fuel ß-oxidation. The fact that photoreceptor specific knockdown of *CPT2* did not lead to LD accumulation suggest that LDs are not degraded to fuel ß-oxidation in neurons. It also suggests that the contacts between mitochondria and LDs observed in photoreceptor neurons may have a distinct purpose, which remains unclear and will require further investigation.

Previous reports indicated that the knockdown of CPT2 in Drosophila brain glial cells leads to abnormal accumulation of LDs (Schulz et al., 2015), which is coherent with our own observation in retina glial cells (Figure 25) . We then tested whether the knockdown of Bmm in the whole brain using a pan-glial driver (repo-GAL4) would also increase LD content in brain glia as well. We observed an increase in bodipy staining in the brain of flies lacking Bmm in glial cells (Figure 25) suggesting that brain and retina glial cells actively degrade TAG to fuel beta-oxidation.

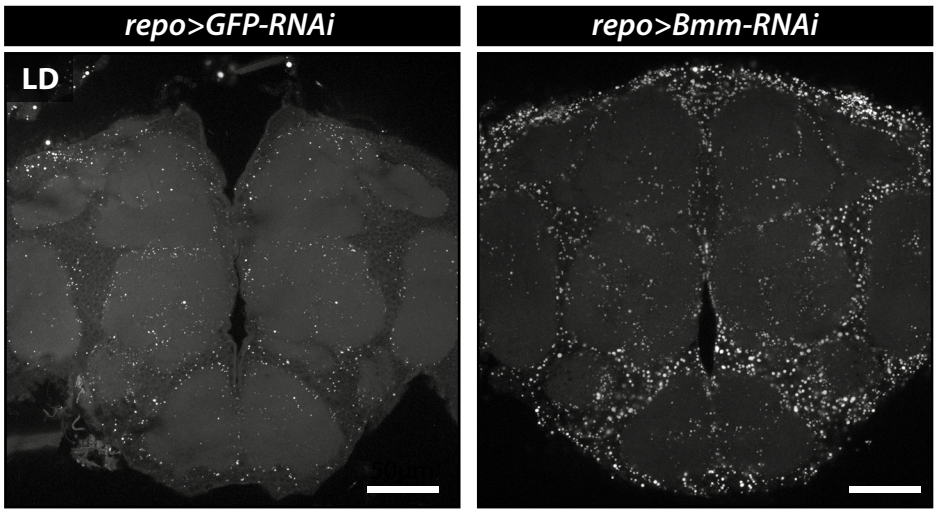

Figure 25. Knockdown of Bmm in Brain glia.
Longitudinal optical sections of whole-mount brain from flies expressing *GFP-RNAi* (control) or *Bmm-RNAi* with pan-glial driver (*repo-GAL4*). LDs are labeled grey (lipophilic dye Bodipy D3922). Scale bar, 50 µm.

1.2.6. Impaired PE synthesis contributes to LD formation in photoreceptor neurons.

Phospholipids such as PC or PE are produced by addition of choline or ethanolamine respectively to a DAG molecule. It has been shown that impairment of phospholipid synthesis can interfere with LD homeostasis. For example, lack of PC synthesis enzyme leads to increase TAG synthesis and LD accumulation in yeast (Vevea et al., 2015). Interestingly,

knockdown of CCT1, the rate-limiting enzyme of PC synthesis, promotes LD fusion (Krahmer et al., 2011). In this context, a decrease in PC synthesis could reduce phospholipid packing at the surface of LDs and promote LD fusion. In order to investigate whether the lack of phospholipid synthesis could promote LD expansion in photoreceptor, I knocked-down either *CCT1* or *CG7149*, a *Drosophila* homolog of *Ethanolaminephosphotransferase 1* (*EPT1*) (Vacaru et al., 2013), in flies expressing *aSynA53T-CG7900*. While CCT1 led to noticeable loss of rhabdomeres integrity, LD content was not modified compared to control expressing GFP-RNAi (Figure 26, A). In contrast, the knock-down of *dEPT1*, the rate limiting enzyme of PE synthesis, further increased accumulation of LDs in flies expressing *aSynA53T-CG7900* (Figure 26, A-B). I also knocked-down *dEPT1* in control flies

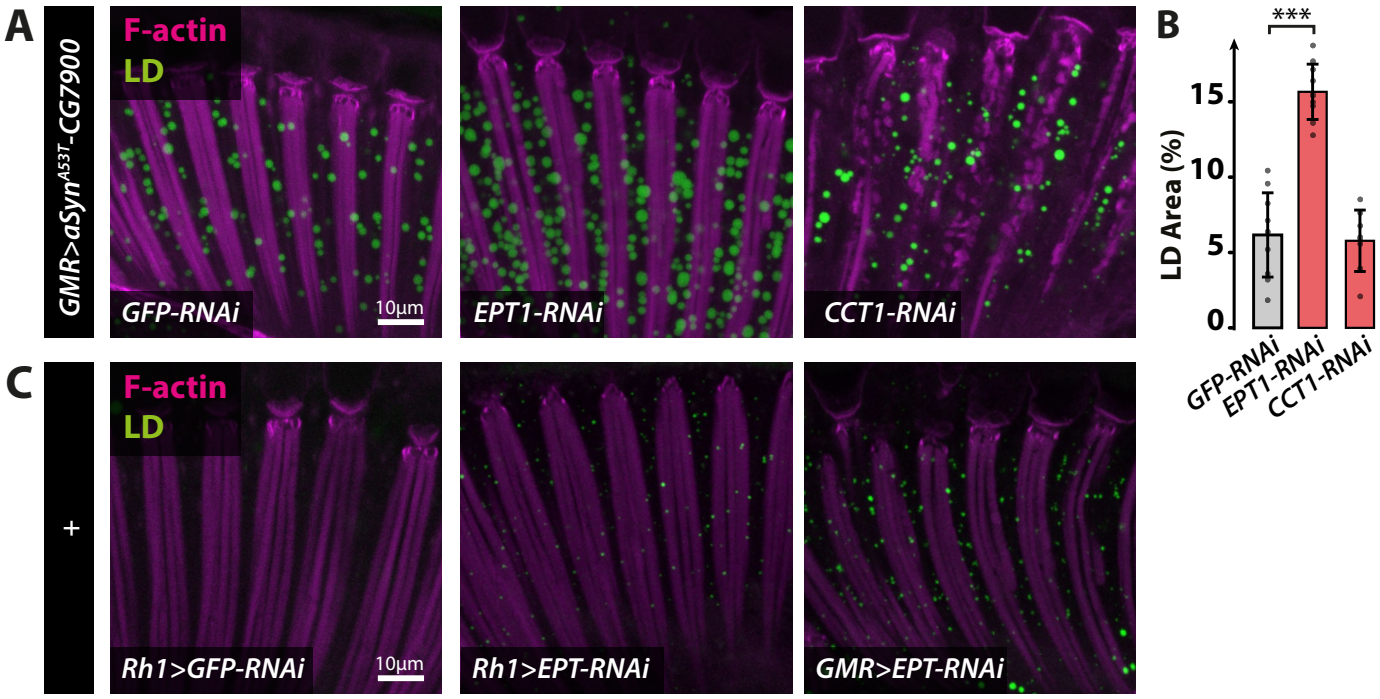

Figure 26. Knockdown of dEPT1 increases LD accumulation in photoreceptors.
(A) Longitudinal optical sections of whole-mount retinas from flies expressing *aSynA53T-CG7900* in conjunction with *GFP-RNAi* (control), dEPT1-*RNAi* or *CCT1-RNAi* using a pan-retinal driver (*GMR-GAL4*). LDs are labeled green (lipophilic dye Bodipy D3922) and photoreceptor rhabdomeres are in magenta (phalloidin-rhodamine labeling of F-actin). Scale bar, 20 µm. (B) Quantification of LD area expressed as % of total retinal area. Data are from the images shown in (A). Mean ± SD. ***p<0.001 by ANOVA with Tukey's HSD test. (C) Longitudinal optical sections of whole-mount retinas from flies expressing *GFP-RNAi* (control) or d*EPT1-RNAi* using a photoreceptor (*Rh1-GAL4) or* pan-retinal driver (*GMR-GAL4*)). LDs are labeled green (lipophilic dye Bodipy D3922) and photoreceptor rhabdomeres are in magenta (phalloidin-rhodamine labeling of F-actin). Scale bar, 10 µm.

and observed that knockdown of *dEPT1* using photoreceptor or pan-retinal driver led also to a noticeable increase in LD accumulation (Figure 26, C). Collectively these results suggest that reducing PE synthesis in photoreceptor neurons, increases TAG synthesis and LD growth in both control and flies expressing *aSynA53T-CG7900*.

1.2.7. dPlin2 expression allows the detection of LDs in *Drosophila* dopaminergic neurons.

Our results suggest that expression of perilipins or several other LD-binding proteins, promote the accumulation of LDs in photoreceptors by a mechanism independent of ER-located TAG synthesis enzymes and Bmm lipase inhibition. We also show that lack of Bmm or CPT2 in otherwise healthy retina glial cells, leads to LD accumulation by a mechanism that involves Mdy and dFatp. Whether those distinct mechanisms regulating LD biosynthesis can also be observed in other neuronal and glial populations of *Drosophila* brain, remains a major question. I focused specifically on dopaminergic neurons as they are the principal neuronal population affected by PD. Photoreceptors have particularly large cell bodies that span the entire retina, compared to other neurons of the central brain, which greatly facilitates the observation of bodipy-stained LDs. For example, lipids can be washed away by permeabilization which considerably limits the use of immunostaining

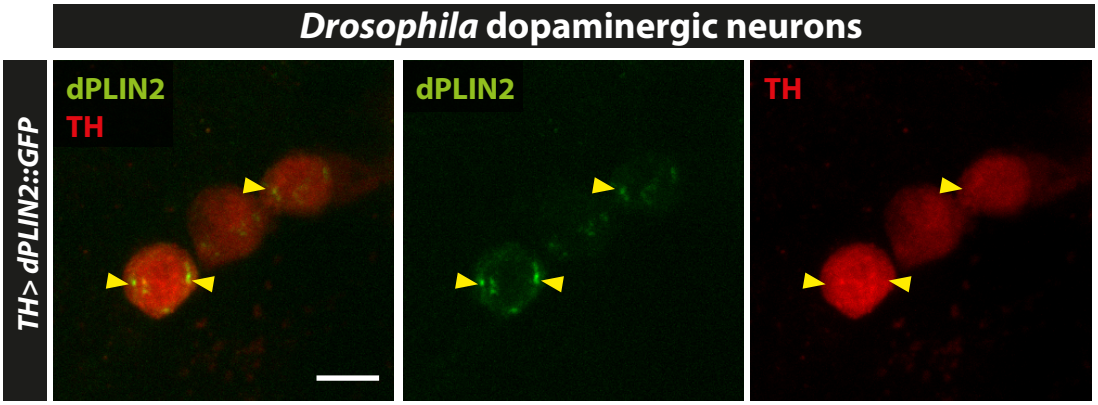

Figure 27. *Drosophila* dopaminergic neurons contain LDs carrying-dPlin2.
Confocal micrograph of whole mount adult brain of flies expressing dPLIN2::GFP under the control of dopaminergic neuron driver *TH-GAL4*. LDs are labeled with GFP antibody (dPLIN2::GFP, green) and dopaminergic neurons are labeled with an antibody against tyrosine hydroxylase (TH, red). LDs in the cytoplasm of dopaminergic neurons are indicated with yellow arrowheads. Scale bars: 5µm.

to localize neuronal population. To circumvent the issue of Bodipy detection in the central brain, I used the expression of dPlin2 with a pan-neuronal driver, associated with tyrosine-hydroxylase (TH) immunostaining to identify whether dopaminergic neurons contained LDs. Co-labelling of dPlin2::GFP and TH revealed small GFP positive ring like shape in the cytoplasm of dopaminergic neurons (Figure 27). The small size of the LDs makes them

very hard to distinguish using the classical bodipy staining, it is thus difficult to determine whether expression of dPlin2 stabilize LD formation in these cells or if dPlin2 labelling reveals endogenous LDs. To test the contribution of aSyn in LD accumulation in DA, we could test if the combined expression of aSyn and dPlin2 increases the LD content of dopaminergic neurons compared to dPlin2 alone. This could thus provide a model to test LDs influence on aSyn-dependent PD-related symptoms such as impaired locomotion and dopaminergic neuron cell death.

There are interesting parallels between cell from the retina and the brain, such as the active degradation of FA by a mechanism involving Bmm and CPT2. The study of lipid storage mechanisms in the retina, are thus relevant for the brain as well. Interestingly, glial LDs accumulate upon oxidative stress resistance and contribute to neurodegeneration in the retina. We further investigated whether brain glia LDs could contribute to neurodegeneration in a model of pesticide-induced PD using paraquat exposure.

2. Split-ends modulates LD content in adult *Drosophila* glial cells and protects against paraquat toxicity.

2.1. Girard et al. (2)

LD accumulation in glial cells has been shown to promote oxidative stress-induced neurodegeneration (Liu et al., 2015; Van Den Brink et al., 2018). In this paper, I investigated glial LD accumulation in a model of pesticide induced PD. Chronic exposure to Paraquat is associated with increased risk of PD (Lee et al., 2012). Paraquat impairs mitochondria respiratory chain and leads to accumulation of ROS and it is widely used to model sporadic PD in model organisms including flies (Cassar et al., 2015). Indeed, *Drosophila* treated with Paraquat, develop progressive motor symptoms and die prematurely. A previous student from the lab M. Querenet conducted a screen to identify factors express in glial cells important for resistance to paraquat exposure. Several candidates were identified including split-ends (Spen). Spen is an RNA binding proteins expressed both in glia and neurons that was previously characterized in our lab as a glial pro-survival factor during retina development (Querenet et al., 2015). Interestingly, Spen has also been shown to have critical function in the regulation of lipid metabolism in *Drosophila* fat body (Hazegh et al., 2017). We thus investigated the functions of Spen in the resistance to paraquat exposure and lipid metabolism in *Drosophila* adult brain. We found that Spen is required specifically in glial cells for the resistance to paraquat-induced neurotoxicity. Moreover, knockdown of *Spen* in glia induced accumulation of LDs and is necessary to maintain Notch expression in adult glial cells. Collectively, these results suggest that abnormal lipid accumulation in glia can increase the sensitivity to paraquat exposure.

scientific reports

Check for updates

OPEN

Spen modulates lipid droplet content in adult *Drosophila* glial cells and protects against paraquat toxicity

Victor Girard[1], Valérie Goubard[1], Matthieu Querenet[1], Laurent Seugnet[4], Laurent Pays[2,3], Serge Nataf[2,3], Eloïse Dufourd[1], David Cluet[1], Bertrand Mollereau[1,5]✉ & Nathalie Davoust[1]✉

Glial cells are early sensors of neuronal injury and can store lipids in lipid droplets under oxidative stress conditions. Here, we investigated the functions of the RNA-binding protein, *SPEN/SHARP*, in the context of Parkinson's disease (PD). Using a data-mining approach, we found that *SPEN/SHARP* is one of many astrocyte-expressed genes that are significantly differentially expressed in the *substantia nigra* of PD patients compared with control subjects. Interestingly, the differentially expressed genes are enriched in lipid metabolism-associated genes. In a *Drosophila* model of PD, we observed that flies carrying a loss-of-function allele of the ortholog *split-ends* (*spen*) or with glial cell-specific, but not neuronal-specific, *spen* knockdown were more sensitive to paraquat intoxication, indicating a protective role for Spen in glial cells. We also found that Spen is a positive regulator of Notch signaling in adult *Drosophila* glial cells. Moreover, Spen was required to limit abnormal accumulation of lipid droplets in glial cells in a manner independent of its regulation of Notch signaling. Taken together, our results demonstrate that Spen regulates lipid metabolism and storage in glial cells and contributes to glial cell-mediated neuroprotection.

Parkinson's disease (PD) is a neurodegenerative disorder characterized by the selective loss of dopaminergic neurons in the *substantia nigra pars compacta* (SN). Although the etiology of PD remains unclear, environmental factors combined with a permissive genetic background are thought to contribute. Epidemiologic studies have shown that chronic exposure to pesticides is one environmental factor involved in the development of PD[1]. Several models of PD have been developed in *Drosophila*, among which the paraquat-induced model reproduces several important pathophysiological features of the disease, thereby enabling causal links between chronic pesticide intoxication and PD to be investigated in detail. In particular, oxidative stress and reactive oxygen species (ROS) production in the brain of paraquat-intoxicated flies has been shown to induce the degeneration of dopaminergic neurons, leading to severe motor disability and premature death[2–4].

In many species including *Drosophila* and humans, non-neuronal glial cells are early sensors of central nervous system injury[5]. Glial cells such as microglia and astrocytes respond to neuronal damage by changing their morphology and proliferation and activating specific transcriptomic programs. We and others recently demonstrated that intracytoplasmic accumulation of lipid droplets (LDs) is a hallmark of the glial cell response to stress[6–10]. Recent work has shown that the regulation of lipid metabolism and formation of LDs requires the RNA-binding protein Split-ends (*spen*), the *Drosophila* ortholog of *SPEN/SHARP*, in *Drosophila* adipose tissue[11,12]. Spen also regulates midline glia specification and survival of glial cells in the *Drosophila* embryo[13] and pupal retina[14], respectively. However, the role of Spen in the regulation of lipid metabolism in glial cells is unknown. Spen proteins contain two conserved functional domains: an RNA Recognition Motif (RMM) and a Spen Paralog and Ortholog C-terminal (SPOC) domain[13,15–17], which mediate its biological effects through transcription, RNA silencing, RNA splicing, and direct interactions with chromatin[18–23].

[1]Laboratory of Biology and Modelling of the Cell, UMR5239 CNRS, INSERM U 1210, ENS de Lyon, UMS 344 Biosciences Lyon Gerland, Université de Lyon, Lyon, France. [2]CarMeN Laboratory, INSERM UMR-1060, INRA U1235, INSA of Lyon, Charles Merieux Medical School, Université Claude Bernard Lyon1, Université de Lyon, Lyon, France. [3]Banque de Tissus et de Cellules des Hospices Civils de Lyon, Hôpital Edouard Herriot, Lyon, France. [4]Centre de Recherche en Neurosciences de Lyon, UMR5292, INSERM U1028, Equipe Physiologie Intégrée du Système d'éveil, Université Claude Bernard Lyon1, Lyon, France. [5]Institut Universitaire de France, Paris, France. ✉email: bertrand.mollereau@ens-lyon.fr; nathalie.davoust-nataf@ens-lyon.fr

Pathway	Human genes	Adjusted P-value
Phospholipid metabolism	*ARF3, ASAH1, CERS6, CERK, PITPNB, PIK3R3, OCRL, MTMR4, PLD3, AGPAT4, INPP4A, PTDSS1, COL4A3BP, STS, SYNJ1, VAPB, OSBP, PI4KA, PIP5K1B, GPD1L, PI4K2A, CDS2*	0.0003
Lipid and lipoprotein metabolism	*ARF3, IDI1, ASAH1, ALAS1, CERK, PITPNB, PIK3R3, HMGCR, MTMR4, PLD3, AGPAT4, PTDSS1, COL4A3BP, STS, OXCT1, OSBP, PIP5K1B, PRKACB, CERS6, HMGCS1, SRD5A1, OCRL, MED7, INPP4A, ACLY, SYNJ1, VAPB, AGPS, PI4KA, GPD1L, PI4K2A, CDS2*	0.0180
Sphingolipid metabolism	*COL4A3BP, ASAH1, STS, CERS6, CERK, VAPB, OSBP, B4GALT6*	0.0488

Table 1. Genes involved in lipid metabolism that are downregulated in the *substantia nigra pars compacta* of PD patients compared with control subjects.

SPEN/SHARP can act as both a negative and positive regulator of the Notch signaling pathway, which plays a major role in cell fate specification in many species[24–27]. A recent study showed that SPEN acts as co-repressor of the transcription of genes responsive to Notch signaling[25] by binding to the recombinant binding protein J-kappa (RBP-Jκ) during *Drosophila* eye development[26]. Conversely, SPEN can act as a positive regulator of Notch signaling by recruiting the lysine methyl transferase 2D (KMT2D) co-activator complex to Notch target genes[27]. Spen has also been shown to promote Notch receptor activation by regulating trafficking of the Notch ligand Delta in intestinal stem cells of adult flies[28].

Given that Spen promotes survival in glial cells of the developing *Drosophila*, we hypothesized that Spen expression in glial cells could confer neuroprotection in a model of PD. In the present study, we investigated the role of Spen as a potential regulator of lipid metabolism and Notch signaling in adult *Drosophila* glial cells, and determined the possible involvement of *spen* in the paraquat intoxication model of PD.

Results

SPEN, the human ortholog of _Drosophila spen_, is upregulated in the _substantia nigra pars compacta_ of PD patients. *SPEN* has been reported to be expressed by human astrocytes[29], but whether its expression is differentially regulated in the brains of patients with PD is unknown. To address this, we exploited the findings of a recent meta-analysis of microarray datasets obtained from the SN of PD patients compared with control subjects[30]. From the list of differentially expressed genes (data Supplement 1), we performed a tissue enrichment analysis using the TargetMine webtool[31]. This analysis identified 197 genes that were both upregulated in the SN of PD patients and expressed in astrocytes; one which was SPEN. SPEN is known to be expressed by both astrocytes and neurons in the normal human brain[29] (data Supplement 2); however, it is not clear whether the upregulation of SPEN in the brains of PD patients occurs in glia or neurons. We also identified 469 genes that were both downregulated in the SN of PD patients compared with control subjects and expressed in astrocytes (data Supplement 2). Interestingly, we detected significant enrichment of lipid metabolism-associated genes, as determined using the BioPlanet pathway enrichment tool[32], in the gene set downregulated, but not upregulated, in the SN of PD patients (data Supplement S3, S4, Table 1). Taken together, these analyses indicate that *SPEN* expression is upregulated in astrocytes and/or neurons of PD patients compared with normal subjects, which prompted us to investigate its function in the *Drosophila* paraquat model of PD.

Glia-specific overexpression of _spen_ protects _Drosophila_ from paraquat-induced neurotoxicity. We first investigated whether *spen* mRNA levels in the brain of adult *Drosophila* were altered under conditions of paraquat-induced toxicity. RT-qPCR revealed a significant upregulation of *spen* expression in the brains of paraquat-treated flies compared with control flies (Fig. 1A). To obtain insights on the potential function of Spen upregulation, we examined the survival of flies heterozygous for *spen* loss-of-function mutations[17] ($spen^{k07612}$/+ and $spen^{03350}$/+) after paraquat intoxication. Both of the *spen* heterozygous mutant lines exhibited a higher sensitivity to paraquat compared with control flies (Fig. 1B, Supplemental Fig. S1), suggesting that Spen protects against paraquat-induced neurotoxicity. As previously reported[33], *spen* expression, as revealed by P-lacW inserts, was detectable in both neurons and glial cells of *Drosophila* adult brain (Supplemental Fig. S2). To determine whether the neuroprotective function of *spen* results from its expression in glial or neuronal cells, we generated flies in which *spen* was selectively knocked down in either cell type using a pan-glial (*repo*) or pan-neuronal (*elav*) driver. We found that downregulation of *spen* in glial cells, but not neuronal cells, increased the sensitivity of male flies to paraquat (Fig. 1C, Supplemental Fig. S3). Knockdown of *spen* in adult glia using an alternative genetic method, the temperature-sensitive TARGET system[45], had the same effect of increasing *Drosophila* sensitivity to paraquat (Fig. 1D). Conversely, glia-specific overexpression of *spen* protected against paraquat toxicity (Fig. 1C). Collectively, these results show that Spen expression in glial cells protects *Drosophila* from paraquat-induced toxicity.

Spen regulates the Notch signaling pathway in adult Drosophila glial cells. Because Spen/SPEN has been shown to positively or negatively regulate Notch signaling pathway, depending on the molecular context and cell type[25,27,28], we next determined how Spen regulates Notch pathway in adult glial cells. To this end, we knocked down *spen* expression using an *Eaat1* (excitatory amino acid transporter 1) driver, which is mainly expressed in astrocyte-like glial cells[34,35], and monitored Notch pathway activation using a reporter transgene, Notch Responsive Element (*NRE)-GFP*. This transgene carries a minimal promoter containing Su(H)-DNA binding sites upstream of the *EGFP* coding sequence[36] (Fig. 2A). As previously reported, basal expression of

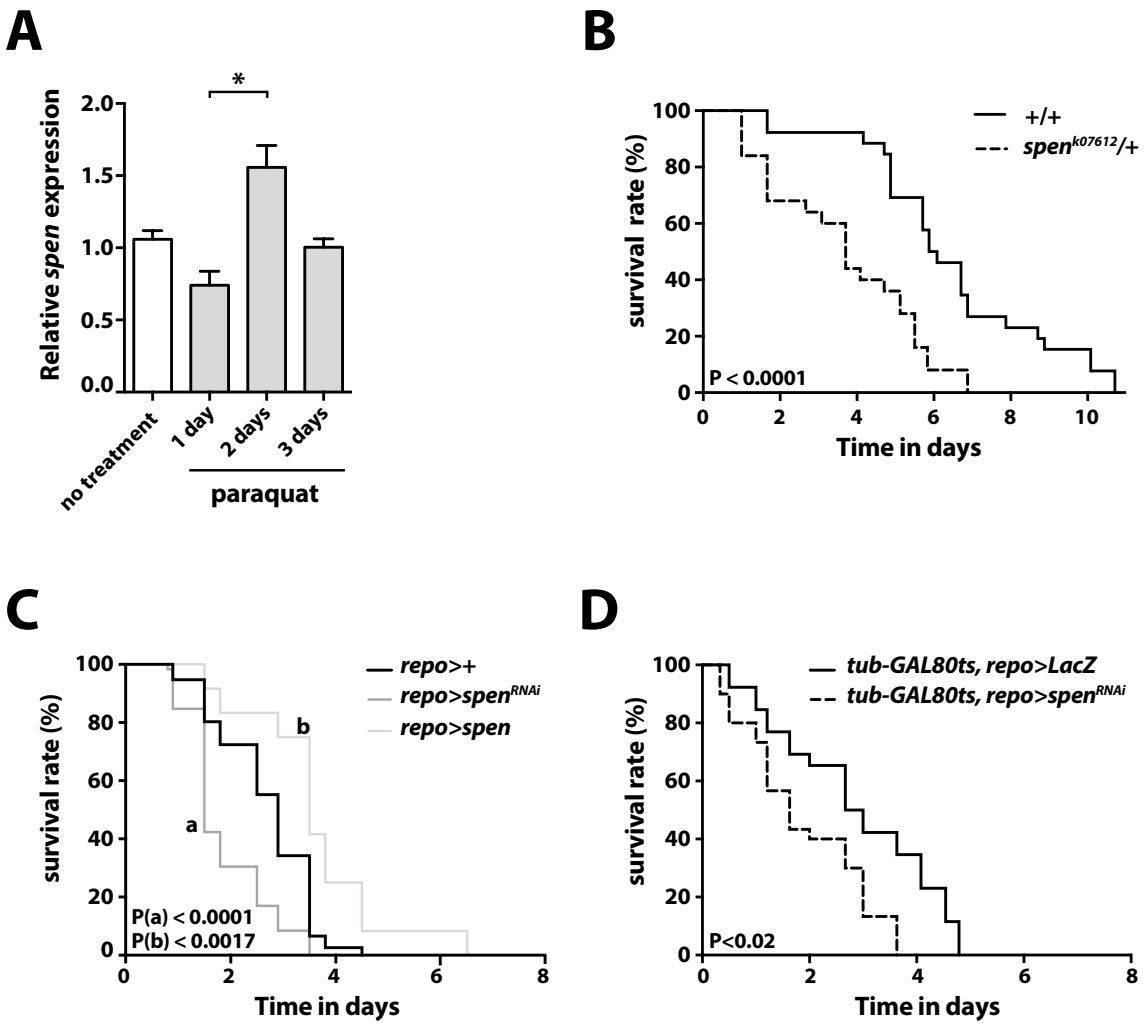

Figure 1. Glia-specific *spen* expression protects *Drosophila* against paraquat-induced lethality. (**A**) RT-qPCR analysis of *spen* mRNA expression in the heads of 3-day-old male *Drosophila* at the indicated times after feeding with a standard sucrose solution lacking (no treatment) or containing 10 mM paraquat for the indicated times (4 independent experiments). Results are expressed relative to the no-treatment condition. *P < 0.03 by nonparametric Mann–Whitney test. (**B**) Survival curves of wild-type (w^{1118}) and *spen* loss-of-function heterozygous mutant ($spen^{k07612}$/+) adult male flies fed with 10 mM paraquat. The curves represent one experiment with N = 16–20 flies per genotype, representative of three independent experiments. P < 0.0001 by the log-rank Mantel–Cox test. (**C**) Survival curves of adult male control flies (*repo-GAL4*/+) or flies with glial cell-specific *spen* knockdown (*UAS-*$spen^{RNAi}$/+;*repo-GAL4*/+) or *spen* overexpression (*UAS-spen*/+;*repo-GAL4*/+) fed with 10 mM paraquat. The curves represent one experiment with N = 20 flies per genotype, representative of three independent experiments. (a) P < 0.0001 for control vs *repo* > $spen^{RNAi}$, (b) P < 0.0017 for control vs *repo* > *spen* by the log-rank Mantel–Cox test. (**D**) Survival curves of adult male flies with expression of *LacZ* (control) or $spen^{RNAi}$ restricted to adult glial cells using the TARGET system[45]. Flies were fed 10 mM paraquat for the indicated times. The curves represent one experiment with N = 16–20 flies per genotype, representative of three independent experiments. P < 0.02 by the log-rank Mantel–Cox test.

NRE-GFP, reflecting basal activity of the Notch pathway, was observed in glial cells of control flies (*Eaat1* > +), particularly in the antennal lobe[37] (Fig. 2B,C, Supplemental Fig. S4) and the dorsal part of the central brain. Interestingly, however, basal activity of Notch signaling was strongly diminished in flies with glia-specific expression of $spen^{RNAi}$ (Fig. 2C,D). These data indicate that Spen is required for basal Notch activity in glial cells in the adult *Drosophila* brain. To extend these observations, we performed an epistasis experiment between the Notch intracellular domain ($Notch^{intra}$), an activator of the Notch pathway, and $spen^{RNAi}$ in Eaat1+ cells. As expected, $Notch^{intra}$ expression resulted in a strong and uniform induction of *NRE-GFP* reporter expression; however, *spen* knockdown significantly reduced the induction of NRE-GFP by $Notch^{intra}$, indicating that Spen is necessary to maintain Su(H)-dependent Notch signaling in adult glia (Fig. 2D,E). The induction of NRE-GFP was not associated with a change in glial cell survival rate, as assessed by quantification of Repo-positive cells in control and *spen* knockdown flies (Fig. 2F). Collectively, these results show that Spen acts as a positive regulator of Notch signaling in adult *Drosophila* glial cells (Fig. 2G).

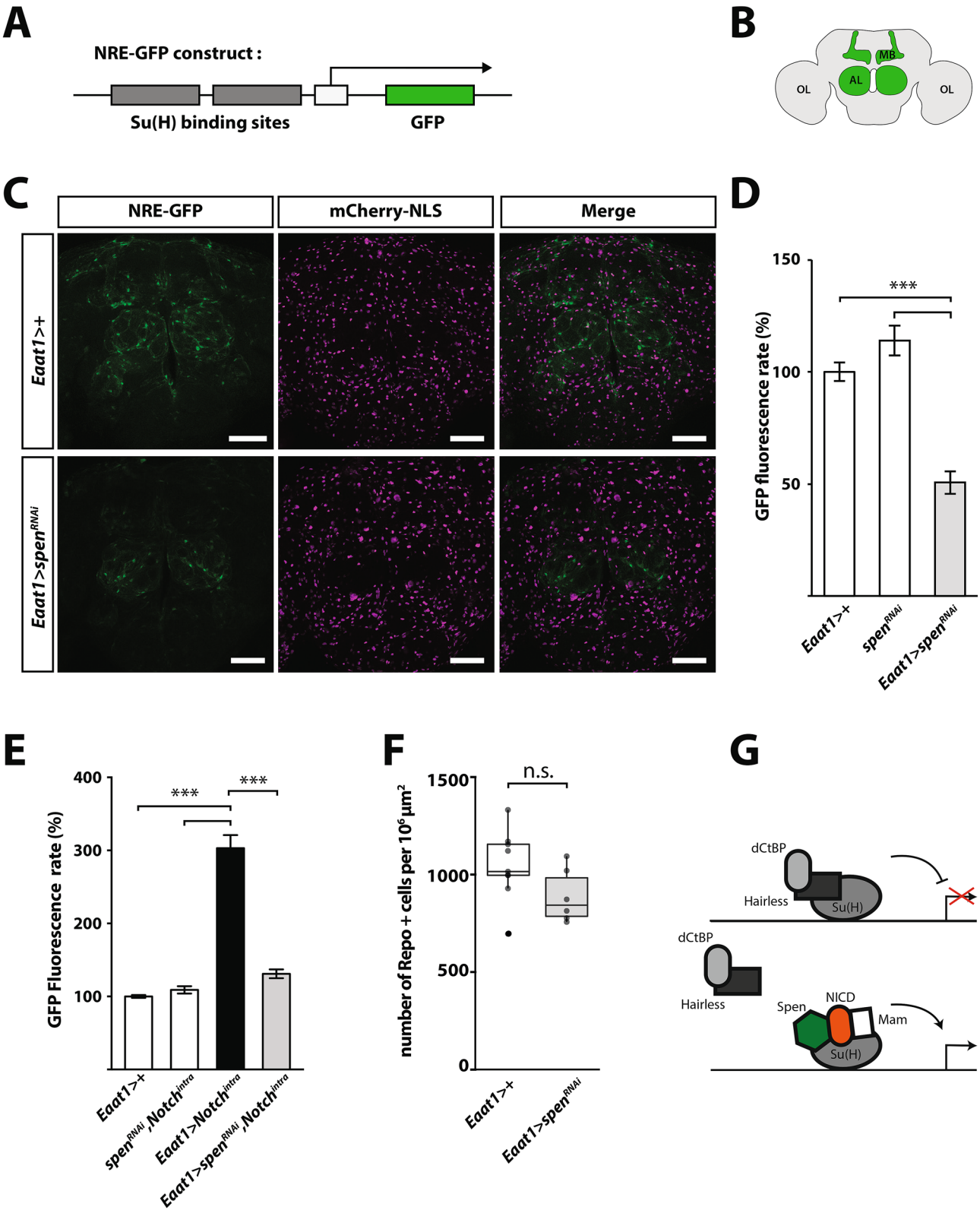
A
NRE-GFP construct :
Su(H) binding sites
GFP
B
MB
AL
OL
OL
C
NRE-GFP
mCherry-NLS
Merge
Eaat1>+
Eaat1>spen^RNAi
D
GFP fluorescence rate (%)
150
100
50
***
Eaat1>+
spen^RNAi
Eaat1>spen^RNAi
E
GFP Fluorescence rate (%)
400
300
200
100
***
***
Eaat1>+
spen^RNAi;Notch^intra
Eaat1>Notch^intra
Eaat1>spen^RNAi;Notch^intra
F
number of Repo+ cells per 10^6 µm^2
1500
1000
500
0
n.s.
Eaat1>+
Eaat1>spen^RNAi
G
dCtBP
Hairless
Su(H)
dCtBP
Hairless
Spen
NICD
Mam
Su(H)

◂**Figure 2.** Spen regulates Notch signaling in *Drosophila* adult glial cells. (**A**) Schematic of the Notch reporter construct *NRE-GFP* used to monitor Notch activity in *Drosophila* brain. The *EGFP* coding sequence (green) is under the control of a promoter containing multiple Su(H) binding sites (dark gray). (**B**) Simplified schematic of *Drosophila* adult brain, showing mushroom bodies (MB) and antennal lobes (AL), which are known to have high Notch activity (green). OL, optic lobes. (**C**) Immunofluorescence confocal micrographs of whole-mount brains from control flies (*Eaat1* glial driver alone: *Eaat1-GAL4/+;NRE-GFP/+*) or flies with glia-specific $spen^{RNAi}$ (*Eaat1-GAL4/UAS-*$spen^{RNAi}$*;NRE-GFP/+*). Flies also harbored the nuclear marker mCherry-NLS expressed under the control of the *Eaat1* driver (magenta). GFP fluorescence was detected in MB and AL lobes in close proximity with *Eaat1* + glial cells. The NRE-GFP signal is reduced in *Eaat1* > $spen^{RNAi}$ (*Eaat1-GAL4/UAS-*$spen^{RNAi}$*; NRE-GFP/+*) flies compared with controls. Scale bar, 50 µm. (**D**) Quantification of NRE-GFP fluorescence in flies with driver alone *Eaat1* > + (*Eaat1-GAL4/+;NRE-GFP/+*), *UAS-*$spen^{RNAi}$ alone (*UAS-*$spen^{RNAi}$*/+;NRE-GFP/+*), or $spen^{RNAi}$ *Eaat1* > $spen^{RNAi}$ (*Eaat1-GAL4/UAS-*$spen^{RNAi}$*; NRE-GFP/+*). N = 18 flies per genotype from 3 independent experiments. (**E**) NRE-GFP fluorescence was quantified in *Eaat1* > + (*Eaat1-GAL4/+;NRE-GFP/+*), *UAS-*$spen^{RNAi}$ (*UAS-*$spen^{RNAi}$*, UAS-*$Notch^{intra}$*;NRE-GFP/*), or Notch intracellular domain-overexpressing (*Eaat1-GAL4/UAS-*$Notch^{intra}$*; NRE-GFP/+*) flies alone or together with $spen^{RNAi}$ (*Eaat1-GAL4/UAS-*$spen^{RNAi}$*, UAS-*$Notch^{intra}$*;NRE-GFP/+*). N = 18 flies per genotype from 3 independent experiments. $P < 0.001$ by the nonparametric Kruskal–Wallis test. (**F**) Density of Repo-positive glial cells in control (*Eaat1-GAL4/+*) or $spen^{RNAi}$ flies (*Eaat1-GAL4/UAS-*$spen^{RNAi}$). Boxes show the median and upper, and lower quartiles, and the whiskers represent 1.5 times the interquartile range. Repo-positive glial cells were quantified over 12 confocal slices across one 12 µm-thick brain section from each of *Drosophila* brains. Circles represent individual data points. (**G**) Simplified proposed scheme showing the Notch activator complex in adult glial cells, which includes the Notch intracellular domain (NICD), Suppressor of hairless (Su(H)), mastermind (Mam), and Spen. The Notch repressor complex includes Su(H), Hairless, and dCtBP (*Drosophila* C-terminal Binding Protein). Adapted from[38].

Spen regulates the number, size, and localization of lipid droplets in glial cells. *Drosophila* glial cells have been shown to accumulate LDs under conditions of oxidative stress[6,7], and Spen is known to control lipid metabolism in the fat body of *Drosophila* larvae[11]. We thus investigated whether Spen expression affects LD expansion and/or accumulation in *Drosophila* glial cells. To this end, we developed an ImageJ[39] macro to quantify fluorescence from BODIPY staining of LDs in serial confocal sections of adult *Drosophila* brain. Quantification was based on an automated detection of BODIPY-positive particles that were distinguished from non-specific fluorescence by successive iterations. This new method allows not only discrimination of LDs from doublet foci on successive confocal stacks but also evaluation of the density, size, and circularity of LDs (see "Materials and methods" section for details). As visualized in the fluorescence micrographs (Fig. 3A) and quantified in the antennal lobe neuropil (Fig. 3B,C), *spen* knockdown in glial cells induced a significant increase in LD number and size. A similar accumulation of LDs was seen when $spen^{RNAi}$ was expressed using the pan-glial driver *repo-GAL4*, but not the pan-neuronal driver *elav-GAL4* (Supplemental Fig. S5). The accumulation of LDs induced by glia-specific knockdown of *spen* was also detected when LDs were visualized by staining of whole-mount brains for PLIN2[40,41], a peridroplet protein anchored to the phospholipid monolayer surrounding LDs (Fig. 3D). In addition to the immunostaining approach, we expressed the *UAS-PLIN1::GFP* genetically encoded LD reporter[40,41] under the control of the *Eaat1-GAL4* driver and confirmed that glia-specific *spen* knockdown induced accumulation of LDs in the brain of adult flies (Fig. 3E,F). Interestingly, inhibition of the canonical Notch pathway in glia by knockdown of *Su(H)* did not affect the number or size of LDs (Supplemental Fig. S6). Collectively these results suggest that LD accumulation in flies with *spen* knockdown occurs specifically in glial cells and is not due to the inhibition of canonical Notch signaling.

Discussion

Several studies have reported that dysregulation of lipids, including LDs, is a component of the glial cell response to stress during neurodegeneration[6,8–10], including that associated with PD[42]. Here, we identified *SPEN/SHARP* as an astrocyte-expressed gene that is significantly overexpressed in the SN of PD patients compared with control subjects. In *Drosophila*, *spen* expression in glial cells mediates the resistance of *Drosophila* to paraquat treatment. We also show that Spen is a positive regulator of Notch signalling in adult glial cells. Finally, we found that glia-specific expression of *spen* regulates LD accumulation in glial cells, in a manner independent of its regulation of Notch signaling. Collectively, our results suggest that the regulation of lipid metabolism by Spen contribute to the glia stress response.

SPEN was one of many astrocyte-expressed genes found to be significantly differentially expressed in the brains of PD patients compared with control subjects. Interestingly, the differentially expressed genes were enriched in genes involved in lipid metabolism, which was of particular interest given the previously reported role of Spen as a regulator of lipid storage in adipocyte-like cells in *Drosophila*. Indeed, Spen was identified in two independent screens as a modulator of fat content in *Drosophila* larvae and adults[43,44]. A more recent study showed that *spen* manipulation in adipocyte-like cells correlated with alterations in the expression of key metabolic enzymes, supporting a role for Spen in energy catabolism[11]. In the present study, we found that glia-specific silencing of *spen* also affected lipid metabolism, as reflected by an increase in the number and size of LDs in *Drosophila* glial cells. While the mechanism underlying this effect is unclear, it is possible that *spen* downregulation may lead to a decrease in LD degradation or an increase in expression of triacylglycerol biosynthesis genes. Further investigations will be required to determine if Spen acts as a positive or negative regulator of lipid metabolism in different physiological and pathological contexts.

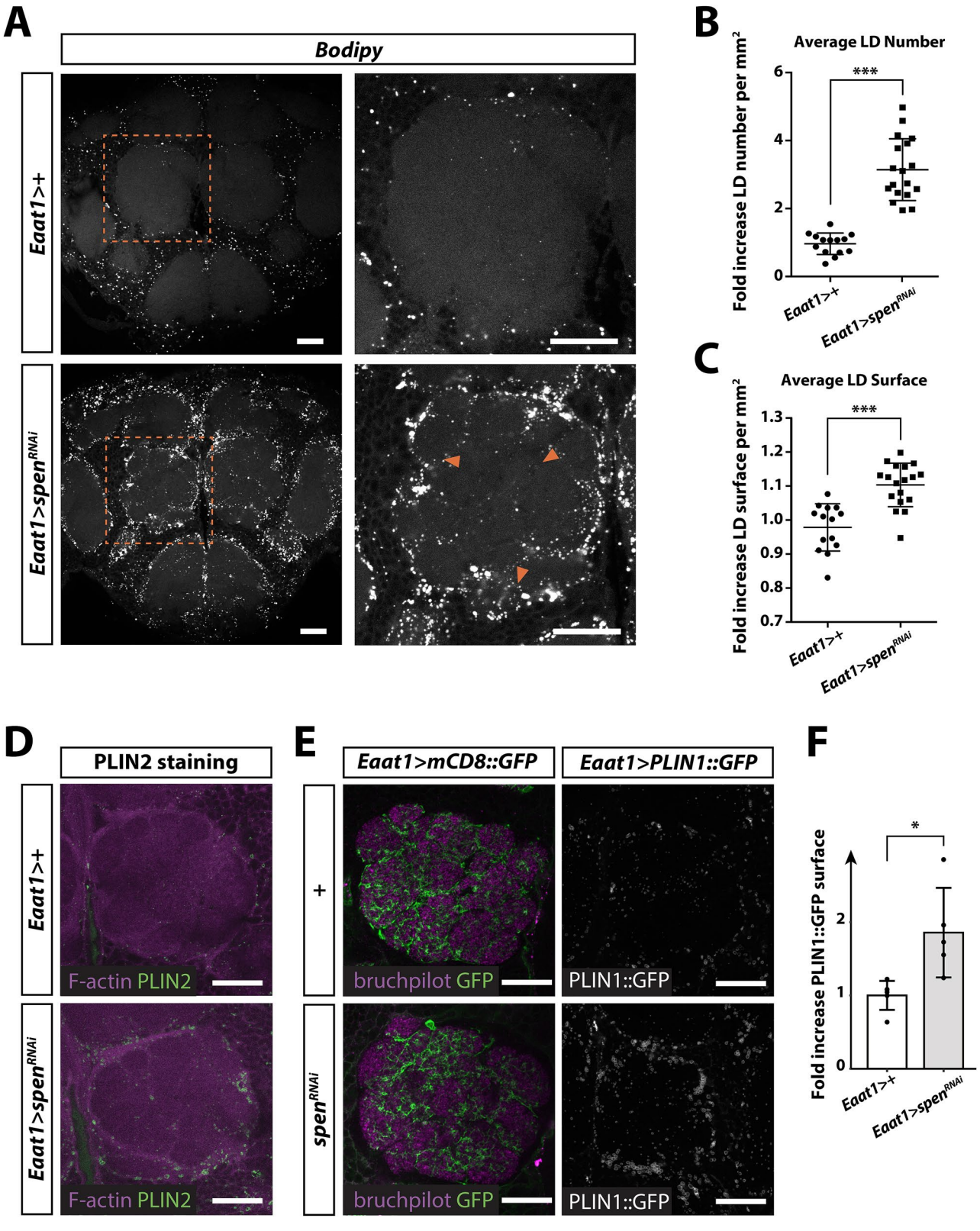
A
Bodipy
Eaat1>+
Eaat1>spen^RNAi
B
Average LD Number
Fold increase LD number per mm²
***
Eaat1>+
Eaat1>spen^RNAi
C
Average LD Surface
Fold increase LD surface per mm²
***
Eaat1>+
Eaat1>spen^RNAi
D
PLIN2 staining
Eaat1>+
Eaat1>spen^RNAi
F-actin PLIN2
E
Eaat1>mCD8::GFP
Eaat1>PLIN1::GFP
+
spen^RNAi
bruchpilot GFP
PLIN1::GFP
F
Fold increase PLIN1::GFP surface
*
Eaat1>+
Eaat1>spen^RNAi

◂**Figure 3.** Spen regulates lipid droplet number, size, and localization in *Drosophila* glial cells. (**A**) Fluorescence micrographs showing lipid droplets (LDs; white dots, BODIPY 493/503) in whole-mount brains of control flies *Eaat1* > + (*Eaat1-GAL4/+*) or flies expressing $spen^{RNAi}$ in glial cells *Eaat1* > $spen^{RNAi}$ (*Eaat1-GAL4/UAS-*$spen^{RNAi}$). Right panels show magnifications of the boxes outlined in the left panels. Orange arrowheads indicate LDs accumulated in the neuropil area of the antennal lobe in $spen^{RNAi}$ flies. Scale bar, 25 µm. (**B**,**C**) Quantification of LD number (**B**) and LD surface (**C**) in *Eaat1* > $spen^{RNAi}$ flies relative to the control flies *Eaat1* > + (*Eaat1-GAL4/+*). N = 14–18 brains per genotype from 3 independent experiments. Circles represent individual data points. LDs were quantified using an automated ImageJ plugin (see "Materials and methods" section). $P < 0.0001$ by unpaired Student's t test. (**D**) Fluorescence micrographs showing PLIN2 antibody staining (green) in whole-mount brains from control flies *Eaat1* > + (*Eaat1-GAL4/+*) and $spen^{RNAi}$ flies (*Eaat1-GAL4/UAS-*$spen^{RNAi}$). Brains were counterstained with phalloidin-rhodamine to detect F-actin (magenta). (**E**) Fluorescence micrographs of the antennal lobe of: (left panel) flies expressing the membrane reporter *mCD8::GFP* alone or in conjunction with $spen^{RNAi}$ under the control of the *Eaat1-GAL4* driver to label astrocyte-like glial processes infiltrating the antennal lobe, and (right panel) flies expressing the lipid droplet reporter *UAS-PLIN1::GFP (PLIN1::GFP)* alone or in conjunction with $spen^{RNAi}$ under the control of *Eaat1-GAL4.* Scale bar, 25 µm. (**F**) Quantification of PLIN1::GFP-positive staining in *Eaat1* > $spen^{RNAi}$ flies relative to control flies *Eaat1* > + (*Eaat1-GAL4/+*) flies. N = 5 brains per genotype. Circles represent individual data points. *$P < 0.05$ by unpaired Student's t test.

Spen has been shown to function as a negative regulator of Notch signaling at the morphogenetic furrow during eye development in *Drosophila*[26]. Here, we showed that Spen positively regulates Notch signaling in adult *Drosophila* glial cells. Spen-dependent activation of the Notch pathway has also been observed in intestinal stem cells of adult flies[28], substantiating the role of Spen as a positive regulator of Notch in adult tissues. Thus, Spen appears to differentially regulate Notch signaling in cell type-, context-, and developmental stage-specific manners. The ability of Spen to differentially affect Notch signaling may be mediated via recruitment of intermediate positive or negative regulatory factors, resulting in activation or repression of Notch responsive-genes expression, respectively.

Our results show that the accumulation of LDs induced by *spen* knockdown is independent of Notch/Su(H) signaling, as reflected by the lack of effect of glia-specific *Su(H)* knockdown on LD size or number. Rather, Spen may directly affect mRNA stability or splicing of lipid metabolism genes to promote gene expression independently of Notch[11]. Finally, it is possible that the LD accumulation may be due to increased oxidative stress in *spen*-mutant flies, as previously observed in flies with defective mitochondrial respiration or after exposure to hypoxia[6,7,9]. Our results showing that *spen*-mutant flies exhibited increased sensitivity to paraquat toxicity are consistent with a mechanism involving oxidative stress.

Our findings are also in accord with a role for glia-expressed Spen in lipid metabolism in the context of PD pathophysiology. Using a data-mining approach, we found that genes differentially expressed in the SN of PD patients are not only enriched in astrocyte-expressed genes (e.g., *SPEN/SHARP*) but also include a significant number of genes annotated with the Gene Ontology terms "phospholipid metabolism", "lipid and lipoprotein metabolism", and "sphingolipid metabolism". These results point to a potential pathological role for lipid metabolism in PD, which is in accordance with a meta-analysis of genome-wide association studies of PD[46]. Among the lipid-related genes identified here to be differentially expressed in the SN of PD patients are several that could contribute to the regulation of LD formation and/or fate. For example, *AGPAT4* (1-acylglycerol-3-phosphate O-acyltransferase 4) is involved in the synthesis of precursors of TAGs, the major lipid component of LDs. Similarly, *SCD5* (stearoyl-CoA desaturase 5), a recently identified new target for PD treatment[47], catalyzes free fatty acid desaturation and plays an important role in the early steps of LD formation. Finally, *Arf79F* and *schlank*, the *Drosophila* orthologs of two lipid-related genes found to be downregulated in the SN of PD patients, have been shown to control the homeostasis of LDs in *Drosophila*[48,49].

Taken together, our data support a central role for *spen* expressed in glial cells in the control of lipid metabolism and resistance to paraquat-induced toxicity in *Drosophila*. Further studies on the function of Spen will contribute to our understanding of the involvement of lipid dyshomeostasis in neurodegeneration.

Materials and methods

Fly strains. Flies were maintained on standard yeast medium at 25 °C unless otherwise noted. Flies bearing the following mutations and transgenes were obtained from the Bloomington Drosophila Stock Center (Indiana University, IN, USA): w^{1118}, *repo-GAL4* (BL7415), *UAS-mCherry-NLS* (BL38424), *tubulin-GAL80*^{ts} (BL7019), *UAS-mCD8::GFP* (BL32186), *NRE-EGFP1* (referred to as NRE-GFP, BL30728), *UAS-Notch*^{intra} (BL52008), an *Eaat1-GAL4*[34] (BL8849), *elav-GAL4* (BL458). $spen^{k07612}$ and $spen^{03350}$ P element insertions (*Drosophila* Genomics Resource Center [DGRC] #102574 and BL11295) were previously characterized as homozygous lethal *spen* loss-of-function mutations[17] and were used here as heterozygotes. *UAS-PLIN1::GFP*[40] was obtained from RP Kuhnlein (University of Graz, Austria). The EP line *spen-GS2279* (Kyoto DGRC Stock Center) was used to overexpress *spen,* and is referred to as *UAS-spen*. The *UAS-*$spen^{RNAi}$ line was a gift from KM Cadigan[50] and was previously characterized in studies of *Drosophila* retina development[14]. *spen* mutants and transgenic flies were outcrossed to a w^{1118} control stock. We used the temperature-sensitive TARGET system[45] to restrict spen RNAi expression to adult glial cells. Briefly, flies carrying repo-GAL4, *tubulin-GAL80*^{ts}, and *UAS-*$spen^{RNAi}$ were raised at 18 °C to inhibit GAL4 activity and switched to 29 °C as adults to induce expression of $spen^{RNAi}$.

RT-qPCR. Total RNA was isolated from 25 to 35 *Drosophila* heads using RNeasy mini kits (Qiagen) and reverse transcribed with oligo(dT)15 primers and the ImProm-II Reverse Transcription System (Promega)

according to manufacturers' instructions. Quantitative PCR reactions were carried out on a StepOnePlus system (Applied Biosystems) using FastStart Universal SYBR Green Master (Roche Applied Science). Efficiency (E) of the primer sets was assessed using serial dilutions of cDNA preparations. Standard curves were generated to quantify mRNA abundance and PCR cycle numbers (Ct) for calculation of the relative mRNA expression level (Qr = E − Ct)[51]. Values were normalized to Rp49 mRNA levels. Primers for qPCR were: *spen* forward 5′-TTC GTTGTGGGATAGCAGCA-3′ and reverse 5′-CGTTCGAAGCTGTTTGTCG-3′ and *Rp49* forward 5′-ATC GTGAAGAAGCGCACCAAG-3′ and reverse 5′-ACCAGGAACTTCTTGAATCCG-3′.

Immunostaining. *Drosophila* heads were removed and placed in a drop of fresh Hemolymph-Like 3 dissection buffer[52] (HL3) supplemented with D-glucose (120 mM). The proboscis was removed and the cuticle was opened to access the brain, and the brains were dissected and fixed overnight at 4 °C in 1% paraformaldehyde (PFA) diluted in HL3 medium. Fixed brains were washed 3 times for 10 min each in phosphate-buffered saline (PBS) containing 0.5% Triton X-100 and 5 mg/ml bovine serum albumin, and then incubated for 1 h in the same buffer containing 4% normal goat serum to prevent non-specific antibody binding (blocking solution). The brains were then incubated overnight at 4 °C with the following primary antibodies diluted in blocking solution: mouse anti-Repo (1:400, Developmental Studies Hybridoma Bank, 8D12), rabbit anti-GFP (1:400, Invitrogen, A6455), and rabbit anti-PLIN2 (1:1000, a gift from RP Kuhnlein[40]). The samples were washed 3 times with PBS-T and incubated overnight at 4 °C with anti-mouse Alexa Fluor 647 (1:400, Invitrogen, A31571) or anti-rabbit Alexa Fluor 488 (1:400, Invitrogen A11008) secondary antibodies diluted in blocking solution. Samples were washed 3 times and then mounted in Vectashield mounting medium (AbCys) on a bridge slide to prevent tissue flattening. Samples were stored at − 20 °C until visualized.

For experiments with the NRE-GFP-expressing *Drosophila* line, the heads were removed and placed in a drop of fresh PBS. The brains were dissected and fixed in 4% PFA/PBS for 20 min at room temperature. The brains were then washed in PBS and mounted directly in Vectashield medium (AbCys). As controls for the NRE-GFP experiments, brains from *Drosophila* not expressing GFP were also processed to evaluate background fluorescence.

Image processing. Images of whole-mount brains were acquired at the LYMIC-PLATIM Imaging and Microscopy Core Facility of SFR Biosciences (UMS3444, ENS de Lyon, France). For PLIN1::GFP, Repo, and BODIPY fluorescence, images were acquired on a Zeiss LSM800 confocal microscope and analyzed with the ImageJ[39] software (see section below). For NRE-GFP fluorescence, images were acquired on a Leica epifluorescence microscope. In each experiment, the mean GFP fluorescence of control brains (*Eaat1-GAL4/+*) was used to normalize the results. The NRE reporter is a synthetic construct with three copies of SPS sites taken from the E(spl) regulatory region[36]. SPS (Su(H) paired sites) are binding sites for the Notch activity-dependent transcription factor Su(H).

Automated image analysis. We developed an ImageJ macro (https://gitbio.ens-lyon.fr/dcluet/Lipid_Droplets) to identify fluorescent particles on confocal stacks using *Drosophila* brains stained with the lipid-binding dye BODIPY 493/503 (Molecular Probes, D-3922) or labeled with the glial cell-specific marker Repo. The program requires ImageJ[39] v1.49 g or higher and is based on an iterative detection of the brightest particles followed by removal of "doublets" of the same particle over the stack. Briefly, the program first delineates the brain region of interest and then identifies particles within that region along the stack. The signal is intensified using the Gaussian blur function and the maximum entropy treatment. The "Max-Entropy" threshold method[53] is then applied to detect the particles of interest. The detected particles are stored in a transient matrix and removed from the image. The next iteration is able to detect less bright particles. Finally, the program removes all doublets of the same particle along the z-dimension of the stack (keeping the largest candidate as the best) to enable optimal counting of labeled particles. The program can calculate multiple parameters, such as particle density, size, and circularity.

Paraquat-induced PD model. Paraquat medium was prepared fresh shortly before each experiment. Paraquat (Sigma, 36541) was added at 10 or 20 mM to PBS (as indicated in the corresponding figure legends) containing 0.8% low-melting agarose (Sigma, A9414) and 10% sucrose (Sigma, S0389). Three-day-old male flies were fasted for 4 h on 0.8% agarose medium and then transferred to 10 or 20 mM paraquat-containing medium for 5–7 days for survival experiments or the indicated times for RT-qPCR analysis. At least three independent experiments were performed, each with $n \geq 20$ flies per condition per experiment.

Lipid droplet staining. Heads were removed from 6-day-old flies and placed in a drop of fresh HL3 dissection buffer supplemented with D-glucose (120 mM). Brains were dissected and fixed overnight at 4 °C in 1% PFA/HL3 medium. Fixed brains were washed 3 times for 10 min each in PBS/01.% Triton X-100 and then incubated overnight at 4 °C with 15 mg/ml BODIPY 493/503 (Molecular Probes, D-3922) diluted in the same buffer. The brains were washed 3 additional times with PBS/0.1% Triton X-100, mounted in Vectashield medium (AbCys) on a bridge slide, and stored at − 20 °C until imaged.

Statistical analysis. Data are presented as the means ± standard deviation from three independent experiments unless noted. Statistical analyses were performed using R (R Core Team) and Prism software (GraphPad, San Diego, CA). The statistical tests applied are given in the figure legends.

Received: 26 May 2020; Accepted: 16 October 2020
Published online: 18 November 2020

References

1. Tanner, C. M. *et al.* Rotenone, paraquat, and Parkinson's disease. *Environ. Health Perspect.* **119**, 866–872 (2011).
2. Cassar, M. *et al.* A dopamine receptor contributes to paraquat-induced neurotoxicity in Drosophila. *Hum. Mol. Genet.* **24**, 197–212 (2015).
3. Filograna, R. *et al.* Superoxide dismutase (SOD)-mimetic M40403 is protective in cell and fly models of paraquat toxicity: Implications for Parkinson disease. *J. Biol. Chem.* **291**, 9257–9267 (2016).
4. Robin, M. *et al.* Drosophila p53 integrates the antagonism between autophagy and apoptosis in response to stress. *Autophagy* **15**, 771–784 (2019).
5. Yildirim, K., Petri, J., Kottmeier, R. & Klämbt, C. Drosophila glia: Few cell types and many conserved functions: YILDIRIM et al.. *Glia* **67**, 5–26 (2019).
6. Liu, L. *et al.* Glial lipid droplets and ROS induced by mitochondrial defects promote neurodegeneration. *Cell* **160**, 177–190 (2015).
7. Van Den Brink, D. M. *et al.* Physiological and pathological roles of FATP-mediated lipid droplets in Drosophila and mice retina. *PLoS Genet.* **14**, e1007627 (2018).
8. Ioannou, M. S. *et al.* Neuron-astrocyte metabolic coupling protects against activity-induced fatty acid toxicity. *Cell* **177**, 1522-1535. e14 (2019).
9. Bailey, A. P. *et al.* Antioxidant role for lipid droplets in a stem cell niche of drosophila. *Cell* **163**, 340–353 (2015).
10. Marschallinger, J. *et al.* Lipid-droplet-accumulating microglia represent a dysfunctional and proinflammatory state in the aging brain. *Nat. Neurosci.* **23**, 194–208 (2020).
11. Hazegh, K. E. *et al.* An autonomous metabolic role for Spen. *PLoS Genet.* **13**, e1006859 (2017).
12. Gillette, C. M. *et al.* Gene–diet interactions: Dietary rescue of metabolic effects in spen-depleted *Drosophila melanogaster*. *Genetics* **214**, 961–975 (2020).
13. Chen, F. & Rebay, I. Split ends, a new component of the Drosophila EGF receptor pathway, regulates development of midline glial cells. *Curr. Biol.* **10**, 943-S2 (2000).
14. Querenet, M., Goubard, V., Chatelain, G., Davoust, N. & Mollereau, B. Spen is required for pigment cell survival during pupal development in Drosophila. *Dev. Biol.* **402**, 208–215 (2015).
15. Kuang, B., Wu, S. C., Shin, Y., Luo, L. & Kolodziej, P. split ends encodes large nuclear proteins that regulate neuronal cell fate and axon extension in the Drosophila embryo. *Dev. Camb. Engl.* **127**, 1517–1529 (2000).
16. Rebay, I. *et al.* A genetic screen for novel components of the Ras/Mitogen-activated protein kinase signaling pathway that interact with the yan gene of Drosophila identifies split ends, a new RNA recognition motif-containing protein. *Genetics* **154**, 695–712 (2000).
17. Wiellette, E. L. *et al.* spen encodes an RNP motif protein that interacts with Hox pathways to repress the development of head-like sclerites in the Drosophila trunk. *Dev. Camb. Engl.* **126**, 5373–5385 (1999).
18. Chu, C. *et al.* Systematic discovery of Xist RNA binding proteins. *Cell* **161**, 404–416 (2015).
19. Jin, L. H. *et al.* Requirement of split ends for epigenetic regulation of notch signal-dependent genes during infection-induced hemocyte differentiation. *Mol. Cell. Biol.* **29**, 1515–1525 (2009).
20. McHugh, C. A. *et al.* The Xist lncRNA interacts directly with SHARP to silence transcription through HDAC3. *Nature* **521**, 232–236 (2015).
21. Moindrot, B. *et al.* A pooled shRNA screen identifies Rbm15, Spen, and Wtap as factors required for Xist RNA-mediated silencing. *Cell Rep.* **12**, 562–572 (2015).
22. Monfort, A. *et al.* Identification of Spen as a crucial factor for Xist function through forward genetic screening in haploid embryonic stem cells. *Cell Rep.* **12**, 554–561 (2015).
23. Yan, D. & Perrimon, N. *Spenito* is required for sex determination in *Drosophila melanogaster*. *Proc. Natl. Acad. Sci.* **112**, 11606–11611 (2015).
24. Oswald, F. SHARP is a novel component of the Notch/RBP-Jkappa signalling pathway. *EMBO J.* **21**, 5417–5426 (2002).
25. Yuan, Z. *et al.* Structural and functional studies of the RBPJ-SHARP complex reveal a conserved corepressor binding site. *Cell Rep.* **26**, 845-854.e6 (2019).
26. Doroquez, D. B., Orr-Weaver, T. L. & Rebay, I. Split ends antagonizes the Notch and potentiates the EGFR signaling pathways during Drosophila eye development. *Mech. Dev.* **124**, 792–806 (2007).
27. Oswald, F. *et al.* A phospho-dependent mechanism involving NCoR and KMT2D controls a permissive chromatin state at Notch target genes. *Nucleic Acids Res.* **44**, 4703–4720 (2016).
28. Andriatsilavo, M. *et al.* Spen limits intestinal stem cell self-renewal. *PLoS Genet.* **14**, e1007773 (2018).
29. Zhang, Y. *et al.* Purification and characterization of progenitor and mature human astrocytes reveals transcriptional and functional differences with mouse. *Neuron* **89**, 37–53 (2016).
30. Kelly, J., Moyeed, R., Carroll, C., Albani, D. & Li, X. Gene expression meta-analysis of Parkinson's disease and its relationship with Alzheimer's disease. *Mol. Brain* **12**, 16 (2019).
31. Chen, Y.-A. *et al.* The TargetMine data warehouse: Enhancement and updates. *Front. Genet.* **10**, 934 (2019).
32. Huang, R. *et al.* The NCATS BioPlanet—An integrated platform for exploring the universe of cellular signaling pathways for toxicology, systems biology, and chemical genomics. *Front. Pharmacol.* **10**, 445 (2019).
33. Davie, K. *et al.* A single-cell transcriptome atlas of the aging Drosophila brain. *Cell* **174**, 982-998.e20 (2018).
34. Rival, T. *et al.* Decreasing glutamate buffering capacity triggers oxidative stress and neuropil degeneration in the Drosophila brain. *Curr. Biol.* **14**, 599–605 (2004).
35. Freeman, M. R., Delrow, J., Kim, J., Johnson, E. & Doe, C. Q. Unwrapping glial biology: Gcm target genes regulating glial development, diversification, and function. *Neuron* **38**, 567–580 (2003).
36. Saj, A. *et al.* A combined ex vivo and in vivo RNAi screen for notch regulators in Drosophila reveals an extensive notch interaction network. *Dev. Cell* **18**, 862–876 (2010).
37. Seugnet, L. *et al.* Notch signaling modulates sleep homeostasis and learning after sleep deprivation in Drosophila. *Curr. Biol.* **21**, 835–840 (2011).
38. Morel, V. *et al.* Transcriptional repression by suppressor of hairless involves the binding of a hairless-dCtBP complex in Drosophila. *Curr. Biol.* **11**, 789–792 (2001).
39. Schneider, C. A., Rasband, W. S. & Eliceiri, K. W. NIH image to ImageJ: 25 years of image analysis. *Nat. Methods* **9**, 671–675 (2012).
40. Beller, M. *et al.* PERILIPIN-dependent control of lipid droplet structure and fat storage in Drosophila. *Cell Metab.* **12**, 521–532 (2010).
41. Grönke, S. *et al.* Control of fat storage by a Drosophila PAT domain protein. *Curr. Biol.* **13**, 603–606 (2003).
42. Fanning, S., Selkoe, D. & Dettmer, U. Parkinson's disease: Proteinopathy or lipidopathy?. *NPJ Park. Dis.* **6**, 3 (2020).
43. Baumbach, J. *et al.* A Drosophila in vivo screen identifies store-operated calcium entry as a key regulator of adiposity. *Cell Metab.* **19**, 331–343 (2014).

44. Reis, T., Van Gilst, M. R. & Hariharan, I. K. A buoyancy-based screen of Drosophila Larvae for fat-storage mutants reveals a role for Sir2 in coupling fat storage to nutrient availability. *PLoS Genet.* **6**, e1001206 (2010).
45. Mcguire, S. Gene expression systems in Drosophila: A synthesis of time and space. *Trends Genet.* **20**, 384–391 (2004).
46. Klemann, C. J. H. M. *et al.* Integrated molecular landscape of Parkinson's disease. *Npj Park. Dis.* **3**, 14 (2017).
47. Fanning, S. *et al.* Lipidomic analysis of α-Synuclein neurotoxicity identifies stearoyl CoA desaturase as a target for Parkinson treatment. *Mol. Cell* **73**, 1001-1014.e8 (2019).
48. Bauer, R. *et al.* Schlank, a member of the ceramide synthase family controls growth and body fat in Drosophila. *EMBO J.* **28**, 3706–3716 (2009).
49. Guo, Y. *et al.* Functional genomic screen reveals genes involved in lipid-droplet formation and utilization. *Nature* **453**, 657–661 (2008).
50. Chang, J. L., Lin, H. V., Blauwkamp, T. A. & Cadigan, K. M. Spenito and Split ends act redundantly to promote Wingless signaling. *Dev. Biol.* **314**, 100–111 (2008).
51. Jamilloux, Y. *et al.* Inflammasome activation restricts *Legionella pneumophila* replication in primary microglial cells through flagellin detection. *Glia* **61**, 539–549 (2013).
52. Stewart, B. A., Atwood, H. L., Renger, J. J., Wang, J. & Wu, C. F. Improved stability of Drosophila larval neuromuscular preparations in haemolymph-like physiological solutions. *J. Comp. Physiol. A* **175**, 179–191 (1994).
53. Sahoo, P. K., Soltani, S. & Wong, A. K. C. A survey of thresholding techniques. *Comput. Vis. Graph. Image Process.* **41**, 233–260 (1988).

Acknowledgements

This work was supported by the French National Research Agency (award ANR-12-BSV1-0019 to BM), SFR Biosciences Projets Développement Technologique (to ND and BM). VG was supported by grants from Fondation Servier, ENS Fond Recherche, and a FRM fellowship. MQ was supported by fellowships from the French Ministry of Research and Education and Association France Parkinson. We thank ARTHRO-TOOLS and PLATIM facilities for fly medium preparation and confocal imaging, respectively.

Author contributions

V.Gi., V.Go., M.Q., E.D. and N.D. performed the *Drosophila* experiments. N.D. and B.M. designed the experiments and obtained funding to support this research. L.S. designed and performed the Notch experiments with the help of V.Go. L.P. and S.N. performed the data-mining experiments. D.C. wrote the ImageJ macro code. V.Gi. and N.D. prepared the figures and drawings. N.D. designed the study and wrote the first draft of the manuscript. V.Gi., S.N., L.S. and BM revised the manuscript for critical content.

Competing interests

The authors declare no competing interests.

Additional information

Supplementary information is available for this paper at https://doi.org/10.1038/s41598-020-76891-9.

Correspondence and requests for materials should be addressed to B.M. or N.D.

Reprints and permissions information is available at www.nature.com/reprints.

Publisher's note Springer Nature remains neutral with regard to jurisdictional claims in published maps and institutional affiliations.

Supplemental Files

Spen modulates lipid droplet content in adult Drosophila glial cells and protects against paraquat toxicity

Victor Girard, Valérie Goubard, Matthieu Querenet, Laurent Seugnet, Laurent Pays, Serge Nataf, Eloïse Dufourd, David Cluet, Bertrand Mollereau[#] and Nathalie Davoust[#]

[#] Corresponding authors: Nathalie Davoust (nathalie.davoust-nataf@ens-lyon.fr) and Bertrand Mollereau (bertrand.mollereau@ens-lyon.fr)

Girard et al, Supplemental Figure 1

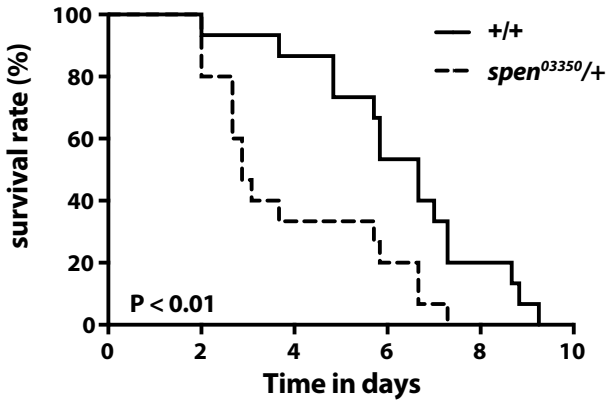

Figure S1. *spen* heterozygous mutant flies are more sensitive to paraquat-induced lethality. Survival rate of *spen* loss of function heterozygous mutants (*P{lacW}spen[03350]/+*) adult flies fed with paraquat (10 mM). *spen*^{03350} heterozygous flies are more sensitive to paraquat than wild-type flies (*w1118*). Log-rank Mantel-Cox test, P<0.0001.

Girard et al, Supplemental Figure 2

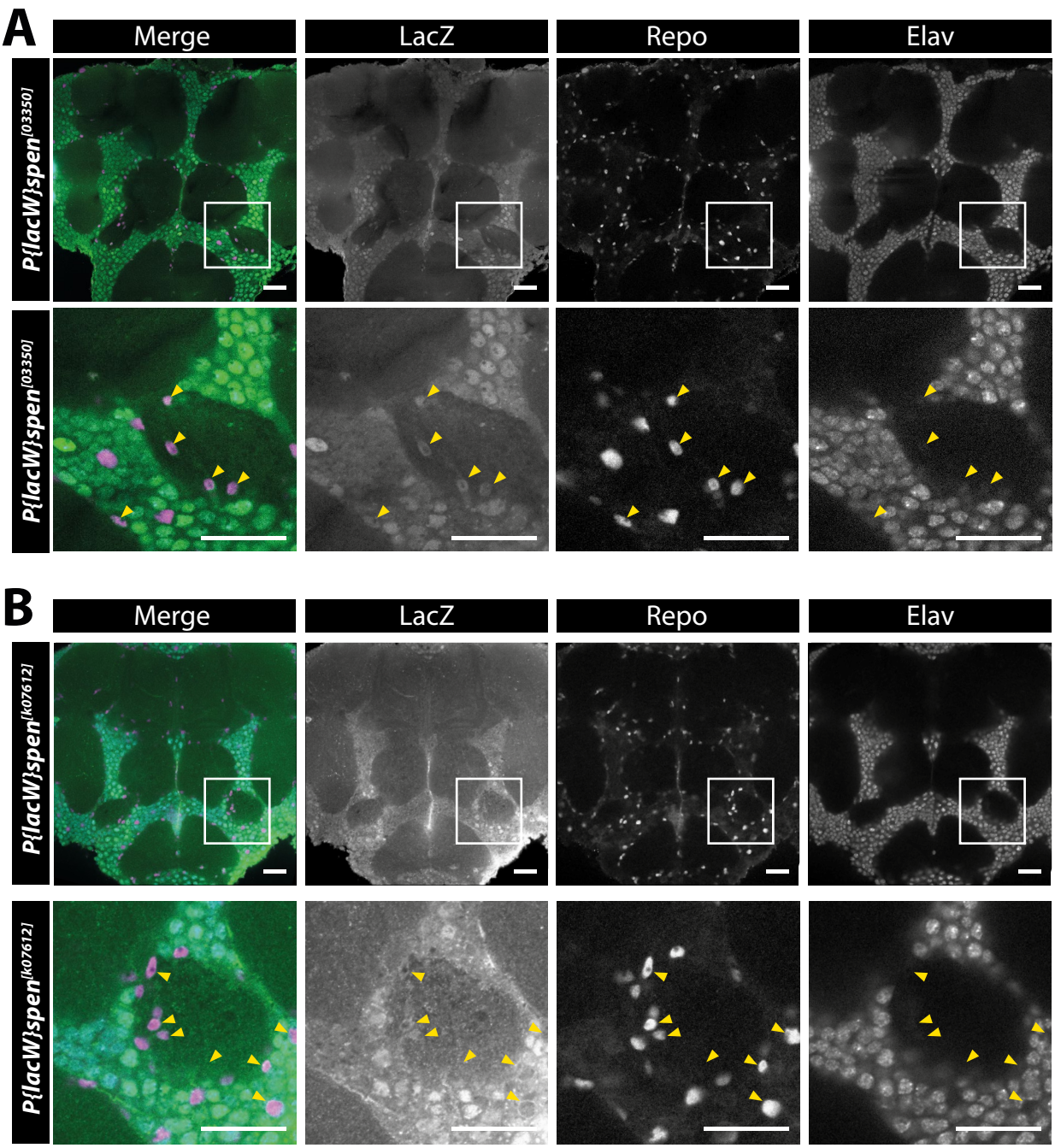

Figure S2. *spen* is expressed in both glia and neurons in *Drosophila* adult brain.
(A) *spen* expression domain in adult brain was assessed by immunostaining of LacZ (green) reporter gene in whole mount brain of 2 enhancer trap lines: *P{lacW}spen[03350]*, **(A)** and *P{lacW}spen[k07612]*, **(B)**. Glial cell nuclei are visualized using Repo staining (magenta) and neuron nuclei using Elav staining (cyan). Expression of *spen* in glial cells is indicated with yellow arrowheads. Scale bar: 25µm.

Girard et al, Supplemental Figure 3

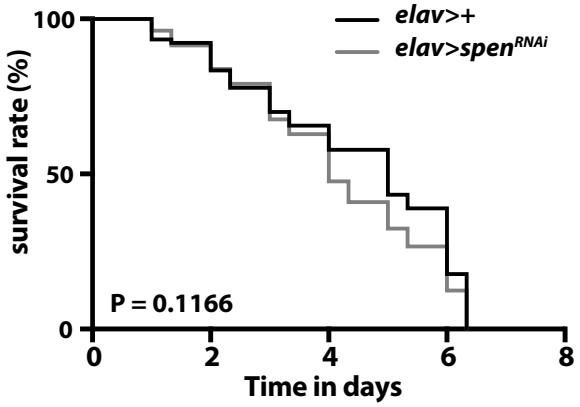

Figure S3. Knockdown of *spen* in neurons does not enhance the fly sensitivity to paraquat treatment.

Survival curves of adult male control flies (*elav-GAL4/+;;*) or flies with glial cell-specific spen knockdown (*elav-GAL4 ;UAS-spen^{RNAi} /+;*) fed with 20 mM paraquat. The curves represent the sum of three independent experiments with each N=20 flies per genotype. P=0.1166, not significant, by the log-rank Mantel–Cox test.

Girard et al, Supplemental Figure 4

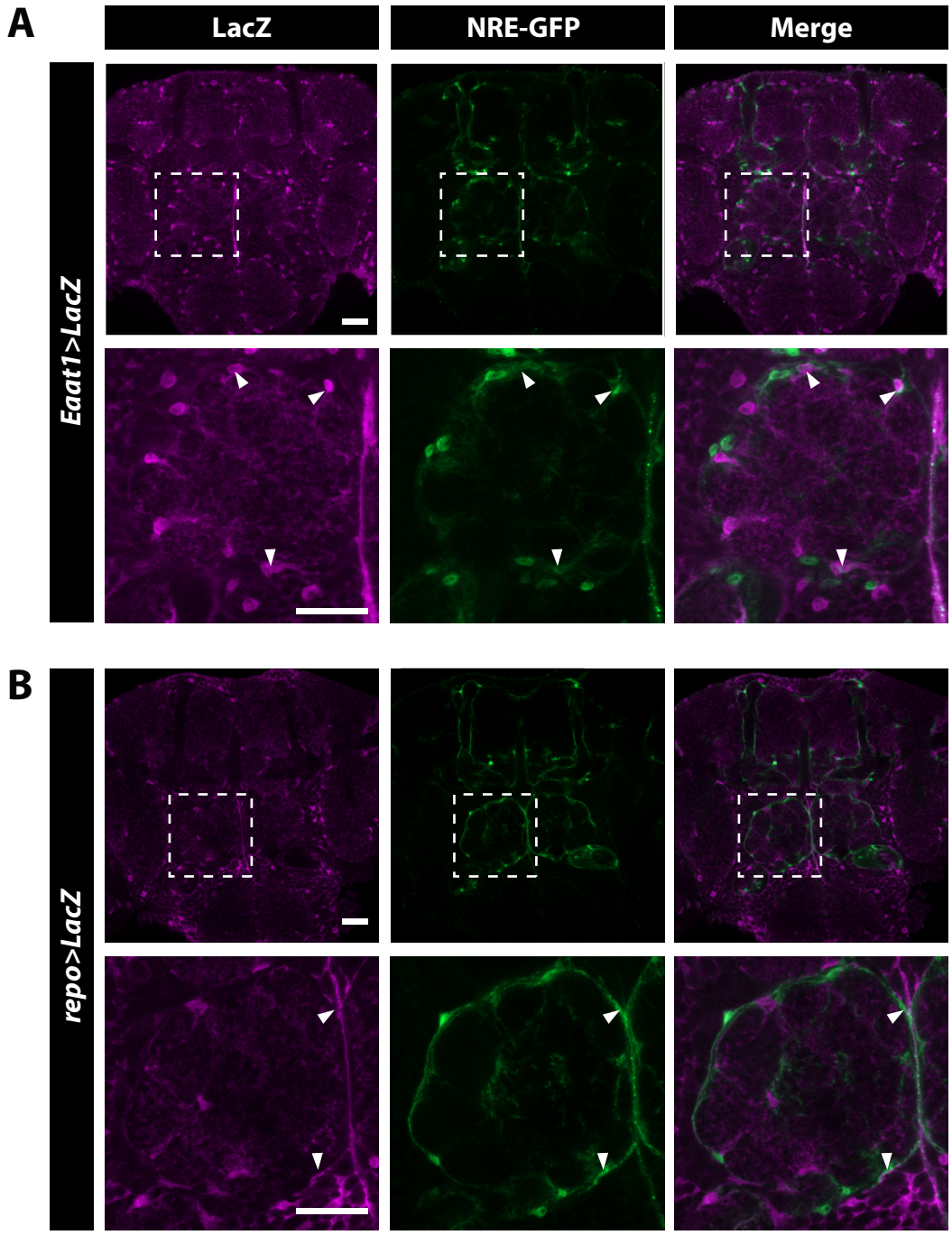

Figure S4. Notch signaling is activated in adult Eaat1+ glial cells .
Confocal microscopy of whole-mount brain of flies carrying Notch activation reporter NRE-GFP (green) expressing LacZ (magenta) under the control of glial driver *Eaat1-Gal4* (A) and *repo-Gal4* (B). NRE-GFP and LacZ co-localisation in glial cells Eaat1 or repo positive is indicated with white arrowheads. Scale bar: 25µm.

Girard et al, Supplemental Figure 5

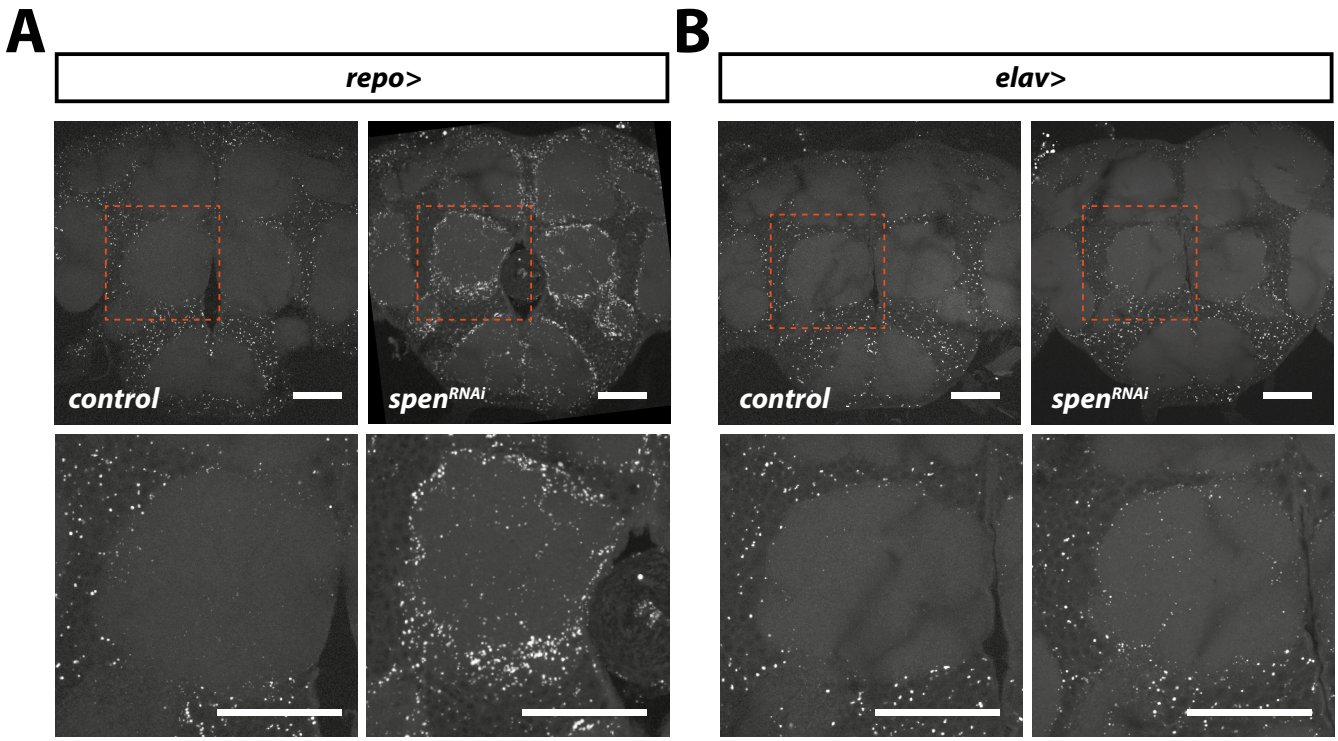

Figure S5. Lack of *spen* in glia but not in neurons promotes lipid droplet accumulation in adult *Drosophila* brain.
Lipid droplets labelled with BODIPY 493/503 (white dots) in whole-mount brain of flies expressing *spen*^{RNAi} specifically in glia (**A**, *repo-GAL4*) or neurons (**B**, *elav-GAL4*) compare to their respective control. As shown in the close-up, lipid droplets are accumulating in the neuropil area of the antennal lobe only flies lacking *spen* in glia but not in neurons. Scale bar: 25µm.

Girard et al, Supplemental Figure 6

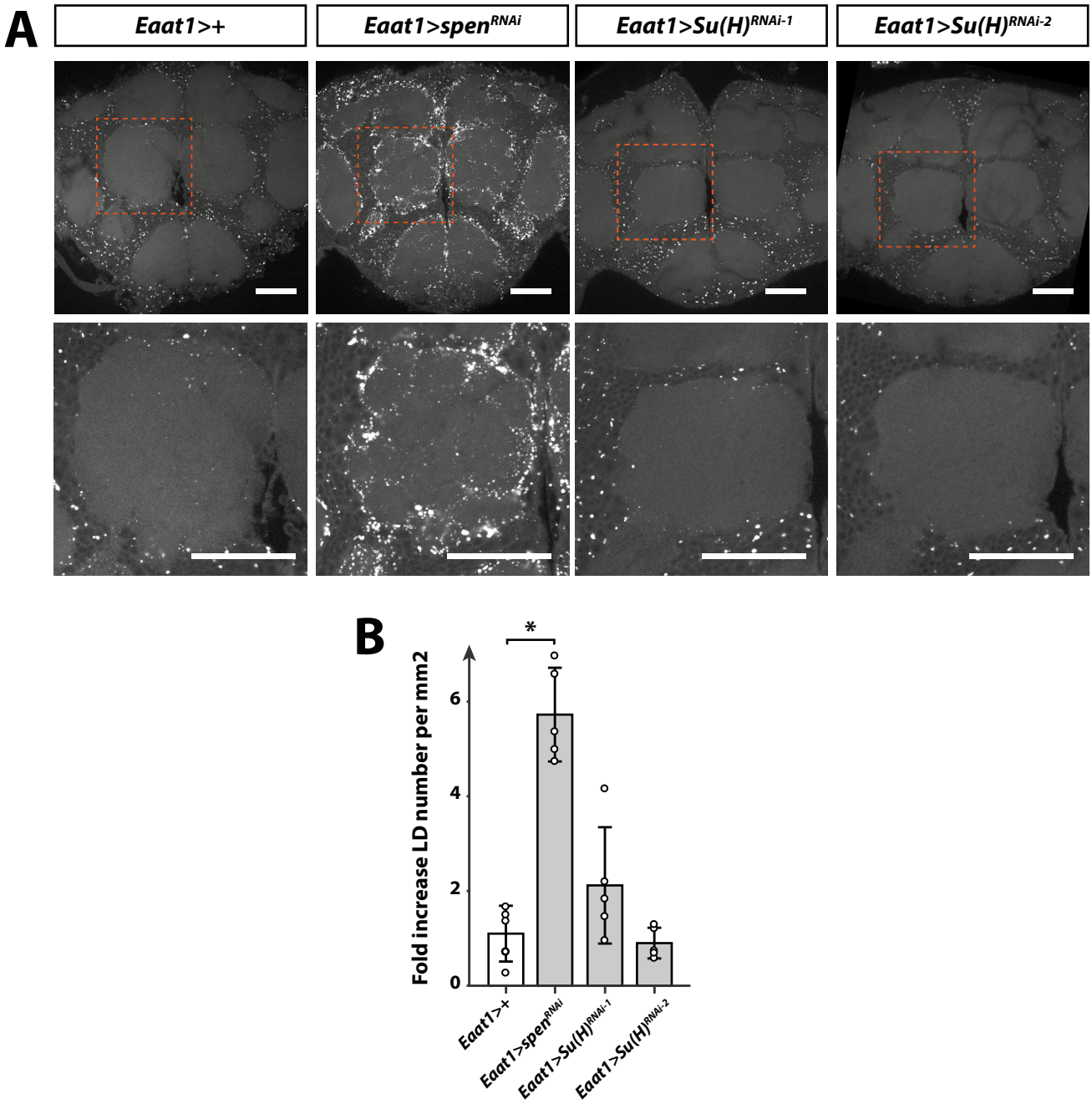

Figure S6. *Su(H)* knockdown do not modify glial cell lipid droplet in adult *Drosophila* brain. **(A)** Lipid droplets labelled with BODIPY 493/503 (white dots) in whole-mount brain of control flies *Eaat1*>+ (;*Eaat1-GAL4*/+;) and flies expressing *spen*^{RNAi} in glial cells *Eaat1*>*spen*^{RNAi} (;*Eaat1-GAL4/UAS-spen*^{RNAi};) was compared to flies expressing two different *Su(H)*^{RNAi} (RNAi-1 : HMS05110 , RNAi-2: KK101550). As shown in the close-up, lipid droplets are accumulating in the neuropil area of the antennal lobe in *spen* knockdown but not in *Su(H)* knockdown. Scale bar: 25µm. **(B)** Quantification of BODIPY 493/503 labelled lipid droplets. Data are presented as the fold change in lipid droplets number (B) relative to control flies *Eaat1*>+ (;Eaat1-GAL4/+;). n=5 brains per condition. Droplets were quantified using an automated ImageJ plugin described in the material and methods section. Non-parametric Kruskal-Wallis test, * P<0.05. Scale bar: 50µm.

2.2. Additional results not included in Girard et al. (2)

2.2.1. Glial cells lacking *spen* show signs of lipid peroxidation

We found that knockdown of *spen* increased lipid storage in glial cells and fly sensitivity to paraquat intoxication. This result is coherent with previous reports indicating that loss of spen increased lipid storage in a cell-autonomous manner in *Drosophila* larvae fat body (Hazegh et al., 2017). Hazegh et al., found that spen promotes lipid catabolism as lack of *spen* reduced the expression of enzymes involved in lipolysis and ß-oxidation (Hazegh et al., 2017). We hypothesized that if spen is involved in lipid catabolism in glia as well, glial cells lacking spen may accumulate abnormal levels of lipids. Lipid overload can damage mitochondria and lead to lipid peroxidation in non-adipose tissue (Nguyen et al., 2017). To

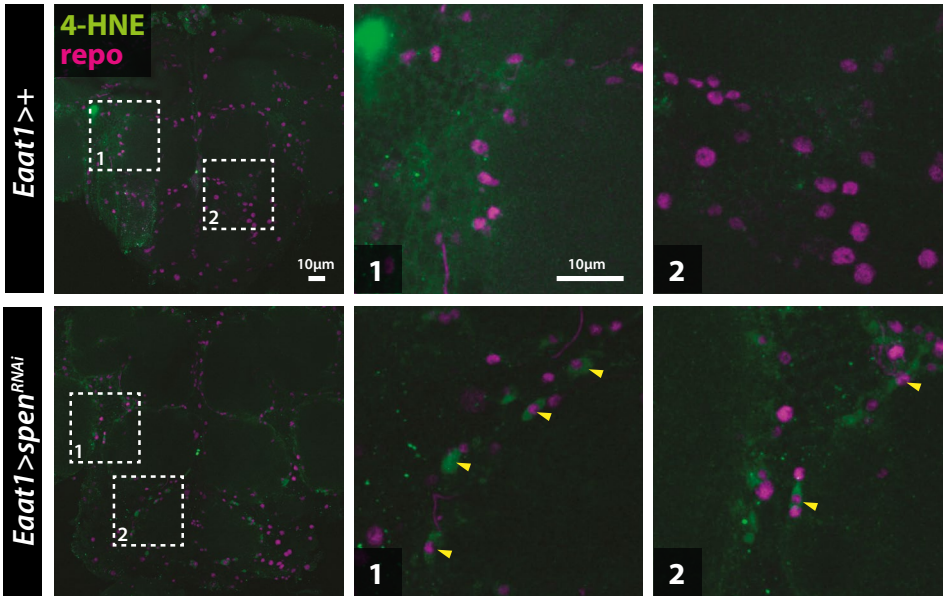

Figure 28. 4-HNE protein adducts accumulate in glial cells knockdown of *spen*.
Longitudinal optical sections of whole-mount brain from 6 day-old flies expressing *spen-RNAi* in astrocyte glia (Eaat1-*GAL4*). 4-HNE protein adducts are labeled in green (4-HNE immunostaining) and glial nuclei are in magenta (repo immunostaining). Scale bar, 10 µm.

test this hypothesis, we stained brains for 4-HNE adduct, a product of lipid peroxidation previously shown to increase during oxidative stress (Bailey et al., 2015).

While the brain of control flies did not show any noticeable level of 4-HNE adducts, the brain of glial Spen knockdown flies showed an increase in 4-HNE staining in glial cells labelled by repo immunostaining. Moreover, cells with high 4-HNE signal were located around the neuropil, in a way reminiscent of the cells accumulating LDs (Girard et al.

(2) Figure 3). From these results, we hypothesize that loss of Spen in glia increases lipid peroxidation. Collectively these results indicate that glial cells lacking *Spen* already show signs of lipid peroxidation, which may increase their sensitivity to paraquat-induced oxidative stress and their subsequent precipitated death.

DISCUSSION

During my thesis, I investigated the mechanisms underlying LD accumulation in both glia and neurons and their contribution to the progression of PD pathology using *Drosophila* as a model system.

1. How do LD-binding proteins promote LD accumulation in neurons?

LDs are rarely seen in healthy neurons, but strikingly mutation in genes important for lipid metabolism and regulation of LD homeostasis are associated with neurodegenerative disorders including HSPs, AD and PD. In addition, neurons containing LDs can be detected in the brain of aged mice, indicating that LDs can appear in neurons during normal aging (Shimabukuro et al., 2016). We found that, in young flies, LDs could be observed in photoreceptor neurons, suggesting that *Drosophila* retina could be a suitable model to study neuronal LD formation *in vivo* (Van Den Brink et al., 2018). I found that expression of dPlin1 and dPlin2 induce long-term LD accumulation in adult *Drosophila* photoreceptor neurons (20 day-old and beyond). This phenotype was specific to neuronal cells as I did not observe any LD in glial cells in 20 day-old flies. The accumulation of LDs in cells overexpressing perilipins is in agreement with previous reports indicating that human perilipins increase lipid storage in murine fibroblast and yeast (Brasaemle et al., 2000; Imamura et al., 2002; Jacquier et al., 2013). While perilipins are known to limit lipolysis, and in particular ATGL-mediated TAG hydrolysis, they can also maintain LD integrity by acting as scaffolds and are required for the maturation of LDs (Beller et al., 2010; Bulankina et al., 2009; Gao et al., 2017; Listenberger et al., 2007; Skinner et al., 2009). Interestingly, the silencing of Bmm lipase did not recapitulate the phenotype of LD accumulation seen in flies expressing dPlin1 or dPlin2 suggesting that Bmm inhibition is not sufficient to induce LDs in neurons. This result also further supports that the accumulation of LDs in neurons induced by Plins occurs independently of lipolysis inhibition but possibly by another mechanism, such as the maintenance of LD stability. To support that hypothesis, I found that expression of several other LD-binding proteins (LDPs) including CG7900, Klarsicht LD-binding domain (LD^{BD}::GFP) and Bmm^{S38A} induce a similar phenotype of LD accumulation in *Drosophila* photoreceptor. The fact that this phenotype of LD accumulation is induced by 1) several non-related proteins sharing only a LD-binding domains and 2) LD^{BD}::GFP, a LD-binding domain fused to GFP, strongly suggest that this phenotype involves the LD-binding itself rather than a specific protein function. I will therefore refer to the mechanism of LD accumulation in photoreceptor expressing LDPs as, LDP-induced LDs.

LD formation requires either an increased synthesis (at the ER or at the surface of LDs), or a decreased degradation of neutral lipids. My results strongly suggest that ER-resident TAG synthesis enzymes, dFatp and Mdy, are dispensable for LDP-induced LDs in

photoreceptors in clear contrast with LD accumulation in retina glial cells. If the induction of LDs in photoreceptor neurons does not require canonical actors of the LD formation at the ER or Bmm inhibition, one could wonder by which mechanism TAG-filled LDs can accumulate in neurons? We thus propose three non-exclusive hypotheses to explain LDP-induced LDs in photoreceptors: 1) an increase of local TAG synthesis at the surface of LDs, 2) a decrease in lipolysis mediated by specific neuronal lipases distinct from Bmm 3) an increase in neutral lipid accumulation dependent on the scaffolding properties of LDPs. Indeed, LDPs such as perilipins could be sufficient to stabilize existing unstable LDs. These stabilize LDs could then expand with the influx of neutral lipids carried by circulating lipoproteins.

Neutral lipid accumulating in LDs can be synthesized either within the ER membrane or locally at the surface of LDs. I found that knockdown of dFatp and Mdy, which are required for LD accumulation in glia, are dispensable for LDP-induced LDs in photoreceptor neurons. In glia, these enzymes located at the ER, produce the TAG necessary for the formation of new LDs. The second mechanism of TAG synthesis involves specific isoforms of the TAG synthesis pathway such as GPAT4 and DGAT2, which have been found on the surface of a subset of growing LDs (Wilfling et al., 2013). In *Drosophila*, the gene encoding DGAT2 is triplicated which precludes an easy ablation of all three *DGAT2* genes to determine the contribution of TAG synthesis in LD formation (Heier and Kühnlein, 2018). Because I was only able to do individual knockdowns (Figure 20), I cannot completely rule out a contribution for DGAT2-mediated local TAG synthesis at the LD surface. To assess if an increase in TAG synthesis is sufficient to induce LDs in photoreceptor, I artificially increased TAG synthesis and measured LD accumulation in photoreceptors. One possible way is to ablate phospholipids synthesis. Indeed, in condition of impaired PC synthesis, DAG are converted to TAG and LDs in yeast (Vevea et al., 2015). Interestingly, I found that knockdown of *dEPT1*, the rate limiting enzyme of PE synthesis, but not CCT1, the rate limiting enzyme of PC synthesis led to a small increase in LD accumulation in photoreceptors of control flies in which they are otherwise absent. In addition, knockdown of *dEPT1* also exacerbated LDP-induced LDs in photoreceptors which already contained abundant LDs (Figure 26). These results suggest that in conditions of limited PE synthesis, DAG are converted to TAG in photoreceptors likely through DGAT enzymes. Importantly, LDs induced by the knockdown of *dEPT1* alone never reached the size of LDP-induced LDs (Figure 26). This indicate that even though TAG can accumulate in *dEPT1* knockdown, the resulting LDs may be unstable compared to LDs carrying LDPs. These results further suggest that TAG synthesis alone is not sufficient to explain LDP-induced LDs in photoreceptors. In support of this result, it was found that yeast deficient for TAG synthesis enzymes and expressing human Perilipins could accumulate LDs when treated with exogenous DAG (Jacquier et al., 2013). Collectively, these results support a structural function of LDP, which promote LD accumulation through stabilization by a scaffold function at the LD rather than an increase

in TAG synthesis in photoreceptor neurons.

Perilipins expression has been associated with a decrease lipolysis rate in *Drosophila* and mammals. ATGL is the main TAG lipase in most cell types examined, however it seems that neurons could express other cytoplasmic lipases. Indeed, mutation in the lipase gene DDHD2 involved in HSP, leads to accumulation of LDs in mice neurons whereas ATGL knockout does not (Etschmaier et al., 2011; Inloes et al., 2014). Interestingly, *Drosophila* genome encodes a possible DDHD2 homolog called *Phosphatidic Acid Phospholipase A1* (*PAPLA1*). I thus knocked-down *PAPLA1* in photoreceptors, but did observe any LD accumulation phenotype in the retina (Figure 21). Likewise, the knockdown of *inactivation no afterpotential E* (*inaE*), another lipase expressed in photoreceptors, did not lead to LD accumulation neither. These results suggest that individual lipase knockdown does not lead to LD accumulation in photoreceptors. However, I cannot exclude that LDP could shield LD from other photoreceptor-specific lipase or multiple lipases acting redundantly in photoreceptors.

I also investigated whether LD accumulation in neurons requires the transfer of metabolites between neuron and glial cells, previously described(Ioannou et al., 2019; Liu et al., 2017). Neurons have been shown to exhibit an increase de-novo synthetize of FA, in condition of oxidative stress or excitotoxicity (Ioannou et al., 2019; Liu et al., 2015, 2017). In these models, neuronal lipids are transferred via ApoE/ApoD-dependent lipid transport from neurons to glia, where they accumulate in LDs. Liu et al., reported also that neuronal *de novo* FA synthesis requires lactate imported from glia (Liu et al., 2017). Indeed, they hypothesized that lactate transferred from glia to neurons, by MCT transporters, is used as substrate for *de-novo* lipid synthesis in neurons through a mechanism requiring Citrate Synthase and Acetyl-CoA Carboxylase. These lipids are then transferred to the adjacent glial cells by ApoD homologs Nlaz and Glaz (Liu et al., 2017). My results indicate that the LDP-induced LDs are not reduced by simultaneous knockdown in glia and photoreceptors of *Glaz*, *Nlaz* or MCT transporters (*Silnoon*, *Outsider* and *Basigin*) (Figure 20). Moreover, neither *Citrate Synthase* nor *Acetyl-CoA Carboxylase* knockdown prevented LD accumulation (Figure 20). Collectively these results indicate that LDP-induced LDs in photoreceptor neurons accumulate by a mechanism independent of the lactate shuttle, neuronal de-novo FA synthesis, and ApoD-dependent FA transport, which is strikingly different from retina glia LDs.

If *de-novo* FA, and TAG synthesis are not required for LDP-induced LD formation in photoreceptor neurons, neutral lipids may enter photoreceptors already in the form of DAG or TAG. In *Drosophila*, DAG and TAG are transported in the hemolymph to organs as lipoprotein complexes secreted by fat body (Palm et al., 2012). Adult flies contain fat body in contact with the brain and the retina called the pericerebral fat body, thus the physical proximity of these structures may facilitate the transfer of lipids to the central nervous system (Hwangbo et al., 2004). It was previously shown by the team of Susan Eaton that

lipoproteins can cross *Drosophila* BBB to reach brain cells (Brankatschk and Eaton, 2010). Neurons need high levels of lipids as membrane recycling a very important process to maintain neuronal integrity. This is especially important for photoreceptors, which contain a large amount of membrane microvilli packed in rhabdomeres that are constantly recycled for proper light detection (Thakur et al., 2016). Thus, in normal condition neutral lipids carried by lipoproteins could enter photoreceptors, aggregate transiently as cytoplasmic unstable LDs, and being then used as substrate to produce membrane lipid for rhabdomeres recycling. In this context, some of these unstable LDs might be captured by increased levels of intracytoplasmic LDPs, that could act as surfactant and stabilize LDs (Čopič et al., 2018). Demonstrating that lipids accumulating in photoreceptors came from circulation would require additional experiments such as the expression of LDP in *Drosophila* photoreceptors lacking both lipoprotein receptors LRP1 and LRP2. Collectively my results support of a stabilization of LDs by LDP, which would support the progressive expansion of LDs.

2. Aging, aSyn, and the formation of neuronal LDs in PD

aSyn has been shown to impact LD homeostasis in yeast and mammalian cells (Cole et al., 2002; Fanning et al., 2019; Outeiro and Lindquist, 2003; Sánchez Campos et al., 2018). In Girard et al. (1), we show that aSyn and dPlin2 act in synergy to promote LD accumulation in photoreceptor neurons in adult *Drosophila*. aSyn was detected on the surface of LDs in close proximity with *Drosophila* Plin2 and human PLIN3 in *Drosophila* photoreceptor and human neuroblastoma cells SH-SY5Y, respectively. Interestingly, it was previously hypothesized that aSyn binding to LDs could delay lipolysis, a function reminiscent of perilipins (Cole et al., 2002). In contrast, Fanning et al., found that aSyn-induced LDs rely on the synthesis of TAG in yeast. Specifically, they showed that aSyn promotes an elevated activity of SCD-1, that leads to accumulation of monounsaturated Oleic Acid (OA), which are rapidly converted to DAG and TAG to form LDs (Fanning et al., 2019). However, the mechanism by which aSyn expression increases SCD1 levels and whether aSyn binding to LDs is involved in this mechanism remains unclear. Here, we provide evidence that the expression of LD-binding proteins promotes the accumulation of LDs in photoreceptors, and that aSyn binds LDs in *Drosophila* photoreceptors and human neuroblastoma cells. These results suggest that the physical binding of aSyn to LDs could also directly contribute LD accumulation in neurons. Indeed, accumulation of LDPs such as aSyn may compete at the surface of LDs with other proteins involved in the utilization/degradation of neutral lipids.

In our model, aSyn expression alone did not increase LD accumulation and required co-expression of another LDP. As it has been observed that LD-binding is dependent on LD properties such as size, nature of the stored FA, phospholipid packing and protein abundance (Chorlay and Thiam, 2018; Kory et al., 2015; Thiam et al., 2013a; Thul et al.,

2017). For example, aSyn binding to LDs was reduced in condition of high phospholipid packing on synthetic LDs (Thiam et al., 2013a). In Girard et al. (1), we hypothesized that without a priming step of stabilization induced by dPlin2, LDs might be too small or unstable to favor association with aSyn. Interestingly, aSyn binds on large LDs in wild-type yeast loaded with lipids but not on smaller LDs found peroxisome–deficient mutant yeast (Wang et al., 2013).

During aging, age-dependent changes in metabolism are associated with LD accumulation in non-adipose tissues including in neurons and glial cells(Shimabukuro et al., 2016). While age-dependent fat accumulation is associated with a decrease in the rate of FA consumption, recent evidences indicate that the LDP abundance dysregulation may also be involved (Yan et al., 2017). Indeed, both the autophagy and the proteasome, which are associated with perilipin degradation, are impaired in old organisms (Hipp et al., 2019; Kaushik and Cuervo, 2015). For example, impaired dPlin2 degradation leads to ectopic LDs in flight muscles of aged *Drosophila* (Yan et al., 2017). Furthermore, PD is also associated with impaired protein degradation mechanisms which contributes to increase aSyn levels in neurons (Cuervo et al., 2004). Collectively, these data suggest that perilipins proteins levels may increase in aging and in the brain of PD patients. I thus propose that an elevation of perilipins levels during aging could disrupt LD homeostasis in neurons, and provide a platform for aSyn deposition. Validating this hypothesis would require to compare perilipins levels in the brain of wild-type, aging flies and fly models of PD. Alternatively, animals lacking perilipins, may modulate aSyn-induced neurotoxicity.

3. LDs, mitochondria and aSyn

PD is tightly associated with defects in mitochondria morphology and functions. Indeed, mutation in genes involved in the selective degradation of mitochondria by mitophagy, are associated with familial forms of PD. Loss of pink1 and parkin are associated with accumulation of damaged mitochondria, increased ROS production and can ultimately neuronal death in animal models of PD (Wang et al., 2006; Yang et al., 2006). Furthermore, neurotoxins such as MPTP or Paraquat, which inhibit the mitochondria respiratory chain complex I are also associated with increased PD risks (Tanner et al., 2011). Interestingly, aSyn has been observed in proximity with mitochondria and could also contribute to their dysfunction in PD. Indeed, aSyn could directly bind to cardiolipids at the mitochondrial membrane, or to mitochondrial proteins such as TOM20 (Di Maio et al., 2016). In our model, we found a close association between LDs and mitochondria in photoreceptor neurons expressing *aSynA53T-CG7900*. It raises several questions such as what is the physiological function of LD-mitochondria contacts? and whether aSyn is involved in this contact. Previous reports indicate that aSyn can affects mitochondria dynamics and functions. For example, aSyn can bind alpha-spectrin, which interferes with the actin cytoskeleton, and impairs mitochondria morphology in *Drosophila* photoreceptors

(Ordonez et al., 2018). Other report, indicate that only abnormal aSyn can associate with mitochondria (Wang et al., 2019), which could indicate that this association is one of the consequence of aSyn aggregation. While we did not find any sign of obvious morphological defect of the mitochondria of flies expressing *aSynA53T-CG7900*, we did not investigate mitochondria respiratory chain activity. One possible explanation for LD-mitochondria is that LDs provide FA for energy production. However, it seems unlikely that photoreceptor use lipid as an energy source, as photoreceptor knockdown of ß-oxidation rate limiting enzyme CPT2, did not lead to LD accumulation. Our model of induced neuronal LD could contribute to the investigation of the interaction between LDs, mitochondria and aSyn in PD. For example, is aSyn co-localized with LDs, and required for LD-aSyn binding? Does the association between LDs and mitochondria affects mitochondria functions? Could LDs be involved in mitochondria recycling?

4. A feed-forward loop contributing to aSyn aggregation

We found that in conditions of high LD accumulation in photoreceptors, such as co-expression of aSynA53T and CG7900 or co-expression of aSyn and dPlin2, aSyn was more resistant to mild proteolysis using proteinase K. It has been shown with a misfolded conformation of aSyn (Cremades et al., 2012; Miake et al., 2002; Neumann et al., 2002). Interestingly, lipid vesicles trigger recombinant aSyn aggregation *in vitro* (Galvagnion et al., 2015). We thus hypothesized that aSyn may be converted to pathological forms more prone to aggregate at the surface of LDs. Indeed, it has been suggested that aggregates may localized preferentially in proximity with lipid droplets (Dettmer et al., 2017). Although we did not directly demonstrate αSyn forms aggregates in our model, there is a tight association between increase resistance to proteinase K and αSyn aggregation. aSyn is converted to compact oligomers resistant to proteinase K degradation is as step in the formation of aggregation (Cremades et al., 2012). In addition, oligomers resistant to digestion are toxic in primary cultures of rat neurons. Additional experiments are required to demonstrate that proteinase-K resistant aSyn forms aggregates in our system. Several approaches could be used to detect aggregates *in situ*, such as fluorometric dyes like Thioflavin S that recognize amyloid deposition or conformation specific aSyn antibodies (Olsen and Feany, 2019; Periquet et al., 2007). Other promising methods, have recently been developed such as bimolecular fluorescence complementation (BiFC) to detect aSyn oligomerization and aggregation *in vivo* (Prasad et al., 2019). This method is based on the reconstitution of a Venus fluorescent protein, which is dependent on the interaction of two aSyn proteins fused to two complementary Venus fragment (Prasad et al., 2019). We could then verify whether these aggregates form are indeed in proximity to lipid droplets as it has been previously suggested (Dettmer et al., 2017).

5. Spen and LD formation in glial cells

LD content in glia is highly dynamic and has been shown to increase in response to neuronal injuries, such as oxidative stress and excitotoxicity in insect and mammals (Bailey et al., 2015; Ioannou et al., 2019; Liu et al., 2015, 2017). In contrast to retina glial cells that contain LDs only transiently, brain glial cells of healthy adult flies contain LDs, especially in the cortex area surrounding neuronal nuclei of healthy adult flies (Figure 25). We found that LD content increased in brain glial cells by knocking-down *Spen* using a pan-glial (*repo-GAL4*) or an astrocyte-like glia driver (*Eaat1-GAL4)*. Interestingly, LDs did not accumulate uniformly, and were increased in the area surrounding the dense synaptic zones of neuropils suggesting that astrocytes are particularly sensitive to the loss of Spen. Astrocytes may be associated with a specific lipid storage regulation that require Spen. Collectively, these results suggest that Spen could either limit lipid synthesis or promote LD degradation in glial cells. As a RNA binding protein Spen can modulate expression of a large variety of genes. For example, Spen was shown to regulate the expression of genes involved in lipid catabolism in *Drosophila* fat body (Hazegh et al., 2017). In particular, loss of *Spen* in fat body reduces the expression of lipases and several ß-oxidation enzymes (Hazegh et al., 2017). The fact that loss of spen also increased lipid storage in adult glia, suggest that Spen promotes lipid catabolism in glial cells as well. Inhibition of lipid catabolism in adult glia using knockdown of *Bmm* lipase or *CPT2* leads to LD accumulation in both retina and brain glia (Figure 24, Figure 25, (Schulz et al., 2015). Importantly in these latter, LDs accumulated uniformly in contrast to LDs localized around the neuropil area in *Spen* knockdown. This specific localization of LDs suggests that LD accumulation in *Spen*-deficient glia are not simply the result of a global impaired ß-oxidation. One explanation is that Spen is required for lipid catabolism in glia subtype surrounding the neuropil such as astrocytes.

Another possible explanation to explain the accumulation of LDs in Spen mutant is that loss of *Spen* increases oxidative stress in glial cells. Indeed, impairment mitochondrial respiratory chain complex I in glia using knockdown of *ND23*, the homolog of *NDUFS8* led to a phenotype of LD accumulation reminiscent of *Spen* (Cabirol-Pol et al., 2018). This is in agreement with the fact that overexpression of Spen was protective against paraquat-induced oxidative stress and neurodegeneration (Girard et al. (2) - Figure 1). In addition, we showed that Spen-deficient glia had increased level of 4-HNE an indicator of oxidative damages and lipid peroxidation, which further support that oxidative stress is induced in Spen mutants (Figure 28). Indeed, increased 4-HNE has been observed in larvae CNS in hypoxia (Bailey et al., 2015). Collectively these results indicate that loss of Spen, could induce LD though a mechanism involving an increase oxidative stress.

Alternatively, *Spen* could also impair other astrocyte-specific functions leading to LD accumulation. Indeed, astrocyte glia, are especially important to recapture glutamate at

the synapse to prevent neuronal excitotoxicity and failure to do so results in excitotoxicity and glial LD accumulation (Ioannou et al., 2019). Indeed, Ioannou et al. showed that in mammalian glia-neurons co-culture, neurons treated with glutamate agonist NMDA, release ApoE lipoprotein that are recaptured by glia and induce accumulation of LDs (Ioannou et al., 2019). *In Drosophila*, astrocyte glia that express the glutamate receptor Eaat1, are located around the neuropil and project processes inside this dense zone of synaptic connections (Rival et al., 2004). Interestingly, GRLD-1, a member of the Spen RNA binding protein family in *C. elegans*, maintain the abundance of α-amino-3-hydroxy-5-methyl-4-isoxazolepropionic acid (AMPA)-type glutamate receptors, GRL-1, in a subset of neurons, by regulating alternative splicing of *grl-1* transcript (Wang et al., 2010). It is thus possible that lack of *Spen* could impair expression of neurotransmitter receptors in glial cells as well. This would impair the recapture of glutamate, resulting in neuronal excitotoxicity and LD formation in glia. Further experiments would be required to investigate whether Spen regulates the abundance of receptors such as Eaat1 in *Drosophila* astrocyte-glia.

Spen is an RNA binding protein that can act as a regulator of transcription, a splicing factor and a nuclear export factor of transcripts. As such, Spen regulates the expression of a large variety of genes in different pathways (Andriatsilavo et al., 2018; Hazegh et al., 2017). Identifying the differentially regulated genes in glia using RNA-seq, would be required to identify Spen targets in this particular tissue as it was performed in fat body and intestinal stem cells (Andriatsilavo et al., 2018; Hazegh et al., 2017).

6. The contribution of glial LDs to PD

PD is a complex neurodegenerative disorder that involves neurons but also glia. As the primary sensor of neuronal injury, glial cells activate the inflammatory response, engulf neuronal debris, and buffer stress by accumulating LD. In PD, astrocytes have been shown to take up aSyn secreted by neurons, and contribute to the disease spreading. Also, Lewy Body can be observed in astrocytes and have been shown to participate to neurodegeneration in Multiple System Atrophy (Tu et al., 1998). Furthermore, simultaneous expression of aSyn in neuron and glia, exacerbates neurotoxicity in *Drosophila*, indicating that glia a involved in aSyn-induced neurodegeneration (Olsen and Feany, 2019). Importantly, the status of neuronal mitochondria could be a putative link between neuronal dysfunction and glia LD accumulation (Ioannou et al., 2019; Liu et al., 2015; Van Den Brink et al., 2018). In Girard et al. (2), we found that flies lacking *Spen* in glia accumulate LDs and have an exacerbated sensitivity to paraquat, a toxin targeting mitochondria respiratory chain. These results suggest that accumulation of LDs in glia may exacerbate the toxicity associated with paraquat-induced mitochondria damages. This observation is coherent with the fact that preventing LD accumulation, by *dFatp* knockdown, or *Bmm* lipase overexpression, delays neurodegeneration in *Aats-Met* mutant photoreceptor neurons (Liu et al., 2015; Muliyil et al., 2020; Van Den Brink et al., 2018). In contrast, accumulation

of LDs in absence of mitochondrial damages was not associated with neurodegeneration in flies overexpressing *dFatp* retina glial cells (Van Den Brink et al., 2018). Collectively these results suggest that the LD content in glia could be detrimental for neuronal survival in conditions of damaged mitochondria. Thus, it would be important to test whether remobilization of LDs in *Spen* mutant flies, using expression of Bmm lipase, would be sufficient to increase the resistance to paraquat of Spen mutant flies. In addition, if LDs, by themselves, increase cells sensitivity to oxidative stress, we could hypothesize that flies lacking the lipase Bmm, which accumulate high levels of LD, would be more sensitive to paraquat-induced toxicity as well.

Collectively my result support that both glial and neuronal LD accumulation contribute to the progression of PD.

CONCLUSION

During my thesis, I investigated the mechanisms of LD formation in glia and neurons in two Drosophila models of PD. I found that LDs in neurons and glia contribute both to different aspects of PD.

Firstly, I found indication that expression of LD-binding proteins and aSyn increase the accumulation of LDs in neurons. Neuronal LDs accumulated independently of TAG synthesis enzyme and Bmm inhibition. In addition, neuronal LDs increase aSyn resistance to proteinase K, a hallmark of pathological forms of aSyn. I propose that LDs may be involved in a feed-forward mechanism with aSyn: aSyn promotes LD accumulation on one hand, and LDs provide a platform for aSyn deposition and conversion to pathological forms.

Secondly, is associated with increase *Drosophila* resistance to Paraquat-induced neurotoxicity. Specifically, I found that Spen, a RNA-binding protein whose expression is increased in PD, restricts abdnormal LD accumulation in *Drosophila* glia. Lack of Spen in glia was associated with LD accumulation and increase sensitivity to Paraquat.

Collectively, my findings indicate that LD accumulation in glia and neurons both contribute to the progression of PD.

MATERIAL AND METHODS OF ADDITIONAL RESULTS NOT INCLUDED IN PAPERS

1. Drosophila Stocks

All flies used for this study were raised on regular yeast medium at 25°C on a 12h light/ dark cycle. The fly stocks were obtained as follows.

Genotype	Stock	Reference
; dHSL^{b24}/Cyo;		(Bi et al., 2012)
; Eaat1-GAL4;	BDSC#8849	(Rival et al., 2004)
Rh1-Gal4, ey-FLP; FRT40A Rh1-tomato^{ninaC}/Cyo;		(Gambis et al., 2011)
FRT40A dFatp^{k10307}/Cyo		(Gambis et al., 2011)
y^{1} sc v^{1}; P{ TRiP.HMS01230}attP2 (ACC-RNAi)*	BDSC#34885	(Liu et al., 2017)
P{KK108281}VIE-260B (CCT1 RNAi)	VDRC#100575	
P{KK113284}VIE-260B (CG1941 RNAi)	VDRC#106800	
P{KK112067}VIE-260B (CG1946 RNAi)	VDRC#108495	
y^{1} sc* v^{1} sev^{21}; P{ TRiP.HMS02556}attP40 (GPAT4 RNAi)	BDSC#42863	
y^{1} sc v^{1}; P{ TRiP.HMS01631}attP40 (CS-RNAi)*	BDSC#36740	(Liu et al., 2017)
P{KK106488}VIE-260B (dEPT1 RNAi)	VDRC#102304	
P{KK109140}VIE-260B (DGAT2 RNAi)	VDRC#107788	
P{KK104809}VIE-260B (Fatp RNAi)	VDRC#100124	(Van Den Brink et al., 2018)
y^{1} sc v^{1} sev^{21}; P{VALIUM20-EGFP.shRNA.1}attP40 (GFP RNAi)*	BDSC#41555	
P{KK106377}VIE-260B (Glaz RNAi)	VDRC#107433	(Liu et al., 2017)
y1 sc v1; P{TRiP.HMC05758}attP40 (InaE RNAi)*	BDSC#64885	
P{KK108334}VIE-260B (LPCAT RNAi)	VDRC#104570	
y^{1} sc v^{1} sev^{21}; P{TRiP.HMC06242}attP40/CyO (Mdy RNAi)*	BDSC#65963	(Bailey et al., 2015)
P{VSH330126}attP40 (Minotaur RNAi)	VDRC#330126	
P{KK107553}VIE-260B (Nlaz RNAi)	VDRC#101321	(Liu et al., 2017)
y^{1} sc v^{1}; P{TRiP.HMS05671}attP40 (Outsider RNAi)*	BDSC#67858	(Liu et al., 2017)
y1 v1; P{TRiP.HMJ30172}attP40 (PAPLA1 RNAi)	BDSC#63605	
y1 sc v1; P{ TRiP.HMS01292}attP2 (Plin2 RNAi)*	BDSC#34617	(Bailey et al., 2015)
y1 sc v1; P{TRiP.HMS01643}attP40 (Seipin RNAi)*	BDSC#37501	
P{KK104306}VIE-260B (Silnoon RNAi)	VDRC#109464	(Liu et al., 2017)
UAS-Spen-RNAi	Cagan R.	
Rh1-GAL4;;	BDSC#8688	
;; UAS-aSynA53T-CG7900	BDSC#8148	(Auluck et al., 2002)
y^{1} v^{1}; P{TRiP.HMJ23935}attP40/CyO (CPT2 RNAi)	BDSC#62455	(Schulz et al., 2015)
;; Bmm^{1}/TM3	Kuhnlein RP	(Grönke et al., 2005)
;sGMR-GAL4, UAS-mito-GFP/Cyo;	BDSC#8842	
;; UAS-Bmm-RNAi/TM3, sb	BDSC#25926	
;; Repo-GAL4/TM3, sb	BDSC#7415	

y1 v1; P{ TRiP.HMC03195}attP40 (Basigin RNAi)	BDSC#52110	(Liu et al., 2017)

VDRC: Vienna *Drosophila* Resource Center. BDSC: Bloomington *Drosophila* Stock Center.

2. 4-HNE detection

Flies were sedated on ice, decapitated, and brains were dissected in a drop of HL3 medium supplemented with D-glucose (120 mM) (Stewart et al., 1994). Whole-mount brains were fixed in 1% PFA overnight at 4°C and permeabilized in PBS supplemented with 0.5% Triton X-100 and 5 mg/mL BSA (blocking solution). Primary antibodies mouse anti-Repo (8D12, DSHB) and rabbit anti-4-HNE protein adduct were diluted in blocking solution and incubated with the retinas overnight at 4°C. The samples were then washed and incubated overnight at 4°C in blocking solution containing Alexa Fluor-conjugated anti-mouse Alexa647, anti-rabbit Alexa488 secondary antibodies.

REFERENCES

Abeliovich, A., and Gitler, A.D. (2016). Defects in trafficking bridge Parkinson's disease pathology and genetics. Nature *539*, 207–216.

Abeliovich, A., Schmitz, Y., Fariñas, I., Choi-Lundberg, D., Ho, W.H., Castillo, P.E., Shinsky, N., Verdugo, J.M., Armanini, M., Ryan, A., et al. (2000). Mice lacking alpha-synuclein display functional deficits in the nigrostriatal dopamine system. Neuron *25*, 239–252.

Agarwal, A.K., Simha, V., Oral, E.A., Moran, S.A., Gorden, P., O'Rahilly, S., Zaidi, Z., Gurakan, F., Arslanian, S.A., Klar, A., et al. (2003). Phenotypic and Genetic Heterogeneity in Congenital Generalized Lipodystrophy. J Clin Endocrinol Metab *88*, 4840–4847.

Ajjaji, D., Ben M'barek, K., Mimmack, M.L., England, C., Herscovitz, H., Dong, L., Kay, R.G., Patel, S., Saudek, V., Small, D.M., et al. (2019). Dual binding motifs underpin the hierarchical association of perilipins1-3 with lipid droplets. Mol. Biol. Cell *30*, 703–716.

Allen, N.J., and Lyons, D.A. (2018). Glia as architects of central nervous system formation and function. Science *362*, 181–185.

Anand, P., Cermelli, S., Li, Z., Kassan, A., Bosch, M., Sigua, R., Huang, L., Ouellette, A.J., Pol, A., Welte, M.A., et al. (2012). A novel role for lipid droplets in the organismal antibacterial response. Elife *1*, e00003.

Andriatsilavo, M., Stefanutti, M., Siudeja, K., Perdigoto, C.N., Boumard, B., Gervais, L., Gillet-Markowska, A., Al Zouabi, L., Schweisguth, F., and Bardin, A.J. (2018). Spen limits intestinal stem cell self-renewal. PLoS Genet *14*, e1007773.

Arrasate, M., Mitra, S., Schweitzer, E.S., Segal, M.R., and Finkbeiner, S. (2004). Inclusion body formation reduces levels of mutant huntingtin and the risk of neuronal death. Nature *431*, 805–810.

Arrese, E.L., and Soulages, J.L. (2010). Insect Fat Body: Energy, Metabolism, and Regulation. Annu. Rev. Entomol. *55*, 207–225.

Arrese, E.L., Patel, R.T., and Soulages, J.L. (2006). The main triglyceride-lipase from the insect fat body is an active phospholipase A(1): identification and characterization. Journal of Lipid Research *47*, 2656–2667.

Arrese, E.L., Rivera, L., Hamada, M., and Soulages, J.L. (2008). Purification and Characterization of Recombinant Lipid Storage Protein-2 from Drosophila melanogaster. Protein Pept Lett *15*, 1027–1032.

Arribat, Y., Grepper, D., Lagarrigue, S., Qi, T., Cohen, S., and Amati, F. (2020). Spastin mutations impair coordination between lipid droplet dispersion and reticulum. PLOS Genetics *16*, e1008665.

Auluck, P.K., Chan, H.Y.E., Trojanowski, J.Q., Lee, V.M.-Y., and Bonini, N.M. (2002). Chaperone Suppression of a-Synuclein Toxicity in a Drosophila Model for Parkinson's Disease. Science *295*, 862–865.

Bailey, A.P., Koster, G., Guillermier, C., Hirst, E.M.A., MacRae, J.I., Lechene, C.P., Postle, A.D., and Gould, A.P. (2015). Antioxidant Role for Lipid Droplets in a Stem Cell Niche of Drosophila. Cell *163*, 340–353.

Baldi, I., Lebailly, P., Mohammed-Brahim, B., Letenneur, L., Dartigues, J.-F., and Brochard, P. (2003). Neurodegenerative diseases and exposure to pesticides in the elderly. American Journal of Epidemiology *157*, 409–414.

Barone, P., Erro, R., and Picillo, M. (2017). Quality of Life and Nonmotor Symptoms in Parkinson's Disease. Int. Rev. Neurobiol. *133*, 499–516.

Bartels, T., Choi, J.G., and Selkoe, D.J. (2011). α-Synuclein occurs physiologically as a helically folded tetramer that resists aggregation. Nature *477*, 107–110.

von Bartheld, C.S. (2018). Myths and truths about the cellular composition of the human brain: A review of influential concepts. Journal of Chemical Neuroanatomy *93*, 2–15.

von Bartheld, C.S., Bahney, J., and Herculano-Houzel, S. (2016). The search for true numbers of neurons and glial cells in the human brain: A review of 150 years of cell counting. The Journal of Comparative Neurology *524*, 3865–3895.

Bélanger, M., Allaman, I., and Magistretti, P.J. (2011). Brain energy metabolism: focus on astrocyte-neuron metabolic cooperation. Cell Metab. *14*, 724–738.

Beller, M., Riedel, D., Jansch, L., Dieterich, G., Wehland, J., Jackle, H., and Kuhnlein, R.P. (2006). Characterization of the Drosophila Lipid Droplet Subproteome. Molecular & Cellular Proteomics.

Beller, M., Bulankina, A.V., Hsiao, H.-H., Urlaub, H., Jäckle, H., and Kühnlein, R.P. (2010). PERILIPIN-Dependent Control of Lipid Droplet Structure and Fat Storage in Drosophila. Cell Metabolism *12*, 521–532.

Beller, M., Herker, E., and Füllekrug, J. (2020). Grease on—Perspectives in lipid droplet biology. Seminars in Cell & Developmental Biology.

Ben M'barek, K., Ajjaji, D., Chorlay, A., Vanni, S., Forêt, L., and Thiam, A.R. (2017). ER Membrane Phospholipids and Surface Tension Control Cellular Lipid Droplet Formation. Dev. Cell *41*, 591-604.e7.

Benador, I.Y., Veliova, M., Mahdaviani, K., Petcherski, A., Wikstrom, J.D., Assali, E.A., Acín-Pérez, R., Shum, M., Oliveira, M.F., Cinti, S., et al. (2018). Mitochondria Bound to Lipid Droplets Have Unique Bioenergetics, Composition, and Dynamics that Support Lipid Droplet Expansion. Cell Metab. *27*, 869-885.e6.

Benador, I.Y., Veliova, M., Liesa, M., and Shirihai, O.S. (2019). Mitochondria Bound to Lipid Droplets: Where Mitochondrial Dynamics Regulate Lipid Storage and Utilization. Cell Metabolism *29*, 827–835.

Bendor, J., Logan, T., and Edwards, R.H. (2013). The Function of α-Synuclein. Neuron *79*.

Bensaad, K., Favaro, E., Lewis, C.A., Peck, B., Lord, S., Collins, J.M., Pinnick, K.E., Wigfield, S., Buffa, F.M., Li, J.-L., et al. (2014). Fatty Acid Uptake and Lipid Storage Induced by HIF-1α Contribute to Cell Growth and Survival after Hypoxia-Reoxygenation. Cell Reports *9*, 349–365.

Bersuker, K., and Olzmann, J.A. (2017). Establishing the lipid droplet proteome: Mechanisms of lipid droplet protein targeting and degradation. Biochimica et Biophysica Acta (BBA) - Molecular and Cell Biology of Lipids *1862*, 1166–1177.

Bersuker, K., Peterson, C.W.H., To, M., Sahl, S.J., Savikhin, V., Grossman, E.A., Nomura,

D.K., and Olzmann, J.A. (2018). A Proximity Labeling Strategy Provides Insights into the Composition and Dynamics of Lipid Droplet Proteomes. Dev. Cell *44*, 97-112.e7.

Bi, J., Xiang, Y., Chen, H., Liu, Z., Grönke, S., Kühnlein, R.P., and Huang, X. (2012). Opposite and redundant roles of the two Drosophila perilipins in lipid mobilization. J. Cell. Sci. *125*, 3568–3577.

Bier, E. (2005). Drosophila, the golden bug, emerges as a tool for human genetics. Nat Rev Genet *6*, 9–23.

Bisaglia, M., Schievano, E., Caporale, A., Peggion, E., and Mammi, S. (2006). The 11-mer repeats of human alpha-synuclein in vesicle interactions and lipid composition discrimination: a cooperative role. Biopolymers *84*, 310–316.

Bosco, D.A., Fowler, D.M., Zhang, Q., Nieva, J., Powers, E.T., Wentworth, P., Lerner, R.A., and Kelly, J.W. (2006). Elevated levels of oxidized cholesterol metabolites in Lewy body disease brains accelerate alpha-synuclein fibrilization. Nat. Chem. Biol. *2*, 249–253.

Bouab, M., Paliouras, G.N., Aumont, A., Forest-Bérard, K., and Fernandes, K.J.L. (2011). Aging of the subventricular zone neural stem cell niche: evidence for quiescence-associated changes between early and mid-adulthood. Neuroscience *173*, 135–149.

Braak, H., Del Tredici, K., Rüb, U., De Vos, R.A., Steur, E.N.J., and Braak, E. (2003). Staging of brain pathology related to sporadic Parkinson's disease. Neurobiology of Aging *24*, 197–211.

Brand, A.H., and Perrimon, N. (1993). Targeted gene expression as a means of altering cell fates and generating dominant phenotypes. Development *118*, 401–415.

Brankatschk, M., and Eaton, S. (2010). Lipoprotein Particles Cross the Blood–Brain Barrier in Drosophila. J. Neurosci. *30*, 10441–10447.

Brankatschk, M., Dunst, S., Nemetschke, L., and Eaton, S. (2014). Delivery of circulating lipoproteins to specific neurons in the Drosophila brain regulates systemic insulin signaling. ELife *3*.

Brasaemle, D.L., Rubin, B., Harten, I.A., Gruia-Gray, J., Kimmel, A.R., and Londos, C. (2000). Perilipin A increases triacylglycerol storage by decreasing the rate of triacylglycerol hydrolysis. J. Biol. Chem. *275*, 38486–38493.

Broersen, K., van den Brink, D., Fraser, G., Goedert, M., and Davletov, B. (2006). Alpha-synuclein adopts an alpha-helical conformation in the presence of polyunsaturated fatty acids to hinder micelle formation. Biochemistry *45*, 15610–15616.

Bruce, K.D., Zsombok, A., and Eckel, R.H. (2017). Lipid Processing in the Brain: A Key Regulator of Systemic Metabolism. Front Endocrinol (Lausanne) *8*, 60.

Buell, A.K., Galvagnion, C., Gaspar, R., Sparr, E., Vendruscolo, M., Knowles, T.P.J., Linse, S., and Dobson, C.M. (2014). Solution conditions determine the relative importance of nucleation and growth processes in α-synuclein aggregation. Proceedings of the National Academy of Sciences of the United States of America *111*, 7671–7676.

Bulankina, A.V., Deggerich, A., Wenzel, D., Mutenda, K., Wittmann, J.G., Rudolph, M.G., Burger, K.N.J., and Höning, S. (2009). TIP47 functions in the biogenesis of lipid droplets. The Journal of Cell Biology *185*, 641–655.

Burré, J., Sharma, M., and Südhof, T.C. (2014). α-Synuclein assembles into higher-order multimers upon membrane binding to promote SNARE complex formation. Proceedings of the National Academy of Sciences of the United States of America *111*, E4274-4283.

Bussell, R., and Eliezer, D. (2003). A Structural and Functional Role for 11-mer Repeats in α-Synuclein and Other Exchangeable Lipid Binding Proteins. Journal of Molecular Biology *329*, 763–778.

Cabirol-Pol, M.-J., Khalil, B., Rival, T., Faivre-Sarrailh, C., and Besson, M.T. (2018). Glial lipid droplets and neurodegeneration in a Drosophila model of complex I deficiency. Glia *66*, 874–888.

Campuzano, V., Montermini, L., Lutz, Y., Cova, L., Hindelang, C., Jiralerspong, S., Trottier, Y., Kish, S.J., Faucheux, B., Trouillas, P., et al. (1997). Frataxin is reduced in Friedreich ataxia patients and is associated with mitochondrial membranes. Hum Mol Genet *6*, 1771–1780.

Capilla-Gonzalez, V., Cebrian-Silla, A., Guerrero-Cazares, H., Garcia-Verdugo, J.M., and Quiñones-Hinojosa, A. (2014). Age-related changes in astrocytic and ependymal cells of the subventricular zone. Glia *62*, 790–803.

Cassar, M., Issa, A.-R., Riemensperger, T., Petitgas, C., Rival, T., Coulom, H., Iché-Torres, M., Han, K.-A., and Birman, S. (2015). A dopamine receptor contributes to paraquat-induced neurotoxicity in Drosophila. Human Molecular Genetics *24*, 197–212.

Cermelli, S., Guo, Y., Gross, S.P., and Welte, M.A. (2006). The lipid-droplet proteome reveals that droplets are a protein-storage depot. Curr. Biol. *16*, 1783–1795.

Chandra, S., Fornai, F., Kwon, H.-B., Yazdani, U., Atasoy, D., Liu, X., Hammer, R.E., Battaglia, G., German, D.C., Castillo, P.E., et al. (2004). Double-knockout mice for alpha- and beta-synucleins: effect on synaptic functions. Proceedings of the National Academy of Sciences of the United States of America *101*, 14966–14971.

Chang, C.-L., Weigel, A.V., Ioannou, M.S., Pasolli, H.A., Xu, C.S., Peale, D.R., Shtengel, G., Freeman, M., Hess, H.F., Blackstone, C., et al. (2019). Spastin tethers lipid droplets to peroxisomes and directs fatty acid trafficking through ESCRT-III. J. Cell Biol. *218*, 2583–2599.

Chang, D., Nalls, M.A., Hallgrímsdóttir, I.B., Hunkapiller, J., van der Brug, M., Cai, F., International Parkinson's Disease Genomics Consortium, 23andMe Research Team, Kerchner, G.A., Ayalon, G., et al. (2017). A meta-analysis of genome-wide association studies identifies 17 new Parkinson's disease risk loci. Nature Genetics *49*, 1511–1516.

Chapman, K.D., Aziz, M., Dyer, J.M., and Mullen, R.T. (2019). Mechanisms of lipid droplet biogenesis. Biochem. J. *476*, 1929–1942.

Chartier-Harlin, M.-C., Kachergus, J., Roumier, C., Mouroux, V., Douay, X., Lincoln, S., Levecque, C., Larvor, L., Andrieux, J., Hulihan, M., et al. (2004). Alpha-synuclein locus duplication as a cause of familial Parkinson's disease. Lancet (London, England) *364*, 1167–1169.

Chen, L., and Feany, M.B. (2005). α-Synuclein phosphorylation controls neurotoxicity and inclusion formation in a Drosophila model of Parkinson disease. Nature Neuroscience *8*, 657–663.

Chitraju, C., Mejhert, N., Haas, J.T., Diaz-Ramirez, L.G., Grueter, C.A., Imbriglio, J.E., Pinto,

S., Koliwad, S.K., Walther, T.C., and Farese, R.V. (2017). Triglyceride Synthesis by DGAT1 Protects Adipocytes from Lipid-Induced ER Stress during Lipolysis. Cell Metab. *26*, 407-418.e3.

Chorlay, A., and Thiam, A.R. (2018). An Asymmetry in Monolayer Tension Regulates Lipid Droplet Budding Direction. Biophys. J. *114*, 631–640.

Chorlay, A., and Thiam, A.R. (2020). Neutral lipids regulate amphipathic helix affinity for model lipid droplets. J Cell Biol *219*.

Choudhary, V., Ojha, N., Golden, A., and Prinz, W.A. (2015). A conserved family of proteins facilitates nascent lipid droplet budding from the ER. J Cell Biol *211*, 261–271.

Choudhary, V., El Atab, O., Mizzon, G., Prinz, W.A., and Schneiter, R. (2020). Seipin and Nem1 establish discrete ER subdomains to initiate yeast lipid droplet biogenesis. J Cell Biol *219*.

Chouhan, A.K., Guo, C., Hsieh, Y.-C., Ye, H., Senturk, M., Zuo, Z., Li, Y., Chatterjee, S., Botas, J., Jackson, G.R., et al. (2016). Uncoupling neuronal death and dysfunction in Drosophila models of neurodegenerative disease. Acta Neuropathologica Communications *4*.

Chughtai, A.A., Kaššák, F., Kostrouchová, M., Novotný, J.P., Krause, M.W., Saudek, V., Kostrouch, Z., and Kostrouchová, M. (2015). Perilipin-related protein regulates lipid metabolism in C. elegans. PeerJ *3*, e1213.

Chung, J., Wu, X., Lambert, T.J., Lai, Z.W., Walther, T.C., and Farese, R.V. (2019). LDAF1 and Seipin Form a Lipid Droplet Assembly Complex. Dev. Cell *51*, 551-563.e7.

Clark, I.E., Dodson, M.W., Jiang, C., Cao, J.H., Huh, J.R., Seol, J.H., Yoo, S.J., Hay, B.A., and Guo, M. (2006). Drosophila pink1 is required for mitochondrial function and interacts genetically with parkin. Nature *441*, 1162–1166.

Clark, L.N., Ross, B.M., Wang, Y., Mejia-Santana, H., Harris, J., Louis, E.D., Cote, L.J., Andrews, H., Fahn, S., Waters, C., et al. (2007). Mutations in the glucocerebrosidase gene are associated with early-onset Parkinson disease. Neurology *69*, 1270–1277.

Cole, N.B., Murphy, D.D., Grider, T., Rueter, S., Brasaemle, D., and Nussbaum, R.L. (2002). Lipid droplet binding and oligomerization properties of the Parkinson's disease protein alpha-synuclein. J. Biol. Chem. *277*, 6344–6352.

Cooper, A.A., Gitler, A.D., Cashikar, A., Haynes, C.M., Hill, K.J., Bhullar, B., Liu, K., Xu, K., Strathearn, K.E., Liu, F., et al. (2006). α-Synuclein Blocks ER-Golgi Traffic and Rab1 Rescues Neuron Loss in Parkinson's Models. Science *313*, 324–328.

Čopič, A., Antoine-Bally, S., Giménez-Andrés, M., La Torre Garay, C., Antonny, B., Manni, M.M., Pagnotta, S., Guihot, J., and Jackson, C.L. (2018). A giant amphipathic helix from a perilipin that is adapted for coating lipid droplets. Nat Commun *9*.

Corder, E.H., Saunders, A.M., Strittmatter, W.J., Schmechel, D.E., Gaskell, P.C., Small, G.W., Roses, A.D., Haines, J.L., and Pericak-Vance, M.A. (1993). Gene dose of apolipoprotein E type 4 allele and the risk of Alzheimer's disease in late onset families. Science *261*, 921–923.

Coulom, H., and Birman, S. (2004). Chronic exposure to rotenone models sporadic Parkinson's disease in Drosophila melanogaster. J. Neurosci. *24*, 10993–10998.

Cremades, N., Cohen, S.I.A., Deas, E., Abramov, A.Y., Chen, A.Y., Orte, A., Sandal, M., Clarke,

R.W., Dunne, P., Aprile, F.A., et al. (2012). Direct Observation of the Interconversion of Normal and Toxic Forms of α-Synuclein. Cell *149*, 1048–1059.

Cruz, A.L.S., Barreto, E. de A., Fazolini, N.P.B., Viola, J.P.B., and Bozza, P.T. (2020). Lipid droplets: platforms with multiple functions in cancer hallmarks. Cell Death Dis *11*.

Cuervo, A.M., Stefanis, L., Fredenburg, R., Lansbury, P.T., and Sulzer, D. (2004). Impaired degradation of mutant alpha-synuclein by chaperone-mediated autophagy. Science *305*, 1292–1295.

Currie, E., Guo, X., Christiano, R., Chitraju, C., Kory, N., Harrison, K., Haas, J., Walther, T.C., and Farese, R.V. (2014). High confidence proteomic analysis of yeast LDs identifies additional droplet proteins and reveals connections to dolichol synthesis and sterol acetylation. J. Lipid Res. *55*, 1465–1477.

Daemen, S., van Zandvoort, M.A.M.J., Parekh, S.H., and Hesselink, M.K.C. (2016). Microscopy tools for the investigation of intracellular lipid storage and dynamics. Mol Metab *5*, 153–163.

Dalen, K.T., Dahl, T., Holter, E., Arntsen, B., Londos, C., Sztalryd, C., and Nebb, H.I. (2007). LSDP5 is a PAT protein specifically expressed in fatty acid oxidizing tissues. Biochim. Biophys. Acta *1771*, 210–227.

Datta, S., Liu, Y., Hariri, H., Bowerman, J., and Henne, W.M. (2019). Cerebellar ataxia disease–associated Snx14 promotes lipid droplet growth at ER–droplet contacts. J Cell Biol *218*, 1335–1351.

Davidson, W.S., Jonas, A., Clayton, D.F., and George, J.M. (1998). Stabilization of alpha-synuclein secondary structure upon binding to synthetic membranes. The Journal of Biological Chemistry *273*, 9443–9449.

Davis, G.C., Williams, A.C., Markey, S.P., Ebert, M.H., Caine, E.D., Reichert, C.M., and Kopin, I.J. (1979). Chronic Parkinsonism secondary to intravenous injection of meperidine analogues. Psychiatry Research *1*, 249–254.

De Franceschi, G., Frare, E., Pivato, M., Relini, A., Penco, A., Greggio, E., Bubacco, L., Fontana, A., and de Laureto, P.P. (2011). Structural and morphological characterization of aggregated species of α-synuclein induced by docosahexaenoic acid. J. Biol. Chem. *286*, 22262–22274.

Delgado, M.G., Oliva, C., López, E., Ibacache, A., Galaz, A., Delgado, R., Barros, L.F., and Sierralta, J. (2018). Chaski, a novel Drosophila lactate/pyruvate transporter required in glia cells for survival under nutritional stress. Sci Rep *8*, 1186.

Deruyffelaere, C., Purkrtova, Z., Bouchez, I., Collet, B., Cacas, J.-L., Chardot, T., Gallois, J.-L., and D'Andrea, S. (2018). PUX10 Is a CDC48A Adaptor Protein That Regulates the Extraction of Ubiquitinated Oleosins from Seed Lipid Droplets in Arabidopsis. Plant Cell *30*, 2116–2136.

Desalvo, M.K., Mayer, N., Mayer, F., and Bainton, R.J. (2011). Physiologic and anatomic characterization of the brain surface glia barrier of Drosophila. Glia *59*, 1322–1340.

DeSalvo, M.K., Hindle, S.J., Rusan, Z.M., Orng, S., Eddison, M., Halliwill, K., and Bainton, R.J. (2014). The Drosophila surface glia transcriptome: evolutionary conserved blood-brain barrier processes. Front Neurosci *8*, 346.

Dettmer, U., Newman, A.J., Luth, E.S., Bartels, T., and Selkoe, D. (2013). In vivo cross-linking reveals principally oligomeric forms of α-synuclein and β-synuclein in neurons and non-neural cells. J. Biol. Chem. *288*, 6371–6385.

Dettmer, U., Newman, A.J., Soldner, F., Luth, E.S., Kim, N.C., von Saucken, V.E., Sanderson, J.B., Jaenisch, R., Bartels, T., and Selkoe, D. (2015). Parkinson-causing α-synuclein missense mutations shift native tetramers to monomers as a mechanism for disease initiation. Nature Communications *6*, 7314.

Dettmer, U., Ramalingam, N., von Saucken, V.E., Kim, T.-E., Newman, A.J., Terry-Kantor, E., Nuber, S., Ericsson, M., Fanning, S., Bartels, T., et al. (2017). Loss of native α-synuclein multimerization by strategically mutating its amphipathic helix causes abnormal vesicle interactions in neuronal cells. Hum. Mol. Genet. *26*, 3466–3481.

Dhiman, R., Caesar, S., Thiam, A.R., and Schrul, B. (2020). Mechanisms of protein targeting to lipid droplets: A unified cell biological and biophysical perspective. Semin. Cell Dev. Biol.

Di Maio, R., Barrett, P.J., Hoffman, E.K., Barrett, C.W., Zharikov, A., Borah, A., Hu, X., McCoy, J., Chu, C.T., Burton, E.A., et al. (2016). α-Synuclein binds to TOM20 and inhibits mitochondrial protein import in Parkinson's disease. Sci Transl Med *8*, 342ra78.

Dichlberger, A., Schlager, S., Maaninka, K., Schneider, W.J., and Kovanen, P.T. (2014). Adipose triglyceride lipase regulates eicosanoid production in activated human mast cells. J Lipid Res *55*, 2471–2478.

Doherty, J., Logan, M.A., Taşdemir, O.E., and Freeman, M.R. (2009). Ensheathing glia function as phagocytes in the adult Drosophila brain. The Journal of Neuroscience: The Official Journal of the Society for Neuroscience *29*, 4768–4781.

Dorsey, E.R., Sherer, T., Okun, M.S., and Bloem, B.R. (2018). The Emerging Evidence of the Parkinson Pandemic. J Parkinsons Dis *8*, S3–S8.

Dourlen, P., Bertin, B., Chatelain, G., Robin, M., Napoletano, F., Roux, M.J., and Mollereau, B. (2012). Drosophila fatty acid transport protein regulates rhodopsin-1 metabolism and is required for photoreceptor neuron survival. PLoS Genetics *8*, e1002833.

Dourlen, P., Sujkowski, A., Wessells, R., and Mollereau, B. (2015). Fatty acid transport proteins in disease: New insights from invertebrate models. Prog. Lipid Res. *60*, 30–40.

Dunn, T.N., Akiyama, T., Lee, H.W., Kim, J.B., Knotts, T.A., Smith, S.R., Sears, D.D., Carstens, E., and Adams, S.H. (2015). Evaluation of the synuclein-γ (SNCG) gene as a PPARγ target in murine adipocytes, dorsal root ganglia somatosensory neurons, and human adipose tissue. PLoS ONE *10*, e0115830.

Edwards, T.N., and Meinertzhagen, I.A. (2010). The functional organisation of glia in the adult brain of Drosophila and other insects. Progress in Neurobiology *90*, 471–497.

Etschmaier, K., Becker, T., Eichmann, T.O., Schweinzer, C., Scholler, M., Tam-Amersdorfer, C., Poeckl, M., Schuligoi, R., Kober, A., Chirackal Manavalan, A.P., et al. (2011). Adipose triglyceride lipase affects triacylglycerol metabolism at brain barriers. J. Neurochem. *119*, 1016–1028.

Falk, J., Rohde, M., Bekhite, M.M., Neugebauer, S., Hemmerich, P., Kiehntopf, M., Deufel, T., Hübner, C.A., and Beetz, C. (2014). Functional mutation analysis provides evidence for a role of REEP1 in lipid droplet biology. Human Mutation *35*, 497–504.

Fanning, S., Haque, A., Imberdis, T., Baru, V., Barrasa, M.I., Nuber, S., Termine, D., Ramalingam, N., Ho, G.P.H., Noble, T., et al. (2019). Lipidomic Analysis of α-Synuclein Neurotoxicity Identifies Stearoyl CoA Desaturase as a Target for Parkinson Treatment. Molecular Cell *73*, 1001-1014.e8.

Farmer, B.C., Kluemper, J., and Johnson, L.A. (2019). Apolipoprotein E4 Alters Astrocyte Fatty Acid Metabolism and Lipid Droplet Formation. Cells *8*.

Fauny, J.D., Silber, J., and Zider, A. (2005). Drosophila Lipid Storage Droplet 2 gene (Lsd-2) is expressed and controls lipid storage in wing imaginal discs. Dev. Dyn. *232*, 725–732.

Feany, M.B., and Bender, W.W. (2000). A Drosophila model of Parkinson's disease. Nature *404*, 394–398.

Featherstone, D.E. (2011). Glial solute carrier transporters in Drosophila and mice. Glia *59*, 1351–1363.

Fecchio, C., Palazzi, L., and de Laureto, P.P. (2018). α-Synuclein and Polyunsaturated Fatty Acids: Molecular Basis of the Interaction and Implication in Neurodegeneration. Molecules *23*.

Fei, W., Li, H., Shui, G., Kapterian, T.S., Bielby, C., Du, X., Brown, A.J., Li, P., Wenk, M.R., Liu, P., et al. (2011). Molecular characterization of seipin and its mutants: implications for seipin in triacylglycerol synthesis. J. Lipid Res. *52*, 2136–2147.

Flagmeier, P., Meisl, G., Vendruscolo, M., Knowles, T.P.J., Dobson, C.M., Buell, A.K., and Galvagnion, C. (2016). Mutations associated with familial Parkinson's disease alter the initiation and amplification steps of α-synuclein aggregation. Proc. Natl. Acad. Sci. U.S.A. *113*, 10328–10333.

Foley, P. (2010). Lipids in Alzheimer's disease: A century-old story. Biochim. Biophys. Acta *1801*, 750–753.

Freeman, M.R. (2015). Drosophila Central Nervous System Glia. Cold Spring Harb Perspect Biol *7*.

Gai, W.P., Yuan, H.X., Li, X.Q., Power, J.T., Blumbergs, P.C., and Jensen, P.H. (2000). In situ and in vitro study of colocalization and segregation of alpha-synuclein, ubiquitin, and lipids in Lewy bodies. Experimental Neurology *166*, 324–333.

Gáliková, M., Klepsatel, P., Münch, J., and Kühnlein, R.P. (2017). Spastic paraplegia-linked phospholipase PAPLA1 is necessary for development, reproduction, and energy metabolism in Drosophila. Scientific Reports *7*, 46516.

Galvagnion, C. (2017). The Role of Lipids Interacting with α-Synuclein in the Pathogenesis of Parkinson's Disease. JPD *7*, 433–450.

Galvagnion, C., Buell, A.K., Meisl, G., Michaels, T.C.T., Vendruscolo, M., Knowles, T.P.J., and Dobson, C.M. (2015). Lipid vesicles trigger α-synuclein aggregation by stimulating primary nucleation. Nat. Chem. Biol. *11*, 229–234.

Gambis, A., Dourlen, P., Steller, H., and Mollereau, B. (2011). Two-color in vivo imaging of photoreceptor apoptosis and development in Drosophila. Dev Biol *351*, 128–134.

Gao, Q., Binns, D.D., Kinch, L.N., Grishin, N.V., Ortiz, N., Chen, X., and Goodman, J.M. (2017). Pet10p is a yeast perilipin that stabilizes lipid droplets and promotes their assembly. J.

Cell Biol. *216*, 3199–3217.

Gaschler, M.M., and Stockwell, B.R. (2017). Lipid peroxidation in cell death. Biochem Biophys Res Commun *482*, 419–425.

Geller, S., Arribat, Y., Netzahualcoyotzi, C., Lagarrigue, S., Carneiro, L., Zhang, L., Amati, F., Lopez-Mejia, I.C., and Pellerin, L. (2019). Tanycytes Regulate Lipid Homeostasis by Sensing Free Fatty Acids and Signaling to Key Hypothalamic Neuronal Populations via FGF21 Secretion. Cell Metab. *30*, 833-844.e7.

Goedert, M. (2015). NEURODEGENERATION. Alzheimer's and Parkinson's diseases: The prion concept in relation to assembled Aβ, tau, and α-synuclein. Science *349*, 1255555.

Goedert, M., and Compston, A. (2018). Parkinson's disease - the story of an eponym. Nat Rev Neurol *14*, 57–62.

Gómez-Ramos, P., and Asunción Morán, M. (2007). Ultrastructural localization of intraneuronal Abeta-peptide in Alzheimer disease brains. J. Alzheimers Dis. *11*, 53–59.

Gong, J., Sun, Z., Wu, L., Xu, W., Schieber, N., Xu, D., Shui, G., Yang, H., Parton, R.G., and Li, P. (2011). Fsp27 promotes lipid droplet growth by lipid exchange and transfer at lipid droplet contact sites. J Cell Biol *195*, 953–963.

Gould, N., Mor, D.E., Lightfoot, R., Malkus, K., Giasson, B., and Ischiropoulos, H. (2014). Evidence of native α-synuclein conformers in the human brain. The Journal of Biological Chemistry *289*, 7929–7934.

Greenberg, A.S., and Coleman, R.A. (2011). Expanding roles for lipid droplets. Trends in Endocrinology and Metabolism: TEM *22*, 195–196.

Greenberg, A.S., Egan, J.J., Wek, S.A., Garty, N.B., Blanchette-Mackie, E.J., and Londos, C. (1991). Perilipin, a major hormonally regulated adipocyte-specific phosphoprotein associated with the periphery of lipid storage droplets. The Journal of Biological Chemistry *266*, 11341–11346.

Greene, J.C., Whitworth, A.J., Kuo, I., Andrews, L.A., Feany, M.B., and Pallanck, L.J. (2003). Mitochondrial pathology and apoptotic muscle degeneration in Drosophila parkin mutants. Proc Natl Acad Sci U S A *100*, 4078–4083.

Greten-Harrison, B., Polydoro, M., Morimoto-Tomita, M., Diao, L., Williams, A.M., Nie, E.H., Makani, S., Tian, N., Castillo, P.E., Buchman, V.L., et al. (2010). αβγ-Synuclein triple knockout mice reveal age-dependent neuronal dysfunction. PNAS *107*, 19573–19578.

Grönke, S., Beller, M., Fellert, S., Ramakrishnan, H., Jäckle, H., and Kühnlein, R.P. (2003). Control of fat storage by a Drosophila PAT domain protein. Curr. Biol. *13*, 603–606.

Grönke, S., Mildner, A., Fellert, S., Tennagels, N., Petry, S., Müller, G., Jäckle, H., and Kühnlein, R.P. (2005). Brummer lipase is an evolutionary conserved fat storage regulator in Drosophila. Cell Metab. *1*, 323–330.

Gutierrez, E., Wiggins, D., Fielding, B., and Gould, A.P. (2007). Specialized hepatocyte-like cells regulate Drosophila lipid metabolism. Nature *445*, 275–280.

Hamada, S., Kishikawa, A., and Yoshida, M. (2020). Proteomic Analysis of Lipid Droplets in Sesamum indicum. Protein J *39*, 366–376.

Hamilton, J.A., and Brunaldi, K. (2007). A Model for Fatty Acid Transport into the Brain.

J Mol Neurosci *33*, 12–17.

Hamilton, J.A., Hillard, C.J., Spector, A.A., and Watkins, P.A. (2007). Brain Uptake and Utilization of Fatty Acids, Lipids and Lipoproteins: Application to Neurological Disorders. J Mol Neurosci *33*, 2–11.

Hamilton, L.K., Dufresne, M., Joppé, S.E., Petryszyn, S., Aumont, A., Calon, F., Barnabé-Heider, F., Furtos, A., Parent, M., Chaurand, P., et al. (2015). Aberrant Lipid Metabolism in the Forebrain Niche Suppresses Adult Neural Stem Cell Proliferation in an Animal Model of Alzheimer's Disease. Cell Stem Cell *17*, 397–411.

Hariri, H., Speer, N., Bowerman, J., Rogers, S., Fu, G., Reetz, E., Datta, S., Feathers, J.R., Ugrankar, R., Nicastro, D., et al. (2019). Mdm1 maintains endoplasmic reticulum homeostasis by spatially regulating lipid droplet biogenesis. J. Cell Biol. *218*, 1319–1334.

Harris, J.J., Jolivet, R., and Attwell, D. (2012). Synaptic Energy Use and Supply. Neuron *75*, 762–777.

Hauck, A.K., and Bernlohr, D.A. (2016). Oxidative stress and lipotoxicity. J. Lipid Res. *57*, 1976–1986.

Hazegh, K.E., Nemkov, T., D'Alessandro, A., Diller, J.D., Monks, J., McManaman, J.L., Jones, K.L., Hansen, K.C., and Reis, T. (2017). An autonomous metabolic role for Spen. PLoS Genet *13*, e1006859.

Heier, C., and Kühnlein, R.P. (2018). Triacylglycerol Metabolism in Drosophila melanogaster. Genetics *210*, 1163–1184.

Henne, W.M., Reese, M.L., and Goodman, J.M. (2018). The assembly of lipid droplets and their roles in challenged cells. EMBO J. *37*.

Hipp, M.S., Kasturi, P., and Hartl, F.U. (2019). The proteostasis network and its decline in ageing. Nature Reviews Molecular Cell Biology *20*, 421–435.

Hölttä-Vuori, M., Salo, V.T., Ohsaki, Y., Suster, M.L., and Ikonen, E. (2013). Alleviation of seipinopathy-related ER stress by triglyceride storage. Hum. Mol. Genet. *22*, 1157–1166.

Hsieh, K., Lee, Y.K., Londos, C., Raaka, B.M., Dalen, K.T., and Kimmel, A.R. (2012). Perilipin family members preferentially sequester to either triacylglycerol-specific or cholesteryl-ester-specific intracellular lipid storage droplets. J. Cell. Sci. *125*, 4067–4076.

Hwangbo, D.S., Gersham, B., Tu, M.-P., Palmer, M., and Tatar, M. (2004). Drosophila dFOXO controls lifespan and regulates insulin signalling in brain and fat body. Nature *429*, 562–566.

Ibáñez, P., Lesage, S., Janin, S., Lohmann, E., Durif, F., Destée, A., Bonnet, A.-M., Brefel-Courbon, C., Heath, S., Zelenika, D., et al. (2009). Alpha-synuclein gene rearrangements in dominantly inherited parkinsonism: frequency, phenotype, and mechanisms. Archives of Neurology *66*, 102–108.

Imamura, M., Inoguchi, T., Ikuyama, S., Taniguchi, S., Kobayashi, K., Nakashima, N., and Nawata, H. (2002). ADRP stimulates lipid accumulation and lipid droplet formation in murine fibroblasts. Am J Physiol Endocrinol Metab *283*, E775-783.

Imberdis, T., Negri, J., Ramalingam, N., Terry-Kantor, E., Ho, G.P.H., Fanning, S., Stirtz, G., Kim, T.-E., Levy, O.A., Young-Pearse, T.L., et al. (2019). Cell models of lipid-rich α-synuclein

aggregation validate known modifiers of α-synuclein biology and identify stearoyl-CoA desaturase. Proc. Natl. Acad. Sci. U.S.A. *116*, 20760–20769.

Inloes, J.M., Hsu, K.-L., Dix, M.M., Viader, A., Masuda, K., Takei, T., Wood, M.R., and Cravatt, B.F. (2014). The hereditary spastic paraplegia-related enzyme DDHD2 is a principal brain triglyceride lipase. Proc. Natl. Acad. Sci. U.S.A. *111*, 14924–14929.

Inloes, J.M., Kiosses, W.B., Wang, H., Walther, T.C., Farese, R.V., and Cravatt, B.F. (2018). Functional Contribution of the Spastic Paraplegia-Related Triglyceride Hydrolase DDHD2 to the Formation and Content of Lipid Droplets. Biochemistry *57*, 827–838.

Ioannou, M.S., Jackson, J., Sheu, S.-H., Chang, C.-L., Weigel, A.V., Liu, H., Pasolli, H.A., Xu, C.S., Pang, S., Matthies, D., et al. (2019). Neuron-Astrocyte Metabolic Coupling Protects against Activity-Induced Fatty Acid Toxicity. Cell *177*, 1522-1535.e14.

Itabe, H., Yamaguchi, T., Nimura, S., and Sasabe, N. (2017). Perilipins: a diversity of intracellular lipid droplet proteins. Lipids Health Dis *16*, 83.

Ito, K., Shinomiya, K., Ito, M., Armstrong, J.D., Boyan, G., Hartenstein, V., Harzsch, S., Heisenberg, M., Homberg, U., Jenett, A., et al. (2014). A Systematic Nomenclature for the Insect Brain. Neuron *81*, 755–765.

Jacquier, N., Mishra, S., Choudhary, V., and Schneiter, R. (2013). Expression of oleosin and perilipins in yeast promotes formation of lipid droplets from the endoplasmic reticulum. J. Cell. Sci. *126*, 5198–5209.

den Jager, W.A. (1969). Sphingomyelin in Lewy inclusion bodies in Parkinson's disease. Archives of Neurology *21*, 615–619.

Kaczocha, M., Glaser, S.T., Chae, J., Brown, D.A., and Deutsch, D.G. (2010). Lipid droplets are novel sites of N-acylethanolamine inactivation by fatty acid amide hydrolase-2. J. Biol. Chem. *285*, 2796–2806.

Kalia, L.V., and Lang, A.E. (2015). Parkinson's disease. Lancet (London, England) *386*, 896–912.

Kassan, A., Herms, A., Fernández-Vidal, A., Bosch, M., Schieber, N.L., Reddy, B.J.N., Fajardo, A., Gelabert-Baldrich, M., Tebar, F., Enrich, C., et al. (2013). Acyl-CoA synthetase 3 promotes lipid droplet biogenesis in ER microdomains. The Journal of Cell Biology *203*, 985–1001.

Kaushik, S., and Cuervo, A.M. (2015). Degradation of lipid droplet-associated proteins by chaperone-mediated autophagy facilitates lipolysis. Nat. Cell Biol. *17*, 759–770.

Khaliullina, H., Bilgin, M., Sampaio, J.L., Shevchenko, A., and Eaton, S. (2015). Endocannabinoids are conserved inhibitors of the Hedgehog pathway. PNAS *112*, 3415–3420.

Khatchadourian, A., Bourque, S.D., Richard, V.R., Titorenko, V.I., and Maysinger, D. (2012). Dynamics and regulation of lipid droplet formation in lipopolysaccharide (LPS)-stimulated microglia. Biochim Biophys Acta *1821*, 607–617.

Kimmel, A.R., and Sztalryd, C. (2016). The Perilipins: Major Cytosolic Lipid Droplet-Associated Proteins and Their Roles in Cellular Lipid Storage, Mobilization, and Systemic Homeostasis. Annu. Rev. Nutr. *36*, 471–509.

Kimmel, A.R., Brasaemle, D.L., McAndrews-Hill, M., Sztalryd, C., and Londos, C. (2010).

Adoption of PERILIPIN as a unifying nomenclature for the mammalian PAT-family of intracellular lipid storage droplet proteins. The Journal of Lipid Research *51*, 468–471.

Kirkland, J.L., Tchkonia, T., Pirtskhalava, T., Han, J., and Karagiannides, I. (2002). Adipogenesis and aging: does aging make fat go MAD? Experimental Gerontology *37*, 757–767.

Kis, V., Barti, B., Lippai, M., and Sass, M. (2015). Specialized Cortex Glial Cells Accumulate Lipid Droplets in Drosophila melanogaster. PLoS ONE *10*, e0131250.

Klemann, C.J.H.M., Martens, G.J.M., Sharma, M., Martens, M.B., Isacson, O., Gasser, T., Visser, J.E., and Poelmans, G. (2017). Integrated molecular landscape of Parkinson's disease. Npj Parkinson's Disease *3*, 14.

Klemm, R.W., Norton, J.P., Cole, R.A., Li, C.S., Park, S.H., Crane, M.M., Li, L., Jin, D., Boye-Doe, A., Liu, T.Y., et al. (2013). A conserved role for atlastin GTPases in regulating lipid droplet size. Cell Rep *3*, 1465–1475.

Knowles, T.P.J., Waudby, C.A., Devlin, G.L., Cohen, S.I.A., Aguzzi, A., Vendruscolo, M., Terentjev, E.M., Welland, M.E., and Dobson, C.M. (2009). An analytical solution to the kinetics of breakable filament assembly. Science *326*, 1533–1537.

Kory, N., Thiam, A.-R., Farese, R.V., and Walther, T.C. (2015). Protein Crowding Is a Determinant of Lipid Droplet Protein Composition. Dev. Cell *34*, 351–363.

Krahmer, N., Guo, Y., Wilfling, F., Hilger, M., Lingrell, S., Heger, K., Newman, H.W., Schmidt-Supprian, M., Vance, D.E., Mann, M., et al. (2011). Phosphatidylcholine synthesis for lipid droplet expansion is mediated by localized activation of CTP:phosphocholine cytidylyltransferase. Cell Metab. *14*, 504–515.

Krahmer, N., Hilger, M., Kory, N., Wilfling, F., Stoehr, G., Mann, M., Farese, R.V., and Walther, T.C. (2013). Protein correlation profiles identify lipid droplet proteins with high confidence. Mol. Cell Proteomics *12*, 1115–1126.

Kremer, M.C., Jung, C., Batelli, S., Rubin, G.M., and Gaul, U. (2017). The glia of the adult *Drosophila* nervous system: Glia Anatomy in Adult Drosophila Nervous System. Glia *65*, 606–638.

Kretzschmar, F.K., Mengel, L.A., Müller, A.O., Schmitt, K., Blersch, K.F., Valerius, O., Braus, G.H., and Ischebeck, T. (2018). PUX10 Is a Lipid Droplet-Localized Scaffold Protein That Interacts with CELL DIVISION CYCLE48 and Is Involved in the Degradation of Lipid Droplet Proteins. Plant Cell *30*, 2137–2160.

Kühnlein, R.P. (2011). The contribution of the Drosophila model to lipid droplet research. Progress in Lipid Research *50*, 348–356.

Kühnlein, R.P. (2012). Lipid droplet-based storage fat metabolism in Drosophila. J Lipid Res *53*, 1430–1436.

Kurant, E., Axelrod, S., Leaman, D., and Gaul, U. (2008). Six-microns-under acts upstream of Draper in the glial phagocytosis of apoptotic neurons. Cell *133*, 498–509.

Kysenius, K., and Huttunen, H.J. (2016). Stress-induced upregulation of VLDL receptor alters Wnt-signaling in neurons. Experimental Cell Research *340*, 238–247.

Kyu, H.H., Abate, D., Abate, K.H., Abay, S.M., Abbafati, C., Abbasi, N., Abbastabar, H., Abd-

Allah, F., Abdela, J., Abdelalim, A., et al. (2018). Global, regional, and national disability-adjusted life-years (DALYs) for 359 diseases and injuries and healthy life expectancy (HALE) for 195 countries and territories, 1990–2017: a systematic analysis for the Global Burden of Disease Study 2017. The Lancet *392*, 1859–1922.

Langston, J.W., Ballard, P., Tetrud, J.W., and Irwin, I. (1983). Chronic Parkinsonism in humans due to a product of meperidine-analog synthesis. Science (New York, N.Y.) *219*, 979–980.

Lass, A., Zimmermann, R., Oberer, M., and Zechner, R. (2011). Lipolysis – A highly regulated multi-enzyme complex mediates the catabolism of cellular fat stores. Prog Lipid Res *50*, 14–27.

Lázaro, D.F., Rodrigues, E.F., Langohr, R., Shahpasandzadeh, H., Ribeiro, T., Guerreiro, P., Gerhardt, E., Kröhnert, K., Klucken, J., Pereira, M.D., et al. (2014). Systematic Comparison of the Effects of Alpha-synuclein Mutations on Its Oligomerization and Aggregation. PLoS Genetics *10*, e1004741.

Lee, J.A., Hall, B., Allsop, J., Alqarni, R., and Allen, S.P. (2020). Lipid metabolism in astrocytic structure and function. Semin. Cell Dev. Biol.

Lee, P.-C., Bordelon, Y., Bronstein, J., and Ritz, B. (2012). Traumatic brain injury, paraquat exposure, and their relationship to Parkinson disease. Neurology *79*, 2061–2066.

Leeuwenhoek, A.V., and Chamberlayne, J. (1723). II. A letter to the Royal Society concerning the particles of fat. By Mr. Leeuwenhoek, F. R. S. Translated from the Dutch by John Chamberlayne, Esq; Philosophical Transactions of the Royal Society of London *32*, 93–99.

Lessing, D., and Bonini, N.M. (2009). Maintaining the brain: insight into human neurodegeneration from Drosophila melanogaster mutants. Nature Reviews Genetics *10*, 359–370.

Leung, H.-T., Tseng-Crank, J., Kim, E., Mahapatra, C., Shino, S., Zhou, Y., An, L., Doerge, R.W., and Pak, W.L. (2008). DAG lipase activity is necessary for TRP channel regulation in Drosophila photoreceptors. Neuron *58*, 884–896.

Listenberger, L.L., Han, X., Lewis, S.E., Cases, S., Farese, R.V., Ory, D.S., and Schaffer, J.E. (2003). Triglyceride accumulation protects against fatty acid-induced lipotoxicity. Proc. Natl. Acad. Sci. U.S.A. *100*, 3077–3082.

Listenberger, L.L., Ostermeyer-Fay, A.G., Goldberg, E.B., Brown, W.J., and Brown, D.A. (2007). Adipocyte differentiation-related protein reduces the lipid droplet association of adipose triglyceride lipase and slows triacylglycerol turnover. J. Lipid Res. *48*, 2751–2761.

Liu, L., Zhang, K., Sandoval, H., Yamamoto, S., Jaiswal, M., Sanz, E., Li, Z., Hui, J., Graham, B.H., Quintana, A., et al. (2015). Glial Lipid Droplets and ROS Induced by Mitochondrial Defects Promote Neurodegeneration. Cell *160*, 177–190.

Liu, L., MacKenzie, K.R., Putluri, N., Maletić-Savatić, M., and Bellen, H.J. (2017). The Glia-Neuron Lactate Shuttle and Elevated ROS Promote Lipid Synthesis in Neurons and Lipid Droplet Accumulation in Glia via APOE/D. Cell Metabolism *26*, 719-737.e6.

Logan, T., Bendor, J., Toupin, C., Thorn, K., and Edwards, R.H. (2017). α-Synuclein promotes dilation of the exocytotic fusion pore. Nature Neuroscience *20*, 681–689.

Londos, C., Brasaemle, D.L., Schultz, C.J., Segrest, J.P., and Kimmel, A.R. (1999). Perilipins, ADRP, and other proteins that associate with intracellular neutral lipid droplets in animal cells. Semin. Cell Dev. Biol. *10*, 51–58.

Luk, K.C., Kehm, V., Carroll, J., Zhang, B., O'Brien, P., Trojanowski, J.Q., and Lee, V.M.-Y. (2012). Pathological α-synuclein transmission initiates Parkinson-like neurodegeneration in nontransgenic mice. Science (New York, N.Y.) *338*, 949–953.

Maroteaux, L., Campanelli, J.T., and Scheller, R.H. (1988). Synuclein: a neuron-specific protein localized to the nucleus and presynaptic nerve terminal. The Journal of Neuroscience: The Official Journal of the Society for Neuroscience *8*, 2804–2815.

Marschallinger, J., Iram, T., Zardeneta, M., Lee, S.E., Lehallier, B., Haney, M.S., Pluvinage, J.V., Mathur, V., Hahn, O., Morgens, D.W., et al. (2020). Lipid-droplet-accumulating microglia represent a dysfunctional and proinflammatory state in the aging brain. Nat. Neurosci. *23*, 194–208.

Martinez-Vicente, M., Talloczy, Z., Wong, E., Tang, G., Koga, H., Kaushik, S., de Vries, R., Arias, E., Harris, S., Sulzer, D., et al. (2010). Cargo recognition failure is responsible for inefficient autophagy in Huntington's disease. Nature Neuroscience *13*, 567–576.

Maruyama, T., Baba, T., Maemoto, Y., Hara-Miyauchi, C., Hasegawa-Ogawa, M., Okano, H.J., Enda, Y., Matsumoto, K., Arimitsu, N., Nakao, K., et al. (2018). Loss of DDHD2, whose mutation causes spastic paraplegia, promotes reactive oxygen species generation and apoptosis. Cell Death Dis *9*, 797.

Mazzulli, J.R., Xu, Y.-H., Sun, Y., Knight, A.L., McLean, P.J., Caldwell, G.A., Sidransky, E., Grabowski, G.A., and Krainc, D. (2011). Gaucher disease glucocerebrosidase and α-synuclein form a bidirectional pathogenic loop in synucleinopathies. Cell *146*, 37–52.

Miake, H., Mizusawa, H., Iwatsubo, T., and Hasegawa, M. (2002). Biochemical characterization of the core structure of alpha-synuclein filaments. J Biol Chem *277*, 19213–19219.

Millership, S., Ninkina, N., Guschina, I.A., Norton, J., Brambilla, R., Brambilla, R., Oort, P.J., Adams, S.H., Dennis, R.J., Voshol, P.J., et al. (2012). Increased lipolysis and altered lipid homeostasis protect γ-synuclein-null mutant mice from diet-induced obesity. Proc Natl Acad Sci U S A *109*, 20943–20948.

Miura, S., Gan, J.-W., Brzostowski, J., Parisi, M.J., Schultz, C.J., Londos, C., Oliver, B., and Kimmel, A.R. (2002). Functional conservation for lipid storage droplet association among Perilipin, ADRP, and TIP47 (PAT)-related proteins in mammals, Drosophila, and Dictyostelium. J. Biol. Chem. *277*, 32253–32257.

Moessinger, C., Kuerschner, L., Spandl, J., Shevchenko, A., and Thiele, C. (2011). Human Lysophosphatidylcholine Acyltransferases 1 and 2 Are Located in Lipid Droplets Where They Catalyze the Formation of Phosphatidylcholine. J. Biol. Chem. *286*, 21330–21339.

Montesinos, J., Guardia-Laguarta, C., and Area-Gomez, E. (2020). The fat brain. Curr Opin Clin Nutr Metab Care *23*, 68–75.

Mougenot, A.-L., Nicot, S., Bencsik, A., Morignat, E., Verchère, J., Lakhdar, L., Legastelois, S., and Baron, T. (2012). Prion-like acceleration of a synucleinopathy in a transgenic mouse model. Neurobiol Aging *33*, 2225–2228.

Muliyil, S., Levet, C., Düsterhöft, S., Dulloo, I., Cowley, S.A., and Freeman, M. (2020). ADAM17-triggered TNF signalling protects the ageing Drosophila retina from lipid droplet-mediated degeneration. EMBO J. *39*, e104415.

Murphy, D.J. (2012). The dynamic roles of intracellular lipid droplets: from archaea to mammals. Protoplasma *249*, 541–585.

Musacchio, T., Zaum, A.-K., Üçeyler, N., Sommer, C., Pfeifroth, N., Reiners, K., Kunstmann, E., Volkmann, J., Rost, S., and Klebe, S. (2017). ALS and MMN mimics in patients with BSCL2 mutations: the expanding clinical spectrum of SPG17 hereditary spastic paraplegia. Journal of Neurology *264*, 11–20.

Muthusamy, N., Sommerville, L.J., Moeser, A.J., Stumpo, D.J., Sannes, P., Adler, K., Blackshear, P.J., Weimer, J.M., and Ghashghaei, H.T. (2015). MARCKS-dependent mucin clearance and lipid metabolism in ependymal cells are required for maintenance of forebrain homeostasis during aging. Aging Cell *14*, 764–773.

Nag, T.C., and Wadhwa, S. (2012). Accumulation of lipid inclusions in astrocytes of aging human optic nerve. Acta. Biol. Hung. *63 Suppl 1*, 54–64.

Nagoshi, E. (2018). Drosophila Models of Sporadic Parkinson's Disease. Int J Mol Sci *19*.

Nalls, M.A., Pankratz, N., Lill, C.M., Do, C.B., Hernandez, D.G., Saad, M., DeStefano, A.L., Kara, E., Bras, J., Sharma, M., et al. (2014). Large-scale meta-analysis of genome-wide association data identifies six new risk loci for Parkinson's disease. Nature Genetics *46*, 989–993.

Navarro, J.A., Ohmann, E., Sanchez, D., Botella, J.A., Liebisch, G., Moltó, M.D., Ganfornina, M.D., Schmitz, G., and Schneuwly, S. (2010). Altered lipid metabolism in a Drosophila model of Friedreich's ataxia. Hum. Mol. Genet. *19*, 2828–2840.

Navarro, J.A., Heßner, S., Yenisetti, S.C., Bayersdorfer, F., Zhang, L., Voigt, A., Schneuwly, S., and Botella, J.A. (2014). Analysis of dopaminergic neuronal dysfunction in genetic and toxin-induced models of Parkinson's disease in Drosophila. J. Neurochem. *131*, 369–382.

Neumann, M., Kahle, P.J., Giasson, B.I., Ozmen, L., Borroni, E., Spooren, W., Müller, V., Odoy, S., Fujiwara, H., Hasegawa, M., et al. (2002). Misfolded proteinase K–resistant hyperphosphorylated α-synuclein in aged transgenic mice with locomotor deterioration and in human α-synucleinopathies. J Clin Invest *110*, 1429–1439.

Nguyen, T.B., Louie, S.M., Daniele, J.R., Tran, Q., Dillin, A., Zoncu, R., Nomura, D.K., and Olzmann, J.A. (2017). DGAT1-Dependent Lipid Droplet Biogenesis Protects Mitochondrial Function during Starvation-Induced Autophagy. Dev. Cell *42*, 9-21.e5.

Nishino, N., Tamori, Y., Tateya, S., Kawaguchi, T., Shibakusa, T., Mizunoya, W., Inoue, K., Kitazawa, R., Kitazawa, S., Matsuki, Y., et al. (2008). FSP27 contributes to efficient energy storage in murine white adipocytes by promoting the formation of unilocular lipid droplets. J Clin Invest *118*, 2808–2821.

Nuber, S., Rajsombath, M., Minakaki, G., Winkler, J., Müller, C.P., Ericsson, M., Caldarone, B., Dettmer, U., and Selkoe, D.J. (2018). Abrogating Native α-Synuclein Tetramers in Mice Causes a L-DOPA-Responsive Motor Syndrome Closely Resembling Parkinson's Disease. Neuron *100*, 75-90.e5.

Oakes, S.A., and Papa, F.R. (2015). The role of endoplasmic reticulum stress in human

pathology. Annu Rev Pathol *10*, 173–194.

Ogrodnik, M., Zhu, Y., Langhi, L.G.P., Tchkonia, T., Krüger, P., Fielder, E., Victorelli, S., Ruswhandi, R.A., Giorgadze, N., Pirtskhalava, T., et al. (2019). Obesity-Induced Cellular Senescence Drives Anxiety and Impairs Neurogenesis. Cell Metab. *29*, 1061-1077.e8.

Ohhara, Y., Kobayashi, S., and Yamanaka, N. (2017). Nutrient-Dependent Endocycling in Steroidogenic Tissue Dictates Timing of Metamorphosis in Drosophila melanogaster. PLOS Genetics *13*, e1006583.

Olsen, A.L., and Feany, M.B. (2019). Glial α-synuclein promotes neurodegeneration characterized by a distinct transcriptional program in vivo. Glia *67*, 1933–1957.

Olzmann, J.A., and Carvalho, P. (2019). Dynamics and functions of lipid droplets. Nat. Rev. Mol. Cell Biol. *20*, 137–155.

Ordonez, D.G., Lee, M.K., and Feany, M.B. (2018). α-synuclein Induces Mitochondrial Dysfunction through Spectrin and the Actin Cytoskeleton. Neuron *97*, 108-124.e6.

Outeiro, T.F., and Lindquist, S. (2003). Yeast cells provide insight into alpha-synuclein biology and pathobiology. Science *302*, 1772–1775.

Pagac, M., Cooper, D.E., Qi, Y., Lukmantara, I.E., Mak, H.Y., Wu, Z., Tian, Y., Liu, Z., Lei, M., Du, X., et al. (2016). SEIPIN Regulates Lipid Droplet Expansion and Adipocyte Development by Modulating the Activity of Glycerol-3-phosphate Acyltransferase. Cell Rep *17*, 1546–1559.

Palm, W., Sampaio, J.L., Brankatschk, M., Carvalho, M., Mahmoud, A., Shevchenko, A., and Eaton, S. (2012). Lipoproteins in Drosophila melanogaster—Assembly, Function, and Influence on Tissue Lipid Composition. PLOS Genetics *8*, e1002828.

Papadopoulos, C., Orso, G., Mancuso, G., Herholz, M., Gumeni, S., Tadepalle, N., Jüngst, C., Tzschichholz, A., Schauss, A., Höning, S., et al. (2015). Spastin Binds to Lipid Droplets and Affects Lipid Metabolism. PLOS Genetics *11*, e1005149.

Park, J., Lee, S.B., Lee, S., Kim, Y., Song, S., Kim, S., Bae, E., Kim, J., Shong, M., Kim, J.-M., et al. (2006). Mitochondrial dysfunction in Drosophila PINK1 mutants is complemented by parkin. Nature *441*, 1157–1161.

Pennetta, G., and Welte, M.A. (2018). Emerging Links between Lipid Droplets and Motor Neuron Diseases. Dev. Cell *45*, 427–432.

Periquet, M., Fulga, T., Myllykangas, L., Schlossmacher, M.G., and Feany, M.B. (2007). Aggregated -Synuclein Mediates Dopaminergic Neurotoxicity In Vivo. Journal of Neuroscience *27*, 3338–3346.

Pineau, L., Colas, J., Dupont, S., Beney, L., Fleurat-Lessard, P., Berjeaud, J.-M., Bergès, T., and Ferreira, T. (2009). Lipid-induced ER stress: synergistic effects of sterols and saturated fatty acids. Traffic *10*, 673–690.

Ploegh, H.L. (2007). A lipid-based model for the creation of an escape hatch from the endoplasmic reticulum. Nature *448*, 435–438.

Pocas, G.M., Branco-Santos, J., Herrera, F., Outeiro, T.F., and Domingos, P.M. (2015). α-Synuclein modifies mutant huntingtin aggregation and neurotoxicity in Drosophila. Human Molecular Genetics *24*, 1898–1907.

Poewe, W., Seppi, K., Tanner, C.M., Halliday, G.M., Brundin, P., Volkmann, J., Schrag, A.-E.,

and Lang, A.E. (2017). Parkinson disease. Nature Reviews Disease Primers *3*, 17013.

Polymeropoulos, M.H., Lavedan, C., Leroy, E., Ide, S.E., Dehejia, A., Dutra, A., Pike, B., Root, H., Rubenstein, J., Boyer, R., et al. (1997). Mutation in the alpha-synuclein gene identified in families with Parkinson's disease. Science *276*, 2045–2047.

Prasad, V., Wasser, Y., Hans, F., Goswami, A., Katona, I., Outeiro, T.F., Kahle, P.J., Schulz, J.B., and Voigt, A. (2019). Monitoring α-synuclein multimerization in vivo. The FASEB Journal *33*, 2116–2131.

Pyc, M., Cai, Y., Greer, M.S., Yurchenko, O., Chapman, K.D., Dyer, J.M., and Mullen, R.T. (2017). Turning Over a New Leaf in Lipid Droplet Biology. Trends Plant Sci *22*, 596–609.

Qiu, Y., Hassaninasab, A., Han, G.-S., and Carman, G.M. (2016). Phosphorylation of Dgk1 Diacylglycerol Kinase by Casein Kinase II Regulates Phosphatidic Acid Production in Saccharomyces cerevisiae. J Biol Chem *291*, 26455–26467.

Querenet, M., Goubard, V., Chatelain, G., Davoust, N., and Mollereau, B. (2015). Spen is required for pigment cell survival during pupal development in Drosophila. Developmental Biology *402*, 208–215.

Rambold, A.S., Cohen, S., and Lippincott-Schwartz, J. (2015). Fatty acid trafficking in starved cells: regulation by lipid droplet lipolysis, autophagy, and mitochondrial fusion dynamics. Dev. Cell *32*, 678–692.

Renvoisé, B., Malone, B., Falgairolle, M., Munasinghe, J., Stadler, J., Sibilla, C., Park, S.H., and Blackstone, C. (2016). Reep1 null mice reveal a converging role for hereditary spastic paraplegia proteins in lipid droplet regulation. Hum. Mol. Genet. *25*, 5111–5125.

Rival, T., Soustelle, L., Strambi, C., Besson, M.-T., Iché, M., and Birman, S. (2004). Decreasing glutamate buffering capacity triggers oxidative stress and neuropil degeneration in the Drosophila brain. Curr. Biol. *14*, 599–605.

Rossi, A., Berger, K., Chen, H., Leslie, D., Mailman, R.B., and Huang, X. (2018). Projection of the prevalence of Parkinson's disease in the coming decades: Revisited. Mov. Disord. *33*, 156–159.

Rovere, M., Powers, A.E., Jiang, H., Pitino, J.C., Fonseca-Ornelas, L., Patel, D.S., Achille, A., Langen, R., Varkey, J., and Bartels, T. (2019). E46K-like α-synuclein mutants increase lipid interactions and disrupt membrane selectivity. J. Biol. Chem. *294*, 9799–9812.

Rowe, E.R., Mimmack, M.L., Barbosa, A.D., Haider, A., Isaac, I., Ouberai, M.M., Thiam, A.R., Patel, S., Saudek, V., Siniossoglou, S., et al. (2016). Conserved Amphipathic Helices Mediate Lipid Droplet Targeting of Perilipins 1-3. J. Biol. Chem. *291*, 6664–6678.

Sánchez Campos, S., Alza, N.P., and Salvador, G.A. (2018). Lipid metabolism alterations in the neuronal response to A53T α-synuclein and Fe-induced injury. Archives of Biochemistry and Biophysics *655*, 43–54.

Savage, M.J., Goldberg, D.J., and Schacher, S. (1987). Absolute specificity for retrograde fast axonal transport displayed by lipid droplets originating in the axon of an identified Aplysia neuron in vitro. Brain Res. *406*, 215–223.

Schirmeier, S., and Klämbt, C. (2015). The Drosophila blood-brain barrier as interface between neurons and hemolymph. Mech. Dev. *138 Pt 1*, 50–55.

Schönfeld, P., and Reiser, G. (2013). Why does brain metabolism not favor burning of fatty acids to provide energy? Reflections on disadvantages of the use of free fatty acids as fuel for brain. J. Cereb. Blood Flow Metab. *33*, 1493–1499.

Schönfeld, P., and Reiser, G. (2017). Brain energy metabolism spurns fatty acids as fuel due to their inherent mitotoxicity and potential capacity to unleash neurodegeneration. Neurochem. Int. *109*, 68–77.

Schuldiner, M., and Bohnert, M. (2017). A different kind of love - lipid droplet contact sites. Biochim Biophys Acta Mol Cell Biol Lipids *1862*, 1188–1196.

Schulz, J.G., Laranjeira, A., Van Huffel, L., Gärtner, A., Vilain, S., Bastianen, J., Van Veldhoven, P.P., and Dotti, C.G. (2015). Glial β-Oxidation regulates Drosophila Energy Metabolism. Scientific Reports *5*.

Schwabe, T., Bainton, R.J., Fetter, R.D., Heberlein, U., and Gaul, U. (2005). GPCR signaling is required for blood-brain barrier formation in drosophila. Cell *123*, 133–144.

Selkoe, D.J. (2017). Showing transmitters the door: synucleins accelerate vesicle release. Nat. Neurosci. *20*, 629–631.

Shahmoradian, S.H., Lewis, A.J., Genoud, C., Hench, J., Moors, T.E., Navarro, P.P., Castaño-Díez, D., Schweighauser, G., Graff-Meyer, A., Goldie, K.N., et al. (2019). Lewy pathology in Parkinson's disease consists of crowded organelles and lipid membranes. Nat Neurosci *22*, 1099–1109.

Sharon, R., Goldberg, M.S., Bar-Joseph, I., Betensky, R.A., Jie, S., and Selkoe, D.J. (2001). a-Synuclein occurs in lipid-rich high molecular weight complexes, binds fatty acids, and shows homology to the fatty acid-binding proteins. PNAS.

Sharon, R., Bar-Joseph, I., Mirick, G.E., Serhan, C.N., and Selkoe, D.J. (2003). Altered Fatty Acid Composition of Dopaminergic Neurons Expressing -Synuclein and Human Brains with -Synucleinopathies. Journal of Biological Chemistry *278*, 49874–49881.

Shimabukuro, M.K., Langhi, L.G.P., Cordeiro, I., Brito, J.M., Batista, C.M. de C., Mattson, M.P., and Mello Coelho, V. de (2016). Lipid-laden cells differentially distributed in the aging brain are functionally active and correspond to distinct phenotypes. Sci Rep *6*, 23795.

Siddiqui, I.J., Pervaiz, N., and Abbasi, A.A. (2016). The Parkinson Disease gene SNCA: Evolutionary and structural insights with pathological implication. Scientific Reports *6*, 24475.

Singh, R., Kaushik, S., Wang, Y., Xiang, Y., Novak, I., Komatsu, M., Tanaka, K., Cuervo, A.M., and Czaja, M.J. (2009). Autophagy regulates lipid metabolism. Nature *458*, 1131–1135.

Singleton, A.B., Farrer, M., Johnson, J., Singleton, A., Hague, S., Kachergus, J., Hulihan, M., Peuralinna, T., Dutra, A., Nussbaum, R., et al. (2003). alpha-Synuclein locus triplication causes Parkinson's disease. Science (New York, N.Y.) *302*, 841.

Skinner, J.R., Shew, T.M., Schwartz, D.M., Tzekov, A., Lepus, C.M., Abumrad, N.A., and Wolins, N.E. (2009). Diacylglycerol enrichment of endoplasmic reticulum or lipid droplets recruits perilipin 3/TIP47 during lipid storage and mobilization. J Biol Chem *284*, 30941–30948.

Soste, M., Charmpi, K., Lampert, F., Gerez, J.A., Oostrum, M. van, Malinovska, L., Boersema,

P.J., Prymaczok, N.C., Riek, R., Peter, M., et al. (2019). Proteomics-Based Monitoring of Pathway Activity Reveals that Blocking Diacylglycerol Biosynthesis Rescues from Alpha-Synuclein Toxicity. Cels *9*, 309-320.e8.

Spillantini, M.G., Schmidt, M.L., Lee, V.M.-Y., Trojanowski, J.Q., Jakes, R., and Goedert, M. (1997). α-Synuclein in Lewy bodies. Nature *388*, 839–840.

Spillantini, M.G., Crowther, R.A., Jakes, R., Hasegawa, M., and Goedert, M. (1998). alpha-Synuclein in filamentous inclusions of Lewy bodies from Parkinson's disease and dementia with lewy bodies. Proc Natl Acad Sci U S A *95*, 6469–6473.

Stewart, B.A., Atwood, H.L., Renger, J.J., Wang, J., and Wu, C.F. (1994). Improved stability of Drosophila larval neuromuscular preparations in haemolymph-like physiological solutions. J. Comp. Physiol. A *175*, 179–191.

Surguchov, A. (2008). Molecular and cellular biology of synucleins. Int Rev Cell Mol Biol *270*, 225–317.

Suzuki, M., Fujikake, N., Takeuchi, T., Kohyama-Koganeya, A., Nakajima, K., Hirabayashi, Y., Wada, K., and Nagai, Y. (2015). Glucocerebrosidase deficiency accelerates the accumulation of proteinase K-resistant α-synuclein and aggravates neurodegeneration in a *Drosophila* model of Parkinson's disease. Human Molecular Genetics *24*, 6675–6686.

Sztalryd, C., Xu, G., Dorward, H., Tansey, J.T., Contreras, J.A., Kimmel, A.R., and Londos, C. (2003). Perilipin A is essential for the translocation of hormone-sensitive lipase during lipolytic activation. The Journal of Cell Biology *161*, 1093–1103.

Takeuchi, K., and Reue, K. (2009). Biochemistry, physiology, and genetics of GPAT, AGPAT, and lipin enzymes in triglyceride synthesis. Am. J. Physiol. Endocrinol. Metab. *296*, E1195-1209.

Tanner, C.M., Kamel, F., Ross, G.W., Hoppin, J.A., Goldman, S.M., Korell, M., Marras, C., Bhudhikanok, G.S., Kasten, M., Chade, A.R., et al. (2011). Rotenone, paraquat, and Parkinson's disease. Environmental Health Perspectives *119*, 866–872.

Tansey, J.T., Sztalryd, C., Gruia-Gray, J., Roush, D.L., Zee, J.V., Gavrilova, O., Reitman, M.L., Deng, C.X., Li, C., Kimmel, A.R., et al. (2001). Perilipin ablation results in a lean mouse with aberrant adipocyte lipolysis, enhanced leptin production, and resistance to diet-induced obesity. Proc. Natl. Acad. Sci. U.S.A. *98*, 6494–6499.

Teixeira, L., Rabouille, C., Rørth, P., Ephrussi, A., and Vanzo, N.F. (2003). Drosophila Perilipin/ADRP homologue Lsd2 regulates lipid metabolism. Mech. Dev. *120*, 1071–1081.

Thakur, R., Panda, A., Coessens, E., Raj, N., Yadav, S., Balakrishnan, S., Zhang, Q., Georgiev, P., Basak, B., Pasricha, R., et al. (2016). Phospholipase D activity couples plasma membrane endocytosis with retromer dependent recycling. ELife *5*, e18515.

Thiam, A.R., and Beller, M. (2017). The why, when and how of lipid droplet diversity. J. Cell. Sci. *130*, 315–324.

Thiam, A.R., and Dugail, I. (2019). Lipid droplet-membrane contact sites - from protein binding to function. J. Cell. Sci. *132*.

Thiam, A.R., Antonny, B., Wang, J., Delacotte, J., Wilfling, F., Walther, T.C., Beck, R., Rothman, J.E., and Pincet, F. (2013a). COPI buds 60-nm lipid droplets from reconstituted water–

phospholipid–triacylglyceride interfaces, suggesting a tension clamp function. Proc Natl Acad Sci U S A *110*, 13244–13249.

Thiam, A.R., Farese, R.V., and Walther, T.C. (2013b). The biophysics and cell biology of lipid droplets. Nat. Rev. Mol. Cell Biol. *14*, 775–786.

Thul, P.J., Tschapalda, K., Kolkhof, P., Thiam, A.R., Oberer, M., and Beller, M. (2017). Targeting of the Drosophila protein CG2254/Ldsdh1 to a subset of lipid droplets. J Cell Sci *130*, 3141–3157.

Tian, Y., Bi, J., Shui, G., Liu, Z., Xiang, Y., Liu, Y., Wenk, M.R., Yang, H., and Huang, X. (2011). Tissue-autonomous function of Drosophila seipin in preventing ectopic lipid droplet formation. PLoS Genetics *7*, e1001364.

Tofaris, G.K., Garcia Reitböck, P., Humby, T., Lambourne, S.L., O'Connell, M., Ghetti, B., Gossage, H., Emson, P.C., Wilkinson, L.S., Goedert, M., et al. (2006). Pathological changes in dopaminergic nerve cells of the substantia nigra and olfactory bulb in mice transgenic for truncated human alpha-synuclein(1-120): implications for Lewy body disorders. J Neurosci *26*, 3942–3950.

Tu, P.H., Galvin, J.E., Baba, M., Giasson, B., Tomita, T., Leight, S., Nakajo, S., Iwatsubo, T., Trojanowski, J.Q., and Lee, V.M. (1998). Glial cytoplasmic inclusions in white matter oligodendrocytes of multiple system atrophy brains contain insoluble alpha-synuclein. Ann Neurol *44*, 415–422.

Ugrankar, R., Bowerman, J., Hariri, H., Chandra, M., Chen, K., Bossanyi, M.-F., Datta, S., Rogers, S., Eckert, K.M., Vale, G., et al. (2019). Drosophila Snazarus Regulates a Lipid Droplet Population at Plasma Membrane-Droplet Contacts in Adipocytes. Dev. Cell *50*, 557-572.e5.

Unger, R.H., Clark, G.O., Scherer, P.E., and Orci, L. (2010). Lipid homeostasis, lipotoxicity and the metabolic syndrome. Biochim. Biophys. Acta *1801*, 209–214.

Vacaru, A.M., van den Dikkenberg, J., Ternes, P., and Holthuis, J.C.M. (2013). Ceramide phosphoethanolamine biosynthesis in Drosophila is mediated by a unique ethanolamine phosphotransferase in the Golgi lumen. The Journal of Biological Chemistry *288*, 11520–11530.

Valm, A.M., Cohen, S., Legant, W.R., Melunis, J., Hershberg, U., Wait, E., Cohen, A.R., Davidson, M.W., Betzig, E., and Lippincott-Schwartz, J. (2017). Applying systems-level spectral imaging and analysis to reveal the organelle interactome. Nature *546*, 162–167.

Van Den Brink, D.M., Cubizolle, A., Chatelain, G., Davoust, N., Girard, V., Johansen, S., Napoletano, F., Dourlen, P., Guillou, L., Angebault-Prouteau, C., et al. (2018). Physiological and pathological roles of FATP-mediated lipid droplets in Drosophila and mice retina. PLOS Genetics *14*, e1007627.

Verghese, P.B., Castellano, J.M., and Holtzman, D.M. (2011). Apolipoprotein E in Alzheimer's disease and other neurological disorders. The Lancet. Neurology *10*, 241–252.

Vevea, J.D., Garcia, E.J., Chan, R.B., Zhou, B., Schultz, M., Di Paolo, G., McCaffery, J.M., and Pon, L.A. (2015). Role for lipid droplet biogenesis and microlipophagy in adaptation to lipid imbalance in yeast. Dev Cell *35*, 584–599.

Volkenhoff, A., Weiler, A., Letzel, M., Stehling, M., Klämbt, C., and Schirmeier, S. (2015). Glial Glycolysis Is Essential for Neuronal Survival in Drosophila. Cell Metabolism *22*, 437–

447.

Volles, M.J., and Lansbury, P.T. (2007). Relationships between the sequence of alpha-synuclein and its membrane affinity, fibrillization propensity, and yeast toxicity. Journal of Molecular Biology *366*, 1510–1522.

Volmer, R., and Ron, D. (2015). Lipid-dependent regulation of the unfolded protein response. Current Opinion in Cell Biology *33*, 67–73.

Vonk, J.J., Yeshaw, W.M., Pinto, F., Faber, A.I.E., Lahaye, L.L., Kanon, B., van der Zwaag, M., Velayos-Baeza, A., Freire, R., van IJzendoorn, S.C., et al. (2017). Drosophila Vps13 Is Required for Protein Homeostasis in the Brain. PLoS ONE *12*, e0170106.

Wang, H., and Eckel, R.H. (2014). What are Lipoproteins doing in the Brain? Trends Endocrinol Metab *25*, 8–14.

Wang, D., Qian, L., Xiong, H., Liu, J., Neckameyer, W.S., Oldham, S., Xia, K., Wang, J., Bodmer, R., and Zhang, Z. (2006). Antioxidants protect PINK1-dependent dopaminergic neurons in Drosophila. Proc Natl Acad Sci U S A *103*, 13520–13525.

Wang, G.J., Kang, L., Kim, J.E., Maro, G.S., Xu, X.Z.S., and Shen, K. (2010). GRLD-1 regulates cell-wide abundance of glutamate receptor through post-transcriptional regulation. Nat Neurosci *13*, 1489–1495.

Wang, H., Hu, L., Dalen, K., Dorward, H., Marcinkiewicz, A., Russell, D., Gong, D., Londos, C., Yamaguchi, T., Holm, C., et al. (2009). Activation of Hormone-sensitive Lipase Requires Two Steps, Protein Phosphorylation and Binding to the PAT-1 Domain of Lipid Droplet Coat Proteins. J. Biol. Chem. *284*, 32116–32125.

Wang, H., Sreenivasan, U., Sreenevasan, U., Hu, H., Saladino, A., Polster, B.M., Lund, L.M., Gong, D., Stanley, W.C., and Sztalryd, C. (2011a). Perilipin 5, a lipid droplet-associated protein, provides physical and metabolic linkage to mitochondria. J. Lipid Res. *52*, 2159–2168.

Wang, H., Zhang, J., Qiu, W., Han, G.-S., Carman, G.M., and Adeli, K. (2011b). Lipin-1γ isoform is a novel lipid droplet-associated protein highly expressed in the brain. FEBS Lett. *585*, 1979–1984.

Wang, H., Becuwe, M., Housden, B.E., Chitraju, C., Porras, A.J., Graham, M.M., Liu, X.N., Thiam, A.R., Savage, D.B., Agarwal, A.K., et al. (2016). Seipin is required for converting nascent to mature lipid droplets. Elife *5*.

Wang, L., Hong, J., Wu, Y., Liu, G., Yu, W., and Chen, L. (2018). Seipin deficiency in mice causes loss of dopaminergic neurons via aggregation and phosphorylation of α-synuclein and neuroinflammation. Cell Death Dis *9*, 440.

Wang, S., Horn, P.J., Liou, L.-C., Muggeridge, M.I., Zhang, Z., Chapman, K.D., and Witt, S.N. (2013). A peroxisome biogenesis deficiency prevents the binding of alpha-synuclein to lipid droplets in lipid-loaded yeast. Biochemical and Biophysical Research Communications *438*, 452–456.

Wang, X., Becker, K., Levine, N., Zhang, M., Lieberman, A.P., Moore, D.J., and Ma, J. (2019). Pathogenic alpha-synuclein aggregates preferentially bind to mitochondria and affect cellular respiration. Acta Neuropathologica Communications *7*, 41.

Wanneveich, M., Moisan, F., Jacqmin-Gadda, H., Elbaz, A., and Joly, P. (2018). Projections of prevalence, lifetime risk, and life expectancy of Parkinson's disease (2010-2030) in France. Movement Disorders *33*, 1449–1455.

Weiler, A., Volkenhoff, A., Hertenstein, H., and Schirmeier, S. (2017). Metabolite transport across the mammalian and insect brain diffusion barriers. Neurobiol. Dis. *107*, 15–31.

Welte, M.A., and Gould, A.P. (2017). Lipid droplet functions beyond energy storage. Biochim Biophys Acta *1862*, 1260–1272.

Welte, M.A., Gross, S.P., Postner, M., Block, S.M., and Wieschaus, E.F. (1998). Developmental Regulation of Vesicle Transport in Drosophila Embryos: Forces and Kinetics. Cell *92*, 547–557.

Welte, M.A., Cermelli, S., Griner, J., Viera, A., Guo, Y., Kim, D.-H., Gindhart, J.G., and Gross, S.P. (2005). Regulation of lipid-droplet transport by the perilipin homolog LSD2. Curr. Biol. *15*, 1266–1275.

Wilfling, F., Wang, H., Haas, J.T., Krahmer, N., Gould, T.J., Uchida, A., Cheng, J.-X., Graham, M., Christiano, R., Fröhlich, F., et al. (2013). Triacylglycerol Synthesis Enzymes Mediate Lipid Droplet Growth by Relocalizing from the ER to Lipid Droplets. Developmental Cell *24*, 384–399.

Windpassinger, C., Auer-Grumbach, M., Irobi, J., Patel, H., Petek, E., Hörl, G., Malli, R., Reed, J.A., Dierick, I., Verpoorten, N., et al. (2004). Heterozygous missense mutations in BSCL2 are associated with distal hereditary motor neuropathy and Silver syndrome. Nature Genetics *36*, 271–276.

Wolins, N.E., Skinner, J.R., Schoenfish, M.J., Tzekov, A., Bensch, K.G., and Bickel, P.E. (2003). Adipocyte protein S3-12 coats nascent lipid droplets. The Journal of Biological Chemistry *278*, 37713–37721.

Xu, N., Zhang, S.O., Cole, R.A., McKinney, S.A., Guo, F., Haas, J.T., Bobba, S., Farese, R.V., and Mak, H.Y. (2012). The FATP1-DGAT2 complex facilitates lipid droplet expansion at the ER-lipid droplet interface. The Journal of Cell Biology *198*, 895–911.

Yamaguchi, T., Omatsu, N., Omukae, A., and Osumi, T. (2006). Analysis of interaction partners for perilipin and ADRP on lipid droplets. Mol Cell Biochem *284*, 167–173.

Yan, Y., Wang, H., Hu, M., Jiang, L., Wang, Y., Liu, P., Liang, X., Liu, J., Li, C., Lindström-Battle, A., et al. (2017). HDAC6 Suppresses Age-Dependent Ectopic Fat Accumulation by Maintaining the Proteostasis of PLIN2 in Drosophila. Developmental Cell *43*, 99-111.e5.

Yang, W., Hamilton, J.L., Kopil, C., Beck, J.C., Tanner, C.M., Albin, R.L., Ray Dorsey, E., Dahodwala, N., Cintina, I., Hogan, P., et al. (2020). Current and projected future economic burden of Parkinson's disease in the U.S. NPJ Parkinson's Disease *6*, 15.

Yang, Y., Gehrke, S., Imai, Y., Huang, Z., Ouyang, Y., Wang, J.-W., Yang, L., Beal, M.F., Vogel, H., and Lu, B. (2006). Mitochondrial pathology and muscle and dopaminergic neuron degeneration caused by inactivation of Drosophila Pink1 is rescued by Parkin. Proc Natl Acad Sci U S A *103*, 10793–10798.

Yellen, G. (2018). Fueling thought: Management of glycolysis and oxidative phosphorylation in neuronal metabolism. J. Cell Biol. *217*, 2235–2246.

Yeshaw, W.M., van der Zwaag, M., Pinto, F., Lahaye, L.L., Faber, A.I., Gómez-Sánchez, R., Dolga, A.M., Poland, C., Monaco, A.P., van IJzendoorn, S.C., et al. (2019). Human VPS13A is associated with multiple organelles and influences mitochondrial morphology and lipid droplet motility. Elife *8*.

Yu, Y.V., Li, Z., Rizzo, N.P., Einstein, J., and Welte, M.A. (2011). Targeting the motor regulator Klar to lipid droplets. BMC Cell Biol. *12*, 9.

Zechner, R., Zimmermann, R., Eichmann, T.O., Kohlwein, S.D., Haemmerle, G., Lass, A., and Madeo, F. (2012). FAT SIGNALS--lipases and lipolysis in lipid metabolism and signaling. Cell Metab. *15*, 279–291.

Zhang, X., Saarinen, A.M., Hitosugi, T., Wang, Z., Wang, L., Ho, T.H., and Liu, J. (2017). Inhibition of intracellular lipolysis promotes human cancer cell adaptation to hypoxia. ELife *6*, e31132.

APPENDIX: ADDITIONAL PAPER

1. Physiological and pathological roles of FATP-mediated lipid droplets in *Drosophila* and mice retina

At the time when I integrated Bertrand Mollereau's research team, former members of the team had identified *Drosophila* Fatp (dFatp), as an important regulator of photoreceptor survival (Dourlen et al., 2012). FATP, predominantly known to be involved in fatty acid activation and can form a complex with DGAT2 to facilitate the expansion of LDs in *C. elegans* (Dourlen et al., 2015; Xu et al., 2012). In 2015, Liu et al. showed that *Drosophila* retina glial cells accumulate LDs in condition of oxidative stress, but whether dFatp was important for this process was not known at the time (Liu et al., 2015). The team thus started to investigate whether dFatp is involved in LD formation in the retina. Importantly, we found that LD accumulation naturally occurred in both retina glial cells and to a lesser extend in photoreceptor neurons in young flies. Moreover, knockdown of *dFatp* in retina glial cells prevented physiological but also oxidative stress-induced LD accumulation. Finally, loss of dFatp in retina glial cells alone, led to progressive photoreceptor degeneration while overexpression of dFatp had no effect. Working as a part of this project helped me learn the technics of LD staining and *Drosophila* retina dissection, that will later be used extensively for my thesis projects.

PLOS GENETICS

RESEARCH ARTICLE

Physiological and pathological roles of *FATP*-mediated lipid droplets in *Drosophila* and mice retina

Daan M. Van Den Brink[1☯], Aurélie Cubizolle[2,3☯], Gilles Chatelain[1], Nathalie Davoust[1], Victor Girard[1], Simone Johansen[1], Francesco Napoletano[4], Pierre Dourlen[5], Laurent Guillou[2,3], Claire Angebault-Prouteau[2,6], Nathalie Bernoud-Hubac[7], Michel Guichardant[7], Philippe Brabet[2,3], Bertrand Mollereau[1]*

1 Université de Lyon, ENSL, UCBL, CNRS, LBMC, UMS 3444 Biosciences Lyon Gerland, Lyon, France, **2** Institut des Neurosciences de Montpellier, INSERM U1051, CHU St Eloi, Montpellier, France, **3** Université de Montpellier, Montpellier, France, **4** Molecular Oncology Unit, Department of Life Sciences, University of Trieste c/o Laboratorio Nazionale CIB, Area Science Park, Trieste, Italy, **5** Institut Pasteur de Lille; Inserm, U1167, RID-AGE-Risk Factors and Molecular Determinants of Aging-Related Diseases; University Lille, U1167-Excellence Laboratory LabEx DISTALZ, Lille, France, **6** INSERM U1046, UMR CNRS 9214, Université de Montpellier, CHRU de Montpellier, Montpellier, France, **7** Univ Lyon, CarMeN laboratory, INSA Lyon, INSERM U1060, INRA U1397, Université Claude Bernard Lyon 1, F-69621, Villeurbanne, France

☯ These authors contributed equally to this work.
* bertrand.mollereau@ens-lyon.fr

OPEN ACCESS

Citation: Van Den Brink DM, Cubizolle A, Chatelain G, Davoust N, Girard V, Johansen S, et al. (2018) Physiological and pathological roles of *FATP*-mediated lipid droplets in *Drosophila* and mice retina. PLoS Genet 14(9): e1007627. https://doi.org/10.1371/journal.pgen.1007627

Editor: Jason M Tennessen, Indiana University, UNITED STATES

Received: December 20, 2017

Accepted: August 13, 2018

Published: September 10, 2018

Data Availability Statement: All relevant data are within the paper and its Supporting Information files.

Funding: This work was supported by the French National Research Agency award ANR-12-BSV1-0019-02 to BM, PB, DMVDB, and AC and by a postdoctoral fellowship to FN from the Association Française contre les Myopathies, a European Union's Seventh Framework Programme/AIRC (Associazione Italiana per la Ricerca sul cancro) Reintegration Grant. The funders had no role in

Abstract

Increasing evidence suggests that dysregulation of lipid metabolism is associated with neurodegeneration in retinal diseases such as age-related macular degeneration and in brain disorders such as Alzheimer's and Parkinson's diseases. Lipid storage organelles (lipid droplets, LDs), accumulate in many cell types in response to stress, and it is now clear that LDs function not only as lipid stores but also as dynamic regulators of the stress response. However, whether these LDs are always protective or can also be deleterious to the cell is unknown. Here, we investigated the consequences of LD accumulation on retinal cell homeostasis under physiological and stress conditions in *Drosophila* and in mice. In wild-type *Drosophila*, we show that *dFatp* is required and sufficient for expansion of LD size in retinal pigment cells (RPCs) and that LDs in RPCs are required for photoreceptor survival during aging. Similarly, in mice, LD accumulation induced by RPC-specific expression of human *FATP1* was non-toxic and promoted mitochondrial energy metabolism in RPCs and non-autonomously in photoreceptor cells. In contrast, the inhibition of LD accumulation by *dFatp* knockdown suppressed neurodegeneration in *Aats-met*^{FB} *Drosophila* mutants, which carry elevated levels of reactive oxygen species (ROS). This suggests that abnormal turnover of LD may be toxic for photoreceptors cells of the retina under oxidative stress. Collectively, these findings indicate that *FATP*-mediated LD formation in RPCs promotes RPC and neuronal homeostasis under physiological conditions but could be deleterious for the photoreceptors under pathological conditions.

study design, data collection and analysis, decision to publish, or preparation of the manuscript.

Competing interests: The authors have declared that no competing interests exist.

Author summary

Lipids are major cell constituents and are present in the membranes, as free lipids in the cytoplasm, or stored in vesicles called lipid droplets (LDs). Under conditions of stress, lipids stored in LDs can be released to serve as substrates for energy metabolism by mitochondria. However, lipid storage is dysregulated in many degenerative disorders such as age-related macular degeneration, Parkinson's and Alzheimer's diseases. Thus, it is unclear whether accumulation of LDs is protective or toxic for neuronal cells. To address this question, we examined the consequences of removal or enforced LD accumulation on the health of retinal cells in flies and mice. Like humans, fly and mouse retinas contain retinal pigment cells (RPC) that support the functions of neighboring photoreceptor cells. We found that overexpression of the fatty acid transport protein (FATP) in RPCs induced accumulation of LDs in both transgenic flies and mice. Moreover, LD accumulation in RPCs was not harmful for juxtaposed photoreceptors during aging, but was toxic under stress conditions. We propose that lipid storage promotes cellular communication that affects photoreceptor health.

Introduction

Photoreceptor neurons are among the highest energy consumers in the body. They are sustained by a layer of retinal pigment epithelial cells (here termed retinal pigment cells [RPC], S1 Fig) that provide photoreceptors with a constant supply of substrates for energy production by mitochondrial oxidation via the tricarboxylic acid (TCA) cycle. An inability of RPCs to perform this role leads to photoreceptor death and is associated with diseases such as age-related macular degeneration (AMD), the most prevalent cause of blindness in developed countries [1].

Injury to RPCs, whether through disease or as part of the normal aging process, is accompanied by an accumulation of lipid deposits, named drusen, in the RPC itself or in the adjacent Bruch's membrane [2–4]. A common cause of injury is reduced blood flow to the retina, which causes hypoxia and a subsequent metabolic shift that results in accumulation in RPCs of intracellular lipid droplets (LDs) composed of neutral lipids, such as triacylglycerides (TAGs) and sterol esters. In AMD, lipids are also deposited extracellularly, further compromising the functions of RPCs and photoreceptors [5]. However, it is not clear whether lipid accumulation is a cause or a consequence of AMD pathology.

Work in *Drosophila* models has contributed greatly to our understanding of the mechanisms of LD biosynthesis and physiological functions [6, 7]. For example, LDs have been shown to play an antioxidant role in the developing *Drosophila* nervous system by protecting polyunsaturated fatty acids from peroxidation under conditions of hypoxia [8]. In contrast, in *Drosophila* carrying mutations with mitochondrial dysfunction, oxidative stress induces glial cells to accumulate LDs that are toxic to the neighboring photoreceptor cells [9]. Thus, LDs are not simply cytoplasmic lipid storage organelles with critical roles in energy metabolism; they also have dynamic functions in regulating the response to stress of many cell types, including those in the nervous system [10–12].

LDs are synthesized on the endoplasmic reticulum membrane by a protein complex composed of diacylglycerol acyltransferase (DGAT-2) and fatty acid transport protein (FATP) [12, 13]. The FATP family (also known as solute carrier family 27 [SLC27]) [14, 15] are acyl-CoA synthetases involved in the cellular import of FAs [16] as well as other processes. FATPs interact physically and functionally with DGAT-2, an enzyme that catalyzes the conjugation of a

fatty acyl-CoA to diacyl glycerol to produce TAGs, which are then incorporated into expanding LDs in *C. elegans* [13]. An important role for *FATP* in TAG storage has also been demonstrated in mammals. In *Fatp1* knockout mice, the uptake of FA and the size of LDs in the brown adipose tissue are reduced compared with wild-type (WT) mice, resulting in defects in non-shivering thermogenesis [17]. The *FATP1* gene is conserved from yeast to humans, where there are six proteins with different tissue distributions and substrate preferences. *Drosophila Fatp* (*dFatp*) shows a high degree of sequence similarity to human (*h*)*FATP1* and *hFATP4*, which have broad expression profiles that include the brain and retina [16, 18, 19].

The *Drosophila* retina is composed of approximately 800 ommatidia, each of which comprises eight photoreceptors surrounded by a hexagonal lattice of nine RPCs (six secondary and three tertiary pigment cells, S1 Fig) [20]. *Drosophila* RPCs (dRPCs) differentiate during the pupal stage and superfluous cells are eliminated by apoptosis [21, 22]. The survival of dRPCs requires cues that are provided by cell-to-cell communication from neighboring cone and primary pigment cells during pupal development [23, 24]. In adult flies, dRPCs have similar functions to mammalian RPCs; that is, they are also juxtaposed to photoreceptor cells and supply metabolites for energy metabolism and other functions [25, 26, 27].

In *Drosophila*, *dFatp* is expressed in both photoreceptors and dRPCs [28], but its physiological role in LD formation in dRPCs and its impact on photoreceptor homeostasis remains to be investigated. Here, we examined the role of *FATP* in LDs formation and in cellular retinal homeostasis in *Drosophila* and in mice. We find that, although the architecture of the mammalian and insect retina are different, RPCs in both organisms play conserved roles in lipid and photoreceptor homeostasis. We show that *FATP* plays a crucial role in regulating LD production in RPCs and, in turn, RPC-derived LDs affect differentially photoreceptor viability in physiological and pathological conditions.

Results

dFatp is necessary and sufficient for LD expansion in *Drosophila* retina under physiological and pathological conditions

To investigate the role of *dFatp* in LD formation and expansion in WT flies and in flies overexpressing *dFatp* (using the pan-retinal *GMR-Gal4* driver), we first measured the uptake of BODIPY$^{500/510}$-C_{12}, a fluorescent long-chain FA analog. We observed an accumulation of LDs (visible as green foci) in the retina of 1-day old WT flies and this accumulation was greatly increased when *dFatp* was overexpressed (Fig 1Aa, 1Ab and 1C). Importantly, expression of *brummer*, a gene encoding a TAG lipase (referred to here as Bmm-lipase) [29], reduced BODIPY$^{500/510}$-C_{12} accumulation further demonstrating the lipid nature of the detected droplets in both WT and *dFatp*-overexpression conditions (Fig 1Ac, 1Ad and 1C). To overexpress *dFatp*, we also used the *54C-Gal4* driver, which was previously used as RPCs specific driver in several publications [9, 24, 27]. *dFatp* overexpression with the *54C* driver induced an important accumulation of LDs similar to the *GMR* driver (Fig 1Ae, 1Af and 1C). We verified the expression pattern of the *54C* driver (*54C-Gal4*, *UAS-GFP*) and confirmed that *54C* driver is strongly expressed in dRPCs (primary, secondary and tertiary pigment cells), although low levels of GFP expression were also observed in one or two photoreceptors per ommatidium, rarely in cone cells and not in bristle cells at 42h after puparium formation (APF) (S2A and S2B Fig). The developmental expression of the *54C* driver suggests that overexpression of *dFatp* during pupal development could account for the observed accumulation of LDs in adult fly retina. To confirm that the accumulation of LDs induced by *54C*-dependent overexpression of *dFatp* is truly RPC specific, we concomitantly expressed *Gal80* the inhibitor of *Gal4* with *Repo*, a panglial driver that is expressed in RPCs [30]. *Repo-Gal80* completely abolished the accumulation

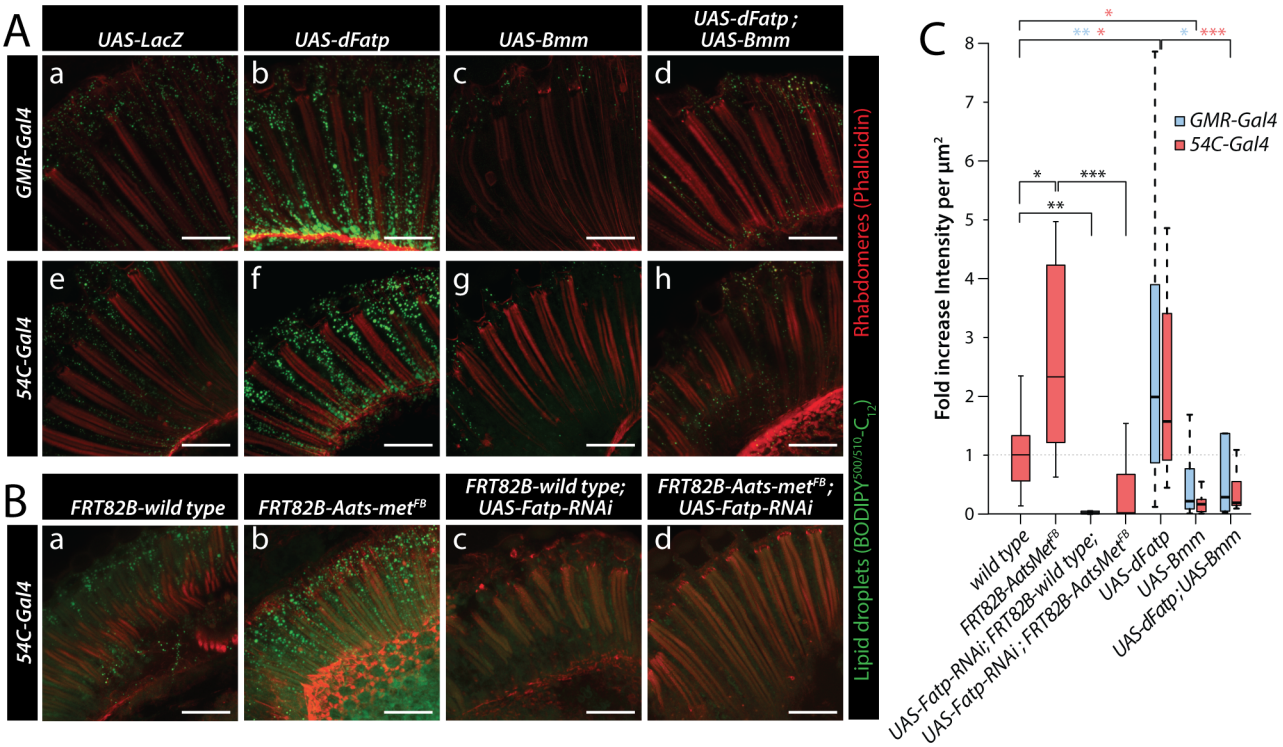

Fig 1. *dFatp* is required for lipid storage in *Drosophila* retina. (**A**) LD labeled with BODIPY$^{500/510}$-C_{12} (green) were revealed using confocal microscopy in horizontal sections of whole mount retinas from one-day-old flies expressing *UAS-LacZ* (control), *UAS-dFatp* and/or *UAS-Bmm-lipase* under the control of a pan-retinal (*GMR-Gal4*) (a–d) or a dRPC-specific (*54C-Gal4*) (e–h) driver. Photoreceptors were counterstained with phalloidin-rhodamine (red). (**B**) BODIPY$^{500/510}$-C_{12} (green) uptake in horizontal sections of whole eye wild-type (FRT82B-wild-type) and mutant (FRT82B-Aats-met^{FB}) clone generated with the GMR-hid/FLP-FRT technique [49] from one-day-old flies in the absence (a, b) or presence of dRPC-specific (driven by *54C-Gal4*) *UAS-dFatp*-RNAi$^{[GD16442]}$ (c, d). Photoreceptors were counterstained with phalloidin-rhodamine (red). Scale bar, 25 µm. (**C**) Quantification of BODIPY$^{500/510}$-C_{12} uptake into lipid droplets from the images shown in (A) and (B). Data are presented as the fold change in fluorescence intensity (dots/µm^2) compared with the FRT82B-wild-type flies. The boxes represent the median and lower and upper quartiles, and the whiskers represent the 1.5 interquartile range. N = 6–41 retinas per condition. Blue and red statistical stars indicate significant differences between wild type and retina overexpressing *dFatp* or *Bmm* with *GMR-Gal4* or *54C-Gal4*, respectively. Log adjusted values: $^{*}p<0.05$, $^{**}p<0.01$, $^{***}p<0.001$ by Tukey's HSD paired sample comparison test.

https://doi.org/10.1371/journal.pgen.1007627.g001

of BODIPY$^{493/503}$ induced by the overexpression of *dFatp* with the *54C* driver (*54C-Gal4*, *UAS-dFatp*) confirming that the induction of LD by *54C* is RPC-specific (S2C and S2D Fig). In this experiment, we used the lipophilic probe BODIPY$^{493/503}$ on fixed tissue instead of the BODIPY$^{500/510}$-C_{12} on live tissue. Because we see increased *dFatp*-induced BODIPY staining in both cases (compare Fig 1Ae and 1Af with S2Ca and S2Cb Fig), this shows that *dFatp* overexpression mediates both the active uptake of BODIPY$^{500/510}$-C_{12} into LD (Fig 1A) and the increase total LD stores revealed with BODIPY$^{493/503}$. Similar to the *GMR* driver, the accumulation of BODIPY$^{500/510}$-C_{12}, induced by overexpression of *dFatp* with the *54C* driver was suppressed by *Bmm-lipase* concomitant overexpression (Fig 1Ag, 1Ah and 1C). We finally examined if the accumulation of LD due to *dFatp* expression requires Vitamin A, a precursor of retinal that is important for *dFatp* function in the regulation of Rh1 in photoreceptors [28]. As previously shown, we observed that the Vitamin A-deficient diet rescued photoreceptor degeneration in *dFatp* whole eye mutant clone ([28] and S3A Fig), but that the accumulation of LD induced by *dFatp* did not require Vitamin A (S3B and S3C Fig). This result suggests *dFatp* functions in LD biogenesis and in Vitamin A-dependent regulation of Rh1 are two distinct processes.

We then examined the requirement of *dFatp* in LD accumulation in retina of WT and *Aats-met*^{FB} mutant flies, which accumulate LD due to high mitochondrial ROS levels. As previously observed [9], BODIPY$^{500/510}$-C_{12} uptake into LDs was increased in the *Aats-met*^{FB} mutant compared with the WT retina (Fig 1Ba, 1Bb and 1C). Expression of *dFatp*-specific dsRNA (RNAi) with the *54C-Gal4* driver abolished BODIPY$^{500/510}$-C_{12} uptake in the WT flies and strongly reduced it in the *Aats-met*^{FB} mutants (Fig 1Bc, 1Bd and 1C). Furthermore, BODIPY$^{500/510}$-C_{12} staining was completely abolished in *dFatp* whole eye mutant clones, confirming the specificity of *dFatp* dsRNA and the role of *dFatp* in LD formation (S3D Fig). Collectively, these data demonstrate that *dFatp* is necessary for LD accumulation in the *Drosophila* retina under physiological and pathological conditions.

To examine the subcellular localization of LDs in the retina, we performed transmission electron microscopy (TEM) of flies overexpressing *dFatp* using *GMR* or *54C* drivers. LDs were typically visible as homogeneous structures surrounded by a monolayer membrane in dRPCs and, to a much lesser extent, in photoreceptor cells (Fig 2A and 2B). Interestingly, *dFatp* overexpression significantly increased the size, but not the number, of LDs in both cell types (Fig 2A–2C). Finally, the expression *Bmm-lipase* with *54C-Gal4* caused a striking reduction in the number of LDs, not only in dRPCs but also in photoreceptors (Fig 2B and S4 Fig). This indicates that the monolayer membrane-encapsulated vesicles observed by TEM are indeed LDs.

The TEM images also indicated the expansion of LDs induced by *dFatp* overexpression concomitantly caused a significant decrease in the size of mitochondria in the photoreceptors (Fig 2D). We confirm that this reduction of mitochondrial size was correlated with LDs accumulation in a *dFatp*-dependent manner since co-expression of *dFatp* and *Bmm-lipase* prevented the decrease in photoreceptor mitochondrial size compared with expression of *dFatp* alone (Fig 2D). Notably, despite the reduction in size, the morphological integrity of mitochondria was preserved, suggesting that their function may remain intact and that accumulation of LD is not toxic to photoreceptors. Collectively, these results show modulating LD levels by increasing LD biogenesis (*54C>dFatp*) or LD lipolysis (*54C>Bmm*) in dRPCs affects LD and mitochondrial sizes in photoreceptor cells.

Evidence of vesicle transfer from RPCs to photoreceptors

TEM images of retina showed various stages suggestive of the transfer of vesicles from dRPCs to photoreceptors in both wild-type and retina overexpressing *dFatp* with the *54C* driver. Vesicles can be seen within the dRPCs (i), in the process of being internalized into the photoreceptor by a process resembling endocytosis (ii), and fully internalized into the photoreceptor, where they appear surrounded by a double membrane (iii) (Fig 3). These vesicles were comparable in size to LDs (~0.25 μm^2) but appeared slightly more electron dense. Due to their double membrane and localization at the proximity of the plasma membrane, these vesicles were distinguished from LD present in the cytoplasm of photoreceptors. These vesicles were seen juxtaposed to one or more mitochondria, which suggests that they contribute to or benefit from mitochondrial energetic function (Fig 3A and 3A'). These results suggest that the non-autonomous transfer of material contributes to the relay of information between dRPCs and photoreceptors.

Expression of *hFATP1* in mRPC increases lipid storage and energy metabolism in the mouse retina

To determine whether the function of *dFatp* is conserved, we first asked whether the loss of photoreceptor cells observed in *dFatp*$^{-/-}$ mutant retinas [28], could be rescued by the expression of the human homolog *hFATP1* in *Drosophila*. Indeed, photoreceptor-specific expression

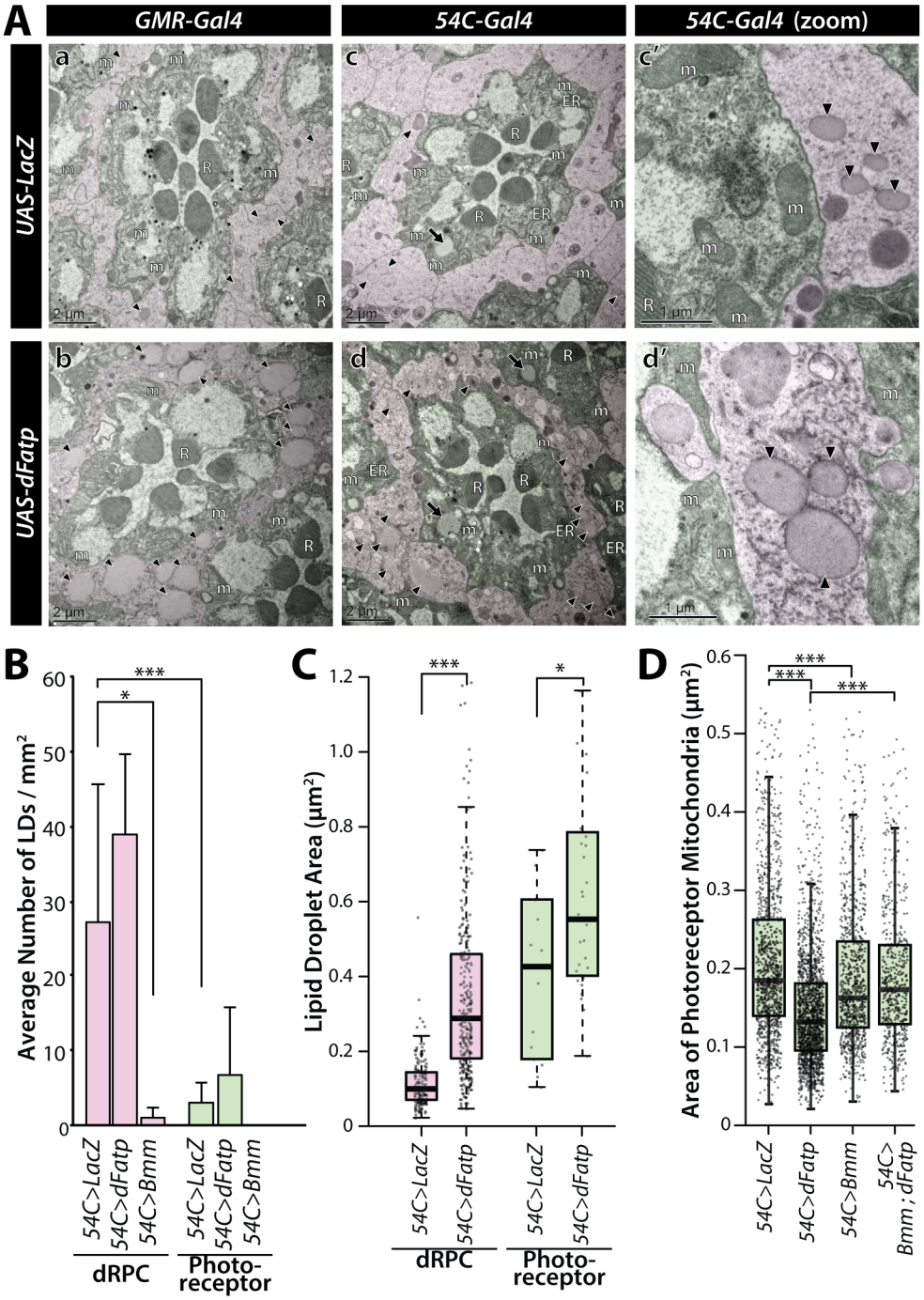

Fig 2. Lipid droplets are mainly localized in dRPCs and are increased by *dFatp* overexpression in *Drosophila* retinas. (**A**) TEM of ommatidia from one-day-old flies expressing *UAS-LacZ* (control) or *UAS-dFatp* under control of the pan-retinal (*GMR-Gal4*) or dRPC-specific (*54C-Gal4*) drivers. One ommatidium in each panel shows seven photoreceptors (false colored green) with central rhabdomeres surrounded by dRPCs (false colored pink). Lipid droplets are mainly located in dRPCs (black arrowheads) but can also be observed in photoreceptors (black arrows). Lipid droplet size was increased by *dFatp* overexpression (b, d, d') compared to control conditions (a, c, c'). Scale bars, 2 µm (a–d), 1 µm (c', d'). m, mitochondria; R rhabdomeres. (**B**) Quantification of lipid droplet density (number per surface area) in dRPCs and photoreceptors in flies with dRPC-specific expression (*54C-Gal4*) of *UAS-LacZ* (control), *UAS-dFatp*, or *UAS-Bmm-lipase*. Means ± SD of n = 4 eyes. (**C**) Quantification of lipid droplet size (area in m^2) in dRPCs of flies with dRPC-specific (*54C-Gal4*) expression of *UAS-LacZ* (control) or *UAS-dFatp*. (**D**) Mitochondrial size (area in m^2) in photoreceptors of flies with dRPC-specific expression of *UAS-LacZ* (control) or *UAS-dFatp*. The boxes

represent the median and lower and upper quartiles, and the whiskers represent the 1.5 interquartile range. N = 4 to 5 flies, from which we analyzed >150 fields of view. Log adjusted values: $^{*}p<0.05$, $^{***}p<0.001$ by Tukey's HSD paired sample comparison tests.

https://doi.org/10.1371/journal.pgen.1007627.g002

of *hFATP1* (driven by the rhodopsin 1 [*Rh1*] promoter) strongly reduced the loss of photoreceptors observed in *dFatp*$^{-/-}$ mutant retinas (S5 Fig). This result supports the conservation of *hFATP1* and *dFatp* function in retinal homeostasis. To investigate the role of *hFATP1* in lipid storage in the mammalian retina, we employed our previously described transgenic mice, in which *hFATP1* is overexpressed using the mammalian RPC-specific VDM2 promoter (referred to as *hFATP1TG* mice) [31]. LDs in the retinas of WT (C57BL/6J) and *hFATP1TG* (Fig 4A and 4B) mice were detected by staining of neutral lipids with Nile Red. Notably, transgenic expression of *hFATP1* significantly increased neutral lipid staining, visible as red foci, in the mRPCs of *hFATP1TG* mice compared with WT mice (Fig 4A–4C). Moreover, lipid profiling of dissected mRPCs by gas-chromatography revealed that levels of sterol esters and TAGs, both of which are components of LDs, were higher in the *hFATP1* mRPCs compared with WT mRPCs (Fig 4D). We also observed that Nile Red staining largely co-localized with perilipin, a

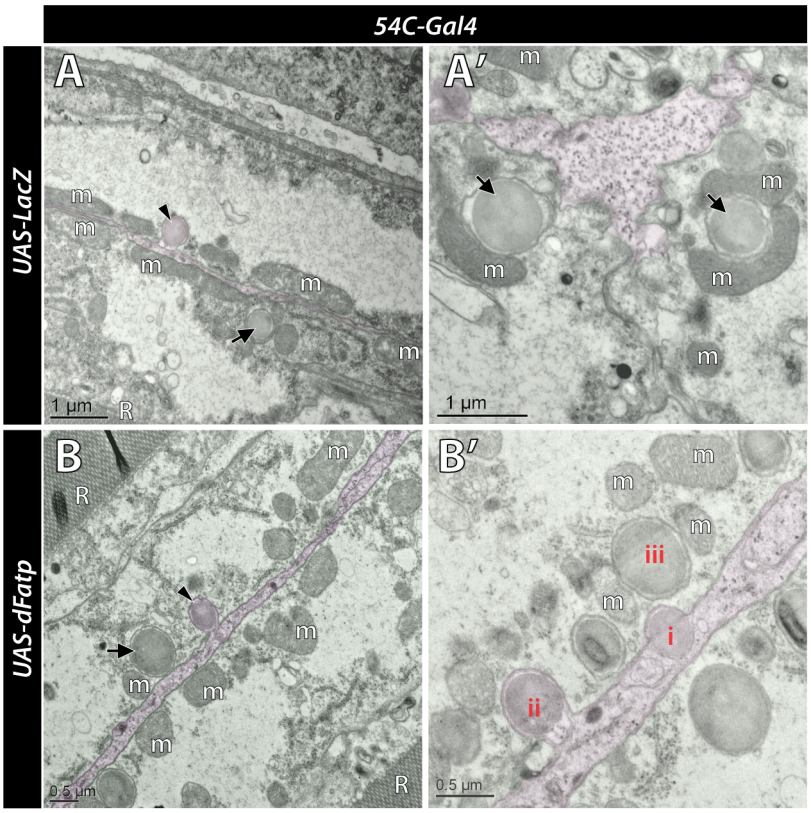

Fig 3. Transfer of vesicles from dRPCs to photoreceptors. Low (left) and high (right) magnification of retina tangential views visualized by TEM in one-day-old flies expressing (**A and A'**) *UAS-LacZ* or (**B and B'**) *UAS-dFatp* under the control of *54C-Gal4* driver. A dRPC (false colored pink) is visible sandwiched between two photoreceptors (false colored green). Arrowheads indicate lipid droplet-like vesicles entering an endocytotic invagination in the photoreceptor plasma membrane. Arrows indicate vesicles within photoreceptors surrounded by a double membrane. **(A')** shows vesicles in close association with mitochondria (m) in a photoreceptor. **(B')** shows various stages of the vesicle transfer from dRPC to photoreceptor. A vesicle within the dRPC (i) is taken up by the photoreceptor (ii), and surrounded by a double membrane once internalized within the photoreceptor (iii). Note the position of mitochondria (m) close to the vesicle. Scale bars, 1 µm (A and A') and 0.5 µm (B and B').

https://doi.org/10.1371/journal.pgen.1007627.g003

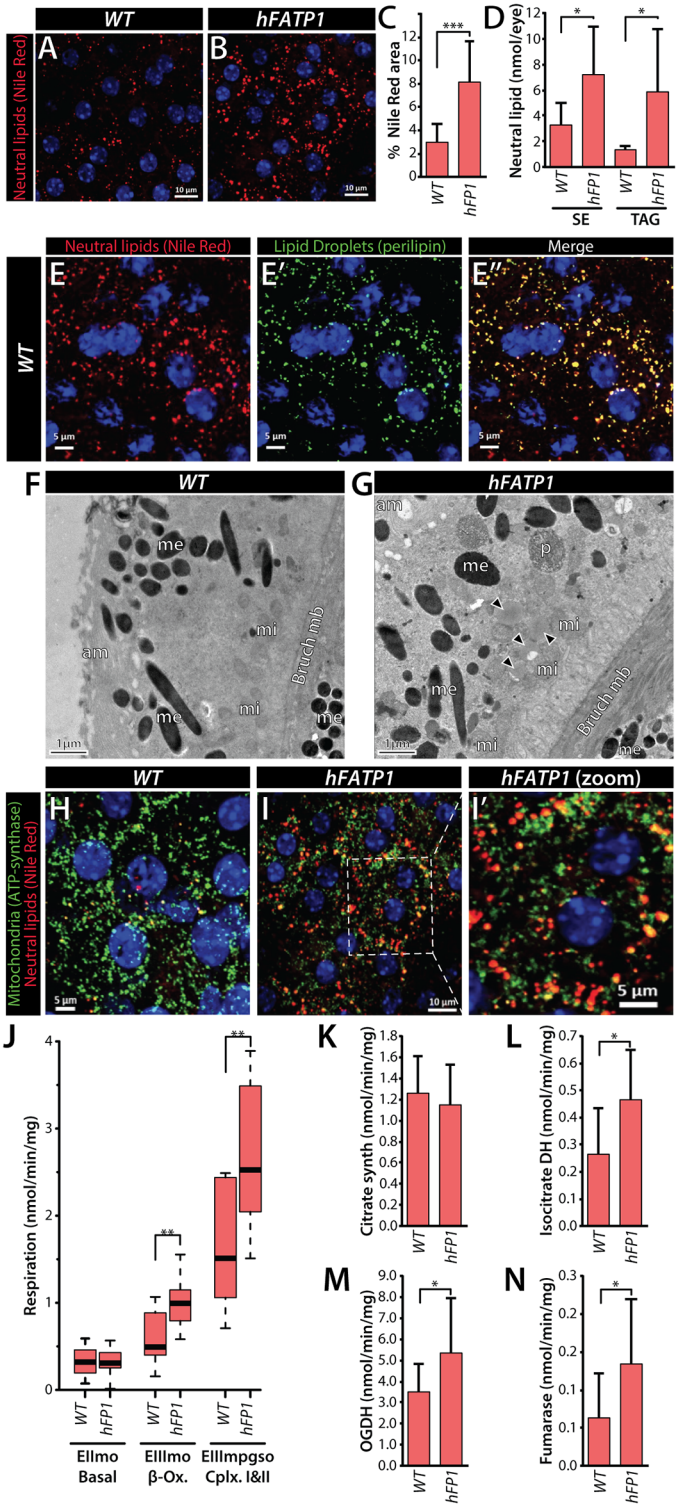

Fig 4. *hFATP1* overexpression in mouse RPCs increases neutral lipid accumulation and mitochondrial respiration. (**A, B**) Nile Red staining of neutral lipids (red) in mRPCs of a flat-mounted eye cup from wild-type (C57BL/6J) mice (**A**) and *hFATP1* transgenic mice (**B**). Nuclei are stained with DAPI (blue). Scale bars, 10 μm. (**C**) Quantification of Nile Red staining in wild-type (WT) and *hFATP1* transgenic (hFP1) mRPCs (as shown in A and B). Mean ± SD of n = 19 and 20 animals, respectively. (**D**) Quantification of sterol esters (SE) and triacylglycerides (TAG) in mRPCs from WT and *hFATP1* transgenic mice. Mean ± SD of n = 5 and 7 animals, respectively. (**E–E"**) mRPCs in

whole-mount retinas from WT mice double-stained with Nile Red (**E**) and anti-perilipin (green, **E'**). The merged image (**E"**) shows extensive overlap between Nile Red and perilipin stainings. Scale bars, 5 μm. (**F, G**) TEM images of mRPCs from wild-type (C57BL/6J) mice (**F**) and *hFATP1* transgenic mice (**G**). am: apical membrane, Bruch mb: Bruch membrane, me: melanosome, mi: mitochondria, p: phagosome. (**H–I'**) mRPCs in whole-mount retinas of WT (**H**) and *hFATP1* transgenic (**I, I'**) mice double-stained with Nile Red and anti-ATP synthase antibody (green, localized to mitochondria). (**I'**) Magnification of the box in (**I**) shows the juxtaposition of mitochondria and neutral lipid stores. Scale bars, 5 μm (**H, I'**), 10 μm (**I**). (**J**) Quantification of mitochondrial respiratory function (O_2 consumption) in RPCs isolated from WT and *hFATP1* transgenic mice. EIImo, basal respiratory rate; EIIImo, β-oxidation, EIIIMPGSO, global respiratory chain function of mitochondrial complexes I and II. The boxes represent the median and lower and upper quartiles, and the whiskers represent the 1.5 interquartile range. N = 21 and 10 WT and transgenic animals, respectively. (**K–N**) Activities of the TCA cycle enzymes, citrate synthase (**K**), isocitrate dehydrogenase (DH) (**L**), oxoglutarate dehydrogenase (OGDH) (**M**), and fumarase (**N**) in RPCs isolated from WT and *hFATP1* transgenic mice. Mean ± SD of n > 10 mice for each condition. $^{*}p<0.05$, $^{**}p<0.01$, $^{***}p<0.001$ for WT vs transgenic groups by two-sample t-test.

https://doi.org/10.1371/journal.pgen.1007627.g004

protein associated with LD membranes (Fig 4E–4E"), supporting the notion that the Nile Red-stained foci were indeed neutral lipid-containing LDs. The presence of LDs was also observed in mRPCs of *hFATP1TG* mice by TEM (Fig 4F and 4G). Taken together, these data indicate that *hFATP1* expression in mouse RPCs leads to accumulation of LDs, consistent with our findings in *Drosophila* RPCs.

Immunofluorescence staining for the mitochondrial marker ATP synthase revealed that LDs and mitochondria were in close proximity in the RPCs of both WT and *hFATP1TG* mice (Fig 4H–4I'), suggesting the possibility that LDs serve as an energy source in mRPCs. To test this hypothesis, we measured the mitochondrial respiratory rate in permeabilized mRPCs by monitoring O_2 consumption after activation of different pathways (β-oxidation and Cx I + II). We found that *hFATP1* increased all respirations tested after addition of ADP to stimulate ATP production (EIIImo β-ox and EIIImpgso CxI+CxII) (Fig 4J). Consistent with this, the activities of the TCA cycle enzymes isocitrate dehydrogenase, 2-oxoglurarate dehydrogenase (OGDH), and fumarase were all significantly increased in retinal extracts from *hFATP1TG* mice compared with WT mice (Fig 4L–4N). This increased respiration rate in transgenic mRPCs is unlikely to be due to an increase in mitochondrial mass because the activity of citrate synthase was unaffected by *hFATP1* overexpression (Fig 4K). Taken together, these data demonstrate that *hFATP1* overexpression in mRPCs increases the size of LDs and suggests that they are substrates for energy production in the mitochondria.

Next, we asked whether *hFATP1* expression and enhanced lipid storage in mRPCs could non-autonomously affect the physiology of juxtaposed neural retinal cells, which includes photoreceptor cells. mRPCs and the neural retina can be dissociated during dissection, which enables the effects of mRPC-specific *hFATP1* expression on the isolated photoreceptor cells to be examined. Lipid profiling of the neural retina revealed that sterol ester and TAG levels were higher while phospholipids levels remained unchanged in the neural retina of transgenic mice compared with WT mice (Fig 5A and 5B). Moreover, the magnitude of the increase was similar to that seen in isolated mRPCs (compare Fig 5A with Fig 4D). These results suggest a non-autonomous effect of mRPC-specific *hFATP1* expression similar to the observed phenotype in *Drosophila*. Next, analyses of the mitochondrial respiratory rate and TCA cycle enzyme activities in neural retinas showed a similar enhancement of O_2 consumption (Fig 5C) and enzyme activities (Fig 5D–5G) in tissue isolated from *hFATP1TG* mice compared with WT mice. Taken together, these results indicate that *hFATP1* expressed in mRPCs not only increased lipid storage and mitochondrial respiration in the mRPCs themselves, but also in the neural retinal cells.

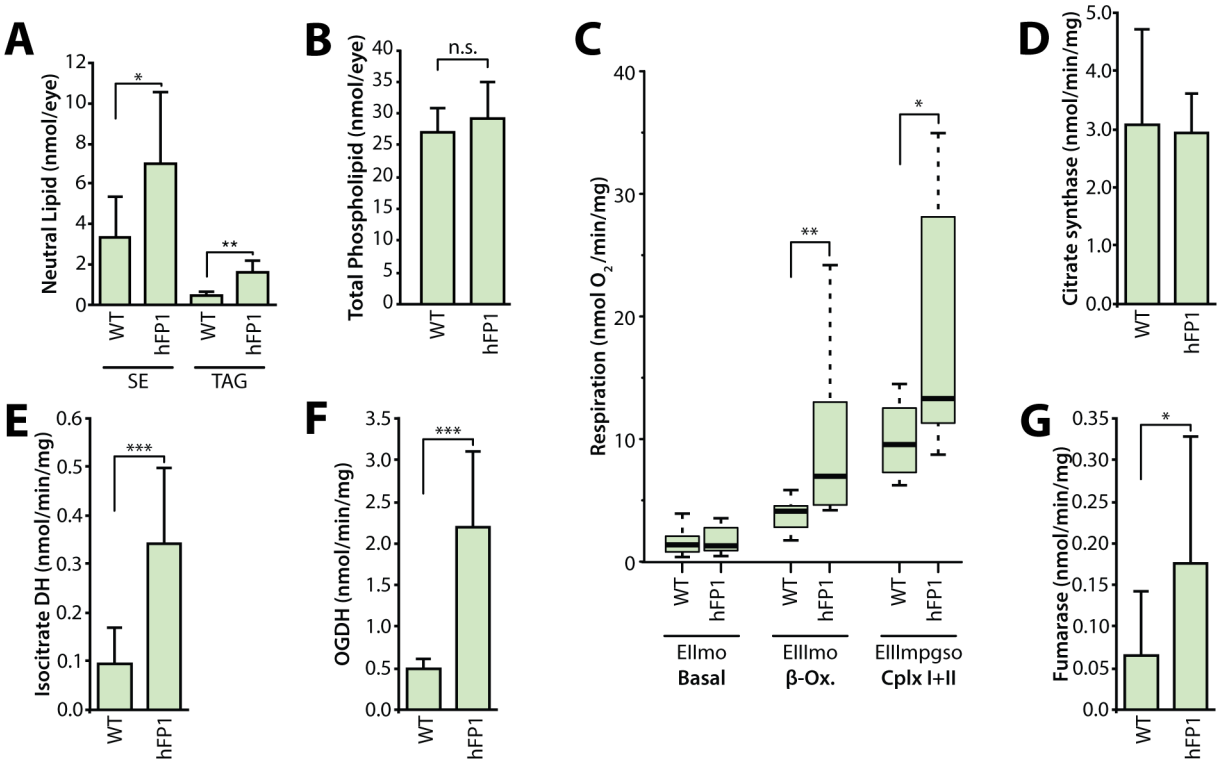

Fig 5. Cell non-autonomous effect of mRPC-specific *hFATP1* overexpression on the lipid content and respiratory rate in the neural retina. (**A**) Quantification of sterol esters (SE) and triacylglycerides (TAG) in the neural retina of 3-month-old WT and *hFATP1* transgenic mice. (**B**) Quantification of total phospholipid content in the neural retina of WT and *hFATP1* transgenic mice. Mean ± SD of n = 5 and 7 retinas, respectively. (**C**) Quantification of mitochondrial respiratory function in the neural retina of WT and *hFATP1* transgenic mice. EIImo, basal respiratory rate; EIIImbgso, β-oxidation; EIIImpgso, global respiratory chain function of complexes I and II. The boxes represent the median and lower and upper quartiles, and the whiskers represent the 1.5 interquartile range. N = 12 and 14 WT and transgenic retinas, respectively. (**D–G**) Activities of citrate synthase (**D**), isocitrate dehydrogenase (DH) (**E**), oxoglutarate dehydrogenase (OGDH) (**F**), and fumarase (**G**) in neural retinal extracts from WT and *hFATP1* transgenic mice. Mean ± SD of n > 9 retinas. $^{*}p<0.05$, $^{**}p<0.01$, $^{***}p<0.001$ for WT vs transgenic groups by two-sample t-test.

https://doi.org/10.1371/journal.pgen.1007627.g005

Genetic modifications of LD accumulation perturb retinal homeostasis

We next examined the consequences of LD accumulation caused by overexpression of *FATP* for the viability of RPCs in mice and *Drosophila*. TEM analyses showed that mRPC-specific expression of *hFATP1* induced vacuolization of the mRPCs and thickening of both mRPC and Bruch's membranes in 3-month-old mice (Fig 6A–6D). Similarly, pan-retinal or dRPC-specific expression of *dFatp* caused a moderate loss of dRPCs (one to two missing dRPCs in most ommatidia), resulting in perturbation of the ommatidia organization in *Drosophila* retina (Fig 6E and 6F). In contrast to dRPCs, photoreceptor cell survival (visualized by expression of Rh1-GFP) was unaffected by *dFatp* overexpression or by the knockdown of the *Bmm-lipase* which induced the accumulation BODIPY$^{493/503}$ similar to *dFatp* overexpression (Fig 6G and 6H and S6 Fig). These results in *Drosophila* retina are in agreement with our previous findings in mouse retina showing that photoreceptor layers were unaffected when *hFATP1* was overexpressed in mRPCs [31]. Therefore, *FATP*-mediated LD accumulation in RPCs does not appear to be deleterious to photoreceptor cells under physiological conditions.

In contrast, knockdown of *dFatp* with the *54C* driver, which is associated with a diminution of LD content, resulted in late onset photoreceptor degeneration in the *Drosophila* retina

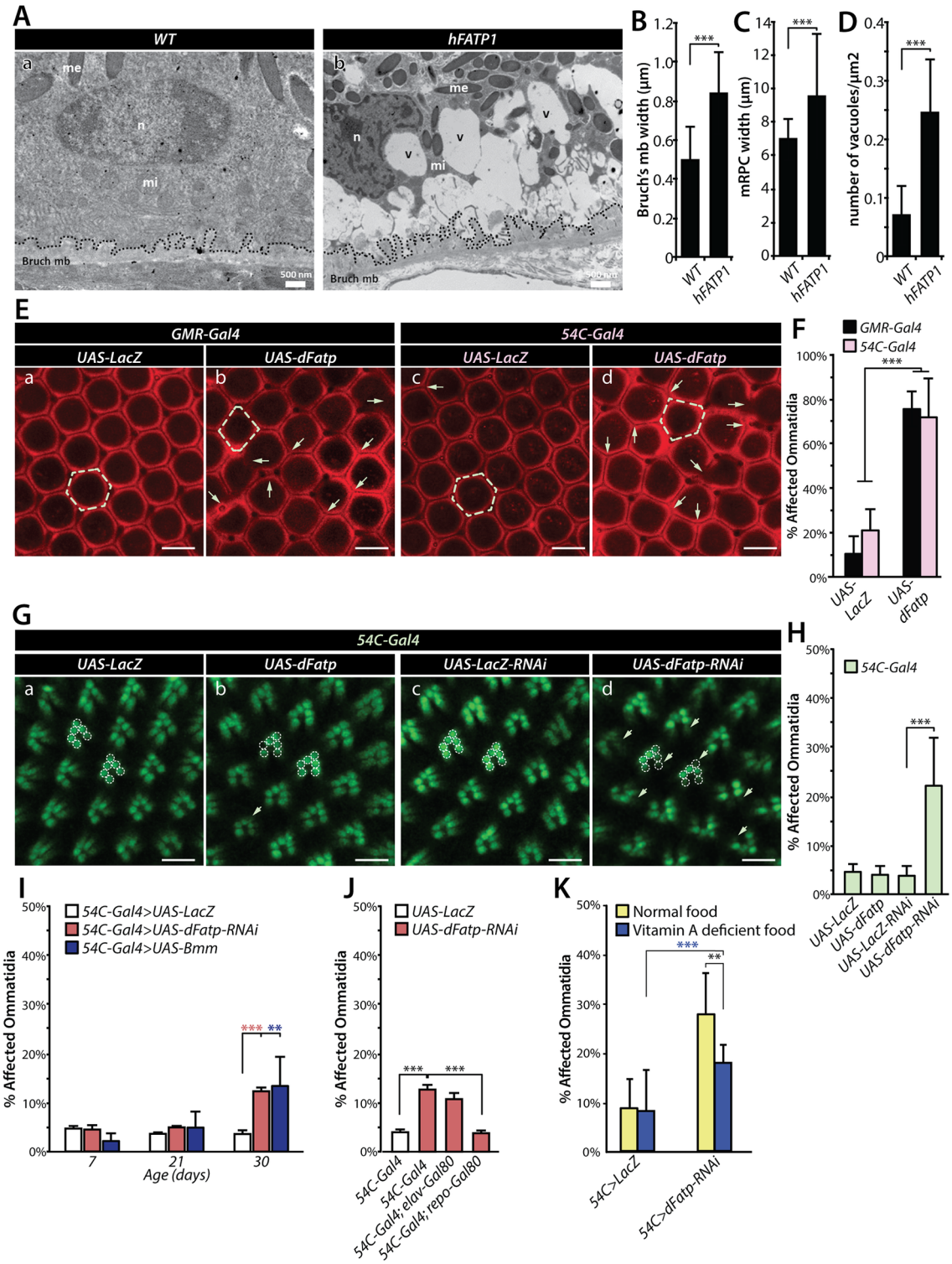

Fig 6. Consequences of *FATP*-depen dent accumulation of LDs on RPCs and photoreceptors in *Drosophila* and mice. (**A**) TEM images of horizontal sections from 3-month-old wild-type (C57BL/6J) and *hFATP1* transgenic mice. Abundant vacuoles (v) and thickened Bruch's membrane (mb, dashed lines) are evident in the aged *hFATP1* mice. me: melanosome, mi: mitochondria, n: nucleus. Scale bars, 500 nm. (**B–D**) Quantification of Bruch's membrane width (**B**), mRPC width (**C**), and vacuole density in mRPCs (**D**) from the images shown in (A). Mean ± SD of n = 14 and 18 WT and transgenic animals, respectively. (**E**) Cornea neutralization method of the retinas using confocal fluorescence microscopy (dRPC autofluorescence) of 30-day-old *Drosophila* expressing (a, c)

UAS-LacZ (control) or (b, d) *UAS-dFatp* throughout the retina (*GMR-Gal4*) or in dRPCs alone (*54C-Gal4*). Arrows show loss of dRPCs resulting in disorganization and loss of typical hexagonal ommatidial shape (dashed outline) upon *dFatp* overexpression. Scale bars, 10 μm. (**F**) Quantification of ommatidia with missing dRPCs (affected ommatidia) in retinas shown in (E). Mean ± SD of n = 5 and 8 control and transgenic flies, respectively. Black bars, *GMR-Gal4*; pink bars, *54C-Gal4*. (**G**) Visualization of retinas of 40-day-old Rh1-GFP-expressing flies by the cornea neutralization method with dRPC-specific expression of (a) *UAS-LacZ* (control), (b) *UAS-dFatp*, (c) *UAS-LacZ* RNAi (control-RNAi), or (d) *UAS-dFatp*-specific RNAi (*dFatp*-RNAi$^{[GD9406]}$). (b) *dFatp* overexpression in dRPCs does not affect photoreceptor survival, as indicated by intact rhabdomeres (dashed outlines). (d) *dFatp*-RNAi$^{[GD9406]}$ expression induces the loss of rhabdomeres (arrows). Scale bars, 10 μm. (**H**) Quantification of ommatidia with one or several missing photoreceptors (affected ommatidia), as shown in (G). (**I**) Quantification of affected ommatidia with missing photoreceptors in 7, 21 and 30 day-old flies expressing *UAS-LacZ*, *UAS-dFatp* or *UAS-Bmm* under the control of *54C-Gal4*. (**J**) Quantification of affected ommatidia with missing photoreceptors in 30 day-old flies expressing *UAS-LacZ*, or *UAS-dFatp* under the control of *54C-Gal4* combined with *repo-Gal80* (white bar), *elav-Gal80* (pink bar) or wild-type (green bar). (**K**) Quantification of affected ommatidia with missing photoreceptors in 30 day-old flies expressing *UAS-LacZ* or *UAS-dFatp-RNAi* under the control of *54C-Gal4* in normal (yellow) or Vitamin A deficient (blue) diet. Mean ± SD of n = 5–7 flies/condition. $^{*}p<0.05$, $^{**}p<0.01$, $^{***}p<0.001$ by two-sample t-test.

https://doi.org/10.1371/journal.pgen.1007627.g006

(Fig 6Gc, 6Gd and 6H). Importantly, this photoreceptor degeneration induced by expression of *dFatp-RNAi* with the *54C* driver was suppressed by Gal80 expression in dRPCs with the Repo driver (Fig 6J). In contrast, blocking the expression of *dFatp-RNAi* specifically in photoreceptors (elav-Gal80) did not inhibit photoreceptor degeneration (Fig 6J). This supports the fact that *dFatp*-dependent accumulation of LD in dRPC is non-autonomously required for photoreceptor viability. In agreement with the idea that LD are required for photoreceptor viability, we also observed a late onset photoreceptor degeneration similar to *dFatp* knockdown, by forcing LD lipolysis by overexpressing the *Bmm-lipase* or inhibiting LD biogenesis by expressing a RNAi against *midway* (*mdy*), a diacylglycerol acyltransferase (DGAT) that functions in the formation of TAG (Fig 6I and S6 Fig).

Next, we examined the effect of Vitamin A-deficient diet on photoreceptor degeneration induced by *54C>dFatp-RNAi*. As previously shown [28], the Vitamin A deficient diet strongly suppressed photoreceptor degeneration in *dFatp* mutant (S3A Fig). In contrast, we only observed a modest rescue of photoreceptor degeneration in flies expressing *dFatp-RNAi* in dRPCs with this diet supporting the idea that a Vitamin A independent dRPC role of *dFatp* in photoreceptor degeneration is predominant (Fig 6K). Collectively, these results indicate that *dFatp*-dependent LDs support photoreceptors viability during the normal aging process.

Finally, we asked whether LD accumulation in dRPCs was beneficial or deleterious to photoreceptors under stress conditions. For this, we examined young (5-day-old) *Aats-met^{FB}* mutant flies, in which *dFatp* RNAi prevents LD accumulation (see Fig 1B and 1C). Importantly, *dFatp* RNAi alone does not induce photoreceptor degeneration in 5-day-old flies [28], but the mutation *Aats-met^{FB}* itself causes some degeneration, allowing us to examine the consequence of *dFatp* RNAi in *Aats-met^{FB}* mutant on photoreceptor survival. We analyzed the apical/distal position of photoreceptor nuclei, which are normally clustered apically in the WT retina but are mislocalized under conditions associated with photoreceptor death [28]. Monitoring of mislocalized nuclei is a useful readout of cell death in situations where photoreceptor rhabdomeres are difficult to count due to their rapid degradation, as is the case for *Aats-met^{FB}* mutants. We observed an increase in the number of nuclei mislocalized between the proximal and distal part of the retina in *Aats-met^{FB}* mutants compared with WT flies (Fig 7Aa, 7Ac and 7B), consistent with previous reports for this mutant [9]. However, the mislocalization was completely reversed by dRPC-specific *dFatp* RNAi (Fig 7Ad and 7B). These results indicate that *FATP*-mediated LD accumulation in dRPCs is harmful to photoreceptors under conditions of pathological oxidative stress (*Aats-met^{FB}* mutants), in stark contrast to the beneficial effect under physiological conditions.

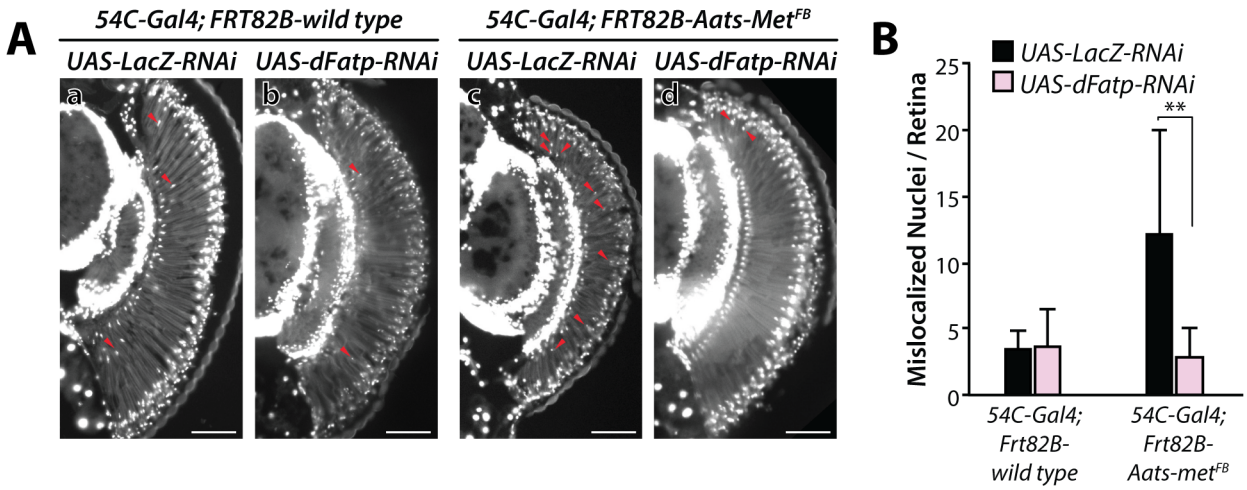

Fig 7. dRPC-specific knockdown of *dFatp* suppresses Aats-met^{FB}-induced photoreceptor degeneration in *Drosophila* retina. (**A**) Epifluorescence microscopy of retinal sections on whole eye clones generated with the GMR-hid/FLP-FRT technique [49] from 5-day-old FRT82B-wild-type (a, b, control) or FRT82B-*Aats-met*^{FB} mutant (c, d) flies expressing *UAS-dFatp-RNAi*$^{[GD16442]}$ (b, d) or *UAS-Lac-RNAi* (a, c) under the control of *54C-Gal4*. In *Aats-met*^{FB} mutant (c), nuclei (stained with DAPI, white) are mislocalized between the distal and proximal part of the retina (red arrows), indicative of dying photoreceptors. dRPC-specific expression of *UAS-dFatp*-RNAi$^{[GD16442]}$ markedly reduces the number of dying photoreceptors in *Aats-met*^{FB} mutant (d). Scale bars, 100 μm. (**B**) Quantification of mislocalized nuclei, as shown in A. Mean ± SD of $n > 6$ retinas. $^{**}p<0.01$ by two-sample t-test.

https://doi.org/10.1371/journal.pgen.1007627.g007

Discussion

Here, we studied the consequences of dysregulated lipid storage in RPCs on photoreceptor structure and function in both *Drosophila* and mouse retinas. Our results show that the *FATP* dependent-mechanisms of lipid storage and communication between RPC and photoreceptor layers are largely conserved in flies and mice. We made several novel observations in this study. We showed that *FATP* expression is required for LD formation in mouse and *Drosophila* RPCs. Interestingly, FATP has an acyl-CoA synthetase activity that is thought to facilitate cellular uptake of FAs (reviewed in [16]). FATP also interacts with DGAT-2 on the endoplasmic reticulum, where it has been show to function in LD expansion in *C. elegans* [13]. The fact that *dFatp* overexpression increases LD size but not number also suggests that the role of *FATP* in LD expansion is conserved in *Drosophila*. Interestingly, retinal LD accumulation induced by *FATP* overexpression resembles one of the key hallmarks of AMD pathology; that is, the accumulation of lipids in RPCs and of drusen in Bruch's membrane [32]. We also found that mRPC-specific *hFATP1* expression increased non-autonomously neutral lipids, β-oxidation, TCA enzyme activity, and mitochondrial respiration in photoreceptors. The fact that overexpression of *FATP* promotes both catabolic (mitochondrial respiration, TCA cycle, β-oxidation) and anabolic (increase of TAG and SE) functions that are distinct processes could be interpreted as followed. First, *FATP* promotes the import of fatty acids, which are used for different metabolic function including catabolism and anabolism within the cell. And second, FATP carries an acyl-coA synthase activity that is central in lipid metabolism for lipid elongation, unsaturation but also β-oxidation [16]. In flies, we did not evaluate the mitochondrial respiration rate due to the technical difficulty of dissociating RPCs from photoreceptor cells. However, mitochondria were intact by TEM and frequently observed juxtaposed to LDs in both flies and mice. The proximity between LD and mitochondria suggests that release of TAGs from LDs mediated by lipases could provide an energy source for the mitochondria. This hypothesis is supported by studies showing that physical proximity between LDs and mitochondria is important for β-oxidation of FAs [33].

In flies, we used the *54C* driver, which is strongly expressed in dRPCs to examine the non-autonomous role of *dFatp* on adjacent photoreceptor as previously described [27]. Because the *54C* driver also showed a low level of expression in few photoreceptors during pupal development, we took advantage of the Gal80 system to show that photoreceptor degeneration observed in flies carrying *54C>dFatp-RNAi* is due to the expression *of dFatp-RNAi* in dRPCs but not in photoreceptors. These results support a non-autonomous role of *dFatp* in fly RPCs as it is observed in the mouse. Altogether, we have shown that both the function of *FATP* in RPCs and its effect on photoreceptor cells are largely conserved between flies and mammals.

Although our data demonstrate that *FATP*-mediated LD accumulation in RPCs provides a metabolic signal to photoreceptors, it is not clear whether the signal itself is a lipid or another signaling molecule. Recent work proposed that in mutants that carry dysfunctional mitochondria, the accumulation of LDs in RPCs requires transfer of lactate from RPCs to photoreceptors [27]. The increased lactate levels in photoreceptors enhanced the activity of the TCA cycle and synthesis of FAs, which then underwent apolipoprotein-mediated transfer back to RPCs and induced LD formation [27]. A similar mechanism was described in mouse neuronal/glial co-cultures, raising the possibility that it may also be operating in the retina of *hFATP1TG* mice [27]. Our ultrastructural analysis supports the possibility of an exchange of electron dense material between RPCs and photoreceptor cells in *Drosophila*. Indeed, electron dense vesicles—similar in appearance and size to LDs—were observed in contact with dRPCs, as invaginations in the photoreceptor membrane, and finally as double-membraned structures in close proximity to the mitochondria in photoreceptors. Associations between LDs and mitochondria have also been observed in skeletal and heart muscle, where it was proposed to facilitate β-oxidation [34, 35, 33]. Although further studies will be required, our ultrastructural findings provide a hint that vesicle transfer could be a route of communication between RPCs and photoreceptors. Collectively, our results demonstrate that crosstalk between RPCs and photoreceptors is crucial for normal photoreceptor homeostasis and that its breakdown may contribute to retinal pathologies.

In our previous work, we showed that *dFatp* is expressed at higher levels in dRPCs than in photoreceptors, and that loss of *dFatp* led to a cell-autonomous photoreceptor degeneration [28]. We had proposed that degeneration of photoreceptors in the *dFatp* mutant is due to a failure to degrade Rh1, which accumulates to toxic levels and triggers apoptosis. Indeed, photoreceptor loss was rescued by down-regulating Rh1 levels in a Vitamin A-deficient diet [28]. We now show that photoreceptor undergo degeneration in flies expressing *dFatp*-RNAi in dRPCs even if fed in a Vitamin A-deficient diet. This indicates that *dFatp* expression in dRPCs also contributes to photoreceptor viability via its role in LD biosynthesis. This is further supported by our results showing that forcing LD lipolysis or inhibiting LD biogenesis induced late onset photoreceptor degeneration similar to *dFatp* knockdown. Therefore, *dFatp* would have two distinct functions in photoreceptors and dRPCs. In photoreceptors, *dFatp* is required for optimal Rh1 metabolism, presumably due to its role in phosphatidic acid synthesis and Rh1 trafficking [16, 36, 37]. In dRPCs, *dFatp* is required for expansion of LDs, which can then be metabolized for energy production. Finally, hFATP1 has been shown to directly interact with visual cycle enzymes in RPC to regulate retinyl-ester-dependent RPE65 isomerase necessary for production of 11-cis-retinal and rhodopsin [38, 39]. In Cubizolle et al., we have also shown by HPLC that retinyl esters accumulate in mRPC of transgenic mice expressing *hFATP1* [31]. We had proposed that the accumulation of retinyl ester could be due to either the inhibition of RPE65 or to an increase of long-chain fatty acids (LCFA) induced by *hFATP1* expression, which results in increased retinyl esters. Indeed, incorporated LCFA can form phosphatidyl choline (PC), which serves in the esterification of all-trans-retinol to form all-trans-retinyl esters in a reaction catalyzed by the Lecithin retinol transferase (LRAT) [40].

Together, our results show that in addition to the role of *FATP* in the regulation of visual cycle precursors in mouse RPC [31] and in the regulation of Rh1 levels in Drosophila photoreceptor [28], *FATP* has a conserved RPC-specific function in lipid storage that promotes the increase of neutral lipids in photoreceptors and the overall energy metabolism by the mitochondria in RPC and photoreceptor layers.

Our results show that the ectopic accumulation of LDs in RPCs induced by overexpression of *FATP* is not toxic to photoreceptors in either *Drosophila* (this study) or mice [31], and that physiological levels of LD are protective for *Drosophila* photoreceptors during aging. The loss of photoreceptors following depletion of LDs may therefore be due to the dwindling supply of energy, especially since photoreceptors have high-energy demands [5]. This hypothesis is supported by the proximity of LD and mitochondria that is observed in both mouse and fly retina that overexpress *FATP*. It is also supported by the increased mitochondrial respiration and β-oxidation rates measured in both RPC and PR layers of mice retina that overexpress *hFATP1*. Another non-exclusive hypothesis supported by recent reports, is that *de novo* LD biogenesis protects against lipotoxicity under conditions of low nutrient supply or high-energy demand as it was shown in adipocytes and mouse embryonic fibroblasts [41, 42]. Collectively, these results indicate that lipid storage in LDs is physiologically required for photoreceptor health during aging. In addition to acting as an energy source, LDs may also reduce the cellular sensitivity to ROS. The latter possibility is supported by the finding that ROS induced by light exposure, which promotes the accumulation of photo-damaged proteins and lipids [43], enhances photoreceptor degeneration to a greater extent in *dFatp* mutant flies than in WT flies [28]. Similarly, LD accumulation in glia protects against ROS-induced damage of the developing nervous system of *Drosophila* upon exposure to hypoxia [8]. Moreover, LDs are not uniform structures but exist in various forms with differing potential functions, such as storage of phospholipids, vitamin E, and cellular toxins [10].

Our data establish that LDs are not toxic to retinal cells under physiological conditions, but that they can contribute to neurodegeneration under some stress conditions as shown here with the *Aats-met*^{FB} mutants (model in Fig 8). In these mutants, suppression of LD accumulation in dRPCs is neuroprotective, suggesting that the LDs non-autonomously promote photoreceptor cell death under conditions of oxidative stress. This is consistent with studies of flies with mitochondrial defects that cause high ROS levels in neurons, which demonstrated that removal of LDs by *dFatp* knockdown rescued retinal degeneration in *sicily* (*Drosophila* homolog of the human nuclear encoded mitochondrial gene NDUFAF6) and *marf* (*Drosophila* homolog of the mitochondrial fusion GTPases, Mitofusin 1 and 2) mutants and that ectopic expression of *Bmm-lipase* rescued photoreceptors in *Aats-met* mutants [9, 27]. One possible explanation as proposed by Liu et al. [27], is that high levels of ROS induce an abnormal initial raise followed by a decrease of LD as the pathology progresses. This perturbed turnover could override LD beneficial role and enhances lipid peroxidation and photoreceptor death. Collectively, our findings and those of others suggest that LDs may play a protective or beneficial role under physiological conditions and be deleterious under pathological conditions.

In conclusion, despite the difference in mouse and fly retinal architecture, RPCs appear to be functionally homologous in both species with respect to providing metabolic support for adjacent photoreceptors. *Drosophila* RPCs form a tight barrier between the hemolymph and photoreceptors, similar to the mammalian outer retina [44], implying that dRPCs, like mammalian RPCs, may play an active role in metabolite exchanges with photoreceptors [32]. Similar to dRPCs, it was recently shown that *Drosophila* cone cells, which are also accessory cells of photoreceptors, express glial cell markers and are important to maintain photoreceptor function in the adult fly [45]. Thus, combined with our data, these results support that both types of accessory cells- dRPCs and cone cells- carry glial functions similar to the support functions

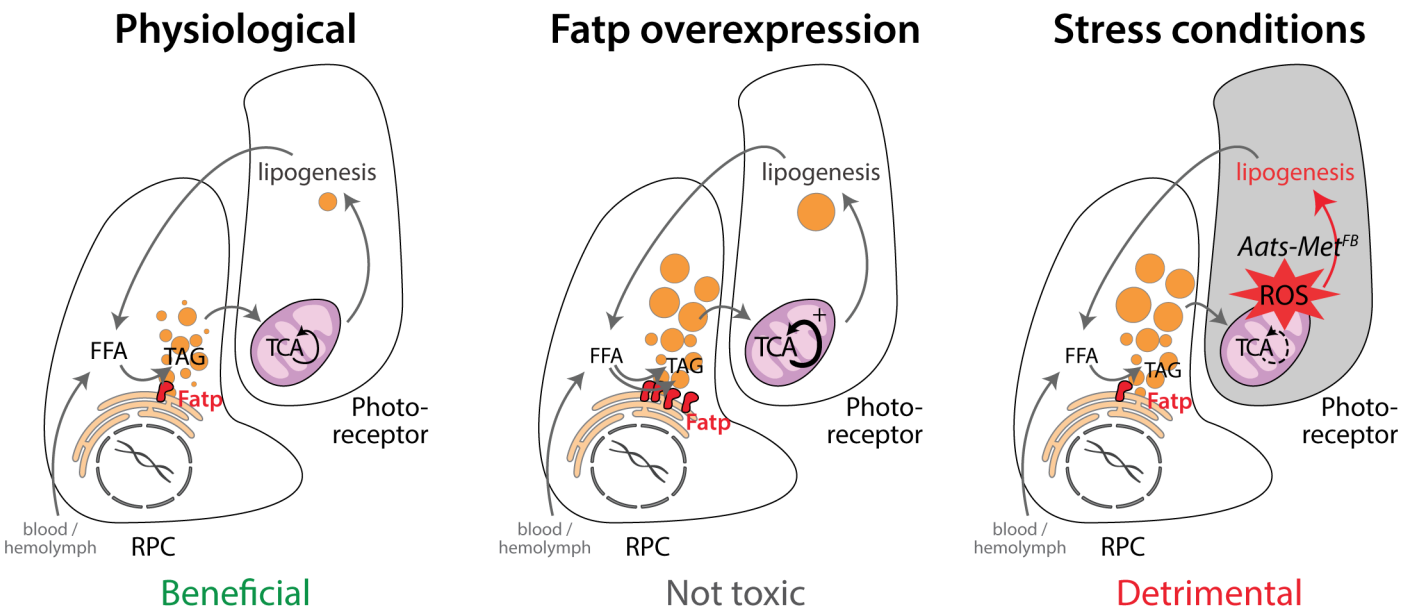

Fig 8. Schematic of the role of *FATP* in the metabolism of lipid droplets and communication between RPCs and photoreceptors under physiological and pathological conditions. Under physiological conditions, *FATP* is involved in the maintenance of LD and their presence in RPCs is required and beneficial for photoreceptor health. Indeed, the removal of LD by expression of *dFatp-RNAi*, *Mdy-RNAi* or *Bmm* induces a progressive photoreceptor degeneration in flies. Overexpression of *FATP* in RPCs expands the cellular LD content, which has a cell non-autonomous stimulatory effect on neighbouring photoreceptors that increases LD (in flies), neutral lipids, mitochondrial respiration and β-oxidation (in mice). LD accumulation in condition of overexpression of *FATP* in RPCs is not toxic for photoreceptors and could be considered beneficial through increased mitochondrial function and nutrient availability in these cells. Under conditions of oxidative stress (e.g., *Aats-met*^{FB} mutant flies, in which ROS levels are elevated in photoreceptors), LD are no longer beneficial. In this scenario, LD could be considered as detrimental which could be due to their abnormal turnover under high ROS leading to enhanced lipid peroxidation.

https://doi.org/10.1371/journal.pgen.1007627.g008

of Müller glia and retinal pigment epithelium (here mRPC) in the vertebrate retina. We propose that the RPC–photoreceptor interaction is a conserved paradigm between *Drosophila* and mammalian that will be a useful model to investigate mammalian RPC disorders, such as AMD, particularly given *Drosophila* genetic tractability.

Material and methods

Ethics statement

Experiments were carried out in accordance with the European Communities Council Directive of 24 November 1986 (86/609/EEC) and the French Ethical Committee (CEEA-LR-12141) guidelines for the care and use of animals for experimental procedures.

Drosophila genetics

The fly stocks used in this study were: *54C-Gal4* (BS#27328) [24], *GMR-Gal4*, *Rh1-Gal4* [46], UAS-dcr2; *eyeless-Gal4 (ey-Gal4)*, *GMR-Gal4*, *Rh1-GFP* (gift from Claude Desplan), *UAS-dFatp*, *FRT40A dFatp*^{k10307} [28], *Rh1-Gal4*, *eyflp; FRT40A Rh1-TdTomatoNinaC ; UAS-GFP* [47], *UAS-bmm* [29], *UAS-dFatp-RNAi* (VDRC stocks GD16442 and GD9604), *UAS-bmm-RNAi* (BS#25926); *UAS-Mdy-RNAi* (VDRC stock GD1749 #6367), *FRT82*^{B} *Aats-met*^{FB} (BS#39747), and *Rh1-GFP* [48]. *Repo-Gal80* and *Elav-Gal80* (gift from Laurent Seugnet, CRNL, Lyon, France). Mitotic whole eye mutant clones for *dFatp*^{k10307} and *Aats-met*^{FB} were generated using GMR-hid/FLP-FRT technique by crossing a mutant line carrying the FRT-containing chromosome with a line containing *ey-flp* and *FRT40A GMR-hid* (for *dFatp*^{k10307})

or *FRT82B GMR-hid* (for *Aats-met*^{FB}) [49]. Human *FATP1* cDNA, a gift from Celine Haby (IGBMC, Strasbourg), was cloned via BamHI and EcoRI into a pUAST-w+-attB transgenic vector. Transgenic lines were generated by Best Gene (Chino Hills, CA, USA) using PhiC31 integrase-mediated transgenesis [50] at the same site used for *dFatp* (65B2). Flies were maintained on standard corn medium at 25˚C or on Vitamin A-deficient medium. Vitamin A-deficient medium contained yeast (12 g), agar (1,5 g), sucrose (7,5 g), cholesterol (0,03 g), sodium methyl-4-hydroxybenzoate (1.15M, 3.75 mL) and propionic acid (0.72 mL) in distilled water (150 mL) as described [28].

Lipid droplet staining using BODIPY lipid probes

The retinas of 1-day-old flies were dissected in ice-cold HL3 medium [51] according to [28]. Tissues were then processed for staining with either C_1-BODIPY$^{500/510}$-C_{12} (D-3823) or BODIPY$^{493/503}$ (D-3922; both acquired from Life Technologies) as stated in figure legends.

For BODIPY$^{500/510}$-C_{12}, dissected retinas were warmed to 25˚C and directly incubated for 30 min with 1.5 μg/mL BODIPY$^{500/510}$-C_{12} (D-3823), washed three times in HL3 medium, fixed in 4% paraformaldehyde (PFA, Electron Microscopy Sciences) for 15 min at room temperature (RT), washed three times in wash buffer (PBS containing 0.1% Triton-X100), and incubated for 16 h at 4˚C in wash buffer supplemented with 25 ng/mL phalloidin-TRITC (Sigma).

For BODIPY$^{493/503}$, dissected retinas were fixed first in 4% PFA for 15 min at RT, washed three times and then incubated with 75 ng/mL BODIPY$^{493/503}$ and 25 ng/mL phalloidin-TRITC for 16 hours at 4˚C.

Subsequently, samples were washed three times in wash buffer, mounted on a bridge slide in Vectashield (Vector Laboratories), and stored at −20˚C until analysis. 16-bit image stacks were acquired on a Zeiss LSM800 microscope and processed for quantification using ImageJ2 software [52]. Images were filtered for noise using Gaussian Blur 3D ($\sigma = 1$), after which a Z-projection was made. LDs were identified by thresholding the images, and the integrated density of the signal and total retinal area were measured. The integrated density of BODIPY staining divided by the total area of the retina was normalized to the control for each experiment.

Statistical analysis

Statistical analyses were performed using R. Group differences were analyzed by t-test or Tukey's HSD paired sample comparison test, as specified in the figure legends.

Imaging of photoreceptors and RPCs by the cornea neutralization method in living flies

Living flies, maintained for 30 days at 25˚C on a 12h light/dark cycle, were anesthetized using CO_2, embedded in 1% agarose covered with cold water [53], and imaged using a Leica SP5 upright confocal microscope. RPCs were visualized by pigment autofluorescence (excitation 514 nm, detection 530–630 nm) and photoreceptors were identified by Rh1-GFP expression (excitation 488 nm, detection 500–570 nm) as described [24, 47, 53]. Ommatidia lacking one or several RPCs lose their lozenge shape and are counted as affected ommatidia. Photoreceptor rhabdomeres were quantified using Fiji cell counter tool.

Transmission electron microscopy of Drosophila eyes

Dissected *Drosophila* eyes were fixed in 0.1 M cacodylate buffer, 2.5% glutaraldehyde, and 2 mM $CaCl_2$ for 16 h at 4˚C. After rinsing with 0.1 M cacodylate buffer at RT, the eyes were

incubated with 1% OsO_4 in 0.1 M cacodylate buffer for 2 h at RT. Tissues were then progressively dehydrated in acetone at RT and mounted in 100% epoxy resin (Epon 812) in silicone-embedding molds. After resin polymerization for 48 h at 60˚C, samples were sliced into 60 nm sections, which were stained with lead citrate and examined with a Philips CM120 transmission electron microscope (TEM) operating at 80 kV. For quantification, only LDs were considered that were clearly localized within either dRPC or photoreceptors. Vesicles surrounded by double membrane layers were excluded.

Mice

Transgenic mice overexpressing human *FATP1* (*hFATP1TG*) specifically in the RPCs (driven by the RPC-specific VDM2 promoter) were generated on a C57BL/6J genetic background as previously described [31]. The *hFATP1TG* mice were maintained on a standard 12 h light (90 lux)/12 h dark cycle at ~22˚C and were fed *ad libitum* with a standard rodent diet. Mice were housed in facilities accredited by the French Ministry of Agriculture and Forestry (B-34 172 36 —March 11, 2010). Mice were euthanized by cervical dislocation and the eyes were enucleated and dissected.

Co-staining of lipids, perilipin, and ATP synthase

Nile Red staining of lipids [54] was used alone or in conjunction with fluorescent protein immunostaining. The eyes of 3-month-old mice were enucleated and the retina was separated from the RPC/choroid layer to obtain an empty eyeball [31]. The eyes were fixed in 4% PFA for 1 h at RT, washed with PBS, and permeabilized with 0.1% sodium dodecyl sulfate. They were then incubated for 20 min at RT in blocking buffer (10% fetal calf serum in PBS), and incubated overnight at 4˚C with a mouse anti-mouse ATP synthase (Millipore MAB3494, 1:500) or rabbit anti-mouse perilipin (D1D8, Cell Signaling Technology # 9349, 1: 200) primary antibody. The tissues were then incubated for 4 h at RT with Alexa Fluor 488-conjugated anti-rabbit or anti-mouse secondary antibodies diluted in blocking buffer. The immunostained eyeballs were gently rinsed in PBS, incubated with Nile Red solution (10 μg/ml) for 30 min at RT in the dark, washed twice in PBS for 5 min at RT, and incubated with 4′,6-diamidino-2-phenylindole (DAPI, 1:1000) for 5 min at RT. The eyeballs were finally rinsed 5 times in PBS for 5 min at RT and mounted in Dako mounting medium. Confocal imaging was performed with a Zeiss LSM 5 LIVE DUO Highspeed/Spectral Confocal system. Images were acquired with Zeiss Zen software, and LDs were counted with ImageJ software.

Quantification of neutral lipids in mouse retina

Mice were euthanized by vertebral dislocation, the eyes were enucleated, and the neural retina was removed from the eye cup. Neural retinas were directly frozen in liquid nitrogen. The RPC/choroid was scraped and collected in PBS, and the samples were centrifuged to remove the PBS. Tissues were stored dry at −80˚C.

Lipids were extracted and analyzed as previously described [55]. Total lipids were extracted twice from tissues with ethanol/chloroform (1:2, v/v). Before extraction, internal standards were added. The organic phases were dried under nitrogen and lipid classes were separated by thin-layer chromatography on silica gel G using a mixture of hexane-ethyl ether -acetic acid (80:20:1 v/v/v). Lipids were transmethylated and the fatty acid methylesters were analyzed by gas chromatography. Briefly, samples were treated with toluene-methanol (1:1, v/v) and boron trifluoride in methanol. Transmethylation was carried out at 100˚C for 90 min in screw-capped tubes. After addition of 1.5 mL, 10% K_2CO_3 in water, the resulting fatty acid methyl

esters were extracted with 2 mL of isooctane and analyzed by gas chromatography, using an HP6890 instrument equipped with a fused silica capillary BPX70 SGE column (60 × 0.25 mm). The vector gas was hydrogen. The temperatures of the Ross injector and the flame ionization detector were set at 230˚C and 250˚C, respectively.

Oxygen consumption

Respiration was measured on RPC/choroid and neural retinas permeabilized by incubation for 2 min with 15 μg digitonin per mg and resuspended in a respiratory buffer (pH 7.4, 10 mM KH_2PO_4, 300 mM mannitol, 10 mM KCl and 5 mM $MgCl_2$). The respiratory rates were recorded at 37˚C in 2 ml glass chambers using a high-resolution Oxygraph respirometer (Oroboros, Innsbruck, Austria). Assays were initiated in the presence of 5 mM malate/0.2 mM octanoyl carnitine to measure state 2, basal respiration (EIImo basal). Complex I-coupled state 3 respiration was measured by adding 0.5 mM NAD^+/1.5 mM ADP (EIIImo β-ox). Then, 5 mM pyruvate and 10 mM succinate were added to reach maximal coupled respiration (EIIImpgso CxI+CxII), and 10 μM rotenone was injected to obtain the CII-coupled state 3 respiration. Oligomycin (8 μg/mL) was added to determine the uncoupled state 4 respiration rate. Finally, carbonyl cyanide-4-(trifluoromethoxy) phenylhydrazone (1 μM) was added to control the permeabilization of the tissues.

Mitochondrial enzymatic activities

The activities of the mitochondrial citrate synthase (CS), oxoglutarate dehydrogenase (OGDH), isocitrate dehydrogenase (IDH) and fumarase were measured in 5 μl RPC/choroid and neural retina homogenates (sonicated in 50 μl PBS) at 37˚C using a Beckman DU-640B spectrophotometer (Beckman Coulter) or a CLARIOstar (BMG LabTech) [56]. Briefly, citrate synthase activity was measured using 0.15 mM DTNB reagent (SIGMA Aldrich) which interacts with CoA-SH to produce TNB. The formation of TNB was followed for 1.5 min at wavelength of 412 nm. IDH and OGDH activities were determined in the presence of respective substrates isocitrate and α-ketoglutarate, by monitoring for 3 min the change in NAD^+ to NADH which absorbs light at 340 nm. Fumarase activity was determined by measuring the conversion of L-malate to fumarate, monitoring the increase in absorbance at 250 nm. The optical density variation per minute is calculated from the curve and the enzymatic activity expressed as nmol of product formed/minute/mg protein.

Electron microscopy of mouse RPCs

The eyes of 3–6 month-old *hFATP1TG* mice were rapidly enucleated, the corneas were removed, and the eyeballs were fixed by immersion in 2.5% glutaraldehyde in Sorensen's phosphate buffer (0.1 M, pH 7.4) overnight at 4˚C. The tissues were then rinsed in Sorensen's buffer and post-fixed in 1% OsO_4 for 2 h in the dark at RT. The tissues were rinsed twice, dehydrated in a graded series of ethanol solutions (30–100%), and embedded in EmBed 812 using a Leica EM AMW (Automated Microwave Tissue Processor for Electronic Microscopy). Sections (60 nm thick) were cut near the optic nerve (Leica-Reichert Ultracut E), counterstained with uranyl acetate, and examined using a Hitachi 7100 TEM (Centre de Ressources en Imagerie Cellulaire de Montpellier, France). The thickness of Bruch's membrane was determined by measuring both the thickest and the thinnest parts of 5 fields throughout the retinal section per mouse. Data are presented as the median value per eye. We also enumerated the vacuoles in 5 fields of retinal sections per mouse at 10,000× magnification.

Supporting information

S1 Fig. Schematic of the mouse and *Drosophila* retina. (**A**) Mouse retinal pigment epithelial cells (mRPCs, pink) support photoreceptor rods and cones (green) by providing them with nutrients, transported across Bruch's membrane from the underlying vasculature. (**B**) Tangential (top) and horizontal (bottom) views through a *Drosophila* ommatidium (of ~800 in total) showing *Drosophila* retinal pigment cells (dRPCs, primary, secondary and tertiary pigment in pink), bristle cells (cone cells are not represented on these drawings) organization around the photoreceptors. In contrast, to mRPCs that are only in contact with photoreceptor outer segments containing disk-filled of opsins (equivalent to rhabdomeres in flies), dRPCs are in contact with the cell bodies of photoreceptors and have a large zone of exchange.
(TIF)

S2 Fig. *dFatp* overexpression with the *54C-Gal4* driver induces a specific accumulation of LDs in dRPCs. (A-A" and B-B") Expression pattern of *54C-Gal4* driver. Expression of the *UAS-GFP* is driven by the *54C-Gal4*, GFP is visualized by confocal fluorescence microscopy on a pupal eye disc at 42 h after puparium formation (AFP). (A) merge, (A') anti-GFP (A") and anti-Elav antibody stainings. (A-A") A strong expression of the GFP in secondary and tertiary pigment cells (dRPCs, arrows), and a weak expression in photoreceptors (Elav positive, arrowheads) at the level of Elav positive nuclei in the apical part of the pupal retina. (B-B") A strong expression of GFP in six secondary (false color in brown) and three tertiary (false color in blue) pigment cells per ommatidium at the basal part of the eye disc. The position of bristle cells that lack GFP expression is shown (*) in A and B. GFP staining in primary pigment cells located above the photoreceptor layer is not apparent in these optical sections. (**C**) LD labeled with BODIPY$^{493/503}$ (D3922) are revealed by confocal microscopy in horizontal sections of whole retinas from one-day-old flies expressing (a, c) *UAS-LacZ* (control) and (b, d) *UAS-dFatp* under the control of *54C-Gal4* driver alone (a, b) or concomitantly with *repo-Gal80* (c, d). Photoreceptors are counterstained with phalloidin-rhodamine (red). (**D**) Quantification of BODIPY$^{493/503}$ (D3922) from the images shown in (C). Data are presented as the fold change in fluorescence intensity (dots/μm^2) compared with the LacZ-control flies. Log adjusted values: $^{*}p<0.05$, $^{**}p<0.01$, $^{***}p<0.001$ by Tukey's HSD paired sample comparison test.
(TIF)

S3 Fig. Vitamin A is not required for *dFatp*-dependent accumulation of LD. (**A**) Quantification of the substantial loss of photoreceptors in whole-eye *dFatp*^{k10307} clone, quantified as % affected rhabdomeres. Whole-eye *dFatp*^{k10307} mutant flies were generated using the GMR-hid/FLP-FRT technique [49] with the following genotype *FRT40A- P{LacW}dFatpk*^{10307}*/ FRT40A-GMR-hid; ey-Gal4, UAS-FLP/TM6B*. For control flies a FRT40A-wild type chromosome was used. Control and *dFatp* mutant flies were fed on a Vitamin A deficient diet, which rescued photoreceptor degeneration in *dFatp* mutant. (**B**) LDs labeled with BODIPY$^{493/503}$ (green) were revealed by confocal microscopy in horizontal sections of whole retinas from one-day-old flies expressing *UAS-dFatp* (b) or *UAS-LacZ* (a) under the control of *54C-Gal4* driver in flies fed with Vitamin A deficient diet. Photoreceptors are counterstained with phalloidin-rhodamine (red). Under vitamin A deficient diet (a, b), accumulation of LDs still occurs. (**C**) Quantification of BODIPY$^{493/503}$ from the images shown in (B). Data are presented as the fold change in fluorescence intensity (dots/μm^2) compared with the *LacZ*-control flies. Log adjusted values: $^{**}p<0.01$, by Tukey's HSD paired sample comparison test. (**D**) The *dFatp*^{k10307} loss of function allele eliminates LD content in the *Drosophila* retina of flies fed with a regular diet. Horizontal sections of wild-type (Control) or *dFatp*^{k10307} mutant retinas, stained with BODIPY$^{500/510}$-C_{12} (green) to visualize LDs. Retinas of one-day-old flies were

used, photoreceptors rhabdomeres were stained with phalloidin-rhodamine (red) and images were acquired by confocal fluorescence microscopy (scale bars 25 μm). Whole-eye *dFatp*^{k10307} mutant flies were generated using the GMR-hid/FLP-FRT technique with the following genotype *FRT40A-P{LacW}dFatp*^{k10307}*/FRT40A-GMR-hid; ey-Gal4, UAS-FLP/TM6B*. For control flies a FRT40A-wild type chromosome was used.
(TIF)

S4 Fig. TEM of retina from flies overexpressing the Bmm lipase. TEM showing ommatidia from one-day-old flies expressing *UAS-Brummer* under control of the dRPC-specific (*54C-Gal4*) driver. One ommatidium in each panel shows seven photoreceptors (false colored green) with central rhabdomeres surrounded by dRPCs (false colored pink). Scale bars, 2 μm (a–d), 1 μm (c', d'). m, mitochondria; R rhabdomeres; arrowhead, small round shaped vesicles with an irregular shape and clear content that are distinct from LD.
(TIF)

S5 Fig. *dFatp* is a functional ortholog of human *FATP1*. (**A, B**) Confocal fluorescence microscopy of retinas from *dFatp*$^{-/-}$ (*dFatp*^{k10307}) mutant flies without (A) or with (B) photoreceptor-specific expression of human *FATP1* (*dFatp*$^{-/-}$*;Rh1>hFATP1*). *hFATP1* rescues the loss of photoreceptors in *dFatp*$^{-/-}$ mutant clones. Retinas were generated using the Tomato/GFP-FLP/FRT technique [47], in which all photoreceptors are marked by GFP, and homozygous mutant mosaic retina is marked by the absence of TdTomato. *dFatp*^{k10307}-mutant tissue shows loss of photoreceptors at 15 days of age (**A**). Scale bars, 10 μm. (**C**) Quantification of affected rhabdomeres, as shown in (A) and (B). Mean ± SD of n = 12 retinas. $^{***}p<0.001$ by two-sample t-test.
(TIF)

S6 Fig. Knock-down of *Mdy* but not *Bmm-lipase* leads to photoreceptor degeneration. (**A**) LD labeled with BODIPY$^{493/503}$ (green) were revealed by confocal microscopy in horizontal optical section of whole mount retinas from one-day-old flies expressing (a) *UAS-LacZ* RNAi (control), (b) *UAS-Bmm-lipase-RNAi* or (c) *UAS-Mdy-RNAi* under the control of a pan-retinal *ey-Gal4/GMR-Gal4* driver. Photoreceptors were counterstained with phalloidin-rhodamine (red). (**B**) Quantification of BODIPY$^{493/503}$ staining from the images shown in (A). Data are presented as the fold change in fluorescence intensity (dots/μm^2) compared with the *LacZ RNAi*-control flies. Mean ± SD of n = 4–10 flies/condition, $^{**}p<0.01$ by Tukey's HSD paired sample comparison test. (**C**) Tangential images of retinas of 20-day-old flies expressing Rh1-GFP visualized by the cornea neutralization method, carrying (a) *UAS-LacZ* RNAi (control), (b) *UAS-Bmm-lipase*-RNAi or (c) *UAS-Mdy*-RNAi induced by *ey-Gal4/GMR-Gal4*. *Bmm-lipase* knock-down does not affect photoreceptor survival, as indicated by intact rhabdomeres (b), while Mdy knock-down induces the loss of rhabdomeres (arrows in c). Scale bars, 10 μm. (**D**) Quantification of ommatidia with missing photoreceptor (affected ommatidia), as shown in (C). Mean ± SD of n = 5–11 flies. $^{***}p<0.001$ by two-sample t-test.
(TIF)

Acknowledgments

We are grateful to the ARTHRO-TOOLS and the PLATIM microscopy platform of SFR Biosciences (UMS3444/CNRS, US8/INSERM, ENS de Lyon, UCBL) and the Centre Technologique des Microstructures CTμ at Lyon1 for assistance with electron microscopy. We would like to thank Chantal Cazevieille from the COMET platform of RHEM for the transmission electron microscopy, the INM facility for the management and maintenance of mice, and Montpellier RIO Imaging for the use of imaging tools. We are grateful to Charlotte Scholtes for her

help in the analysis of mitochondrial integrity on TEM images. Stocks were obtained from the Bloomington Drosophila Stock Center (NIH P40OD018537).

Author Contributions

Conceptualization: Daan M. Van Den Brink, Aurélie Cubizolle, Nathalie Davoust, Philippe Brabet, Bertrand Mollereau.

Data curation: Daan M. Van Den Brink.

Formal analysis: Daan M. Van Den Brink, Aurélie Cubizolle, Victor Girard.

Funding acquisition: Daan M. Van Den Brink, Nathalie Bernoud-Hubac, Michel Guichardant, Philippe Brabet, Bertrand Mollereau.

Investigation: Daan M. Van Den Brink, Aurélie Cubizolle, Gilles Chatelain, Nathalie Davoust, Victor Girard, Simone Johansen, Francesco Napoletano, Pierre Dourlen, Laurent Guillou, Claire Angebault-Prouteau, Philippe Brabet.

Methodology: Daan M. Van Den Brink, Aurélie Cubizolle.

Project administration: Bertrand Mollereau.

Resources: Philippe Brabet, Bertrand Mollereau.

Software: Daan M. Van Den Brink.

Supervision: Nathalie Davoust, Nathalie Bernoud-Hubac, Michel Guichardant, Philippe Brabet, Bertrand Mollereau.

Validation: Philippe Brabet, Bertrand Mollereau.

Visualization: Daan M. Van Den Brink, Aurélie Cubizolle, Victor Girard, Philippe Brabet, Bertrand Mollereau.

Writing – original draft: Daan M. Van Den Brink, Bertrand Mollereau.

Writing – review & editing: Daan M. Van Den Brink, Nathalie Davoust, Victor Girard, Philippe Brabet, Bertrand Mollereau.

References

1. Sparrow JR, Hicks D, Hamel CP. The retinal pigment epithelium in health and disease. Curr Mol Med. 2010; 10(9):802–23. Epub 2010/11/26. PMID: 21091424.
2. Pauleikhoff D, Barondes MJ, Minassian D, Chisholm IH, Bird AC. Drusen as risk factors in age-related macular disease. Am J Ophthalmol. 1990; 109(1):38–43. Epub 1990/01/15. PMID: 1688685.
3. Holz FG, Sheraidah G, Pauleikhoff D, Bird AC. Analysis of lipid deposits extracted from human macular and peripheral Bruch's membrane. Arch Ophthalmol. 1994; 112(3):402–6. PMID: 8129668.
4. Sheraidah G, Steinmetz R, Maguire J, Pauleikhoff D, Marshall J, Bird AC. Correlation between lipids extracted from Bruch's membrane and age. Ophthalmology. 1993; 100(1):47–51. PMID: 8433826.
5. Kurihara T, Westenskow PD, Gantner ML, Usui Y, Schultz A, Bravo S, et al. Hypoxia-induced metabolic stress in retinal pigment epithelial cells is sufficient to induce photoreceptor degeneration. Elife. 2016; 5. Epub 2016/03/16. https://doi.org/10.7554/eLife.14319 PMID: 26978795.
6. Kuhnlein RP. The contribution of the Drosophila model to lipid droplet research. Prog Lipid Res. 2011; 50(4):348–56. https://doi.org/10.1016/j.plipres.2011.04.001 PMID: 21620889.
7. Kuhnlein RP. Thematic review series: Lipid droplet synthesis and metabolism: from yeast to man. Lipid droplet-based storage fat metabolism in Drosophila. J Lipid Res. 2012; 53(8):1430–6. Epub 05/09. PMID: 22566574.
8. Bailey AP, Koster G, Guillermier C, Hirst EM, MacRae JI, Lechene CP, et al. Antioxidant Role for Lipid Droplets in a Stem Cell Niche of Drosophila. Cell. 2015; 163(2):340–53. Epub 10/10. https://doi.org/10.1016/j.cell.2015.09.020 PMID: 26451484.

9. Liu L, Zhang K, Sandoval H, Yamamoto S, Jaiswal M, Sanz E, et al. Glial Lipid Droplets and ROS Induced by Mitochondrial Defects Promote Neurodegeneration. Cell. 2015; 160(1–2):177–90. Epub 01/17. https://doi.org/10.1016/j.cell.2014.12.019 PMID: 25594180.
10. Welte MA, Gould AP. Lipid droplet functions beyond energy storage. Biochim Biophys Acta. 2017; 1862 (10 Pt B):1260–72. https://doi.org/10.1016/j.bbalip.2017.07.006 PMID: 28735096.
11. Wang CW. Lipid droplets, lipophagy, and beyond. Biochim Biophys Acta. 2016; 1861(8 Pt B):793–805. Epub 2015/12/30. https://doi.org/10.1016/j.bbalip.2015.12.010 PMID: 26713677.
12. Gross DA, Silver DL. Cytosolic lipid droplets: from mechanisms of fat storage to disease. Crit Rev Biochem Mol Biol. 2014; 49(4):304–26. https://doi.org/10.3109/10409238.2014.931337 PMID: 25039762.
13. Xu N, Zhang SO, Cole RA, McKinney SA, Guo F, Haas JT, et al. The FATP1-DGAT2 complex facilitates lipid droplet expansion at the ER-lipid droplet interface. J Cell Biol. 2012; 198(5):895–911. Epub 08/29. https://doi.org/10.1083/jcb.201201139 PMID: 22927462.
14. Anderson CM, Stahl A. SLC27 fatty acid transport proteins. Mol Aspects Med. 2013; 34(2–3):516–28. Epub 2013/03/20. https://doi.org/10.1016/j.mam.2012.07.010 PMID: 23506886.
15. Kazantzis M, Stahl A. Fatty acid transport proteins, implications in physiology and disease. Biochim Biophys Acta. 2012; 1821(5):852–7. Epub 2011/10/08. https://doi.org/10.1016/j.bbalip.2011.09.010 PMID: 21979150.
16. Dourlen P, Sujkowski A, Wessells R, Mollereau B. Fatty acid transport proteins in disease: New insights from invertebrate models. Prog Lipid Res. 2015; 60:30–40. Epub 09/30. https://doi.org/10.1016/j.plipres.2015.08.001 Epub 2015 Sep 28. PMID: 26416577.
17. Wu Q, Kazantzis M, Doege H, Ortegon AM, Tsang B, Falcon A, et al. Fatty acid transport protein 1 is required for nonshivering thermogenesis in brown adipose tissue. Diabetes. 2006; 55(12):3229–37. Epub 2006/11/30. https://doi.org/10.2337/db06-0749 PMID: 17130465.
18. Sujkowski A, Saunders S, Tinkerhess M, Piazza N, Jennens J, Healy L, et al. dFatp regulates nutrient distribution and long-term physiology in Drosophila. Aging Cell. 2012. Epub 07/20. https://doi.org/10.1111/j.1474-9726.2012.00864.x PMID: 22809097.
19. Chekroud K, Guillou L, Gregoire S, Ducharme G, Brun E, Cazevieille C, et al. Fatp1 deficiency affects retinal light response and dark adaptation, and induces age-related alterations. PLoS ONE. 2012; 7 (11):e50231. Epub 11/21. https://doi.org/10.1371/journal.pone.0050231 Epub 2012 Nov 16. PMID: 23166839.
20. Mollereau B, Domingos PM. Photoreceptor differentiation in Drosophila: from immature neurons to functional photoreceptors. Dev Dyn. 2005; 232(3):585–92. https://doi.org/10.1002/dvdy.20271 PMID: 15704118.
21. Miller DT, Cagan RL. Local induction of patterning and programmed cell death in the developing Drosophila retina. Development. 1998; 125(12):2327–35. PMID: 9584131
22. Mendes CS, Arama E, Brown S, Scherr H, Srivastava M, Bergmann A, et al. Cytochrome c-d regulates developmental apoptosis in the Drosophila retina. EMBO Rep. 2006; 7(9):933–9. https://doi.org/10.1038/sj.embor.7400773 PMID: 16906130.
23. Monserrate JP, Brachmann CB. Identification of the death zone: a spatially restricted region for programmed cell death that sculpts the fly eye. Cell Death Differ. 2007; 14(2):209–17. https://doi.org/10.1038/sj.cdd.4401947 PMID: 16710366.
24. Querenet M, Goubard V, Chatelain G, Davoust N, Mollereau B. Spen is required for pigment cell survival during pupal development in Drosophila. Dev Biol. 2015; 402(2):208–15. Epub 2015/04/15. https://doi.org/10.1016/j.ydbio.2015.03.021 PMID: 25872184.
25. Wang X, Wang T, Ni JD, von Lintig J, Montell C. The Drosophila visual cycle and de novo chromophore synthesis depends on rdhB. J Neurosci. 2012; 32(10):3485–91. Epub 03/09. https://doi.org/10.1523/JNEUROSCI.5350-11.2012 PMID: 22399771.
26. Edwards TN, Nuschke AC, Nern A, Meinertzhagen IA. Organization and metamorphosis of glia in the Drosophila visual system. J Comp Neurol. 2012; 520(10):2067–85. https://doi.org/10.1002/cne.23071 PMID: 22351615.
27. Liu L, MacKenzie KR, Putluri N, Maletic-Savatic M, Bellen HJ. The Glia-Neuron Lactate Shuttle and Elevated ROS Promote Lipid Synthesis in Neurons and Lipid Droplet Accumulation in Glia via APOE/D. Cell Metab. 2017; 26(5):719–37.e6. Epub 2017/10/03. https://doi.org/10.1016/j.cmet.2017.08.024 PMID: 28965825.
28. Dourlen P, Bertin B, Chatelain G, Robin M, Napoletano F, Roux MJ, et al. Drosophila fatty acid transport protein regulates rhodopsin-1 metabolism and is required for photoreceptor neuron survival. PLoS Genet. 2012; 8(7):e1002833. Epub 07/31. https://doi.org/10.1371/journal.pgen.1002833 PMID: 22844251.

29. Gronke S, Mildner A, Fellert S, Tennagels N, Petry S, Muller G, et al. Brummer lipase is an evolutionary conserved fat storage regulator in Drosophila. Cell Metab. 2005; 1(5):323–30. https://doi.org/10.1016/j.cmet.2005.04.003 PMID: 16054079.

30. Jung WH, Liu CC, Yu YL, Chang YC, Lien WY, Chao HC, et al. Lipophagy prevents activity-dependent neurodegeneration due to dihydroceramide accumulation in vivo. EMBO Rep. 2017; 18(7):1150–65. Epub 2017/05/17. https://doi.org/10.15252/embr.201643480 PMID: 28507162.

31. Cubizolle A, Guillou L, Mollereau B, Hamel CP, Brabet P. Fatty acid transport protein 1 regulates retinoid metabolism and photoreceptor development in mouse retina. PLoS One. 2017; 12(7):e0180148. Epub 2017/07/04. https://doi.org/10.1371/journal.pone.0180148 PMID: 28672005.

32. Bhutto I, Lutty G. Understanding age-related macular degeneration (AMD): relationships between the photoreceptor/retinal pigment epithelium/Bruch's membrane/choriocapillaris complex. Mol Aspects Med. 2012; 33(4):295–317. https://doi.org/10.1016/j.mam.2012.04.005 PMID: 22542780.

33. Rambold AS, Cohen S, Lippincott-Schwartz J. Fatty acid trafficking in starved cells: regulation by lipid droplet lipolysis, autophagy, and mitochondrial fusion dynamics. Dev Cell. 2015; 32(6):678–92. Epub 03/11. https://doi.org/10.1016/j.devcel.2015.01.029 Epub 2015 Mar 5. PMID: 25752962.

34. Wang H, Lei M, Hsia RC, Sztalryd C. Analysis of lipid droplets in cardiac muscle. Methods Cell Biol. 2013; 116:129–49. Epub 2013/10/09. https://doi.org/10.1016/B978-0-12-408051-5.00008-5 PMID: 24099291.

35. Zhang H, Wang Y, Li J, Yu J, Pu J, Li L, et al. Proteome of skeletal muscle lipid droplet reveals association with mitochondria and apolipoprotein a-I. Journal of proteome research. 2011; 10(10):4757–68. Epub 2011/08/30. https://doi.org/10.1021/pr200553c PMID: 21870882.

36. Coelho DS, Cairrao F, Zeng X, Pires E, Coelho AV, Ron D, et al. Xbp1-independent ire1 signaling is required for photoreceptor differentiation and rhabdomere morphogenesis in Drosophila. Cell Rep. 2013; 5(3):791–801. Epub 11/05. https://doi.org/10.1016/j.celrep.2013.09.046 Epub 2013 Oct 31. PMID: 24183663.

37. Raghu P, Coessens E, Manifava M, Georgiev P, Pettitt T, Wood E, et al. Rhabdomere biogenesis in Drosophila photoreceptors is acutely sensitive to phosphatidic acid levels. J Cell Biol. 2009; 185(1):129–45. Epub 04/08. https://doi.org/10.1083/jcb.200807027 PMID: 19349583.

38. Redmond TM, Yu S, Lee E, Bok D, Hamasaki D, Chen N, et al. Rpe65 is necessary for production of 11-cis-vitamin A in the retinal visual cycle. Nat Genet. 1998; 20(4):344–51. Epub 1998/12/08. https://doi.org/10.1038/3813 PMID: 9843205.

39. Guignard TJ, Jin M, Pequignot MO, Li S, Chassigneux Y, Chekroud K, et al. FATP1 inhibits 11-cis retinol formation via interaction with the visual cycle retinoid isomerase RPE65 and lecithin:retinol acyltransferase. J Biol Chem. 2010; 285(24):18759–68. https://doi.org/10.1074/jbc.M109.064329 PMID: 20356843.

40. Jahng WJ, Xue L, Rando RR. Lecithin retinol acyltransferase is a founder member of a novel family of enzymes. Biochemistry. 2003; 42(44):12805–12. Epub 2003/11/05. https://doi.org/10.1021/bi035370p PMID: 14596594.

41. Chitraju C, Mejhert N, Haas JT, Diaz-Ramirez LG, Grueter CA, Imbriglio JE, et al. Triglyceride Synthesis by DGAT1 Protects Adipocytes from Lipid-Induced ER Stress during Lipolysis. Cell Metab. 2017; 26(2):407–18 e3. https://doi.org/10.1016/j.cmet.2017.07.012 PMID: 28768178.

42. Nguyen TB, Louie SM, Daniele JR, Tran Q, Dillin A, Zoncu R, et al. DGAT1-Dependent Lipid Droplet Biogenesis Protects Mitochondrial Function during Starvation-Induced Autophagy. Dev Cell. 2017; 42(1):9–21 e5. https://doi.org/10.1016/j.devcel.2017.06.003 PMID: 28697336.

43. Strauss O. The retinal pigment epithelium in visual function. Physiol Rev. 2005; 85(3):845–81. Epub 2005/07/01. https://doi.org/10.1152/physrev.00021.2004 PMID: 15987797.

44. Banerjee S, Bainton RJ, Mayer N, Beckstead R, Bhat MA. Septate junctions are required for ommatidial integrity and blood-eye barrier function in Drosophila. Dev Biol. 2008; 317(2):585–99. Epub 2008/04/15. https://doi.org/10.1016/j.ydbio.2008.03.007 PMID: 18407259.

45. Charlton-Perkins MA, Sendler ED, Buschbeck EK, Cook TA. Multifunctional glial support by Semper cells in the Drosophila retina. PLoS Genet. 2017; 13(5):e1006782. Epub 2017/06/01. https://doi.org/10.1371/journal.pgen.1006782 PMID: 28562601.

46. Mollereau B, Wernet MF, Beaufils P, Killian D, Pichaud F, Kuhnlein R, et al. A green fluorescent protein enhancer trap screen in Drosophila photoreceptor cells. Mech Dev. 2000; 93(1–2):151–60. PMID: 10781948

47. Gambis A, Dourlen P, Steller H, Mollereau B. Two-color in vivo imaging of photoreceptor apoptosis and development in Drosophila. Dev Biol. 2011; 351(1):128–34. https://doi.org/10.1016/j.ydbio.2010.12.040 PMID: 21215264.

48. Pichaud F, Desplan C. A new visualization approach for identifying mutations that affect differentiation and organization of the Drosophila ommatidia. Development. 2001; 128(6):815–26. PMID: 11222137.

49. Stowers RS, Schwarz TL. A genetic method for generating Drosophila eyes composed exclusively of mitotic clones of a single genotype. Genetics. 1999; 152(4):1631–9. PMID: 10430588

50. Fish MP, Groth AC, Calos MP, Nusse R. Creating transgenic Drosophila by microinjecting the site-specific phiC31 integrase mRNA and a transgene-containing donor plasmid. Nat Protoc. 2007; 2(10):2325–31. https://doi.org/10.1038/nprot.2007.328 PMID: 17947973.

51. Stewart BA, Atwood HL, Renger JJ, Wang J, Wu CF. Improved stability of Drosophila larval neuromuscular preparations in haemolymph-like physiological solutions. J Comp Physiol A. 1994; 175(2):179–91. PMID: 8071894.

52. Rueden CT, Schindelin J, Hiner MC, DeZonia BE, Walter AE, Arena ET, et al. ImageJ2: ImageJ for the next generation of scientific image data. BMC Bioinformatics. 2017; 18(1):529. https://doi.org/10.1186/s12859-017-1934-z PMID: 29187165.

53. Dourlen P, Levet C, Mejat A, Gambis A, Mollereau B. The Tomato/GFP-FLP/FRT Method for Live Imaging of Mosaic Adult Drosophila Photoreceptor Cells. J Vis Exp. 2013;(79). Epub 10/03. https://doi.org/10.3791/50610 PMID: 24084155.

54. Greenspan P, Mayer EP, Fowler SD. Nile red: a selective fluorescent stain for intracellular lipid droplets. J Cell Biol. 1985; 100(3):965–73. Epub 1985/03/01. PMID: 3972906.

55. Lefils J, Geloen A, Vidal H, Lagarde M, Bernoud-Hubac N. Dietary DHA: time course of tissue uptake and effects on cytokine secretion in mice. Br J Nutr. 2010; 104(9):1304–12. Epub 2010/05/22. https://doi.org/10.1017/S0007114510002102 PMID: 20487585

56. Medja F, Allouche S, Frachon P, Jardel C, Malgat M, Mousson de Camaret B, et al. Development and implementation of standardized respiratory chain spectrophotometric assays for clinical diagnosis. Mitochondrion. 2009; 9(5):331–9. Epub 2009/05/15. https://doi.org/10.1016/j.mito.2009.05.001 PMID: 19439198.